Investigation of diffuse noxious inhibitory controls in the rat monosodium iodoacetate model of osteoarthritis pain

Victoria Simmonds, BSc.

University of Nottingham
UK | CHINA | MALAYSIA

Thesis submitted to the University of Nottingham
for the degree of Doctor of Philosophy

September 2019

Abstract

Osteoarthritis (OA) is the most common form of arthritis, with chronic pain being the most frequent and debilitating consequence. Current analgesics are inadequate in treating OA pain due to poor efficacy or serious side effects. Mechanistic studies in humans suggest dysfunction of descending inhibitory pathways in symptomatic knee OA is a key contributor in the development and maintenance of chronic pain. Such inhibitory pathways are recruited by diffuse noxious inhibitory controls (DNIC), whereby inhibition of spinal dorsal horn neuronal excitability to a 'test' stimulus can be induced by applying a noxious 'conditioning' stimulus to widespread areas of the body outside the peripheral excitatory receptive field (RF) of the neuron (heterotopic stimulation); hence DNIC can be used to study whether inhibition of spinal neural transmission has been compromised. In this respect spinally organised nociceptive withdrawal reflexes (NWRs) are functionally characterised population responses, modularly organised to most effectively move a limb away from a source of pain, with descending inhibitory pathways helping to set an appropriate activation threshold. The aim of this thesis was therefore to investigate whether descending inhibition was altered in an experimental model of OA pain by electrophysiologically measuring DNIC of reflexes in hindlimb muscles.

In alfaxalone-anaesthetised rats, electromyograms (EMGs) to noxious stimulation of the heel or toes were recorded in the ankle extensor medial gastrocnemius (MG), the knee flexor biceps femoris (BF) and the ankle flexor tibialis anterior (TA) of the left hindlimb before and after a noxious 'conditioning' capsaicin injection into the contralateral hind or forelimb. In naïve animals, depending on the reflex, responses were inhibited by capsaicin (50 µg, 500 µg or 5 mg) in a dose-related manner to a median of between 14 – 76% of controls for 29 to 63 min. For all reflexes this inhibition was abolished by spinalization and reduced by decerebration for heel-MG and toes-BF when capsaicin was applied to the contralateral forelimb. For the same reflexes and

conditioning site, reduced alfaxalone levels led to significantly greater inhibition. Reflexes were inhibited to a similar level irrespective of whether electrical (up to 10 mA, 8 x 2 ms pulses at 1 Hz) or graded mechanical (10 – 300 g von Frey (vF) monofilaments) stimuli were used although the latter appeared to offer a better means by which to detect changes in DNIC as both A- and C-fibre responses were measured along with the range of stimulus intensities.

Subsequent experiments investigated DNIC of reflex responses in a model of OA pain induced by knee joint injection of monosodium iodoacetate (MIA). At 28-35 days post-injection, MIA-injected animals had severe cartilage damage and established pain behaviour. However, DNIC of reflex responses was to a similar degree for all three reflexes after injection of capsaicin into the contralateral hind or forelimb. In contrast, 3-4 days post-injection, MIA animals had very little to no cartilage damage accompanied by pain behaviour. Although DNIC of reflex responses was similar following injection of capsaicin into the contralateral forelimb, a reduced efficacy in DNIC inhibition was found after hindlimb injection.

These data show that stimulus-evoked inhibition (DNIC) of spinal reflexes originates from regions caudal to the colliculi (likely within the pons and medulla) but higher brain areas may modify this inhibition. Similar to other general anaesthetics, alfaxalone levels affect the degree of DNIC. A reduction in DNIC efficacy is present in early stages of OA, but there was no evidence of compromised DNIC in established OA. Mechanical test stimuli provided a more sensitive method for detecting changes in DNIC whilst findings were also dependent on choice of conditioning site. Similarly, differential sensitivities to DNIC highlights the importance of studying multiple reflex responses in mechanistic studies of chronic pain.

Abstracts and poster presentations

Simmonds, V, Harris, J. The effect of diffuse noxious inhibitory controls on nociceptive withdrawal reflexes in the monosodium iodoacetate model of osteoarthritis pain. 16th IASP World Congress on Pain, Congress of the European Federation of IASP Chapters, Yokohama, Japan, 2016. PF0371.

Simmonds, V, Kelly, S, Harris, J. The effect of diffuse noxious inhibitory controls on spinal reflexes in the monosodium iodoacetate model of osteoarthritis pain. "Bridging the gaps between pain research and osteoarthritis research" An internal workshop for basic and clinical researchers, Stockholm, Sweden, 2015.

Simmonds, V, Kelly, S, Harris, J. The effect of diffuse noxious inhibitory controls on spinal reflexes in the monosodium iodoacetate model of osteoarthritis pain. 9th Congress of the European Federation of IASP Chapters, Vienna, Austria, 2015. EFIC5-0651.

Acknowledgements

There are many people without whom the completion of this thesis would not have been possible, and whom I would now like to thank.

Firstly, I would like to thank my supervisor Dr John Harris for his help, support and guidance throughout my PhD, for teaching me the intricacies of experimental techniques and always being available for a cup of tea and discussions about experiments or data (or sometimes Game of Thrones!).

I am grateful to Dr Sara Kelly for her help in teaching me the MIA model technique and support in overcoming issues we encountered, as well as Dr Carl Stevenson for his advice and inputs to discussions of my work and thesis.

I would like to acknowledge the BBSRC Doctoral Training Partnership and the University of Nottingham for funding my studies, Professor Kate White for her help organising the lab and obtaining supplies, and the Bio-Support Unit for all their hard work and support.

I would also like to thank my family for their continued encouragement, and friends, especially those made through the DTP, who have been understanding, and invaluable for de-stressing and I know this project would not have been the same without them.

Finally, I am indebted to Tom for his love, patience and listening skills, and without who's computer help I would still be lost. Most of all I owe my deepest thanks to my parents, whose continued love, support and unfailing belief in me has made me the person I am, and I would not be where I am today without them.

Table of Contents

List of figures and tables

Abbreviations

5-HT	5-hydroxytryptamine (serotonin)
5-HTP	5-hydroxytryptophan
ACL	anterior cruciate ligament
ACLT	anterior cruciate ligament transection
ALL	anterolateral ligament
AMPA	alpha-3-hydroxy-5-methyl-4-isoxazolepropionic acid
ANOVA	analysis of variance
ARRIVE	Animal Research: Reporting of In Vivo Experiments
ASICs	acid sensing ion channels
ATP	adenosine triphosphate
AUC	area under the curve
AWERB	Animal Welfare & Ethical Review Body
BF	biceps femoris
BMC	bone mineral content
BMD	bone marrow density
BMI	body mass index
BMLs	bone marrow lesions
BMU	bone multicellular unit
CED	Cambridge Electronic Design
CFA	complete Freund's adjuvant
CGRP	calcitonin gene-related peptide
CNF	cuneiformis nucleus
CNS	central nervous system
COX-2	cyclooxygenase-2
CPM	conditioned pain modulation
CRI	constant rate infusion
CVLM	caudal ventrolateral medulla
DALY	Disability of Adjusted Life Year
DH	Dunkin Hartley
DNIC	diffuse noxious inhibitory controls
DRG	dorsal root ganglia
DRt	Dorsal reticular

ECG	electrocardiogram
ECM	extracellular matrix
EMG	electromyogram
EMLA	Eutectic Mixture of Local Anaesthetics
EPSCs	excitatory postsynaptic currents
FCEs	Finished Consultant Episodes
G3PD	glyceraldehyde-3-phophate dehydrogenase
GABA	gamma-aminobutyric acid
GAGs	glycosaminoglycans
GlyR	glycine receptors
GNP	Gross National Product
GPCR	G protein-coupled receptor
HLA	human leukocyte antigen
HTMs	high-threshold mechanoreceptors
i.p.	intraperitoneal
i.v.	intravenous
IBS	irritable bowel syndrome
IL	interleukin
ILC	Infralimbic cortex
IQR	interquartile range
JOR	jaw-opening reflex
KL	Kellgren and Lawrence
LCL	lateral collateral ligament
LPb	lateral parabrachial
LTMs	low-threshold mechanoreceptors
MCL	medial collateral ligament
MG	medial gastrocnemius
mGluR	metabotropic glutamate receptors
MHRs	mechano-heat receptors
MIA	monosodium iodoacetate
MNX	meniscal transection
MPQ	McGill Pain Questionnaire
MRF	medullary reticular formation
MRI	magnetic resonance imaging

mRNA	messenger ribonucleic acid
N_2O	nitrous oxide
NA	noradrenaline
NGF	nerve growth factor
NHS	National Health Service
NKA	neurokinin A
NMDA	N-methyl-D-aspartate
NpGC	nucleus paragiganto-cellularis
NPY	neuropeptide Y
NRM	nucleus raphe magnus
NRS Pain	Numeric Scale for Pain
NS	nociceptive-specific
NSAIDs	non-steroidal anti-inflammatory drugs
NSIA	noxious stimulus-induced antinociception
NTS	nucleus of the solitary tract
NVS	Named Veterinary Surgeon
NWR	nociceptive withdrawal reflex
OA	osteoarthritis
PAFs	primary afferent fibres
PAG	periaqueductal grey
PB	parabrachial
PCL	posterior cruciate ligament
pCPA	para-chlorophenylalanine
PCS	photographic chondropathy score
PG	prostaglandin
PKA	protein kinase A
PKC	protein kinase C
PLA_2	phospholipase A_2
PLC	phospholipase C
PPT	pressure pain threshold
PWT	paw withdrawal threshold
QST	quantitative sensory testing
RF	receptive field
RMS	Root mean square

RTK	receptor tyrosine kinase
RO	reverse osmosis
RVM	rostral ventromedial medulla
SBCs	subchondral bone cysts
SCI	spinal cord injury
SD	standard deviation
SEM	standard error of means
SFA	Système Française D'Arthroscopie
SHT	spinohypothalamic tract
SNL	spinal nerve ligation
SOP	standard operating procedure
SP	substance P
SPBT	spinoparabrachial pathway
SRD	subnucleus reticularis dorsalis
ST	semitendinosus
STT	spinothalamic tract
TA	tibialis anterior
TENS	transcutaneous electrical nerve stimulation
TKR	total knee replacement
TMD	temporomandibular joint disorder
TNF-α	tumor necrosis factor alpha
TRP	transient receptor potential
TRPA	transient receptor potential ankryin
TRPC	transient receptor potential canonical
TRPM	transient receptor potential melastatin
TRPV	transient receptor potential vanilloid
VAS	Visual Analogue Scale
vF	von Frey
VGCC	voltage-gated calcium channel
VGSC	voltage-gated sodium channel
VMpo	ventromedial posterior
VP	ventral posterior
WDR	wide-dynamic range
WOMAC	Western Ontario and McMaster Universities

WS	Wallenberg's syndrome
YLDs	Years Lived with Disability

Chapter One

General Introduction

1.1. Introduction

Osteoarthritis (OA) is a degenerative musculoskeletal condition affecting structures within joints (Felson, 2006). OA is the most common form of arthritis with an estimated 8.75 million people aged 45 and over having sought treatment in the UK and it is estimated that 8.3 million people could have knee OA alone by 2035 (Arthritis Research UK, 2013). It can be found in any joint in the body; just over half of all people who have sought treatment for OA have knee OA and 24% suffer from hip OA but it can also be found in the hands, wrists, facet joints and feet (Arthritis Research UK, 2013; Litwic et al., 2013). The prevalence of OA varies between geographical locations with hand OA indicated as the most prevalent form of OA in the USA and knee OA being less frequent (Lawrence et al., 2008; Litwic et al., 2013). There are also variations within countries, for example between rural and urban communities where rural communities have a higher prevalence of OA in countries such as China, Bangladesh and India, possibly due to the physical nature of living in a rural community and the overloading of joints (Chopra, 2013). OA sufferers find their lives greatly affected by the disease with crippling pain being the most burdensome symptom associated with the condition (Swagerty and Hellinger, 2001). In 2016 over 33.5 million prescription items were dispensed for musculoskeletal & joint diseases, of which OA is included, at a cost of nearly £206 million to the National Health service (NHS)(NHS Digital, 2017). However, many patients find that their pain relief is inadequate for their condition (Breivik et al., 2006). A worldwide questionnaire study showed that 40% of pain

sufferers felt dissatisfied with the treatment they were receiving for their long lasting pain (Breivik et al., 2006). There are a wide range of analgesics available for treating OA pain, however patients have variable results with all of them. Oral analgesics also have severe side effects, from nausea and vomiting to stomach ulcers and other gastrointestinal problems. This leads to patients having to change analgesics regularly or stop them completely even if they are effective in treating their pain. This has led to the conclusion that the treatment of OA pain is not a "one size fits all" concept that a given efficacious drug will cure all patients of their pain, some drugs work for some and not for others and some patients find no relief from any current treatments. Therefore, a better understanding of the mechanisms underlying OA pain will not only enable us to fully comprehend the changes in the joint but also in the central nervous system (CNS) which occur in an OA patient and so begin to understand why each patients pain is unique. This study uses an animal model to investigate the underlying central mechanisms associated with OA pain by measuring reflex responses to examine the effects of a noxious stimulus on a descending inhibitory pathway.

1.2. The pain pathway

Pain is *"an unpleasant sensory and emotional experience associated with actual or potential tissue damage, or described in terms of such damage"* (Loeser and Treede, 2008). Whilst pain and nociception are linked, there is a distinct separation with nociception being separately defined as *"neural processes of*

encoding and processing noxious stimuli" (Loeser and Treede, 2008). The basic pain pathway for the perception of pain consists of three main stages. The first stage is transduction, where pain is detected in the periphery. The second stage is transmission of the signals from the periphery to the dorsal horn of the spinal cord. The final stage is transmission of signals to higher brain centres via the CNS which is typically via two routes; ascending pathways carrying information from the spinal cord to the brain and descending pathways from the brain to the reflex organs (Yam et al., 2018).

1.2.1. Primary afferent fibres

Primary afferent fibres (PAFs) are sensory neurons in the peripheral nervous system that transduce information on the mechanical, chemical and thermal state of the body to the CNS. They can transmit both innocuous and noxious stimuli and are classified into three groups based on their conduction velocities, sensitivities, structure and size (Lawson, 2002)(Table 1.1).

A-fibres are broadly classified as myelinated fibres, however, can be broken down into smaller sub-categories. Aα and Aβ-fibres have large myelinated axons with average diameters of 20 µm and 10 µm respectively which enables them to have the fastest action potential conduction velocities, between 40 and 120 m s^{-1}, and they are activated by innocuous mechanical stimuli (Harper and Lawson, 1985a; Julius and Basbaum, 2001; McGlone and Reilly, 2010). Aα-fibres are low-threshold mechanoreceptors (LTMs) and mainly have a

proprioceptive function whereas Aβ-fibres were traditionally only thought to be involved in innocuous mechanosensation (Niissalo et al., 2002; Djouhri and Lawson, 2004; Wu and Henry, 2010). However, both Aα and Aβ-fibres have also been shown to be involved in nociception under normal and diseased states such as OA whereby as much as 19% of Aα/β-fibres were nociceptive (Djouhri and Lawson, 2004).

Aδ-fibres are small diameter (2 – 5 μm) myelinated fibres, with slower conduction velocities and their main role is as high-threshold mechanoreceptors (HTMs) or mechano-heat receptors (MHRs)(McGlone and Reilly, 2010). It has been proposed that there are two distinct types of Aδ-fibre, both of which respond to intense mechanical stimuli classified as type I and type II, with approximately 90% as type II responding to chemical stimuli such as capsaicin and moderately noxious temperatures above 45 °C, whilst type I represent 10% of the Aδ-fibres, are capsaicin insensitive and respond to temperatures above 52 °C (Julius and Basbaum, 2001; Ringkamp et al., 2013).

C-fibres are the smallest diameter axons at < 1 μm and are unmyelinated, making them the slowest conducting afferents (< 1.3 m s^{-1})(McGlone and Reilly, 2010). High-threshold C-fibres signal threatening and damaging stimuli in a unique fashion that is not possible for low threshold units (Bessou and Perl, 1969).

Fibre Type	Myelinated	Axon diameter (µm)	Conduction velocity (m s^{-1})	Modality
Aα	Yes	10 – 20	70 – 120	Innocuous mechanical: pressure, vibration, stroking, muscle stretch, proprioception
Aβ	Yes	2.5 – 10	40 – 70	Innocuous mechanical: pressure, vibration, stroking, muscle stretch, proprioception
Aδ (I)	Yes	1 – 2.5	1 – 15	High-threshold heat > 52 °C (thermal receptors)
Aδ (II)	Yes	1 – 2.5	1 – 15	Cooling (thermal receptors), noxious mechanical, chemical and heat > 45 °C (nociceptors)
C – pain	No	< 1	< 1.3	Noxious mechanical, chemical and cold/heat (< 5 °C and > 43 °C)(nociceptors)
C - tactile	No	< 1	< 1.3	Light stroking, gentle touch

Table 1.1. Primary afferent fibre properties (Adapted from Harper and Lawson, 1985a, b).

1.2.2. Sensory receptors

When investigating sensory receptors in the skin it becomes quickly evident that there are different groups of receptors which can be separated by common characteristics and can be grouped based on the stimuli they respond to (Bessou and Perl, 1969).

1.2.2.1. Mechanoreceptors

Mechanoreceptors can be found in a variety of tissues such as skin, muscle spindles and the gastrointestinal tract and are stimulated by changes in pressure, stretch or distortion (Kandel et al., 2013). Mechanoreceptors account for a large proportion of the sensory receptors innervated by unmyelinated fibres of cutaneous nerves (Bessou and Perl, 1969). LTMs respond to innocuous or low intensity mechanical stimuli via Pacinian corpuscles, Meissner's corpuscles, Merkel's discs and Ruffini endings (Basbaum et al., 2009; McGlone and Reilly, 2010). These cutaneous receptors are located in different layers of the skin to differentially adapt to various types of stimuli; with Pacinian corpuscles and Meissner's corpuscles classified as fast adapting, where they react to the initial and final changes in the skin due to the stimuli, and Merkel's discs and Ruffini endings are slow adapting, continuously firing for the duration the stimulus is in contact with the skin (McGlone and Reilly, 2010). All non-nociceptive mechanoreceptors are transduced by Aα or Aβ afferent fibres.

1.2.2.2. Thermoreceptors

Thermal stimuli that differ from a set homeostatic point cause changes in ambient temperature which are detected by thermoreceptors (McGlone and Reilly, 2010). Within these fibres there are two distinct groups; one responding to heat and the other to cold, within the innocuous range of 20 – 45 °C (McGlone and Reilly, 2010). Thermoreceptors are exclusively activated by thermal stimuli, with changes in temperature as slight as 2 °C being detected (Hensel, 1973; Kuhtz-Buschbeck et al., 2010). Rapid changes in temperature produce increases in impulse frequency, therefore thermoreceptors respond to both dynamic and static temperature (Hensel and Boman, 1960; Kuhtz-Buschbeck et al., 2010). Thermal stimuli are detected by a specific family of transduction proteins known as transient receptor potential (TRP) channels which are nonselective cation receptor-channels with six transmembrane domains (Kandel et al., 2013). All TRP channels are gated by temperature and the various chemical ligands that bind to them. There are many subgroups of TRP channels including; TRP melastatin (TRPM), TRP ankryin (TRPA) and TRP canonical (TRPC) of which individual receptors have different functions, for example TRPM8 and TRPA1 are activated by cold stimuli (Kandel et al., 2013). Another subgroup is the TRP vanilloid (TRPV) group of which the TRPV1 channel is a member. This channel is found on a subpopulation of PAFs and activated by noxious heat above 43 °C and acidic conditions of pH < 6.0 (Ringkamp et al., 2013). TRPV1 is a non-selective ion channel, therefore when activated it allows an influx of Na^+ and Ca^{2+} ions causing depolarisation of the peripheral afferent

terminal and generation of an action potential. In inflammatory conditions, TRPV1 is increased in the joint as axonal transport of TRPV1 messenger ribonucleic acid (mRNA) is induced, with TRPV1-labelled unmyelinated axons in the periphery increased by 100% (Ringkamp et al., 2013; Kelly et al., 2013a). Also known as the capsaicin receptor, TRPV1 is activated by this compound, which is the chemical responsible for the pungency of chilli peppers. It binds to TRPV1 proteins in nociceptors and induces the release of substance P (SP) and calcitonin gene-related peptide (CGRP) causing pain in the form of a burning sensation. Injection of capsaicin causes transient pain followed by hypersensitivity to both mechanical and thermal stimuli (Ringkamp et al., 2013).

1.2.2.3. Nociceptors

Nociceptors are sensory receptors responsible for encoding pain by connecting all peripheral tissues such as muscles, tendons and joints to the CNS (Kandel et al., 2013; Malfait and Schnitzer, 2013). They are pseudounipolar and highly specialised primary afferent neurons with their cell bodies lying in the dorsal root ganglia (DRG) and bifurcating axons, projecting to both the periphery and the CNS to terminate in the dorsal horn of the spinal cord or trigeminal nucleus (Malfait and Schnitzer, 2013). Unmyelinated C-fibre nociceptors are the most common fibre type in the peripheral nervous system and represent the vast majority of nociceptors; however a small proportion of nociceptors are thinly myelinated Aδ-fibres (Woolf and Ma, 2007). Together these two fibre types

with their differing conduction velocities produce two distinct perceptions of pain known as first and second pain. First pain is produced by the faster conducting Aδ-fibres and is perceived as an initial sharp or prickling sensation that is responsible for controlling withdrawal reflexes to move the tissue away from the potentially damaging stimuli (McGlone and Reilly, 2010). Second pain is transmitted to the CNS by C-fibres where it evokes an emotional response to the pain and is described by delayed sensations such as dull, aching, radiating, throbbing and burning (Melzack, 1975; Kandel et al., 2013). Nociceptors are all high-threshold receptors and can be divided into four main groups based on the type of noxious stimuli they respond to; mechanical, thermal, polymodal and silent nociceptors (Bessou and Perl, 1969; Kandel et al., 2013).

Mechanical nociceptors are activated by intense pressure and often cannot be activated by or are inconsistently activated by any other form of stimulation (Burgess and Perl, 1967; Bessou and Perl, 1969; Kandel et al., 2013). They are classified as HTMs and account for approximately 15% of the Aδ-fibres (Bessou and Perl, 1969). HTMs adapt to maintained mechanical stimuli fairly rapidly, however if subjected to repeated noxious stimuli become inactive (Bessou and Perl, 1969).

Thermal nociceptors detect extreme temperatures, usually greater than 45 °C or less than 5 °C, and are usually conducted by Aδ-fibres at conduction velocities between 5 and 30 m s^{-1} (Fein, 2012; Kandel et al., 2013). Noxious heat

and cold are conducted by separate groups of fibres, however noxious cold does not produce responses as strongly as noxious heat (Julius and Basbaum, 2001). Whilst noxious heat activates around 50% of fibres, noxious cold only excites approximately 10 – 15% of fibres within the same receptive field (RF) (Julius and Basbaum, 2001).

Polymodal nociceptors respond to noxious thermal, mechanical and chemical stimuli and are usually small unmyelinated C-fibres (Fein, 2012). They are the most common type of nociceptors with around 50% of unmyelinated axons classified as polymodal (Schmidt et al., 1995; McGlone and Reilly, 2010). These units vary in their sensitivity to noxious stimuli and are 5 – 10 times more sensitive than LTMs, however polymodal nociceptors tend to have a pattern in their sensitivity, for example receptors with lower mechanical thresholds also have lower thermal thresholds (Bessou and Perl, 1969). Chemical stimulants such as dilute hydrochloric acid consistently evoke activity in polymodal nociceptors where impulses were low in frequency but maintained for the duration that the stimulant was in contact with the RF (Bessou and Perl, 1969). After noxious stimulation polymodal nociceptors have increased sensitivity to stimuli, resulting in altered responsiveness to rapid cooling and a reduction in thresholds, sometimes for periods of up to 2 hours after the initial stimulus was applied, which may be key in sensitization (see section 1.2.5) (Bessou and Perl, 1969; Basbaum et al., 2009).

Silent nociceptors are unmyelinated heat sensitive fibres that are activated by chemical stimuli and therefore classed as inflammatory mediators (Fein, 2012). During prolonged periods of inflammation or injury, silent or sleeping nociceptors can also become increasingly activated by mechanical stimuli (Basbaum et al., 2009). This would suggest that during states of pain such as in OA, recruitment of silent nociceptors contributes to sensitization in humans by adding a component of spatial summation (Schmidt et al., 1995; McGlone and Reilly, 2010).

1.2.3. Spinal cord dorsal horn

Central terminals of PAFs extend to the dorsal horn of the spinal cord or the trigeminal nucleus in the face where they terminate and synapse onto secondary nociceptive projection neurons or excitatory and inhibitory interneurons (Vanegas et al., 2010; Malfait and Schnitzer, 2013). The spinal cord grey matter is divided into ten distinct laminae, numbered dorsal to ventral from I to X, and separated based on their shape, size and the relative number of nerve cells they contain in both cats (Rexed, 1952) and rats (Molander et al., 1984, 1989)(Figure 1.1). Sensory information from the knee joint enters the spinal cord via primary afferents in the L5 – L7 dorsal roots which terminate in laminae I – VI (Craig et al., 1988; Schaible and Grubb, 1993). Spinal cord neurons in these laminae receive convergent input from the knee and surrounding muscle and subcutaneous tissue (Schaible et al., 1987).

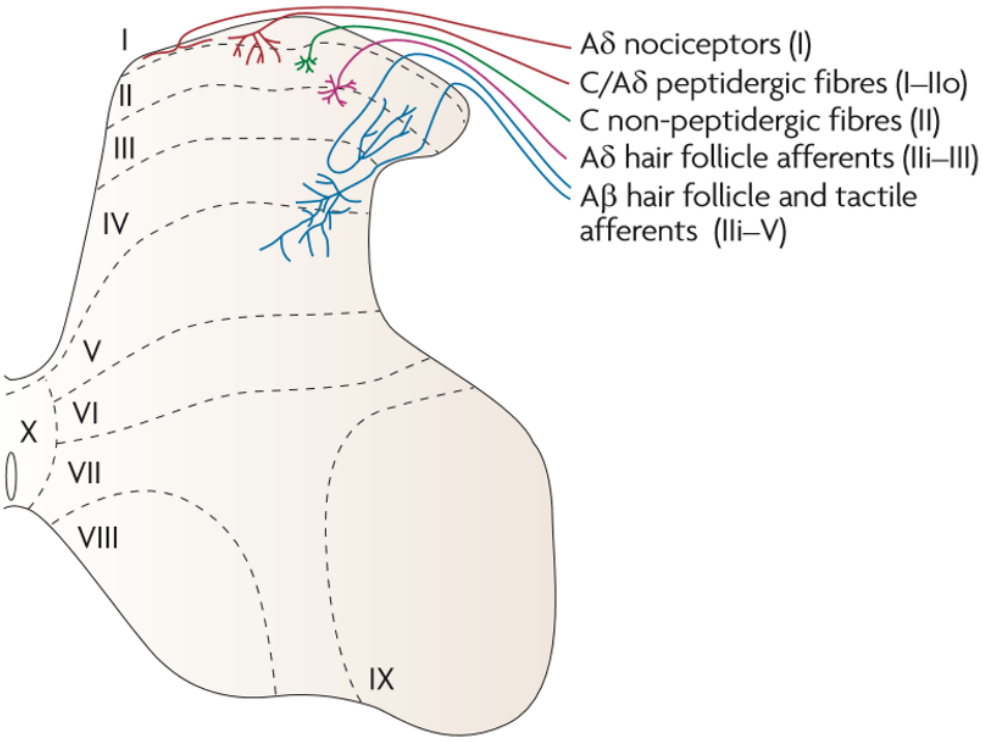

Figure 1.1. Organisation of the Rexed laminae of the spinal cord dorsal horn. Primary afferent fibres (PAFs) terminate in different locations depending on their size and function (Todd, 2010).

Lamina I, or the marginal layer, forms a small outermost cover of the dorsal horn and contains both projection neurons and interneurons (Todd and Koerber, 2013). A large majority of the neurons in lamina I receive inputs from Aδ primary afferents in response to high-threshold mechanical, intense cold, chemical and noxious heat stimulation (Fields and Basbaum, 1978; Longstaff, 2000; Millan, 2002). Due to the selectivity of these neurons to noxious stimuli they are termed nociceptive-specific (NS) neurons (Kandel et al., 2013). Lamina I also receive small inputs from graded innocuous to highly noxious mechanical stimuli and these are termed wide-dynamic range (WDR) neurons (Kandel et al., 2013). However, only 5% of lamina I neuronal population equates to these type of neurons, despite containing the highest density of projection neurons in the dorsal horn (Todd and Koerber, 2013).

Lamina II, the substantia gelatinosa, contains predominantly interneurons which are densely packed and receive nociceptive input from Aδ and C-fibres (Longstaff, 2000; Todd and Koerber, 2013; Todd, 2010). The interneurons in laminae II are both excitatory (glutamatergic) and inhibitory (GABA-ergic or glycinergic), responding selectively to nociceptive inputs or both nociceptive and innocuous inputs (Todd, 2010; Kandel et al., 2013). Lamina II can be subdivided into two regions; the inner region which has lower neuronal density and receives non-peptidergic C-fibre afferents and the outer region receiving peptidergic Aδ and C-fibre afferents (Todd, 2010).

Laminae III – VI form the deep dorsal horn, with lamina III and IV occupying the larger part of the head of the dorsal horn (Rexed, 1952). These laminae contain significantly less nociceptive input than the superficial layers, however some tracing has shown PAFs present in lamina III (Molander and Grant, 1986). Lamina III is characterized by densely populated interneurons, that are slightly larger than those in lamina II, and large projection neurons (Molander et al., 1984; Todd, 2010). Predominantly terminating in lamina III, are Aβ-fibres innervating innocuous mechanoreceptors, however Aβ-fibres also terminate in lamina IV, V and VI but to a much lesser extent (Millan, 1999).

The intermediate and ventral grey matter comprise of lamina VII – X and are targets for both myelinated and non-myelinated primary afferents mostly from visceral inputs (Longstaff, 2000). Lamina VII receives autonomic preganglionic fibres and lamina IX contains cell bodies of both α and γ-motoneurons which extend to skeletal muscles (Longstaff, 2000).

1.2.4. Neurotransmitters

There are many neurotransmitters, neuropeptides, ion channels and receptors expressed by nociceptors. Neuronal components of the dorsal horn are interconnected in a highly complex synaptic circuit, demonstrating the many potential mechanisms that can modulate nociceptor activity and transmission (Table 1.2).

Receptor(s)	Receptor Type	Neurotransmitter	PAF type	Effect
NMDA, AMPA & kainate	Ligand-gated ion channel	Glutamate	C, Aδ, Aβ	Excitation
mGluR	GPCR	Glutamate	C, Aδ	Excitation
NK_1	GPCR	Substance P	C, Aδ	Excitation
NK_2	GPCR	Neurokinin A (NKA)	C, Aδ	Excitation
CGRP receptor	GPCR	CGRP	C, Aδ, Aβ	Excitation
BK_1 & BK_2	GPCR	Bradykinin	C	Excitation
P2X	Ligand-gated ion channel	ATP	C	Excitation
Ca^{2+}	Ion channel	Ca^{2+}	C, Aδ	Excitation
$Na_v1.9$	Ion channel	Na^+	C	Excitation
$Na_v1.7$ & $Na_v1.8$	Ion channel	Na^+	C, Aδ	Excitation
$GABA_A$	Ligand-gated ion channel	GABA	Aδ, Aβ	Inhibition
$GABA_B$	GPCR	GABA	Aδ, Aβ	Inhibition
GlyR	Ligand-gated ion channel	Glycine	C, Aδ	Inhibition
Gal_{1-3}	GPCR	Galanin	C, Aδ	Inhibition
$NPYR_{1-5}$	GPCR	Neuropeptide Y	C	Inhibition
SST_{1-5}	GPCR	Somatostatin	C	Inhibition

Table 1.2. Neurotransmitters and peptides expressed by nociceptors in primary afferent fibres (PAFs). GPCR = G protein-coupled receptor. Table modified from (Lawson, 2005).

Glutamate is the primary excitatory neurotransmitter involved in nociceptive signalling released from primary afferents, projection neurons and excitatory interneurons (Sorkin and Yaksh, 2013). Its release from central terminals of nociceptors generates excitatory postsynaptic currents (EPSCs) in secondary dorsal horn neurons (Basbaum et al., 2009). It is found in both myelinated and unmyelinated fibres and acts at several different receptors including the ionotropic alpha-3-hydroxy-5-methyl-4-isoxazolepropionic acid (AMPA), N-methyl-D-aspartate (NMDA) and kainate receptors as well as many metabotropic glutamate receptors (mGluR). AMPA, NMDA and kainate receptors are all expressed on the spinal terminals of Aδ and C-fibres, however mGluR receptors are differentially expressed by Aδ and C-fibres depending on the receptor subtype (Sorkin and Yaksh, 2013; Todd and Koerber, 2013). Ionotropic Glu receptors directly regulate the opening of ion channels to Na^+ and K^+, and mGluR and NMDA receptors are also permeable to Ca^{2+} (Budai, 2000).

Neuropeptides SP, neurokinin A (NKA) and CGRP are also excitatory neurotransmitters released by primary afferent nociceptors (Todd and Koerber, 2013). SP is found to be present in the central terminals of primary afferent neurons where it produces long-lasting enhancement of dorsal horn neurons, especially when combined with NMDA where it produces profound effects to noxious mechanical stimulation (Budai, 2000). SP also enhances the release of glutamate from the spinal cord dorsal horn to potentiate nociceptive signals (Budai, 2000). SP can also be co-released with NKA from primary afferent

terminals, where NKA has a slower degradation rate and so persists in the dorsal horn for much longer periods. Neurokinin receptors are the main targets for both these neurotransmitters, with SP targeting NK_1 and NKA targeting NK_2 (Levine et al., 1993). CGRP is in high concentrations in the small DRG nerve cells and the majority of PAFs associated with pain transmission contain this peptide, including unmyelinated and small-diameter myelinated fibres (Levine et al., 1993; Budai, 2000). Whilst CGRP has limited effects itself it potentiates the effects of other compounds such as SP in response to noxious thermal, mechanical or electrical stimulation (Levine et al., 1993). Bradykinin is an excitatory peptide neurotransmitter which acts on BK_1 and BK_2 receptors to activate phospholipase C (PLC) and protein kinase C (PKC) pathways and is released in the spinal cord within minutes of nociceptor C-fibre input (Ringkamp et al., 2013; Woolf and Ma, 2007). Adenosine triphosphate (ATP) is expressed by C-fibre nociceptors and released in response to tissue damage or noxious stimulation primarily from heat stimulation (North, 2004). In the presence of its purinogenic receptor (P2X) on the central terminals of PAFs, ATP increases EPSCs by evoking the release of glutamate from DRG cells (Budai, 2000; North, 2004). Ion channels also facilitate excitatory nociception by voltage-gated calcium channels (VGCCs) and voltage-gated sodium channels (VGSCs)(Sorkin and Yaksh, 2013). Depolarization of primary afferent terminals leads to the opening of VGCC, resulting in a number of important functions such as generating depolarizing membrane currents at the terminal, initiating activation via phosphorylation of other receptors, for example NMDA, and propagating further protein cascades, such as phospholipase A_2

(PLA_2)(Malmberg and Yaksh, 1994; Sorkin and Yaksh, 2013). VGSCs are essential for regulating encoding receptor potentials into action potentials, however $Na_v1.7$, $Na_v1.8$ and $Na_v1.9$ are the three main VGSCs that are found in the DRG neurons (Strickland et al., 2008; Fein, 2012). $Na_v1.7$ and $Na_v1.8$ are predominantly found in small diameter nociceptive afferents and in chronic pain states all three receptor sub-types are overexpressed in joint afferent neurons (Strickland et al., 2008).

Inhibitory interneurons in the dorsal horn express the amino acids gamma-aminobutyric acid (GABA) and/or glycine as their main neurotransmitter (Todd, 2010). Immunostaining shows that glycine is only found in GABA containing cells within laminae I – III which suggests these interneurons co-release glycine and GABA or they only release GABA (Todd, 2010). GABA has two receptor targets which are the ionotropic $GABA_A$ and metabotropic $GABA_B$ receptors (Fein, 2012). $GABA_A$ mediates rapid transmission whilst $GABA_B$ mediates a variety of transmissions and is found in greater numbers than $GABA_A$ (Budai, 2000). Glycine is found predominantly in lamina III of the dorsal horn and receives significant inputs from myelinated LTMs as well as small diameter nociceptive afferents (Budai, 2000). Glycine receptors (GlyR) are ligand-gated ion channels which when activated hyperpolarize neurons (Millan, 1999). Galanin, neuropeptide Y (NPY) and somatostatin are inhibitory neuropeptides that in the superficial dorsal horn are exclusively found in GABA-ergic cells (Todd and Koerber, 2013). Galanin acts at its receptors $Gal_{1\text{-}3}$ to inhibit firing of

nociceptive-specific spinal cord neurons by hyperpolarization of the primary afferent and by inhibiting the release of SP (Levine et al., 1993; Sorkin and Yaksh, 2013). NPY and its receptors $NPYR_{1-5}$ are found in lamina III of the dorsal horn where they inhibit the release of bradykinin (Niissalo et al., 2002). The role of NPYRs in the dorsal horn is to differentially decrease nociception by enhancing K^+ currents and reducing Ca^{2+} currents (Millan, 1999). Somatostatin is also a peptide hormone found in limited populations in the small cells of the DRG and small dorsal horn neurons (Sorkin and Yaksh, 2013). It acts through G protein-coupled receptors (GPCRs) SST_{1-5}, some of which inhibit the opening of VGCCs, producing long-lasting depression in response to noxious stimuli (Sorkin and Yaksh, 2013).

1.2.5. Sensitization

Sensitization is defined as "increased responsiveness of neurons to their normal input or recruitment of a response to normally subthreshold inputs" (Loeser and Treede, 2008). There are two main types of sensitization; peripheral sensitization and central sensitization.

1.2.5.1. Peripheral sensitization

The body becomes peripherally sensitized during injury where inflammation drives the sensitization of nociceptors reducing their thresholds and increasing responsiveness to normal stimuli (Loeser and Treede, 2008). Inflammation in

the periphery results in the accumulation of several molecules collectively called an 'inflammatory soup'. Some components of this include bradykinin, protons (H^+), prostaglandins (PGE_2), serotonin or 5-hydroxytryptamine (5-HT), ATP, nerve growth factor (NGF), tumor necrosis factor alpha (TNF-α) and interleukins (IL-1β, IL-6).

Activation of the nociceptors causes the damaged tissue to release adenosine, ATP and protons resulting in activation of P2X receptors and acid sensing ion channels (ASICs) as well as sensitization of TRP channels. Other inflammatory cells such as mast cells, macrophages, platelets and endothelial cells release further chemicals such as bradykinin, interleukins (IL-1β, IL-6), NGF, TNF-α, PGE_2, 5-HT and histamine which act at the peripheral nociceptors on various receptors including GPCRs, receptor tyrosine kinase (RTK) and two-pore potassium channels (K_{2P})(Woolf and Costigan, 1999; Julius and Basbaum, 2001; Ringkamp et al., 2013). Once activated these processes trigger further secondary cascades, protein kinase A and C (PKA, PKC) and these actions can be enhanced by the phosphorylation of receptors, ultimately resulting in primary hyperalgesia (Ringkamp et al., 2013). Sensitization of peripheral nociceptors in conditions such as OA is characterized by primary hyperalgesia or a sensitivity to pain and allodynia or pain in response to previous innocuous stimuli at the site of injury. It is therefore suggested that joint pain is driven by peripheral nociceptors and this is necessary for the development and maintenance of chronic pain (Schaible et al., 2002, 2009).

1.2.5.2. Central sensitization

In many clinical syndromes with pain as the main symptom, pain is no longer a protective mechanism. Ongoing nociceptor activity following peripheral sensitization causes hyperexcitability of neurons in the spinal cord resulting in a phenomena known as central sensitization where nociceptive neurons within the CNS have increased responsiveness (Schaible et al., 2002; Loeser and Treede, 2008). The excessive nociceptor input can increase membrane excitability, facilitate synaptic strength or decrease inhibitory effects in dorsal horn neurons (Latremoliere and Woolf, 2009). This increased responsiveness is initially only in the area of tissue damage (peripheral sensitization) however after excessive stimulation from inflammatory mediators in the periphery, neurons have enhanced responses to pressure applied to normal tissue (Schaible et al., 2002). Key features of these heightened pain situations are allodynia and hyperalgesia at the site of injury in the periphery, however once pain spreads beyond the site of injury this is known as secondary hyperalgesia and is a common symptom of central sensitization (Latremoliere and Woolf, 2009). This phenomenon is facilitated by abnormal inputs to nociceptive pathways such as large Aβ-fibre LTMs which now begin to mediate pain (Latremoliere and Woolf, 2009). Often in musculoskeletal pain conditions, such as OA, another key feature of RFs are also significantly enlarged when compared to pain free individuals which is indicative of secondary hyperalgesia (Biurrun Manresa et al., 2013). Therefore central sensitization is driven and

maintained by the excessive and continuous peripheral inflammatory inputs (Neugebauer et al., 1996; Schaible et al., 2002).

1.2.6. Ascending pain pathways

Projection neurons in the dorsal horn relay nociceptive inputs to the thalamus, brainstem and higher brain centres via several ascending pathways (Malfait and Schnitzer, 2013). There are three main projections which are involved in nociception; the spinothalamic tract (STT), spinobulbar projections and the spinohypothalamic tract (SHT)(Dostrovsky and Craig, 2013).

The STT is the projection pathway most closely linked to pain and temperature and these projection neurons originate in the superficial dorsal horn in lamina I, the deep dorsal horn in laminae IV – IV and the intermediate zone of laminae VII – VIII (Dostrovsky and Craig, 2013). Lamina I contains approximately half of the STT projection neurons and is selectively responsive to nociceptive and thermoreceptive modalities (Zhang and Craig, 1997; Craig et al., 2002). The main supraspinal targets for projection neurons from lamina I are the caudal ventrolateral medulla (CVLM), the nucleus of the solitary tract (NTS), the lateral parabrachial (LPb) area, the periaqueductal grey (PAG) and select nuclei of the thalamus (Todd, 2010). The remaining 50% of STT cells are split equally between laminae IV – V and laminae VII – VIII where they relay high-threshold mechanical stimuli and convergent inputs from large diameter skin and deep muscle input respectively (Dostrovsky and Craig, 2013). The densest

termination field of STT cells is in the posterior region of a dedicated nociceptive and thermoreceptive relay nucleus, the ventromedial posterior (VMpo) nucleus of the thalamus, which primarily originate from lamina I (Zhang and Craig, 1997; Dostrovsky and Craig, 2013). Projections from laminae IV – V primarily terminate in the ventral posterior (VP) nuclei and lamina VII – VIII projection neurons also project to regions of the thalamus, however it is argued how much of a role these projections play in pain perception (Craig, 2003; Dostrovsky and Craig, 2013). The VMpo and VP nuclei then project to the dorsal insular cortex and anterior cingulate cortex which are important for the sensation of pain to be established and are particularly active in chronic pain patients (Craig, 2003).

Spinobulbar projections (spinoparabrachial pathway - SPBT) to the brain stem are important for the integration of nociceptive activity such as behavioural and homeostatic mechanisms (Dostrovsky and Craig, 2013). Spinobulbar projections originate in similar laminae to the STT, especially found in lamina I, V and VII in the monkey, cat and rat (Wiberg et al., 1987). Spinobulbar projections terminate in the lateral parabrachial nucleus of which a high proportion of the neurons (50 – 70%) project to the amygdala or the hypothalamus and are specifically strongly excited by noxious stimuli (Gauriau and Bernard, 2002). These connections are therefore likely to be involved in the emotional and autonomic components of pain including stress responses and influencing fear-learning behaviour (Longstaff, 2000; Todd, 2010). The PAG also

receives significant input from spinobulbar pathways, which is a key site for motor limbic output and homeostatic control, but also due to projections to other brainstem areas such as the rostral ventromedial medulla (RVM) has an important role in antinociception and descending modulation of dorsal horn circuits (see section 1.2.7)(Basbaum and Fields, 1978; Dostrovsky and Craig, 2013; Todd, 2010).

The SHT originates from lamina I, V, VII and X over the entire length of the cord (Dado et al., 1994b). This tract has been identified in rats however is not well known or understood and has only been proposed as a general pathway in mammals with small amounts of evidence for it in primates (Chang and Ruch, 1949; Morin et al., 1951; Dostrovsky and Craig, 2013). Projections from this tract in the rat has shown a complex pathway capable of providing nociceptive input to multiple areas of the thalamus and hypothalamus bilaterally (Dado et al., 1994a). If established fully in primates this tract could have potentially important implications for the autonomic, neuroendocrine and emotional aspects of pain (Dostrovsky and Craig, 2013).

1.2.7. Descending pathways

1.2.7.1. Descending pain modulatory pathways

Regions of the brain are activated by ascending nociceptive afferent terminations and these account for the sensation of pain. However, projections

to other brain regions allow for modulation and control of pain pathways via descending pain modulatory pathways. These pathways originate from various brain regions and can be both facilitatory or inhibitory and when working together they produce a powerful anti-nociceptive system which is able to inhibit dorsal horn neurons in the spinal cord (Gjerstad et al., 2000; Ossipov et al., 2014).

1.2.7.2. Noradrenergic pathways

Noradrenaline (NA) is a catecholamine neurotransmitter along with adrenaline and dopamine, all of which can be found in both the periphery and in central nociception (Goldstein, 2010). The principal descending NA pathways originate in the locus coeruleus and the pontine sub coeruleus regions (Todd, 2010; Ossipov et al., 2014). These regions communicate with both the RVM and PAG and animal studies have shown that stimulation of all these regions releases NA into the spinal cord to produce antinociception (Ossipov et al., 2014). Projections from these NA brain regions terminate in the spinal cord dorsal horn where they release NA via volume transmission to act on spinal α2 adrenoceptors causing dose dependent antinociception in intact spinal but not spinalized animals (Pertovaara, 2006). During weak noxious stimulation, low levels of tonic release of NA causes an inconsistent increase in nociceptive withdrawal reflexes (NWRs) and a mild hypersensitivity to thermal but not mechanical stimulation, showing a weak and selective tonic pain regulatory system (Pertovaara, 2006). However, during prolonged noxious stimulation,

pain regulation via noradrenergic pathways is more prominent with nociceptive responses significantly increased in cases of α2 adrenoceptor knockouts or with the use of an antagonist (Jones, 1991; Pertovaara, 2006). Injury results in increased synthesis and release of NA and enhanced efficacy of spinal α2 adrenoceptors, on the other hand, activation of spinal α1 adrenoceptors results in pain facilitation (Ossipov et al., 2014). Whilst intact and effective, descending NA inhibitory pathways protect against the development of abnormal and enhanced pain, however an imbalance between pain facilitation and inhibition is believed to result in abnormal pain (Ossipov et al., 2014).

1.2.7.3. Serotonergic pathways

5-HT is an important molecule in processing and modulation of pain in peripheral and central mechanisms (Sommer, 2006). Early studies of 5-HT pathways were found to release 5-HT from areas of the brainstem that had an analgesic effect in the spinal cord, it was then regarded as a descending inhibitory system (Yaksh and Tyce, 1979). The RVM contains the major serotonergic nuclei including the nucleus raphe magnus (NRM), the nucleus reticularis gigantocellularis-pars alpha and the nucleus paragiganto-cellularis (NpGC) lateralis which receive input from the PAG, the RVM as well as the thalamus, the parabrachial (PB) region and the locus coeruleus which contains the noradrenergic origins (Todd, 2010; Ossipov et al., 2014). Studies have demonstrated that lesions of the NRM cause significantly greater hyperalgesia in rat pain models, measured with paw inflammation and increased withdrawal

responses to noxious heat (Vanegas and Schaible, 2004). 5-HT terminals are also involved in tonic inhibition of spinal transmission of nociceptive information (Clarke et al., 1996). 5-HT descending pathways are both facilitatory and inhibitory and terminate in the trigeminal nucleus caudalis and throughout the dorsal horn via volume transmission (Ossipov et al., 2014). The various receptor types associated with 5-HT are what determines its analgesic or hyperalgesic effects (Sommer, 2006). There are 7 different 5-HT receptors with more than 15 sub-types identified which are located in various areas of the body including smooth muscle and the gastrointestinal tract (Suzuki et al., 2004). Most notably involved in nociception are 5-HT_{1A}, 5-HT_{1B}, 5-HT_{1D}, 5-HT_{2A}, 5-HT_3 and 5-HT_4 where 5-HT_1 receptors are predominantly antinociceptive and 5-HT_{2A}, 5-HT_3 and 5-HT_4, are pronociceptive in the spinal cord dorsal horn, making 5-HT descending pathways very complex (Sommer, 2004; Bannister et al., 2009).

1.3. Diffuse noxious inhibitory controls

The integrity of descending pathways appears to be necessary for maintaining an appropriate excitability of withdrawal reflexes and for maintaining the dimensions of their RFs (Schouenborg et al., 1992). This tonic control of reflexes by propriospinal and bulbospinal descending neurons from the brain strongly control spinal reflexes, however the integrity of descending pathways can be assessed by phasic controls of the spinal reflexes whereby noxious stimuli evoke withdrawal reflexes (Le Bars et al., 1979a). One example of the latter is

that a painful stimulus applied to one area of the body can elicit analgesic properties in another area outside the RF of the first in both experimentally induced and clinical pain; this phenomenon is a form of "hyperstimulation analgesia" termed "diffuse noxious inhibitory controls" (DNIC)(Le Bars et al., 1979a). Thus, the activity of secondary convergent neurons in the spinal cord i.e. neurons that receive both innocuous and noxious inputs from hindlimb PAFs, can be greatly inhibited (to between 55 and 100%) in response to a noxious stimulus applied elsewhere on the body (Dickenson et al., 1980). This kind of hyperstimulation analgesia is the basis for the use of transcutaneous electrical nerve stimulation (TENS) as therapeutic relief for chronic pain. TENS uses pulses of electrical currents across the surface of the skin with the pulses ranging from low to high intensity depending on the level of pain relief required (Jones and Johnson, 2009). This therapy is designed to stimulate Aβ-fibres and Aδ-fibres that activate endogenous opioid supraspinal anti-nociception pathways (Longstaff, 2000).

DNIC is not confined to the spinal cord but is facilitated by an ascending and descending mechanism from supraspinal structures or a supraspinal loop (Le Bars et al., 1979b). Le Bars and colleagues found that, in the intact rat, WDR neurons responding to both noxious and innocuous test stimuli and receiving both C and Aα-fibre inputs were strongly inhibited by peripheral noxious conditioning stimuli applied to areas of the body outside the peripheral excitatory RF of the WDR neurons including the tail, the contralateral hind paw,

the forepaws, ears, muzzle and from the viscerae (Le Bars et al., 1979a). It was also noted that innocuous stimuli had no effect when applied to these areas (Le Bars et al., 1979a). As well as measuring a range of off-limb sites, Le Bars also studied a range of noxious conditioning stimuli including noxious pinch applied with forceps, an intraperitoneal (i.p.) injection of bradykinin, noxious heat and electrical stimulation (Le Bars et al., 1979a). Le Bars then postulated that in order to obtain clear inhibitory effects a certain number of peripheral nociceptors must first be recruited, as stimulating a small area was not sufficient when using noxious heat applied to the tail, however increasing the surface area inserted into the water gave strong inhibitory effects (Le Bars et al., 1979a). DNIC is specific in its action that the noxious stimuli applied to the distant locations of the body that is the weaker of the two noxious stimuli is the one that is inhibited (Le Bars et al., 1979b). This therefore demonstrates a great deal of interaction between the test and conditioning stimulus. DNIC has been found to inhibit both spontaneous and induced activity using Aα and C-fibres, with the latter being more strongly inhibited by noxious stimuli; C-fibre response is inhibited to a maximal degree of 98% and Aα-fibres to only 45% (Le Bars et al., 1979a). However, this phenomenon is limited to convergent neurons and a lack of effect is observed in non-convergent neurons including NS, innocuous and proprioceptive neurons (Le Bars et al., 1979b). NS, innocuous and proprioceptive cells in the dorsal horn were not affected by various types of noxious conditioning stimuli applied to the tail, muzzle, contralateral hindpaw or ears of rats (Le Bars et al., 1979b). Spinal sectioning of animals results in a lack of DNIC in convergent neurons when using various conditioning

stimuli on a number of locations in the rat, even when these stimuli were increased to a powerfully noxious level (Le Bars et al., 1979b).

1.3.1. Mechanisms mediating diffuse noxious inhibitory controls

Electrical stimulation of the sciatic nerve at high but not low intensities was found to increase spinal release of 5-HT and NA indicating that these descending pathways are influences by noxious stimuli (Tyce and Yaksh, 1981). There is pharmacological evidence to suggest that functioning 5-HT mechanisms are required for the full effect of DNIC as 5-HT receptor blockers, metergoline and cinanserin, strongly reduced the inhibitory effect induced by noxious heat and pinch applied to the tail and nose respectively (Chitour et al., 1982). As well as this, when the serotonin synthesis precursor 5-hydroxytryptophan (5-HTP) was administered the inhibitory effect of noxious heat to the tail was increased (Chitour et al., 1982). When animals are depleted of 5-HT using para-chlorophenylalanine (pCPA) at the level of the spinal cord, the inhibitory effects of DNIC are partially reduced indicating that serotonergic pathways are involved in DNIC but also that they are not the only mechanism involved (Dickenson et al., 1981). This reduced efficacy in DNIC was observed not only in the magnitude of the C-fibre response but also in a reduction of the RF size which would suggest peripheral interactions (Dickenson et al., 1981). Serotonergic pathways from the NRM are therefore believed to be the link between 5-HT and DNIC as electrical stimulation of the NRM produces powerful inhibition of dorsal horn convergent neurons, which mimics the effects of DNIC,

and NRM inhibition is also reduced in depleted 5-HT states suggesting DNIC and NRM-mediated inhibition share common mechanisms (Rivot et al., 1980; Dickenson et al., 1981). It can be postulated that as the majority of 5-HT originates from the NRM this brain region plays a key role in DNIC, however it cannot be ruled out that other raphé nuclei participate in DNIC (Dickenson et al., 1981). These other mechanisms that are involved in DNIC may be noradrenergic descending modulatory pathways or changes in opioid levels within the spinal cord.

When noradrenergic and opioid receptor antagonists are given with capsaicin as a conditioning stimulus, inhibitory effects of DNIC on reflex responses are abolished which indicates that blocking these two descending pathways with antagonists inhibits the inhibitory descending controls which would otherwise have reduced the response seen when only capsaicin was given (Gjerstad et al., 2000). Further investigation into blocking individual receptors indicated that when the μ-opioid receptor was blocked with an antagonist and capsaicin was also given there was a 40% increase in responses, indicating that the μ-receptor has a key role in anti-nociception (Tambeli et al., 2003). When the same tests were completed for the κ and δ-receptors there was no hyperalgesia, however the anti-nociception was to a significant lesser degree in κ-receptors than that seen with only capsaicin but not significant at all with δ-receptors, indicating that κ-receptors also play a role in descending inhibitory pathways but δ-receptors do not (Tambeli et al., 2003). Opioid facilitated analgesia is believed

to be exerted by activating the PAG which contains the 5-HT rich NRM of the RVM which project to the spinal cord. One believed mechanism of opioids is to activate the 5-HT NRM cells which triggers the release of 5-HT in the spinal cord terminals (Matos et al., 1992). Naloxone which blocks opioid actions is often given as pain relief medication and its effects upon the spinal cord are to decrease the inhibitory effects exerted by NRM stimulation, as previously mentioned there is strong evidence to suggest the NRM is linked to DNIC (Rivot et al., 1979). From these findings it can be concluded that μ-opioid receptors are key in the anti-nociceptive pathway as they block DNIC and that κ-opioid receptors partially block this modulatory pathway, which strongly supports the suggestion that tonic inhibitory controls descending from the brain are mediated by these pathways (Tambeli et al., 2003).

The α adrenoceptor antagonist phentolamine given directly onto the spinal cord whilst evoking DNIC using capsaicin produced a slight reduction in the inhibitory effects of DNIC (Gjerstad et al., 2000). Adrenergic α2 agonists administered spinally have enhanced anti-nociceptive potency and activation of the locus coeruleus, which is a key brain structure for descending noradrenergic projections, reduce pain signals at the level of the spinal cord (Pertovaara, 2013). Lesions of the locus coeruleus and sub coeruleus, which are the key nuclei for descending noradrenergic projections, results in a 30 – 40% reduction in spinal cord NA in the rat and higher in other mammals such as the cat (Jones, 1991). Lesioning of the locus coeruleus increased hyperalgesia,

therefore also showing a net loss of descending inhibition (Vanegas and Schaible, 2004). Therefore descending serotonergic and noradrenergic pathways are activated during situations requiring anti-nociception, they are mediated by opioids in the spinal cord and supraspinal structures and these systems must be activated collectively in order for there to be anti-nociception as when only one pathway antagonist was given the anti-nociceptive pathway was not fully activated (Gjerstad et al., 2000).

The subnucleus reticularis dorsalis (SRD) has been implicated as a potential site of action for DNIC. The SRD, also known as the dorsal reticular (DRt) nucleus, is located in the medullary reticular formation (MRF) below the cuneate nucleus and between the spinal trigeminal nucleus and the NTS and contains neurons that respond selectively to and encode noxious stimuli (Bernard et al., 1990; Villanueva et al., 1996; Velo et al., 2013). Neurons in this region can be activated exclusively by noxious thermal, mechanical or chemical stimuli and are involved in pain processing and motor reactions during noxious events (Villanueva et al., 1988; Bernard et al., 1990). They have properties that make them comparable with their involvement in DNIC, as they were preferentially activated by noxious stimuli applied to any part of the body (Bouhassira et al., 1992b). Reduction in DNIC was observed in rats with unilateral SRD lesions which concurred with ideas that the SRD participates in spino-bulbo-spinal loops (Bouhassira et al., 1992b; Patel and Dickenson, 2019). However only partial blocking of DNIC inhibition occurred in these lesions which led the investigators to believe that

bilateral SRD lesions would result in complete abolishment of DNIC inhibition; these studies were not possible to perform as bilaterally operated animals do not maintain a good physiological health state for experiments (Bouhassira et al., 1992b). Bouharissa investigated other brain structures that may be involved in DNIC, suggesting that many mesencephalic structures including the PAG, cuneiformis nucleus (CNF) and the PB nucleus may all be involved in DNIC (Bouhassira et al., 1990). However much to their surprise the study concluded that the PAG, CNF and PB did not participate directly in the inhibitions observed in DNIC and that other candidates included the NRM, the locus coeruleus, although, currently, the SRD is the only supraspinal structure to contain neurons that are responsible for DNIC (Bouhassira et al., 1990).

1.3.2. Diffuse noxious inhibitory controls and chronic pain

In human studies DNIC is usually referred to as “conditioned pain modulation” (CPM), a term introduced in attempt to encapsulate all the pain modulation terms and to include the psychophysical paradigms (Yarnitsky, 2010; Yarnitsky et al., 2010), however DNIC tends to still be used for animal experimental studies therefore for the purposes of this thesis DNIC will be used throughout.

DNIC has been studied in many chronic pain conditions and overwhelmingly the results show that individuals with chronic pain demonstrate compromised DNIC (van Wijk and Veldhuijzen, 2010). Many spinal cord neurons with joint input are tonically inhibited by descending inhibitory systems (Cervero et al., 1991).

However continued input from the periphery leads to central sensitization, which in turn can alter these descending inhibitory pathways resulting in the maintenance of chronic pain (Danziger et al., 1999). Human DNIC studies have demonstrated that DNIC is not only compromised in individuals with OA (Kosek and Ordeberg, 2000) but also in many other chronic pain conditions (Peters et al., 1992; Kosek and Hansson, 1997; Bragdon et al., 2002; Pielsticker et al., 2005; Song et al., 2006).

1.3.3. Factors affecting diffuse noxious inhibitory controls

DNIC efficacy varies greatly between individuals and personal factors that may have an influence on this fluctuation have been largely unexplored. However, some studies have been conducted looking at the effect of various personal factors such as emotional state, age and gender on the efficacy of DNIC in healthy individuals.

Gender has been investigated most frequently in DNIC efficacy studies and although there are many studies investigating sex differences in DNIC there are variable conclusions. Approximately half of the studies do not indicate any effect of sex on the efficacy of DNIC (Baad-Hansen et al., 2005; Ge et al., 2005; Arendt-Nielsen et al., 2008). Studies that indicated a difference between males and females all showed that males have more efficacious DNIC than females (Staud et al., 2003; Ge et al., 2004; Granot et al., 2008; Weissman-Fogel et al., 2008; Goodin et al., 2009) except one study which showed the opposite

(Treister et al., 2010), where the experimenters concluded that their results were inconsistent and needed further support. The studies that determined men had greater DNIC effects than women indicated that both sexes showed a DNIC response, but women showed it to a lesser degree. This may be in part explained by experimental differences in that the conditioning and test stimulus varied greatly between these experiments and therefore a direct comparison is not possible. Also most of these experiments did not control for menstrual cycle or contraceptive use in women which can alter the hormone levels and effect pain processing (Berkley, 1997). As well as this, psychological factors may play a role in the difference between males and females DNIC efficacy as one study's regression model found that gender no longer predicted pain modulation when the subjects were controlled for catastrophizing (Weissman-Fogel et al., 2008). These studies showed variable results indicating that in some cases gender may influence DNIC and that females have compromised DNIC in comparison to males. This conclusion would in part explain why women have higher incidence of clinical pain syndromes than males, however more investigation is required before a firm conclusion is reached.

Aging adults have been found to have inferior DNIC when compared to young adults and middle-aged or older people sometimes don't have DNIC at all (Washington et al., 2000; Edwards et al., 2003; Larivière et al., 2007; Riley et al., 2010; Grashorn et al., 2013; Riley et al., 2014). Most studies looked only at

young and old adults and compared the differences in DNIC, however one study investigated young, middle-aged and elderly healthy individuals which showed that DNIC efficacy was negatively correlated with age and that changes in pain perception and pain modulation occurred at a much earlier age than previously predicted (Larivière et al., 2007). This study contradicts with the results of other studies that showed middle-aged individuals do not have any significant differences in their DNIC to older adults (Grashorn et al., 2013; Riley et al., 2014). From these studies, it can be concluded that younger adults have better DNIC than older adults, however it is still uncertain at what age this shift in pain modulation occurs. Chronic pain is more prevalent in older populations and reduced efficacy of DNIC may partly explain why pain in these individuals is more common than in young adults.

Ethnic differences have an impact on both clinical and experimental pain studies and have continuously demonstrated that African-Americans are more sensitive to experimental pain and report higher levels of clinical pain than other ethnic groups (Edwards et al., 2001). Few studies have directly investigated the effect of different ethnicities on the efficacy of DNIC, however those that have found that some ethnic differences do appear. One study suggests that African-Americans experience reduced DNIC when compared to non-Hispanic whites which may indicate why these individuals have greater clinical pain (Campbell et al., 2008). However other studies reported no differences in the DNIC effect amongst different ethnic groups, therefore more

investigation is required before a full conclusion can be drawn (Goodin et al., 2013; Riley et al., 2014).

A continuous vicious cycle occurs between sleep and pain. Whilst pain disturbs and disrupts sleep it is also believed that poor sleep has a negative impact on pain (Smith and Haythornthwaite, 2004; Lautenbacher et al., 2006). Two studies have both investigated DNIC functionality and its relationship to sleep and both concluded that disrupted sleep may contribute to impaired DNIC function (Smith et al., 2007; Goodin et al., 2009). Edwards et al. (2009) found that patients with chronic pain associated with temporomandibular joint disorder (TMD) had reduced DNIC when they also suffered from insomnia (reduced sleep efficiency or total sleep time). Similarly, Smith et al. concluded that healthy female subjects who had partial sleep deprivation had significant reductions in DNIC and higher incidence of spontaneous pain. As no study has currently investigated the effect of improved sleep on DNIC, only tentative conclusions can be drawn that sleep disturbance has a negative impact on DNIC (Edwards et al., 2009).

Physical activity and pain are closely linked in that, especially for chronic musculoskeletal conditions such as OA, osteoporosis and low back pain, moderate physical activity can improve pain (Vuori, 2001). Very little research has been conducted into the effect of physical activity on DNIC, however one study showed that healthy individuals who self-report greater levels of activity,

both more demanding exercise and increased total exercise, had improved descending pain modulation (Naugle and Riley, 2014). This may be the reason that exercise is so beneficial to individuals with chronic pain.

1.3.4. Relationship between the test and conditioning stimulus

Few studies have directly investigated the link between the test and conditioning stimulus in relation to DNIC. However studies investigating DNIC have recognised that these two are interlinked (Le Bars et al., 1979a; Arendt-Nielsen et al., 2008; Pud et al., 2009). Le Bars first outlined that inhibition can be evoked in animals via DNIC when the conditioning stimulus is greater than that of the test stimulus (Le Bars et al., 1979a). Le Bars also investigated various combinations of noxious stimuli for the test and conditioning stimulus with conditioning stimuli such as noxious pinch and radiant heat, electrical stimulation with various test stimuli such as pinch to the tail, muzzle and ears, heat to the tail, electrical stimulation and bradykinin. The results of these experiments showed that all combinations evoked DNIC, however the most potent was electrical stimulation with noxious heat and bradykinin combined with hot water (Le Bars et al., 1979a). Other studies have likewise tried various combinations such as only electrical stimulation for the test stimulus combined with mechanical pressure, thermal heat or electrical stimulation for the conditioning stimulus and again all three evoked DNIC to differing degrees indicating that the interactions between the test and conditioning stimulus and also that different conditioning stimuli have varying effects on the degree of

DNIC (Danziger et al., 2001). More research has been conducted investigating the different conditioning stimuli and how this affects the degree of DNIC evoked. Dickenson demonstrated that electrical test stimulus combined with bradykinin as the conditioning stimulus resulted in 89% inhibition, however when sustained pinch was combined with bradykinin, heat or pinch as the conditioning stimulus a maximal inhibition of 60% was observed (Dickenson et al., 1980). This demonstrates that certain test and conditioning stimulus combinations have a greater inhibitory effect than others.

1.4. Spinal reflexes

1.4.1. Nociceptive withdrawal reflexes

An NWR is many polysynaptic motor responses to noxious or potentially noxious stimulation. Within a NWR are cutaneomuscular responses to noxious stimuli that involve multiple interneuronal pathways to individual muscles which enables differential control of these muscles to most effectively move the limb from the source of pain (Clarke and Harris, 2004). This process occurs entirely within the spinal cord and this is evidenced by experiments involving complete transection of the spinal cord which still have functional NWRs (Shahani and Young, 1971). To effectively move the limb away from the noxious stimulus the nociceptive PAF which enters the dorsal horn is excited when the threshold level is reached (Figure 1.2). As previously mentioned (see section 1.2.3), the primary afferent nociceptor synapses in the dorsal horn onto various excitatory interneurons (Malfait and Schnitzer, 2013). These interneurons

branch widely with their axons often stretching over several laminae of the dorsal horn or both the dorsal and ventral horn (Jankowska and Lundberg, 1981). The majority of these interneurons appear to be local, synapsing onto various other secondary interneurons within the spinal cord, however others synapse onto ascending projection tracts (Jankowska and Lundberg, 1981). The location and properties of these interneurons is not yet fully established, however it is known that laminae II neurons project to the deeper laminae and therefore could be the source of the secondary interneurons (Schouenborg, 2002). In an NWR, excitatory interneurons synapse onto an effector motoneuron resulting in contraction of the muscle to move the affected limb away from the noxious stimulus (Burke, 1999).

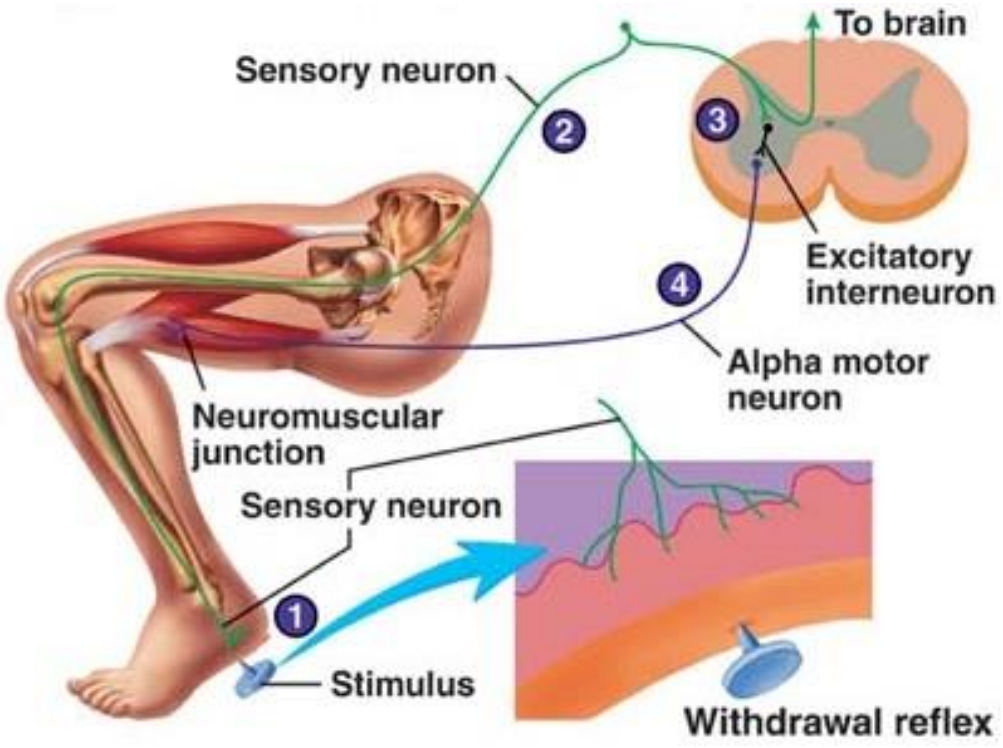

Figure 1.2. Nociceptive withdrawal reflex (NWR) arc (The McGraw-Hill Companies, 2018).

1.4.2. Organisation of reflexes

The initial outline of the organization of withdrawal reflexes was put forward by Sherrington in the late 1800s who studied NWRs in decerebrate cats. He proposed that movement of the hindlimb away from a noxious stimulus was due to activation of flexor muscles of the hip, knee and ankle joints (Sherrington, 1910). He also proposed concomitant inhibition of extensor muscles, hence termed the response the "flexion-reflex of the limb" (Sherrington, 1910). Simultaneous inhibition or relaxation in the antagonistic extensor muscles was termed "reciprocal innervation" (Sherrington, 1898). Sherrington also postulated the "crossed extension reflex" whereby the effect of the noxious input in one limb causes excitation of extensors and inhibition of flexors in the contralateral limb, which serves to maintain balance in the animal (Sherrington, 1906, 1910).

Further research in the flexion reflex realised that if a noxious stimulus was applied to the heel, flexion about the ankle joint would cause the area more damage by moving it towards the stimulus and therefore extension of the ankle was the more appropriate action. This brought about the idea that movement during withdrawal was dependent on the location of the noxious stimulus, and that whilst the main movement may be flexion, there are also local extension reflexes to protect the limb (Hagbarth, 1960; Megirian, 1962). It was therefore proposed that describing NWRs as generally flexion reflexes was inappropriate and they should instead be considered as being modular, whereby reflex

pathways are present in separate muscles or groups of synergistic muscles and the overall withdrawal movement is the result of activation (or inhibition) of these 'modules' (Schouenborg et al., 1994). In this capacity a withdrawal movement would then be facilitated by a number of reflex modules working together or reflex modules would be inhibited in the antagonistic muscles to allow controlled movement (Schouenborg et al., 1994; Schouenborg, 2002).

In modular organisation of reflexes, propriospinal neurons within the CNS could serve to modulate NWRs, via descending controls, as the number of combinations of reflex pathways would be very large and higher thresholds would allow for reactions only in the noxious range (Schouenborg et al., 1994).

1.4.3. Reflex receptive fields

The RF of a reflex was first defined as the "whole area of skin from where the reflex can be elicited" (Sherrington, 1906). This definition provides a simplistic version of the RF as only increased stimulus intensities evoked reflex responses towards the periphery of the RF indicating graded sensitivity (Andersen, 2007). Therefore an innocuous stimulus applied to a given area of skin will excite all neurons with their RF centres in this location, however a noxious stimulus applied to the same place will activate these same neurons as well as other that have edges of their RFs in this location (Le Bars, 2002).

Cutaneous muscle RF patterns are learnt after birth as NWR modules are functionally unadapted at birth, often causing movements towards the noxious stimulus (Schouenborg, 2002; Clarke and Harris, 2004). Spatial organization of RFs is relatively independent to excitability whereby changes in excitability only affect the size of the RF and not the location (Schouenborg et al., 1992; Weng and Schouenborg, 1996). By mapping the RF borders and sensitivity distribution of hindlimb muscles, Schouenborg discovered that each muscle has an individual RF with a characteristic sensitivity distribution and can be activated independently of other muscle modules (Schouenborg, 2002). Proximal muscles tend to have large RFs whilst distally located muscles have smaller RFs (Andersen, 2007). The excitatory RF for a muscle is closely linked to the part of the limb that would be withdrawn from the ground when the muscle is made to contract and the opposite is also true that the inhibitory RF would move the area towards the noxious stimulus (Clarke and Harris, 2004).

1.5. Osteoarthritis and chronic pain

1.5.1. Burden of osteoarthritis to the patient

The impact and burden of OA on daily life differs from individual to individual, however more commonly sufferers find morning stiffness, instability of the joint and pain that worsens with activity and decreases during periods of rest (Swagerty and Hellinger, 2001). This pain is often the most debilitating symptom of the disease and increases during weight bearing and limits activities such as walking, carrying objects or dressing (Swagerty and Hellinger,

2001; Palazzo et al., 2016). Hip and knee OA have the greatest burden, often leading to significant disability and surgical intervention is usually required due to pain (Oliveria et al., 1995). In the UK ranking for leading causes of Years Lived with Disability (YLDs) OA ranked 11th in both 1990 and 2010 (Murray et al., 2013; Cross et al., 2014). Disability of Adjusted Life Year (DALY) is a measure of years of potential life lost due to premature mortality and the years of productive life lost due to disability for a given condition. The DALY for OA has increased by 6.4% between 1990 and 2010 in the UK indicating the ever-increasing burden that OA has on the lives of sufferers (Murray et al., 2013).

As well as the physical disability of OA there is also a great deal of psychological burden that OA places on people's lives. Often the extent of functional disability is an important factor in psychological distress (Penninx et al., 1996). Inability to perform everyday tasks leads people to feel devalued in their self-worth and the constant pain causes a great deal of distress. One study found that the psychological distress is most frequently experienced by patients with OA over diabetic, cardiac or stroke patients (Penninx et al., 1996; Hopman et al., 2009). This negative effect on mental health associated with disability and pain in OA is well established with worse baseline mental health positively correlated with worse knee OA pain indicating that mental health is worsened by the condition (van Baar et al., 1998; Wise et al., 2010). However, mental health can also have adverse effects on OA with one study showing that risk of pain flare is increased by worsened mental health in the week prior to the flare and another showing

treatment of depression can significantly improve pain (Lin et al., 2003; Wise et al., 2010).

OA can often lead to reduction and/or prevention of social interactions with family, friends and partners as well as effecting an individual's working life (Arthritis Research UK, 2013). Sufferers often find themselves having more time off sick or being unable to work at all, having a huge impact on the person's life (Arthritis Research UK, 2013). Patients with severe OA are shown to have an average of 2 and a half 8 hour days off sick in a 2-week period, which is 5 times greater than a healthy individual (Lerner et al., 2002). Employees with OA that are present at work may experience reduced productivity caused by functional limitations of their condition (Meerding et al., 2005). OA employees lose an average of 9% per hour in productivity while the average healthy control is less than 1% (Lerner et al., 2002).

1.5.2. Burden of osteoarthritis to the health services

The total economic cost of OA in the UK has not been studied however a 1997 study indicated the cost of musculoskeletal disorders, of which OA is the most common, totalled 1.1% of the Gross National Product (GNP) of the UK (March and Bachmeier, 1997). Of all the musculoskeletal conditions OA is responsible for the most inpatient Finished Consultant Episodes (FCEs), which are the episodes of admitted patient care with one consultant in a year, at 209,382 instances, most of which are related to orthopaedic surgery (Parsons et al.,

2011). Treatment and management of OA incur significant costs both directly, such as due to medication, hospitalization, ambulatory care or physiotherapy, and indirectly, such as home care or child care costs (March and Bachmeier, 1997; Bitton, 2009). Pain medication accounts for 15% of annual drug costs with nearly 50% of these medications being non-steroidal anti-inflammatory drugs (NSAIDs) which have significant side effects including increased chance of gastric ulcers (Gabriel et al., 1991; March and Bachmeier, 1997; Bitton, 2009). In 2015, 98,951 patients underwent total knee replacement (TKR) surgery and 89,288 patients received a hip replacement of which 98% and 90% were due to OA respectively (National Joint Registry, 2016). In 2015-2016 the average cost of knee and hip procedures on the NHS were £6,253 and £7,089 respectively (Department of Health, 2016). TKR and hip replacements are end stage treatments for OA and for the most part are successful in treating the joint degeneration. Hip and knee replacements in general will last for 10-20 years in 90% of patients, however as people who are developing OA are getting younger, joint replacements revision surgery is becoming more common where the joint replacement is changed (Labek et al., 2011). Revision surgeries are more complex and have higher risks on post-surgery complications leading to greater expense for the NHS (Labek et al., 2011).

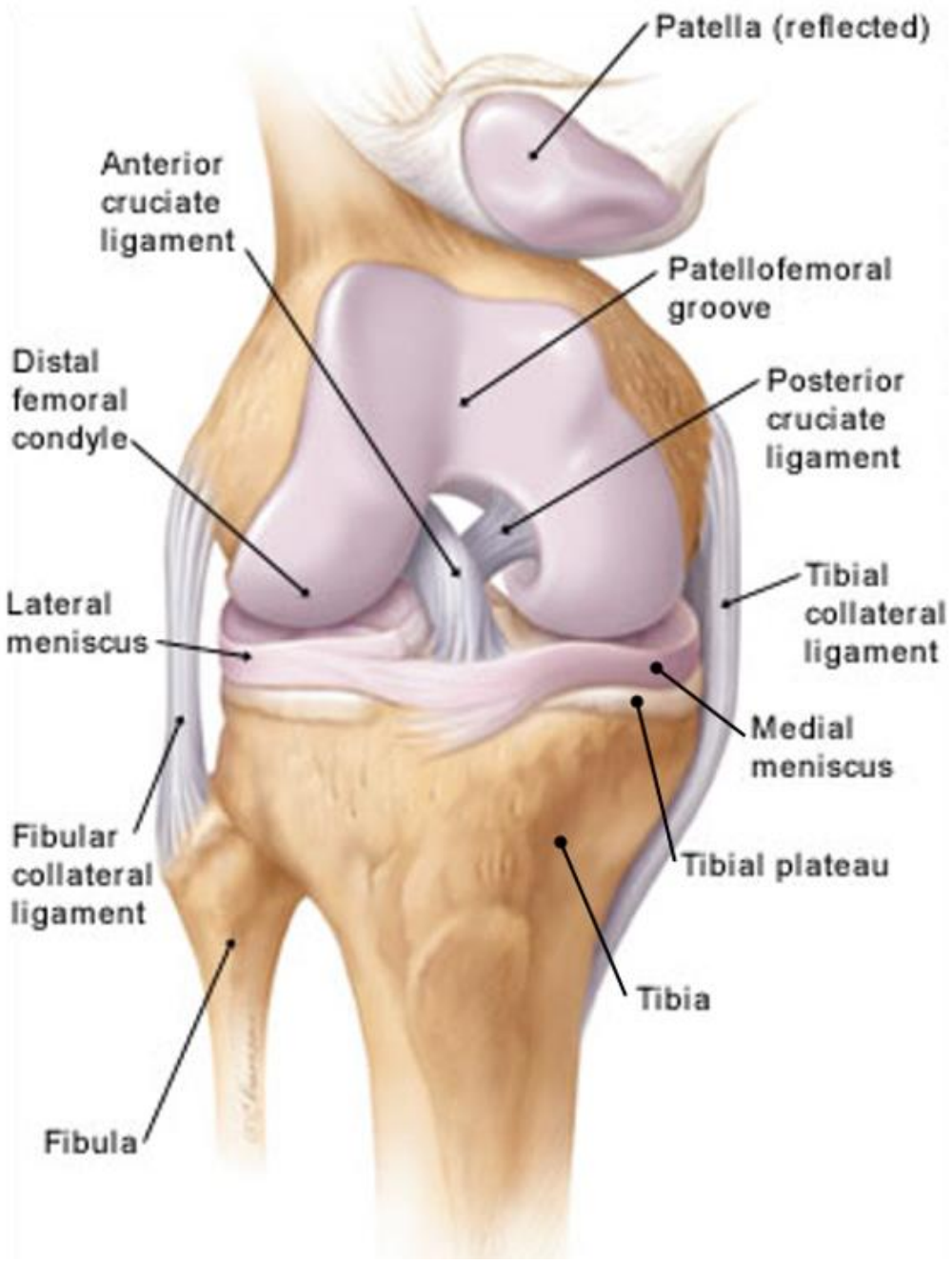

Figure 1.3. Anatomy of the knee joint (Mendez, 2017).

1.5.3. Risk factors

Increased risk of OA is associated with age with 33% of people aged 45 and over having consulted a doctor for their condition, rising to almost half in people over 75 (Arthritis Research UK, 2013). The mechanism leading to joint damage in older individuals is poorly understood, however it is believed to be due to a number of factors including thinning of the cartilage, muscle weakness, oxidative damage and a reduction in proprioception (Litwic et al., 2013). It is also thought that as basic cellular mechanisms that maintain tissue homeostasis decrease with age, older joints inadequately respond to stress or joint injury which causes tissue loss and destruction (Litwic et al., 2013).

OA is positively correlated with a rising body mass index (BMI) making it one of the strongest factors associated with the disease (Litwic et al., 2013; Wluka et al., 2013; Kearns et al., 2014). It has been estimated that 24.6% of new OA cases are related to the patient being obese (Silverwood et al., 2015). In 2015, individuals who underwent hip and knee replacements were found to have average BMI of 28.7 and 30.9 respectively indicating that they were in the overweight and obese classifications of the BMI (National Joint Registry, 2016). Obese patients have increased risk of bilateral OA especially in the case of knee OA but also for hip OA (Cimmino and Parodi, 2004). The mechanisms for links between OA and obesity occur in 2 ways; the first is increased dynamic stress on the joint due to the excess weight (Cimmino and Parodi, 2004). Increased weight adds to joint stress as obese individuals have higher bone mass which

may increase stiffness in the subchondral bone and facilitate cartilage breakdown (Cimmino and Parodi, 2004). Weight distribution may also play a key role in the type of OA observed as weight carried around the waist has to be supported by the knee and hip joints whilst weight carried on the thighs or hip is supported primarily by the knees (Stürmer et al., 2000). The second way is that it may not just be the biomechanical aspects of obesity that gives rise to increased risk of OA. Systemic metabolic and inflammatory factors may also influence OA with a possible link to insulin-like growth factor (Cimmino and Parodi, 2004). One indicator for this is that not just hip and knee OA are associated with obesity, correlations are also found with hand OA which would suggest other routes than just load-bearing joints (Palazzo et al., 2016).

OA is more commonly found in women over men with women accounting for 60% of hip and knee replacement operations (National Joint Registry, 2016). Female knee joints have been found to have various anatomical differences; narrower femurs, a thinner patella, tibial condylar size and a larger quadriceps angle, which have led to the implementation of gender-specific TKRs (Merchant et al., 2008; Hame and Alexander, 2013). Despite these anatomical differences between the male and female knee joint no direct link has been found between this and increased risk of OA in women (Hame and Alexander, 2013). However, women also have differences in the volume of cartilage which may play a key role in their increased risk of developing OA (Hame and Alexander, 2013). One particular study examined 169 women and 102 men with no clinical history of

knee pain using magnetic resonance imaging (MRI) to investigate the cartilage volume and defects (Hanna et al., 2009). After the second MRI 2.3 years later they found that the average annual percentage loss of tibial and patella cartilage volume was significantly greater in women and that women had a greater number of tibiofemoral cartilage defects when compared to men (Hanna et al., 2009). These findings may indicate a contributing factor to the increased knee OA found in women. Hormonal differences in females may also be key to developing OA as postmenopausal women in particular have increased risk of developing arthritis (Hame and Alexander, 2013). Post-menopausal women are more prone to OA due to the reduced levels of oestrogen and oestrogen replacement therapy has protective effects in post-menopausal women (Nevitt et al., 1996; Richmond et al., 2000; Hame and Alexander, 2013). This may be caused by oestrogen modulating the synthesis of the cartilage matrix and production of matrix and this is supported by the presence of oestrogen receptors in articular cartilage (Nevitt et al., 1996; Richmond et al., 2000; Hame and Alexander, 2013). It has also been found that women who take oestrogen replacement therapy post menopause have reduced chances of developing radiographic evidence of knee arthritis (Zhang et al., 1998). This shows that oestrogen may have a protective role on cartilage as this decrease was positively correlated with the duration that the women had been taking the therapy (Zhang et al., 1998).

A traumatic joint injury or surgery is a key risk factor for OA especially for the development of knee OA (Arthritis Research UK, 2013; Litwic et al., 2013). These injuries can occur in any joint from sports injuries in knee joints to dislocations in a finger joint (Arthritis Research UK, 2013). Trauma to any area of the joint that compromises the structural integrity are implicated in the development of OA (Gelber et al., 2000). Injury to a particular joint changes the biomechanics within the joint and this change can lead to secondary OA, especially if the individual has OA present in another joint (Cimmino and Parodi, 2004; Litwic et al., 2013). The knee joint is one of the most commonly injured joints, with anterior cruciate ligament (ACL) injuries showing the closest links to the development of OA (Øiestad et al., 2009; Palazzo et al., 2016). In ACL injuries, 13% of cases develop early-onset knee OA after 10 years of the initial injury, whilst ACL injuries associated with meniscal injury have an increased risk of developing OA of up to 40% within the same time period post-injury (Øiestad et al., 2009).

Certain types of OA have a genetic component making family members more at risk from developing OA in later life (Arthritis Research UK, 2013). It is thought that genetic factors account for 60% hip and hand and 40% knee OA (Spector and MacGregor, 2004). There are many genes that are potentially involved in disease onset with the most likely candidate involving the production and maintenance of collagen, such as collagen type II which is the most abundant protein of the cartilage extracellular matrix (ECM)(Cimmino and

Parodi, 2004; Palazzo et al., 2016). Other contender genes could be those encoding the vitamin D receptor which is located close to the collagen type II gene, such as insulin-like growth factor I, cartilage oligomeric protein and the human leukocyte antigen (HLA) region (Cimmino and Parodi, 2004; Spector and MacGregor, 2004; Palazzo et al., 2016). As well as gene mutations that directly affect the site of OA there may be genetic changes that could indirectly influence the risk of OA for example the response to injury, effects on body weight and muscle mass as well as bone structure and turnover (Spector and MacGregor, 2004).

It is widely acknowledged that physically demanding occupations, that require repetitive and excessive joint loading, can increase the risk of OA in some joints (Arthritis Research UK, 2013; Litwic et al., 2013). Occupations that involve squatting and kneeling were found to increase risk of knee OA whilst lifting and prolonged standing is associated with hip OA (Cimmino and Parodi, 2004; Muraki et al., 2009; Palazzo et al., 2016). Particularly dexterous professions are linked to hand OA as well as certain repetitive movements such as a pincer action or winding (Hadler et al., 1978; Muraki et al., 2009; Palazzo et al., 2016).

1.5.4. Structure of the knee joint: normal versus osteoarthritic

OA is a disease affecting the whole joint, including bone, synovium, cartilage and capsule (Dieppe, 2005). Normal knee joints allow the bones to move freely but within controlled limits which are regulated by the tendons and ligaments

surrounding the joint (Arthritis Research UK, 2012). The bones in the joint are coated in a smooth layer of cartilage that allows the joint to move effortlessly against one another and menisci within the joint act as “shock absorbers” to spread the load over the joint more evenly (Arthritis Research UK, 2012)(Figure 1.3). This section will look at each component of the normal knee joint and discuss the changes during mild to severe OA.

1.5.4.1. Cartilage

Articular cartilage is a specialised tissue that is on average approximately 3-4 mm thick and allows almost frictionless movement across its surface (Brody, 2015). In a healthy state, articular cartilage has the capacity to withstand a lifetime of loading forces, despite its limited ability to repair once damaged which is attributed to its lack of nerves, blood vessels and lymphatics (Fox et al., 2009; Brody, 2015). Articular cartilage comprises of two main parts; cells called chondrocytes which account for approximately 1 – 5% of articular cartilage weight and the ECM which predominantly comprises of water, collagens and proteoglycans but also has small amounts of lipids, phospholipids, non-collagenous proteins and glycoproteins (Bhosale and Richardson, 2008; Fox et al., 2009).

Articular cartilage encompasses four different zones based on the shape and orientation of chondrocytes and the distribution of collagen fibres within the ECM (Brody, 2015). These four zones are the superficial, middle or transitional,

deep and calcified zones representing approximately 15%, 50%, 30% and 5% of the total cartilage thickness respectively (Fox et al., 2009).

As we age articular cartilage changes occur due to continuous wear on the joint; the most obvious structural change to articular cartilage is increased articular surface fibrillation which is abrasions on the surface, which can be characterised by microscopic cracks (Meachim et al., 1977; Pritzker et al., 2006). Chondrocytes, which are cells within the ECM, decrease in density with increasing age which reduces the synthesis of collagen fibres and so alters the structure of the matrix (Brody, 2015). As well as this, chondrocyte function is also reduced during aging as the capacity of the cells to synthesise some types of proteoglycans and their response to stimuli including growth factors decreases (Guerne et al., 1995; Buckwalter and Mankin, 1997). These changes in chondrocyte numbers and function may limit the cells ability to restore and maintain the ECM and therefore contribute to cartilage degeneration (Buckwalter and Mankin, 1997). Other striking changes in the ECM are differences to the proteolytic proteins aggrecans as these macromolecules are synthesised much smaller than they are in younger joints (Thonar et al., 1986). These changes may be due to degradation of the proteoglycans in the ECM or decreased synthesis of proteoglycans (Martin and Buckwalter, 2002). Structural changes also occur within the ECM as changes in the proteins results in the cross-linking of collagens being altered and changes to the osmolarity of the ECM (DeGroot et al., 1999; Verzijl et al., 2000). The overall effects of all these

changes are a decreased water concentration and changes in the tensile stiffness and strength which may make cartilage vulnerable to injury and repair of damaged cartilage slower (Kempson, 1982; Martin and Buckwalter, 2002).

In an OA joint, continuous wear causes damage to the smooth cartilage layer which over time degrades and becomes rough (Swagerty and Hellinger, 2001; Felson, 2006; Arthritis Research UK, 2012). Cartilage damage is one of the main features of the disease and the attempted repair of articular cartilage leads to many of the key clinical symptoms of OA (Buckwalter and Martin, 2006). OA involves the progressive loss of articular cartilage and most commonly occurs in the absence of a known cause which is known as idiopathic or primary OA (Buckwalter and Mankin, 1998). Less frequently OA can develop as a result of joint damage, injuries or infections such as an intra-articular fracture causing damage to the articular cartilage or due to a variety of disorders such as haemophilia which can cause joint haemorrhages; this type of OA is called secondary OA (Buckwalter and Mankin, 1998). Idiopathic OA rarely occurs in people younger than 40 years old, whilst secondary OA can occur in younger individuals (Buckwalter and Martin, 2006). The earliest sign of OA in cartilage is increased water content or oedema in the ECM of all the cartilage zones, however most prominently the pattern of water content is altered, where water is now seen in its highest volumes in the middle or transitional zone whilst in normal cartilage the higher volumes are observed in the superficial zone (Venn and Maroudas, 1977; Calvo et al., 2004). Water content in the

cartilage increases to over 90% during OA which is associated with the loss of negatively charged glycosaminoglycans (GAGs)(Roberts et al., 1986; Guilak et al., 1994; Bhosale and Richardson, 2008). This leads to reduced elasticity of the cartilage and so a reduction in load-bearing capability of the articular cartilage, disruption of the superficial zone alters mechanical properties thus contributing to the development of OA (Bhosale and Richardson, 2008). Early changes in OA cartilage are most apparent at the joint surface where mechanical forces such as shear stress are at their largest (Andriacchi et al., 2004). Early changes in OA can often lead to abnormal motion in the joint which causes a shift in the location of cartilage contact to an area of the joint that is not accustomed to high load-bearing (Andriacchi et al., 2004). This shift in motion of the joint may be caused by a traumatic injury or by a chronic problem in the joint, however it initiates changes in the superficial zone of articular cartilage (Andriacchi et al., 2004). Chondrocytes in normal cartilage are normally reasonably dormant cells, however in OA they become “activated” and this initiates cell proliferation, cluster formation, and increased production of both matrix proteins and matrix-degrading enzymes (Goldring and Marcu, 2009). In early OA, clusters of two to six cells are found along the eroding articular surface, in later stages clusters grow to include up to eight cells or in some cases up to ten cells in one cluster (McGlashan et al., 2008). Disruption of chondrocyte activity may be viewed as an injury response which leads to chondrocytes returning to their developmental programming, causing matrix remodelling and inappropriate hypertrophy-like maturation as well as cartilage calcification (Goldring and Marcu, 2009). These over-active chondrocytes

produce a number of cytokines, which stimulate the production of proteinases, down-regulate aggrecan production and cease synthesis of proteoglycans (Loeser et al., 2012; Roughley and Mort, 2014). Loss of aggrecans and proteoglycans from the ECM subsequently results in the production of collagenases, and a lack of proteoglycans to cover the collagen fibres leaves them vulnerable for degradation, which has been demonstrated in a knockout mouse study (Glasson et al., 2005). This degradation of the collagen fibres within the ECM disrupts the structure of the ECM and initiates fibrillation or microscopic cracks in the superficial zone and erosion of the articular surface (Roughley and Mort, 2014). These cracks eventually develop into deep fissures that extend into the middle and deep cartilage zones, and branch out horizontally across these zones (Pritzker et al., 2006). In late-stage OA, the fissures that develop and expand vertically through the articular cartilage create gaps for angiogenesis or development of new blood vessels down these channels making the normally avascular cartilage a vascular tissue (Walsh et al., 2007). This may be due to pro-angiogenic factors being released from chondrocytes in the deep zone which occurs in hypertrophic chondrocytes, however these vascular channels penetrate the tidemark, a separation line between the deep and calcified zones, and are accompanied by neural components that may play a role in joint pain in later stages of OA (Imhof et al., 2000; Walsh et al., 2007; Goldring and Goldring, 2016). The reintroduction of minerals into this area due to vascularisation of the cartilage results in the calcified zone expanding at the osteochondral junction or the point separating cartilage and bone into the articular cartilage (Imhof et al., 2000; Pritzker et al.,

2006; Loeser et al., 2012). The tidemark also becomes duplicated due to the penetration of vascular tissue into the calcified zone and so this widens the tidemark (Loeser et al., 2012). Vascularisation of the cartilage also results in fragmentation of the ECM, further loss of the matrix structure and introduction of other cytokines, this is believed to be a primary cause of chondrocyte apoptosis or cell death (Pritzker et al., 2006; Loeser et al., 2012; Hwang and Kim, 2015). With the loss of the chondrocytes, no further structural or functional tissues can be synthesised resulting in complete delamination of the articular cartilage whereby all zones are lost down to the calcified zone and widened tidemark (Goldring and Goldring, 2016).

1.5.4.2. Subchondral bone

Beneath the articular cartilage there is a structure known as the cement line and below this is the subchondral bone plate and all of these five components make up the osteochondral junction (Suri and Walsh, 2012). The cement line is a thin line between the calcified cartilage and subchondral bone which is approximately 1 – 5 µm wide (Burr et al., 1988). It is a zone of increased calcification between calcified cartilage and bone (Pritzker et al., 2006). The morphology of the cement line would suggest that it has mechanical role with the surrounding bone matrix in that it is a ductile structure that would allow relatively easy crack initiation within the bone structure, however it would prevent or slow any significant expansion of this crack therefore allowing time for repair of the bone structure (Burr et al., 1988). Beneath this thin cement

line is the subchondral bone, which is a layer of compact bone directly beneath the articular cartilage that is a transition between the articular cartilage and the rigid skeleton (Suri and Walsh, 2012; Goldring and Goldring, 2016). The subchondral bone can be split into three sections; the subchondral bone plate, the subchondral trabecular bone and the bone at the joint margins (Goldring and Goldring, 2010). The subchondral bone plate, sometimes called the cortical endplate, consists of cortical or compact bone which is relatively nonporous and poorly vascularised (Goldring and Goldring, 2010). Calcified cartilage is interlinked with the subchondral bone plate in an irregular fashion which allows for transformation of shear forces during traction and compression (Imhof et al., 1999). Subchondral trabecular bone is a delicate bone consisting of fine straight or curved rods which form together a meshwork often described as looking like a sponge (Singh, 1978). This subchondral trabecular bone is polar opposite to the subchondral bone plate in that it is vastly vascularised with a high number of arterial and venous vessels as well as nerves which have small branches that extend into the calcified cartilage zone (Imhof et al., 1999). These vessels invade the subchondral bone plate to form direct contact passageways which allow opportunities for molecular trafficking and the transmission of physical forces (Lyons et al., 2006). Therefore the key function of this bone region is to supply articular cartilage and more specifically chondrocytes in the deeper articular zones with nutrition and oxygen by diffusion (Coimbra et al., 2004; Suri and Walsh, 2012). Bone is a constantly remodelled structure, and its turnover is facilitated by the cells contained within the structure which include osteoblasts, osteoclasts and osteocytes (Eriksen, 2010). This remodelling has to

be tightly regulated as deviations from neutral balance between resorption and formation would cause increased risk of fracture or compression syndromes (Goldring and Goldring, 2016). Osteoblasts and osteoclasts together form a bone multicellular unit (BMU) which is responsible for remodelling both cortical and trabecular bone via osteoclast resorption supported by a phase of osteoblast-mediated bone formation (Eriksen, 2010). Osteocytes are the third bone cell type and are embedded in the bone matrix, they form an interconnected network with each other in the bone matrix and with the cells on the bone surface to play a critical role in the homeostasis in the adult skeleton by regulating osteoblast and osteoclast function (Dallas et al., 2013).

During the progression of OA, subchondral bone undertakes dramatic changes in its composition and structural organisation (Loeser et al., 2012). The calcified cartilage layer and tidemark above the subchondral bone undergo angiogenesis and these blood vessels infiltrate this zone from the subchondral bone (Walsh et al., 2007). A pro-angiogenic environment in the subchondral bone as well as an increase in NGF expression facilitates the vascularisation and growth of new nerves in the articular cartilage (Walsh et al., 2010). This increases bone cross talk between the subchondral bone and articular cartilage, where osteoblasts, osteoclasts, osteocytes and bone-lining cells engage in molecular interactions with the articular cartilage (Suri and Walsh, 2012). This increased cross-talk between the subchondral bone and the articular cartilage in early OA leads to increased bone remodelling in the subchondral bone plate and the subchondral

trabecular bone (Intema et al., 2010b). Subchondral trabecular bone deteriorates and its density decreases during early OA; trabecular bone thickness decreases as well as increased separation between the trabeculae and a reduction in the number of trabeculae (Bolbos et al., 2008). The subchondral bone plate also sees a reduction in thickness due to increased bone remodelling (Intema et al., 2010b). This is observed in canine animal models of OA where early OA can be observed more closely and this coincides with degeneration in the articular cartilage (Intema et al., 2010b). Subchondral bone plate was found to drastically decrease particularly in the medial part of the joint and the porosity of the plate was also found to increase (Intema et al., 2010a). A feline model of OA investigating early and late stage post-traumatic OA also found that the subchondral bone plate thinned during early OA (Boyd et al., 2005). Density and thickness of subchondral bone is found to decrease with increased age, however this decrease is much more dramatic in cases of OA (Yamada et al., 2002; Boyd et al., 2005). The subchondral bone plate and subchondral trabecular bone change over the course of OA progression, both regions, which decreased in early OA, are found to increase in thickness and density in late OA (Goldring and Goldring, 2016). Bone surface of the subchondral plate and trabecular bone were decreased with OA, however thickness of the subchondral plate was found to positively correlate with increased severity of OA (Finnilä et al., 2017). Trabecular bone is found to increase in density during OA progression, however this increase in bone density also causes increased stiffness in the bone possibly due to the proliferation of defective bone (Li and Aspden, 1997; Ding, 2010). As OA

progresses, subchondral bone changes become more evident. Bone marrow lesions (BMLs) form within the subchondral bone and, observed on MRI, show water signals indicating these are oedema filled regions associated with inflammation (Eriksen, 2015). Previous trabecular bone deterioration in early OA due to increased bone remodelling results in spaces between the marrow trabeculae, these spaces are highly associated with BMLs in the subchondral bone (Eriksen, 2015). BMLs tend to be associated with cartilage pathology in OA and have been found to develop in later stages of OA and depend upon the development of pre-existing cartilage damage and are exacerbated by increased joint loading (Crema et al., 2010; Kothari et al., 2010). BMLs can also develop on MRIs because of fibrovascular replacement of adipose bone marrow in OA, which are associated with osteochondral angiogenesis, suggesting that subchondral pathology drives vascular invasion into articular cartilage or that angiogenesis may stimulate fibrovascular marrow replacement (Walsh et al., 2010). Regions within the subchondral bone develop into so called subchondral bone cysts (SBCs), these regions are fluid filled or can contain fibrous tissue (Li et al., 2013). They are highly correlated with BMLs in that BMLs have found to predict the development of SBCs in OA (Carrino et al., 2006). They are commonly reported in patients with OA and are strongly associated with greater disease progression and severity but also with higher degrees of pain (Tanamas et al., 2010). Formation of cysts is hypothesised via two different mechanisms; the first is the Synovial Breach Theory where cysts form in spaces between trabeculae in the subchondral bone as proliferations of other cells (Carrino et al., 2006). These cells accumulate a mucoid fluid to become

myxomatous (tumourous) in histologic appearance and during their expansion the lesion compresses all surrounding tissues (Milgram, 1983). Enlargement of cysts is undertaken by significant bone resorption occurring and the rupturing of these myxomatous cells leaving the mucous fluid in the centre of the cavity, lots of smaller cysts can also join to create larger mucosal cavity regions within the subchondral bone (Milgram, 1983). Trauma in these regions and on the articular surface causes fissures and breach of the osteochondral junction whereby synovial fluid is able to infiltrate the subchondral bone (Landells, 1953). The other method of cyst development is referred to as Bone Contusion Theory where damage to the subchondral bone, which can develop from the articular surfaces impacting on one another, results in fissures and necrosis of the surrounding tissues (Crema et al., 2010). This theory suggests that SBCs are induced by abnormal mechanical stress and subsequent microcracks which results in inflammation and so oedema of the bone spaces resulting in the observed cysts (Dürr et al., 2004; Crema et al., 2010; Li et al., 2013). New bone often forms around the edges of these large cysts producing structures that are clearly observed radiographically as the new bone is often thicker, a change known as sclerosis (Milgram, 1983). Subchondral bone sclerosis is an indisputable sign of the progression of OA, however it is unknown whether it is present as a driving force for the disease or as a result of damage to the articular cartilage (Burr and Gallant, 2012). It is a striking feature of OA radiographs and is observed as darkened white patterns indicating the thickened bone (Milgram, 1983). Participants in the Framingham Study showed up to 9% increase in bone mineral density in men and women with knee OA than those

with no knee OA, however the mechanical consequences of this are not clear (Hannan et al., 1993; Burr and Gallant, 2012). Bone sclerosis is believed to be caused by dysregulation of bone remodelling whereby abnormal osteoblasts have increased metabolic activity that result in an increase in an under-mineralised osteoid matrix (Hunter and Spector, 2003; Lajeunesse, 2004). Osteophytes are another key feature of late stage OA that are due to changes in the subchondral bone and are easily observed on radiographs (Goldring and Goldring, 2016). Osteophytes are outgrowths of bone at the margin or periphery of the joint and radiographically they appear as lips of new bone around the edges of the joint (Boegård and Jonsson, 1999). They develop by stimulation of cells in the synovial lining of the joint beginning to proliferate, cells inside the developing osteophyte then undergo chondrogenesis and deposit matrix molecules such as aggrecan causing chondrocytes to further differentiate and undergo hypertrophy (van der Kraan and van den Berg, 2007). This is followed by ossification of the site and formation of marrow cavities to create a fully developed osteophyte which is integrated into the subchondral bone (van der Kraan and van den Berg, 2007). It is unclear whether osteophytes develop as a manifestation of pathologic joint changes or whether they are part of normal remodelling in response to articular cartilage changes (Pottenger et al., 1990). It is possible that osteophytes develop as a way of stabilising the joint in OA as, in severe OA, joints are frequently found to be unstable (Kolstad et al., 1980; Goldring and Goldring, 2016). One study has tested whether this hypothesis is true and found that OA knee joints are more unstable than normal knees, however osteophytes prevent greater instability as they may press

against the slackened ligaments (Pottenger et al., 1990). All of these changes to the subchondral bone result in joint space narrowing and bone attrition (Goldring and Goldring, 2016). Joint space narrowing often forms between osteophytes at the joint margin and does not appear to correlate or predict articular cartilage damage (Fife et al., 1991). Joint space narrowing results predominantly from increased thickness of the subchondral bone plate and due to the development of osteophytes (Buckland-Wright, 2004). Bone attrition is an altered bone contour resulting from deformation of the subchondral bone plate (Goldring and Goldring, 2016). Bone attrition is seen as an additional radiographic feature of advanced OA and graded on the degree of flattening of the articular surface and can be observed from mild to severe OA but is more commonly a feature of severe OA (Reichenbach et al., 2008). The presence of bone attrition in sub regions within the knee joint has also been found to predict further cartilage loss in that sub region suggesting that these features of OA are highly correlated (Neogi et al., 2009). Bone attrition occurs in areas of the joint that experienced greater mechanical loading and is increased when the joint is misaligned (Neogi et al., 2010).

1.5.4.3. Meniscus

Meniscus is a smooth lubricated tissue that is crescent shaped wedges of fibrocartilage and in the knee joint there are two menisci located between the femoral condyles and the tibial plateaux on the medial and lateral aspects of the tibial plateaux (Messner and Gao, 1998; Fox et al., 2012a). The menisci of

the knee are specialised tissues that play a key role in load transmission, joint stability and shock absorption as well as stability, nutrition, proprioception and joint lubrication (Fox et al., 2012a; Sun et al., 2012). Functions associated with load transmission are often discovered by the removal of the meniscus or meniscectomy. In 107 cases of meniscectomy individual had overloading of the articular surfaces of the joint and increased compression of the articular cartilage (Fairbank, 1948). Articular cartilage has elastic properties allowing it to withstand forces between the femoral and tibial surfaces, however this is only for small forces applied for short periods of time (Fairbank, 1948). Comparisons between the contact areas of tibial and femoral surfaces show that the contact area with menisci is more than twice as large as knee joints without menisci, indicating menisci play a key role in the distribution of loads (Fukubayashi and Kurosawa, 1980). Under large load conditions the menisci distribute the weight across its surface, placing larger forces on the lateral meniscus whereas the medial meniscus carries less load and shares this load with the exposed articular cartilage (Walker and Erkman, 1975; Fukubayashi and Kurosawa, 1980). The meniscus achieves this load transmission by its distinctive shape (Makris et al., 2011). Under normal physiological conditions there is continuously repetitive loading on a joint during gait which generates intermittent shock waves in every joint and this is attenuated by shock absorbers which in the knee joint is the menisci (Voloshin and Wosk, 1983). Healthy knees have a 20% higher shock absorbing capacity when compared to painful knees or knees which have undergone meniscectomy, however painful knees and meniscectomized knees showed no difference in shock absorption

capacity, indicating menisci can lose their shock absorbing properties even when no knee pathology is present (Voloshin and Wosk, 1983). Menisci also aid in stabilising the knee joint as the geometric structure of the menisci maintains joint congruity and stability (Fox et al., 2012a). The concave and convex shaping of the menisci enables the femoral condyles and tibial plateaus to articulate against each other and, after joint loading, the knee has multi-directional stabilisation, limiting excess motion in all directions (Fox et al., 2012a). When the menisci are removed the joint becomes lax and anterior-posterior flexion in the knee joint becomes more unstable (Markolf et al., 1976). Menisci have a vascular ring which supplies the periphery and sends radial branches into the nearby tissues and the inner two-thirds of the menisci is avascular (Bird and Sweet, 1988). Canal-like openings have been observed in the surface of calf and human menisci which were traced adjacent to blood vessels near the attached edge of the menisci which may provide nutrients to the cells of the menisci and replenish fluid content (Bird and Sweet, 1987). Lubrication is an important part of the menisci as during articulation of the joint there must be the formation of a liquid film between the moving surface and its bearing (MacConaill, 1932). Menisci contribute to joint lubrication due to their high water content by compression forces which squeeze the liquid out into the joint space allowing smoother articulation (Levy et al., 1982; Aagaard and Verdonk, 1999). Proprioception is a sensory modality that encompasses the sense of relative joint position and motion (Karahan et al., 2010). This perception is mediated by mechanoreceptors which have been found to be present in the anterior and posterior horns of the menisci (Jerosch et al., 1996; Akgun et al., 2008). It is

thought that quick-adapting mechanoreceptors such as the Pacinian corpuscles mediate the sensation of joint motion whilst slow-adapting receptors such as Ruffini endings and Golgi tendon organs mediate the sensation of joint position (Reider et al., 2003). These findings along with evidence that there is a reflex arc between the medial meniscus and the semimembranosus muscle in rabbits suggests that the meniscus plays a key role in joint motion and position (Messner and Gao, 1998; Saygi et al., 2005; Akgun et al., 2008).

Injury to the meniscus is a known predisposition of OA and damage of the meniscus occurs in 63% of adults with symptomatic knee OA (Englund et al., 2008). Degeneration of the meniscus is a common feature of OA and this is frequently revealed by MRI scanning (Chan et al., 1991). There is a strong relationship between meniscal abnormalities in MRI scanning and degenerative joint disease (Chan et al., 1991). During OA, the menisci lose their smooth surface and become worn, however this does not occur evenly over the menisci with the medial menisci often showing a greater degree of wear than the lateral menisci (Katsuragawa et al., 2010). Meniscal tears are the most common form of intra-articular injury, with peak incidence occurring between the ages of 20 and 29 and more commonly found in men than women (Bryceland et al., 2017). They can be classified into two main categories; traumatic or degenerative, with traumatic lesions found in younger active individuals which occur when the meniscus becomes trapped between the femoral condyle and the tibial plateau under excessive forces (Englund et al., 2009). They can be further

classified based upon the pattern of the tear seen during an arthroscopy and commonly described patterns include vertical longitudinal, oblique, complex, transverse and horizontal (Figure 1.4)(Greis et al., 2002). Traumatic tears usually occur in younger active individuals and the meniscus often splits vertically and parallel to the collagen fibres, which is known as a vertical longitudinal tear, or perpendicular to the collagen fibres, commonly known as a transverse or radial tear, these are associated with increased risk of knee OA (Englund et al., 2009). Degenerative tears are often described as horizontal cleavages, flaps (oblique), complex tears or meniscal maceration or destruction and are associated with older aged individuals, who already have degenerative diseases, such as OA, and occur due to pre-existing structural changes in the meniscus due to early-stage OA (Noble and Hamblen, 1975; Englund, 2009). Meniscal tears cause prominent mechanical symptoms in OA such as buckling or locking of the joint as well as tenderness over the joint line (Felson, 2005).

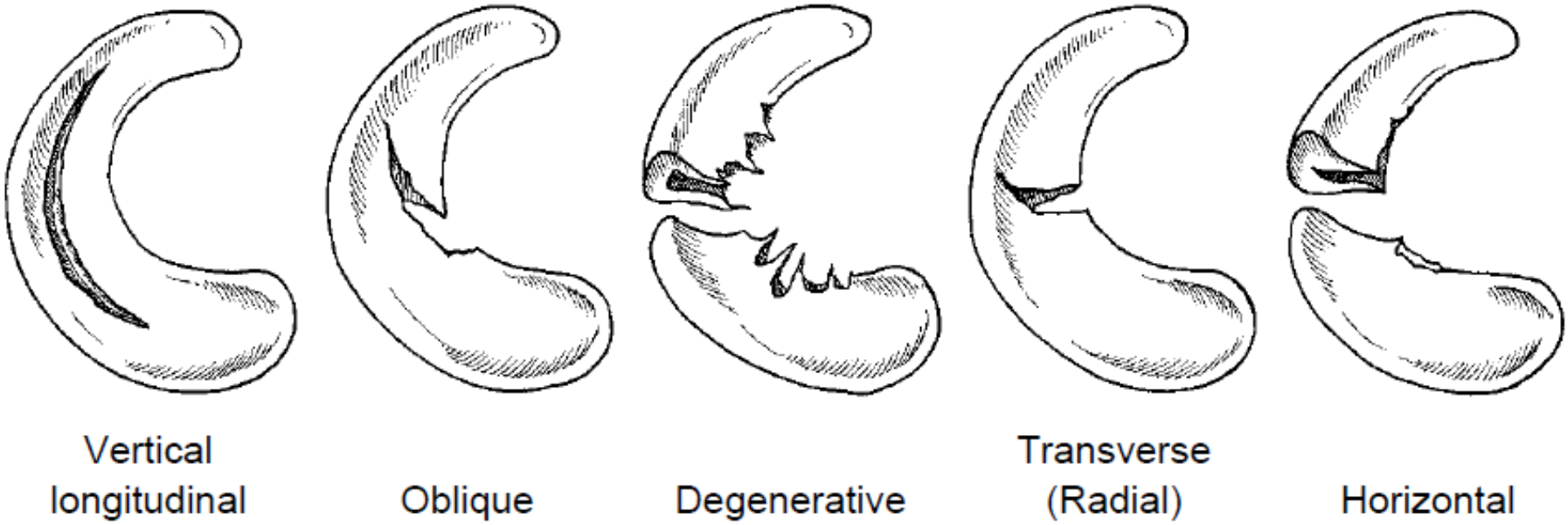

Figure 1.4: Classification of meniscal tears (Greis et al., 2002).

Another change in the meniscus during OA is meniscal subluxation, which is defined as a protrusion over the edge of the tibial plateau whereby pressure within the joint forces the meniscus to displace (Breitenseher et al., 1997). This causes distension of the capsule and retraction of the meniscotibial and meniscofemoral ligaments resulting in retraction of the meniscus from its original position (Breitenseher et al., 1997). Meniscal displacement and extrusion has also been associated with joint space narrowing which is observed on radiographs in OA (Adams et al., 1999; Gale et al., 1999). As well as morphological changes to the menisci during OA there are also changes to the internal structure (Herwig et al., 1984). Examination of the ECM in OA menisci shows that during early degeneration there is a reduction in the diameter of collagen fibres and an increase in water content from 70% to 85% to fill the gaps created by this in the matrix (Adams et al., 1983; Herwig et al., 1984). Collagen fibres start to split initially on the surface and fibril bundles decrease until they are no longer recognisable (Herwig et al., 1984; Katsuragawa et al., 2010). Similarly to OA in articular cartilage, cells within the meniscus start to form clusters, particularly in the surfaces where the meniscus is most damaged (Katsuragawa et al., 2010). This continuous damage and reduction in the collagen fibrils causes the ECM to fill with fluid, resulting in overall thickening of the meniscus (Herwig et al., 1984; Katsuragawa et al., 2010). Changes to the macrostructure of the ECM result in a reduction in stability and strength of the menisci, however there are also molecular changes which occur, such as the levels of GAGs, which are found to decrease during disease progression due to increased binding of proteoglycans with the

increased water content (Herwig et al., 1984). Normal menisci are rarely found in knee joints with OA and are often torn, macerated or totally destroyed (Bhattachayya et al., 2003; Englund et al., 2008). A meniscal lesion in a healthy knee joint may eventually lead to knee OA because of the loss of meniscal function, however knee OA may also lead to meniscal tears (Roos et al., 1995). There is also a strong association between meniscal damage and cartilage loss, where both are exposed to similar stresses and share similar components (Englund, 2009). The active processes in early stage OA lead to cartilage destruction and damage to the meniscus, however a tear in the meniscus with degenerative changes is often associated with pre-existing structural changes in the articular cartilage that are commonly observed in early-onset OA (Noble and Hamblen, 1975). It is therefore difficult to conclude whether meniscal damage is a cause or a consequence of OA however both are strongly associated with each other (Englund, 2009).

1.5.4.4. Ligaments

Skeletal ligaments are dense bands of collagen fibres that span a joint and become anchored to the bone at either end (Frank, 2004). They appear as dense white bands of tissue which have unique bony attachments called insertions and are usually attached in such a way that is crucial for the movement of the ligament and the joint (Frank, 2004; Bray et al., 2005). The general function of ligaments within a joint is to provide passive stability to the joint and guide the joint through their normal range of motion when a tensile

load is applied (Frank, 2004). Other roles include joint homeostasis; due to the viscoelastic properties of ligaments, they are able to reduce stress or load on a joint by being pulled to a constant deformation, and they are involved in joint proprioception where they aid with the perception of the limb position in space (Frank, 2004). This is particularly important in the knee joint where the muscle, joint and cutaneous receptors provide proprioception and ligaments assist this function by invoking neurological feedback signals which activate muscular contraction in response to straining of the ligament (Frank, 2004). Ligaments are the most fibrous component of the knee joint when compared to meniscus and articular cartilage (Eleswarapu et al., 2011). There are three groups of major ligaments in the knee joint; the collateral ligaments, the cruciate ligaments and the patellar ligament (Eleswarapu et al., 2011). The collateral ligaments consist of the medial and lateral collateral ligaments (MCL and LCL) which are extracapsular ligaments located on either side of the knee joint (Woo et al., 2006). The function of the MCL and LCL are to protect the medial and lateral sides of the knee from a contralateral outside or inside bending force, respectively (Eleswarapu et al., 2011). The cruciate ligaments, made up of the ACL and posterior cruciate ligament (PCL), are intracapsular ligaments, named according to their site of attachment to the tibia and, located within the capsule, they cross each other obliquely (Woo et al., 2006). The function of the ACL and PCL is to stabilise the knee during rotation and bending (Eleswarapu et al., 2011). The patellar ligament, sometimes referred to as the patellar tendon, is located between the patella and the tibial tubercule (Amiel et al., 1983). Its function is to provide stability to the patella as it glides over the patellofemoral

grove and femoral condyles (Eleswarapu et al., 2011). One further ligament, only recently described, is the anterolateral ligament (ALL), which is a pearly, fibrous band on the anterolateral side of the knee joint connecting the femur with the tibia (Claes et al., 2013). The hypothesised function of the ALL was to stabilise against internal rotation as it can withstand extreme amounts of tension in this manner (Claes et al., 2013).

Ligament alterations during OA cause similar problems to those observed in the meniscus in that ligament injury particularly to ACL and MCL have a predisposition to OA (Loeser et al., 2012). As well as this, ligament laxity associated with hypermobility is also a risk factor for OA (Bird et al., 1978). It is also acknowledged that ligaments, particularly the ACL, are often ruptured in patients with established OA and examination of 32 ACLs in patients with severe OA in one particular study showed 4 with normal ACL, 10 with lax or ruptured ACLs and 18 where the ACL was completely missing (Wada et al., 1999; Watanabe et al., 2011). However, in severe OA it is difficult to determine whether ACL degeneration is a consequence of cartilage destruction and degradation of the joint or whether a primary lesion within the ACL causes articular cartilage damage (Hasegawa et al., 2012). When examining ACLs across a range of age groups it has been found that ACL degeneration can occur before or progress more rapidly than cartilage degeneration (Hasegawa et al., 2012). With worsening of the disease there is increased varus-valgus rotation which is associated with laxity of ACL and PCL (Wada et al., 1996). It is therefore

clear there is a link between the progression of OA and ACL degradation. There is also evidence that the PCL is correlated with disease progression in OA but to a lesser degree than the ACL, as severe damage to the ACL occurs in 40% of OA knee joints whereas severe PCL damage is seen in only 7% and is very rarely completely absent from the joint (Mullaji et al., 2008). The pathology of these changes to ligaments during OA has been studied very little, however there are known histological changes which occur in the structure of the ligaments during OA which have been clearly documented. In OA knee joints, the ACL and PCL exhibit changes in their collagen fibre orientation, cystic changes and myxoid degeneration as well as mucoid degeneration and loose connective tissue (Cushner et al., 2003; Mullaji et al., 2008). Similar changes are observed in individuals with early onset hand OA where ligament thickening is also observed, this occurs in ligaments during aging and in ligaments in the knee during OA (Tan et al., 2006; Arthritis Research UK, 2012).

1.5.4.5. Patella

The patella is a large flat triangular sesamoid bone located anterior to the knee joint within the tendon of the quadriceps femoris muscle (Fox et al., 2012b). The patella is coated with its own articular cartilage which has a similar structure and the same function as articular cartilage found within the rest of the joint, however patellar cartilage has an increased water content and a lower proteoglycan content (Froimson et al., 1997). The patella is divided into 3 distinct facets; proximal, middle and distal which are separated by two

transverse ridges (Kwak et al., 1997). The primary function of the patella is to improve quadriceps efficiency by increasing the lever arm of the extensor mechanism (Grelsamer and Weinstein, 2001). Its second function is to protect the anterior aspect to the knee joint, it protects the deeper knee joint and the quadriceps tendon from frictional forces. During an increase in patellofemoral force an increase in contact pressure would be expected, however the increase in contact area during flexion of the patellofemoral joint protects the joint from damage (Huberti and Hayes, 1984; Hehne, 1990). In the absence of the patella, such as after patellectomy, the quadriceps tendon is found to thin and elongate which is believed to be prevented by the presence of the patella (Freehafer, 1962).

The patella is a key compartment affected in OA and has previously been overlooked as OA has been considered a tibiofemoral joint disorder with relatively little research into the effects of the patellofemoral compartment (Hinman and Crossley, 2007). Similarly to articular cartilage, any damage to the patella cartilage disrupts the internal structure of the cartilage resulting in a loss of pressure of the internal fluid structure and causing higher stresses on the collagen fibres (Ateshian and Hung, 2013). Increased contact stress may predispose towards more rapid cartilage degeneration and pain due to increased stress on the subchondral bone and the release of cartilage break-down products causing synovial inflammation (Bellemans, 2003). This loss of cartilage is key to development of patellofemoral OA as well as the loss of the

groove the patella sits in known as the trochlear groove (Saleh et al., 2005). Patella malalignment with the femoral trochlea is commonly found in patients with patellofemoral joint OA and patella subluxation is found to be highly associated with OA pain and disease progression (Hunter et al., 2007). Joints with structural changes shown on radiographs in both the tibiofemoral compartment and the patellofemoral compartment are more likely to be painful and are associated with loss of function when compared to knees where only one of these compartments is affected (Szebenyi et al., 2006). Patellofemoral OA is found to be present in approximately 41% of early onset cases of OA and is classified as a risk factor for progression of tibiofemoral osteophytes and joint space narrowing in later stage OA (Mazzuca et al., 2006). Dislocation of the patella has been linked to OA as realignment of the extensor mechanism after dislocation results in reduced risk of OA in later life (Crosby and Insall, 1976). A key indicator of OA is the presence of osteophytes and these are also observed in the patellofemoral compartment where they are significantly associated with OA pain (Hunter et al., 2003; Kornaat et al., 2006).

1.5.4.6. Synovial joint capsule

The synovial joint capsule is a liquid-containing cavity enveloped by dense fibrous connective tissue and lined with synovium, it forms a sleeve around the articulating bones to which it is attached which in the knee is the tibia and the femur (Ralphs and Benjamin, 1994; Iwanaga et al., 2000). The wall of the joint capsule is comprised of 2 distinct layers; an external layer called the fibrous

layer, which is dense fibrous tissue made of bundles of collagen fibres that attach to the articulating bones and tendons, sometimes replacing them such as in the knee joint where the quadriceps and patellar tendons form the anterior portion of the knee joint capsule, and the inner layer which is the synovial membrane or synovium and is more cellular in nature (Ralphs and Benjamin, 1994; Iwanaga et al., 2000). Nerves and blood vessels are able to pass through the joint capsule and there are also gaps where the synovium may protrude to form a pouch (Ralphs and Benjamin, 1994). The synovial membrane is a soft tissue lining the spaces of the knee joint and is composed of 2 to 3 layers of specialised cells called synoviocytes (O'Connell, 2000). There are 2 morphologically different types of synoviocytes; A-cells which are macrophages and B-cells which are fibroblast-like cells (Schmidt and Mackay, 1982). A-cells are located in the upper part of the synovial tissue nearest to the joint cavity and their function is to quickly uptake foreign substances from the joint cavity, absorb and degrade these extracellular bodies which may be microorganisms, cell debris or antigens, by using their vesicular and lysosomal systems (Ball et al., 1964; Southwick and Bensch, 1971; Leach et al., 1988; Iwanaga et al., 2000). B-cells are found at a range of depths but more commonly further away from the cavity have a secretory function as they secrete collagens, fibronectin and other GAGs into the joint cavity (Matsubara et al., 1983; Mapp and Revell, 1985; Leach et al., 1988). The joint space in normal joints contain a small amount of viscous, transparent fluid called synovial fluid which aims to moisten and lubricate the gliding surfaces of the joint as well as supply articular cartilage with nutrition by diffusion (Key, 1928; Coimbra et al., 2004). Synovium contains

an excellent nerve supply of both thinly myelinated and unmyelinated fibres of which there are 2 types; postganglionic sympathetic adrenergic fibres and unmyelinated C-fibres (Mapp, 1995). The postganglionic fibres are located around the larger blood vessels and are responsible for the flow of articular blood, C-fibres, which are responsible for the transmission of pain, are usually inactive and are only activated during tissue damage (Mapp, 1995).

Changes to the synovial joint capsule are key features of OA and could also be an important contributor to pain in OA. The synovial membrane reacts during OA in a number of different ways including synovial hyperplasia where the synovial membrane becomes inflamed and thickened which is also known as synovitis (Scanzello and Goldring, 2012). In a group of individuals with OA, over 95% of them are likely to have synovitis present in their joint in both early and advanced stages (Roemer et al., 2010). Synovitis in OA encompasses various histologic changes including infiltration of macrophages and lymphocytes which can be detected in 50% of patients with OA (Pearle et al., 2007). Synovitis is associated with subsequent development of cartilage erosion indicating that synovial inflammation occurs in early onset OA and predisposes further structural progression of the disease (Roemer et al., 2011). Synovitis is also correlated with changes in knee pain but not cartilage loss when compared on an MRI between the synovial membrane thickening and cartilage loss (Hill et al., 2007). Various studies conducted have indicated that synovial inflammation and abnormalities observed in individuals with knee OA have shown an

increase in their chondropathy score after 1 year or that synovitis is associated with an increased risk of fast cartilage loss (Ayral et al., 2005; Roemer et al., 2009). Angiogenesis, the development of new blood vessels, in OA occurs within the synovium and is associated with chronic synovitis, in particular macrophage infiltration of the synovium (Haywood et al., 2003). Synovial angiogenesis may impair chondrocyte function and affect the homeostasis of articular cartilage (Walsh et al., 2007; Mapp et al., 2008). Angiogenesis alone is not a cause of pain, however it enables the innervation of tissues and facilitates inflammation which in turn contribute to pain in OA (Bonnet and Walsh, 2005). Angiogenesis in OA may therefore contribute to both symptoms and disease progression (Walsh et al., 2007). In OA joints lymphatic vessels are seen in more regions of the synovial membrane rather than just the deep layers (Xu et al., 2003). OA joints that showed little inflammation presented similar lymphatic vessels to normal, however those with inflammation, thickened synovium and scatterings of chronic-inflammatory cells the lymphatic vessels were prominent in all zones and were either highly dilated or compressed with slit-like lumen (Xu et al., 2003). Further inflammatory changes occur in adhesion molecules which are expressed by B-cells and may be important in inflammatory arthritis by trapping macrophages and lymphocytes within the synovial membrane while allowing neutrophils to egress into the synovial fluid (Smith, 2011). These additional inflammatory response can in turn sensitise C-fibres located in the synovium by mediators such as prostaglandins (PG) which can add to OA pain (Mapp, 1995).

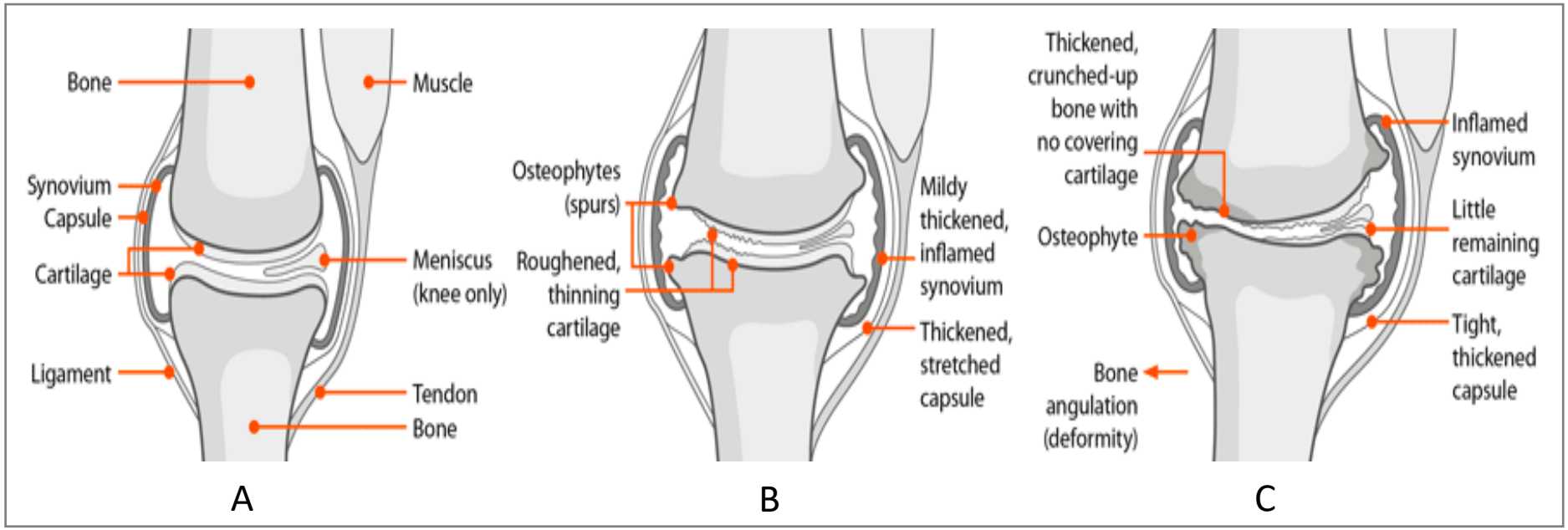

Figure 1.5. Joint degradation in osteoarthritis (OA) from a normal joint (A) to a joint with mild OA (B) and severe OA (C)(Arthritis Research UK, 2012).

1.5.5. Pain structures within the knee joint

The exact source of joint pain after the onset of OA is unknown, although several structures within the joint could be the primary cause of pain. Nociceptors innervate the joint capsule, ligaments, periosteum, menisci, subchondral bone and synovium and pain could therefore arise from any or all of these structures within the joint (Malfait and Schnitzer, 2013)(Figure 1.5).

A key feature of OA is degeneration of the articular cartilage, however as cartilage is aneural and avascular this structure is unlikely to contribute to pain directly (McDougall and Linton, 2012). Correlation between defects in articular cartilage and pain in patients is poor, however there are still ways in which damage to the cartilage may contribute to pain in OA (Wojtys et al., 1990). One way is that nociceptive fibres have been found in the erosion channels running through the subchondral plate to the deep surface of the articular cartilage where the nerve terminals were observed (Wojtys et al., 1990). During OA articular cartilage also becomes vascularised, which in turn leads to innervation of the cartilage via these vascular channels and therefore exposing a potential source of pain from the cartilage (Suri et al., 2007).

Meniscal changes and damage occurs in 63% of adults with symptomatic knee OA including matrix disruption, fibrillation, cell clusters, calcification and cell death (Loeser et al., 2012). These morphological changes correlate with those observed in articular cartilage in the same joint during OA (Pauli et al., 2011).

The menisci are more intensely innervated towards the outer edges with decreasing innervation towards the central thirds which are devoid of innervation (Grönblad et al., 1985). However during injury, such as meniscal tears which can often result in later development of OA, the meniscus has increased levels of vascularisation which is associated with increased sensory nerve growth and may contribute to pain (Mine et al., 2000; Ashraf et al., 2010).

Similarly, ligament injury is closely associated with development of OA and almost 23% of people with symptomatic knee OA have evidence of complete ACL rupture (Loeser et al., 2012). Externally, tenderness is observed in 90% of patients in the anterior medial knee joint which is the location of the MCL (Ikeuchi et al., 2013). Internal staining of knee ligaments in rabbits and humans revealed innervation in the ligaments is comparable between the two species but also is closely associated with the vasculature (McDougall et al., 1997). Ligaments surrounding the joint are densely populated with myelinated and unmyelinated nociceptive fibres making them susceptible to neurogenic inflammation and possible centres of articular nociception (McDougall et al., 1997).

Angiogenesis occurs in the osteochondral junction resulting in a separation of the articular cartilage from the subchondral bone forming a “tide-mark” (Loeser et al., 2012). These vascular channels have been shown to contain sensory nerve fibres expressing NGF which may be a potential cause of symptomatic

pain, as when angiogenesis was inhibited in the osteochondral junction, pain behaviour was significantly reduced (Walsh et al., 2010; Ashraf et al., 2011). BMLs on MRI are also strongly associated with pain in knee OA (Felson et al., 2001; Yusuf et al., 2011; Hunter et al., 2013). BMLs are areas that have high-signals in the medullary space on MRI scans and are thought to represent contusions within the marrow (Felson et al., 2001). BMLs are more prevalent in those with knee pain than those without it, however there appears to be no link to the severity of pain in these individuals therefore showing that OA pain has multiple origins (Felson et al., 2001).

Inflammation of the synovium or synovitis occurs in early stages of disease and may contribute to OA pain by increasing intra-articular pressure (Schaible and Grubb, 1993; Felson, 2006; Yusuf et al., 2011). Nociceptors found in the synovium may also be activated by irritation of the nerve endings within the synovium, the release of PGs and other inflammatory agents and also by osteophytes (Grönblad et al., 1985; Hunter et al., 2013). Whilst there may be many factors that contribute to OA pain in the synovium, it is clear that there is direct correlation between the two as increased synovitis has been found to produce worse pain in subjects with knee OA and that pain changed over time in relation to the change in synovitis (Hill et al., 2007; Loeser et al., 2012).

1.5.6. Treatment of pain in osteoarthritis

Pain in OA is currently assessed via questionnaires inquiring about the presence, severity and intensity of pain the patient is feeling (Neogi and Felson, 2013). The most commonly used is the Western Ontario and McMaster Universities (WOMAC) index which asks patients about pain, stiffness and physical function of their joints, however other pain indices are also used such as the Visual Analogue Scale (VAS), Numeric Scale for Pain (NRS Pain) and the McGill Pain Questionnaire (MPQ)(Hawker et al., 2011).

Current treatments for OA involve attempting to rectify the mechanical malalignment of the joint, repairing joint instability, education about managing the condition and alleviating pain, which will be the focus of this section. There are various types of treatment for pain in OA such as oral medication, topical creams, steroid injections, TENS and surgery as the final resort. Oral medication for the treatment of pain in OA is usually found in NSAIDs, cyclooxygenase-2 (COX-2) inhibitors, cannabinoids, paracetamol/acetaminophen and opioids (Felson, 2006). NSAIDs and COX-2 are the most efficacious for treating knee OA pain, however whilst they do provide some symptomatic relief they do not alleviate pain long-term across the lifespan of the patient (Felson, 2006; McDougall and Linton, 2012). High doses of NSAIDs taken over many years can lead to toxicity, gastrointestinal bleeding, ulcers and increased risk of heart attack and stroke and whilst COX-2 drugs are more specific in their action they also have several side effects such as abdominal pain, nausea, headache and

insomnia (Arthritis Research UK, 2012; Felson, 2006; McDougall and Linton, 2012). Cannabinoids have been found to be very efficacious in treating OA pain however also have centrally-mediated side effects such as motor impairment, dizziness, dysphoria, memory loss and possible dependence (McDougall and Linton, 2012). Paracetamol, also known as acetaminophen, is considered a first action medication in the treatment of OA, in the majority of cases it is self-medicated and useful for mild to moderate pain (Jordan et al., 2003). Short-term paracetamol use has been found to very efficacious and it can be safely taken long term however its efficacy is questionable for long periods of time and there is also controversy over the gastrointestinal safety of using paracetamol (Jordan et al., 2003). Opioids are a useful alternative for patients who have found NSAIDs or COX-2 drugs ineffective however are not without risk as they have high potential for dependency (Jordan et al., 2003).

Topical applications such as capsaicin or NSAIDs are commonly used and well tolerated by patients (Jordan et al., 2003). They can be very effective when administered regularly and the effects can last for several days (Arthritis Research UK, 2012).

Steroid injections are sometimes administered directly into the osteoarthritic joint and are usually corticosteroids. They are useful for short term treatment of OA pain, have fast onset of pain relief and their effects can last for up to two weeks (Bellamy et al., 2006; Arthritis Research UK, 2012).

TENS is a non-invasive analgesic technique used for relieving musculoskeletal pain where electrical impulses are delivered across the surface of the skin (Jones and Johnson, 2009). It is self-administered, inexpensive and useful for treating moderate to severe pain with results showing improved motility (Jones and Johnson, 2009; Osiri et al., 2009; Arthritis Research UK, 2012).

Surgery in the form of a total joint replacement is used if the pain is very severe and motility has become very difficult or impossible (Arthritis Research UK, 2012). The effectiveness of surgeries such as TKR is very good for those who are severely incapacitated however 10 – 20% of patients with knee OA still have persistent severe joint pain after surgery (Suokas et al., 2012).

1.5.7. Animal models of osteoarthritis and their similarities to human osteoarthritis

Animal models provide useful tools for investigating the physiological, pharmacological and psychological mechanisms of pain (Berge, 2013). There is currently no consensus on which animal model best replicates the human condition and which might be the most suitable for studying the underlying pain mechanisms of human OA (Ameye and Young, 2006; Poole et al., 2010). Models are generally developed on how well they mirror the joint structural changes in human OA and few are looked at in relation to whether they imitate

associated pain behaviour in OA (Combe et al., 2004; Fernihough et al., 2004; Pomonis et al., 2005; Ferreira-Gomes et al., 2008; Ferland et al., 2011). Models of OA are found in a variety of species and their validity is determined by joint histopathology (to confirm the presence of the model), physiological assessments (e.g. assessing inflammation), pharmacological assessments (e.g. drug administration) and behavioural tests (e.g. weight bearing and paw withdrawal thresholds (PWTs))(Combe et al., 2004).

1.5.7.1. Models of spontaneously developing osteoarthritis

Spontaneously occurring OA has been found in the joints of animals including guinea pigs, dogs, Syrian hamsters, some strains of mice and non-human primates (Bendele, 2001). However these models are limited by the extended time frame required to allow them to progress, which can be 18 months for severe OA features to develop (Bendele, 2001; Guzman et al., 2003).

The Dunkin Hartley (DH) guinea pig model is considered the most well characterised spontaneous OA model with the earliest changes observed at approximately 3 months old (Bendele and Hulman, 1988; Bendele, 2001). Guinea pigs also indicate a lack of correlation between morphological joint degeneration and joint nociception indicating it's similarity to human OA whereby disease severity is a poor predictor of pain (Mcdougall et al., 2009). Similar to human OA, spontaneously developing OA in DH guinea pigs is both age and weight related (Bendele and Hulman, 1988; Davis et al., 1989; Bendele

and Hulman, 1991; Jimenez et al., 1997; Mcdougall et al., 2009). Guinea pig knee joints are structurally similar to human knee joints and despite being much smaller are prone to a spontaneous OA which has a histopathology that is very similar to human OA (Jimenez et al., 1997). From early signs of OA at 3 months to around 18 months old animals exhibit classical histology of OA including cartilage degeneration, chondrocyte death, proteoglycan loss, fibrillation, osteophytes, degeneration of the menisci, thickening of the synovial membranes due to synoviocyte proliferation and sclerosis of the subchondral bone affecting gait and extension of the knee joint (Bendele, 2001). Guinea pigs reach skeletal maturity at approximately 4 months of age when bone stops growing, giving them an advantage over other spontaneous models and they are very docile and easy to care for (Gregory et al., 2012). However, guinea pigs are renowned for their sedentary lifestyle making studying the role of exercise in OA very difficult and despite the clinical relevance of this model, the severity and onset of OA cannot be controlled between animals (Schuelert and McDougall, 2009). The major disadvantages with this model are that first signs of OA only appear after 3 months, prolonging both the time and cost of any study which is undertaken, and it is difficult to identify an adequate control for aged animals as all animals will develop bilateral OA making pain behaviour tests unsuitable.

Some mice strains are able to spontaneously develop OA, the causes of which are unidentified genetic predispositions or due to genetic mutations (Brandt,

2002). All aging mice develop medial compartment cartilage degeneration; however it is only in some animals that this progresses to OA (Bendele, 2001). Degeneration begins to develop in the medial compartment of the knee at around 6 months old which can become severe with full thickness cartilage loss and large osteophytes by the time the mice are 15 months old (Bendele, 2001). One particular strain, the STR/ort strain, is prone to OA with lesions developing around 10-20 weeks, starting with cartilage degeneration in the medial tibial plateau and eventual exposure of the subchondral bone, resulting in joint instability (Mason et al., 2001). By 35 weeks old, 85% of mice have developed OA lesions (Gaffen et al., 1995). With the mouse having a fully sequenced genome, these models are excellent for investigating the genetic component of OA and the genotypic-phenotypic relationships in OA and have been used for this purpose extensively and with much success (Gregory et al., 2012). However, mouse knee joints are very small, making them difficult to study, especially when investigating load and biomechanic involvement in OA (Glasson et al., 2010). Another issue with spontaneous OA models in mice is that mouse knee cartilage is very thin compared to other mammals which makes grading cartilage lesions very difficult due to lack of cartilage cell layers (Simon, 1970; Glasson et al., 2010).

Naturally occurring OA is considered to be the most common form of joint disease in dogs with an estimated 20% of cases resulting in euthanasia (Lascelles and Main, 2002). Canine OA shows similar pathological, clinical and

developmental features to that observed in human OA with notable signs of pain including lameness and physical disability (Vainio, 2012). Dogs as young as 1 year old can develop OA and it is estimated that 20% of dogs over this age suffer from OA (Johnston, 1997). Similar to spontaneous mouse OA, non-human primates develop OA due to an unidentified genetic predisposition, however it is also age related with older animals exhibiting the most severe lesions (Carlson et al., 1996; Brandt, 2002). OA is found to be most severe in the medial plateau and is characterised by articular cartilage fibrillation, clefting and eventual loss as well as thickening of the subchondral bone (Carlson et al., 1996). Naturally occurring OA in monkeys make an excellent model for studying human OA as the changes in articular cartilage and subchondral bone are very similar to that observed in human OA, although body weight is not found to be correlated with severity of disease (Carlson et al., 1994, 1996). However, both dogs and non-human primates need to be housed in specialist facilities where they are able to be group housed and require the studies to be very long lasting, especially if age-related OA is to be investigated, making these studies very expensive (Gregory et al., 2012). As well as this, public perception of studies in these animals makes these models difficult to use (Gregory et al., 2012).

1.5.7.2. Chemical models of osteoarthritis

The most widely used chemical model of OA pain is the monosodium iodoacetate (MIA) model whereby MIA (typically 1 – 3mg) is administered as an intra-articular injection through the patella ligament under general anaesthesia

(Dunham et al., 1992; Guingamp et al., 1997; Schaible, 2013). MIA is a glycolysis inhibitor, specifically, it inhibits activity of glyceraldehyde-3-phophate dehydrogenase (G3PD), inducing chondrocyte death (Guzman et al., 2003; Sagar et al., 2014). This model mimics the behavioural, pathological and pharmacological features associated with human OA, including synovial inflammation, chondropathy and osteophytosis (Bove et al., 2003; Mapp et al., 2013). Intra-articular injection of MIA disrupts chondrocyte metabolism resulting in OA-like lesions characterised by chondrocyte necrosis, cell-cloning (chondrones), fibrillation and erosion of the cartilage to expose the subchondral bone (Bove et al., 2003; Combe et al., 2004). As early as 1 day after injection of MIA, inflammatory signs of OA are apparent with more structural pathology of OA becoming evident after 14 days and resembling human OA after 20 days (Schaible, 2013; Mapp et al., 2013; Nwosu et al., 2016b). Changes in pain behaviour associated with weight bearing and gait in MIA injected animals can be observed from as early as day 1 post-MIA injection indicating a rapid onset of OA-like symptoms (Bove et al., 2003). The MIA model can be therapeutically treated with analgesics which reduces pain behaviour representing the alleviation of joint pain observed in human OA (Bove et al., 2003; Sagar et al., 2014). This model has prominent osteophytes making it ideal for studying their induction and formation and as well as mimicking the pain, biochemical and structural changes of OA, it is also relatively low cost to implement and easy to induce (Bendele, 2001; Ameye and Young, 2006; Gregory et al., 2012). The MIA model can be easily induced compared to other more complicated surgical models, has a high degree of reproducibility and can

be used in a variety of species including rat, mouse, chicken, horse, guinea pig and rabbit, making it highly versatile (Janusz et al., 2001; Bove et al., 2003; Gregory et al., 2012; Sagar et al., 2014). This model is also a rapid onset model which can exhibit severe OA in short periods of time, this is both an advantage for the time frame of studies and a disadvantage as it strays from the condition in human OA where disease progression occurs at a much slower rate (Janusz et al., 2001). Therefore this model does not mimic the early mechanisms of cartilage damage in human OA (Sagar et al., 2014).

1.5.7.3. Surgical models of osteoarthritis

There are a number of surgical OA models with many of them being widely used, including the ACL transection (ACLT) model in dogs and rodents (Ameye and Young, 2006). ACLT requires a small surgical incision to expose the knee joint and dislocation of the patella, the ACL is then transected (Stoop et al., 2000). This transection results in instability within the joint causing OA lesions that mimic naturally occurring OA but also OA following injury in humans (Bendele, 2001; Hayami et al., 2006). The lesions produced take extended periods of time to progress to OA and so allow the study of developing OA and therefore larger dogs are often used to increase the cartilage degeneration (Bendele, 2001). This model shows early changes in articular cartilage and subchondral bone as well as other key features of OA such as osteophytes and eventually functional loss of the joint (Ameye and Young, 2006; Gregory et al., 2012). This model is excellent for studying OA in a situation that is naturally

occurring, however due to the slow progression of disease, length of time for the study is a key disadvantage (Bendele, 2001). ACLT models are also unhelpful if an assessment of pain behaviour is required as these animals do not develop weight bearing deficiencies or mechanical allodynia (Ferland et al., 2011).

The meniscal transection (MNX) model requires transection of the MCL followed by a half or full thickness cut through the medial meniscus (Sagar et al., 2014). This model is useful because it mimics human injury such as meniscal tears which are common sports injuries and gives an accelerated severity of OA (Sagar et al., 2014). Similarly to the ACLT, this model can be implemented in a number of species such as rats, guinea pigs, rabbits, dogs, sheep, mice and goats (Bendele, 2001; Gregory et al., 2012). This model is a rapidly progressive with cartilage degeneration characterised by chondrocyte and proteoglycan loss as well as fibrillation, and chondrocyte cloning (Bendele, 2001). As well as significant cartilage damage within 3 weeks post-surgery, MNX animals show changes in the subchondral bone by day 7 which are similar to the lesions seen in human OA (Bove et al., 2006). By 14 days post-surgery the presence of osteophytes can be observed as well as synovitis and increasing chondropathy (Mapp et al., 2013). Despite the usefulness of this surgical model it is more technically demanding, requires sham-operated controls and characteristically has a more rapid onset of disease making looking at early onset or progression of the disease more difficult (Sagar et al., 2014).

1.6. Experimental objectives and hypotheses

Previous work in DNIC has notably focussed on single cell dorsal horn recordings and whilst this is an excellent tool for investigating DNIC at the level of the spinal cord this thesis aims to utilise nociceptive withdrawal reflex responses measured from hindlimb muscles as an alternative to develop the field of DNIC. This novel work considered the effects of DNIC at the periphery measuring a whole population response whereby both the sensory and motor component were considered as well as the effect of modifications from interneurons. This is particularly important as DNIC likely reflects the net balance between descending inhibitory and facilitatory signalling (Patel and Dickenson, 2019).

1.6.1. Chapter 3

Chapter 3 explored DNIC and the factors affecting DNIC and were to confirm that the evoked inhibition was of an adequate size for the experiments to be undertaken. These initial experiments ensured that the methodology was working, and that the inhibition could be evoked but also was the inhibition that was intended to evoke. This was important to determine for the background of the rest of the experiments in this thesis and was therefore fundamental to undertake for the development of the thesis. The objectives of Chapter 3 were therefore to:

1. Investigate the ability of capsaicin to evoke DNIC of spinal reflexes from different sites of application and to determine its concentration-effect to find a dose that caused significant, non-transient inhibition.
    - The hypothesis for these experiments was that the largest dose would induce the greatest and longest lasting inhibition of reflexes.
2. Determine whether DNIC of reflexes originated entirely from descending supraspinal pathways or whether a spinal component was also involved.
    - The hypothesis was that spinalization would abolish the observed inhibition.
3. Assess the contribution of higher brain structures to DNIC of reflexes (i.e. regions rostral to the superior colliculi). Hence DNIC would be lessened if frontal structures were involved in DNIC.
    - The hypothesis was that DNIC would not be affected by the removal of forebrain structures.
4. Determine the effect of alfaxalone anaesthesia on DNIC by reducing the anaesthesia levels. As anaesthesia is known to have strong influences on spinal reflexes it was important to acknowledge the effects the anaesthesia had on both the spinal reflexes and the induced inhibition in the current experiments as this has not previously been investigated.
    - The hypothesis was that DNIC inhibition would be greater in the presence of a reduced level of alfaxalone.

5. Compare different modalities of test stimulus (graded mechanical versus electrical) to determine the sensitivity of reflexes evoked by these two modalities to inhibition by a fixed capsaicin conditioning stimulus. The premise was that more 'natural' graded mechanical stimuli would allow clearer analysis of the relationship between the test and conditioning stimuli as well as providing the sensitivity needed to detect changes in DNIC in subsequent studies using the OA model. The test and conditioning stimuli are closely linked and whilst many studies have looked at different modalities of test stimulus and a range of conditioning stimuli few studies have directly compared the induced inhibition across different modalities.
    - The hypothesis for these experiments was that a more noxious test stimulus (i.e. electrical stimulation) would be inhibited to a lesser degree than less noxious (i.e. mechanical) stimulation.

1.6.2. Chapter 4

In Chapter 4 DNIC of spinal reflexes was investigated in the MIA model of OA pain. The objective of these experiments was to determine whether efficacy of DNIC of spinal reflexes was altered in the MIA model 28-35 days after induction, hence provide evidence for OA-induced changes in reflex responses due to modified descending inhibition. To increase the possibility of detecting what may be subtle changes in DNIC in 'normal' versus OA groups both mechanical and electrical stimuli were compared with respect to evoking reflex (test)

responses and two concentrations of capsaicin were evaluated in terms of the conditioning stimulus.

- The hypothesis of these experiments was that MIA animals would have a reduced level of inhibition post-capsaicin injection. Either by a reduction in magnitude of the inhibition, a reduction in the duration of inhibition or of the overall inhibition.

1.6.3. Chapter 5

Chapter 5 investigated an acute OA pain state by exploring DNIC in the MIA model 3-4 days post-injection. The objective of these experiments was to investigate whether the efficacy of DNIC was altered in a 3-4 day MIA model of OA pain. Similarly to Chapter 4, these novel experiments measured from nociceptive withdrawal reflexes in the MIA model however this chapter also allowed the effect of inflammation in the periphery on DNIC to be determined.

- The hypothesis of these experiments was that MIA animals would not have a reduced level of inhibition post-capsaicin injection, as these central changes are expected to occur much later in disease progression.

Chapter Two

Materials and Methods

2.1. Animals

All procedures were performed in accordance with the UK Animals (Scientific Procedures) Act 1986 Amendment Regulations 2012, the European Directive 2010/63/EU and UK Home Office regulations under project licence 30/3156. All experiments undertaken were with the approval of the University of Nottingham's Animal Welfare & Ethical Review Body (AWERB) and reported in accordance with the Animal Research: Reporting of In Vivo Experiments (ARRIVE) guidelines.

Male Sprague Dawley rats (n = 167, 100 – 150 g and 250 – 275 g) were obtained from Charles River (Kent, UK) and housed on a 12 hour light-dark cycle at 19 – 23 °C and 55 ± 10% relative humidity with up to four animals per cage. Animals were provided with *ad libitum* access to food and water as well as environmental enrichment in the form of tunnels and chew sticks.

2.2. Electrophysiology

2.2.1. Surgical preparation for electrophysiological recordings

All animals underwent the following preparatory surgery prior to electrophysiology recordings (Figure 2.1).

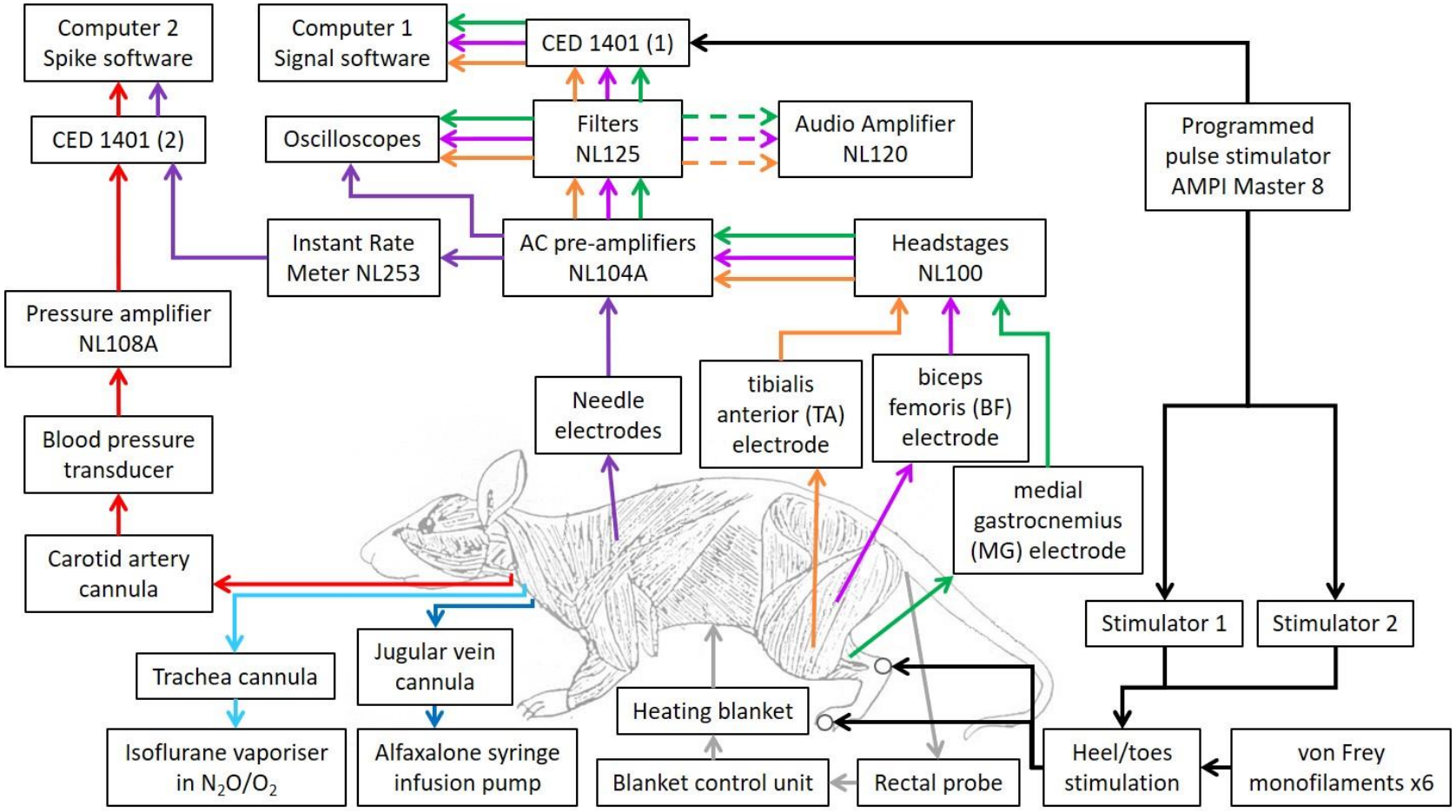

Figure 2.1. Flow diagram of the recording apparatus.

2.2.1.1. Anaesthesia

Rats were deeply anaesthetized until a loss of righting reflex was observed in an anaesthetic chamber using inhalation of 3% isoflurane (IsoFlo; Abbott Laboratories, Maidenhead, UK) in a 2:1 mixture of nitrous oxide (N_2O) and oxygen (O_2)(flow rates 1.2 L min^{-1} and 0.6 L min^{-1} respectively). Animals were then transferred to a nose cone where anaesthesia was maintained using 2 – 2.5% isoflurane in N_2O/O_2 (flow rates 0.8 L min^{-1} and 0.4 L min^{-1} respectively). Core body temperature was maintained at 37.5 ± 0.5 °C via a thermostatically-controlled heating blanket coupled to a rectal probe (Harvard Apparatus Ltd, Edenbridge, UK).

2.2.1.2. Cannulation

Sterilization of surgical instruments was performed to make the procedure more aseptic using Virusolve+ Concentrate solution (5% dilution in reverse osmosis (RO) water; Clinipath Equipment Limited, Hull, UK) for a minimum of 30 minutes prior to surgery. Instruments were then rinsed in RO water prior to use. Virusan gel (Clinipath Equipment Limited, Hull, UK) was also applied to non-sterile gloves periodically throughout the procedure to maintain sterility.

Animals were placed in a supine position, hair overlying the throat was removed and a Rosse sterile drape placed over the animal (The Vet Store, Bradford, UK). This area was then swabbed using dilute Virusolve+ Concentrate

solution (5% dilution in RO water; Clinipath Equipment Limited, Hull, UK) and injected subcutaneously with local anaesthetic (3 x 5 µl injections of 2.0% w/v solution lignocaine hydrochloride, Lignol®; Dechra Veterinary Products, Hadnall, UK) to minimise nociceptive input at the site of the incision. Depth of anaesthesia was checked by pinching the skin overlying the trachea, if no reaction was observed, surgery then continued. An incision approximately 3 cm long was made in the skin along the line of the trachea and the subcutaneous fat and connective tissue over the trachea separated via blunt dissection. Additional lignocaine solution (10 µl) was injected directly into the sternohyoid muscle before it was bisected to reveal the trachea beneath. The trachea was cannulated by inserting 1.5 cm of the cannula into the trachea (Portex, fine bore polythene cannula, 2.4 mm outside diameter, 1.7 mm internal diameter, ~5.5 cm long; Scientific Laboratory Supplies Ltd, Nottingham, UK) to maintain the airway and so that anaesthesia could be continued via a direct connection to this cannula.

Approximately 1 cm of the left carotid artery was cleared of surrounding connective tissue and separated from the vagus nerve via blunt dissection, then cannulated (Portex, iv cannula, outside diameter 1.0 mm, 30 cm long; Scientific Laboratory Supplies Ltd, Nottingham, UK) to allow constant measurement of arterial blood pressure. Prior to insertion the cannula was filled with 10 IU mL^{-1} heparinised Ringer solution to prevent blood clotting. The left jugular vein was then blunt dissected to remove surrounding tissue and cannulated using a

cannula filled with Ringer solution (Portex, iv cannula, outside diameter 0.7 mm, 30 cm long; Scientific Laboratory Supplies Ltd, Nottingham, UK) for administration of intravenous (i.v.) anaesthetic.

After cannulation was complete, a small amount of haemostatic gelatin sponge (Spongostan™; Ferrosan Medical Devices, Søborg, Denmark) was placed around each vessel and the trachea to stem any bleeding and 50 µl of 5% Eutectic Mixture of Local Anaesthetics (EMLA) cream (2.5% lidocaine and 2.5% prilocaine, EMLA™; AstraZeneca, Luton, UK) was applied to the incised muscle and skin. The skin at the neck incision was then sutured (size 5-0; Harvard Apparatus, Kent, UK) to secure the cannulae in place and prevent dehydration of the underlying tissue.

2.2.1.3. Earthing electrode

A section of hair was removed over the upper lumbar vertebrae and after swabbing with Virusolve+ Concentrate solution, a 1-2 cm midline incision was made in the skin. A silver-silver chloride earth pellet was inserted into the exposed muscle and sutured in place. EMLA cream was placed on the incised area and the skin sutured. In the spinalized preparation (section 3.2.2.1) the earth was placed via the laminectomy.

2.2.1.4. Cardiovascular recording

Two needle (length 16 mm, 25-gauge) electrodes were inserted into the subcutaneous tissue either side of the chest to record an electrocardiogram (ECG). These were connected to an amplifier and triggered an instantaneous rate meter (Neurolog NL253; Digitimer Ltd, Hertfordshire, UK). Arterial blood pressure measurements were made using a pressure transducer (NL108A; Digitimer Ltd, Hertfordshire, UK) attached to the carotid artery cannula. Both ECG and blood pressure were recorded on a computer running Spike2 software for Windows (version 3; Cambridge Electronic Design (CED), Cambridge, UK) via a CED micro1401 interface.

2.2.1.5. Maintenance of anaesthesia

Following the completion of surgical methodology, animals were transferred to an i.v. administration of 10 mg mL^{-1} alfaxalone (Alfaxan®; Jurox UK Ltd, Crawley, UK) anaesthesia for the duration of electrophysiological recordings. An initial bolus dose of 3.0 ml hr^{-1} was administered via the jugular cannula using a constant rate infusion (CRI) until a slight drop in blood pressure was observed. At this point, isoflurane anaesthesia and N_2O were immediately ceased, alfaxalone administration was reduced to an appropriate rate and oxygen was reduced to a flow rate of 0.2 L min^{-1} for the duration of the experiment. The rate of alfaxalone anaesthesia was determined by the weight of the animal, specific details of mean rates are provided in individuals experiments.

2.2.2. Stimulation and recording

2.2.2.1. Reflex recording

The majority of hair was removed from the left hindlimb and paired, percutaneous, varnish-insulated copper wire electrodes were inserted into three hindlimb muscles; the ankle extensor medial gastrocnemius (MG), the ankle flexor tibialis anterior (TA) and the knee flexor biceps femoris (BF) using a 25 mm, 23-gauge needle.

Signals were amplified (NeuroLog NL104A, x5000; Digitimer Ltd, Hertfordshire, UK), filtered (NeuroLog NL125; Digitimer Ltd, Hertfordshire, UK), digitised (CED analogue-digital converter, 1401) and sent to a computer running Signal version 2.08 (CED) to be averaged and integrated.

2.2.2.2. Reflex stimulation

Hindlimb NWRs were evoked using either electrical or mechanical stimuli. Stimulation was applied every 2 minutes alternatively to the heel and toes, resulting in a heel stimulation every 4 minutes. Baseline activity was recorded for both electrical and mechanical stimulation. For electrical stimuli, before each 'live' stimulus train, an additional eight sweeps of data were taken with the stimulator switched off to enable subtraction of baseline activity; for mechanical stimulation, a 3 second period of baseline activity prior to von Frey (vF) application was subtracted. Thresholds of reflex responses were

determined before each experiment and were defined as a single motor unit action potential. For electrical stimulation this was established by increasing the stimulus strength until a constant response was observed and for mechanical stimulation the threshold was determined as the first von Frey weight to evoke a response.

2.2.2.2.1. Electrical stimulation

Electrical stimuli were administered via paired stainless steel 27-gauge needle electrodes separated by 2 mm inserted into the plantar skin of the foot at the heel and lateral toe. Electrical stimuli were delivered as eight constant current pulses of 2 ms duration at 1 Hz using AMPI Isoflex stimulators. The stimulus strength was dependent on the threshold of the reflex response but had a maximum intensity of 10 mA (for further details see specific results chapter). The minimum stimulation strength required to evoke a reflex electromyogram (EMG) response in one of the appropriate muscles was recorded as the stimulation threshold. Stimulation strengths in each experiment were determined based on the requirement to evoke control responses that had the capacity to increase as well as decrease in size. Using Signal software, the eight electrical responses were averaged up to 250 ms (Figure 2.2). Using positioned cursors measurements of the area under the peaks was taken for the A-fibre responses (approximately 0.005 – 0.03 seconds) for each of the three muscles, however C-fibre responses were not analysed for electrical stimulation.

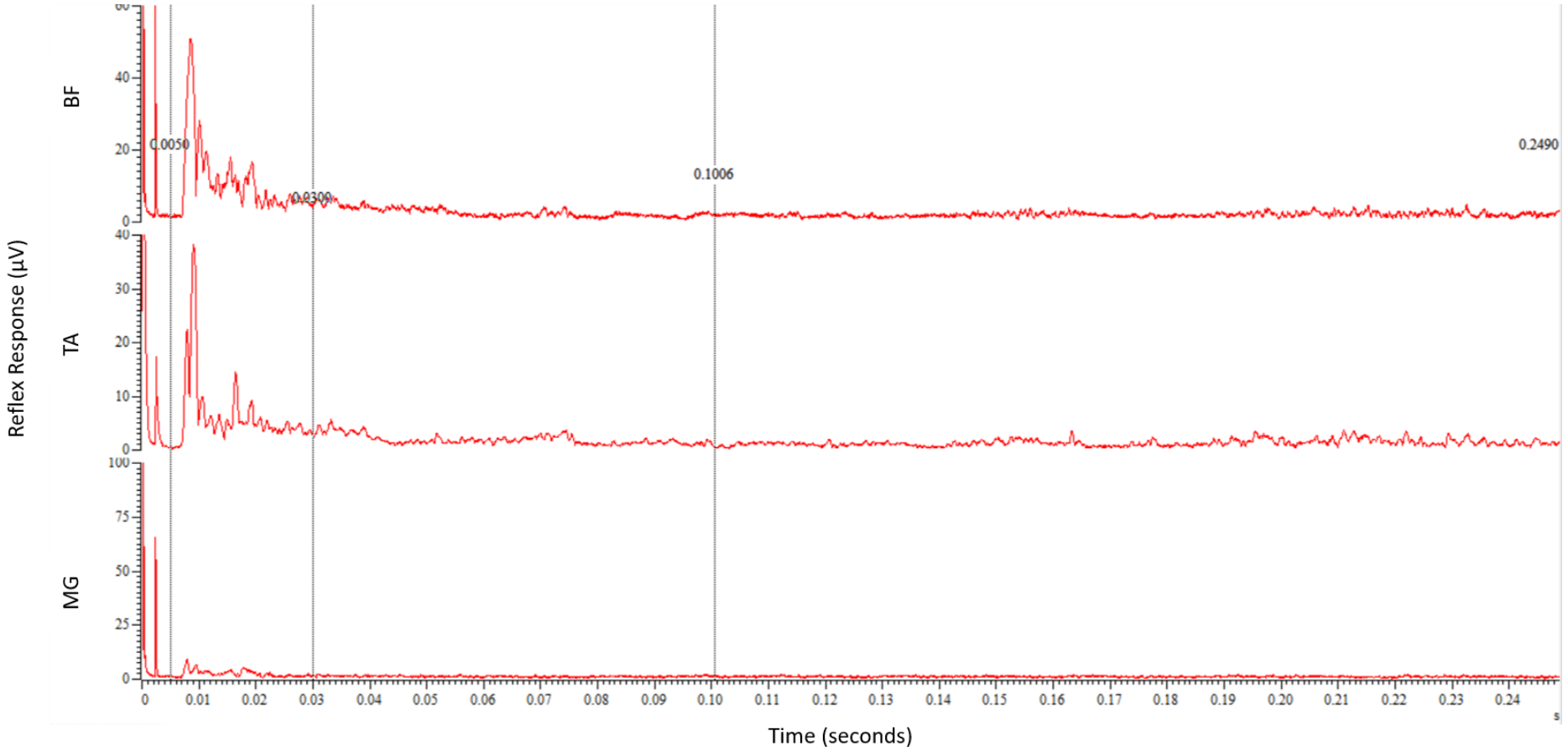

Figure 2.2. Example Signal data trace of electrically-evoked reflex response recorded in a naïve rat after stimulation to the toes. Responses are observed in biceps femoris (BF) and tibialis anterior (TA) but not medial gastrocnemius (MG).

2.2.2.2.2. Mechanical stimulation

Mechanical stimuli were also used to evoke reflex responses via vF monofilaments (Ugo Basile, Varese, Italy) where a range of monofilaments (10 g, 26 g, 60 g, 100 g, 180 g and 300 g) were applied to the skin at the heel and lateral toe for 3 seconds each. In accordance with previous studies, MG was recorded in response to stimulation of the heel and BF and TA in response to stimulation of the toes (Harris and Clarke, 2003). Using Signal software cursors were positioned at the start of the response which was identified using keyboard markers inserted at the time the vF monofilament was applied and at the end of the three second period the monofilament was applied (Figure 2.3). For each three second region the root mean square (RMS) amplitude of the waveform response was analysed. This analysis integrates both A- and C-fibre responses.

2.2.2.3. Analysis of responses

For both electrically and mechanically stimulated responses the baseline responses (see section 2.2.2.2) were subtracted from the reflex response and this value was taken as the reflex response for a given timepoint.

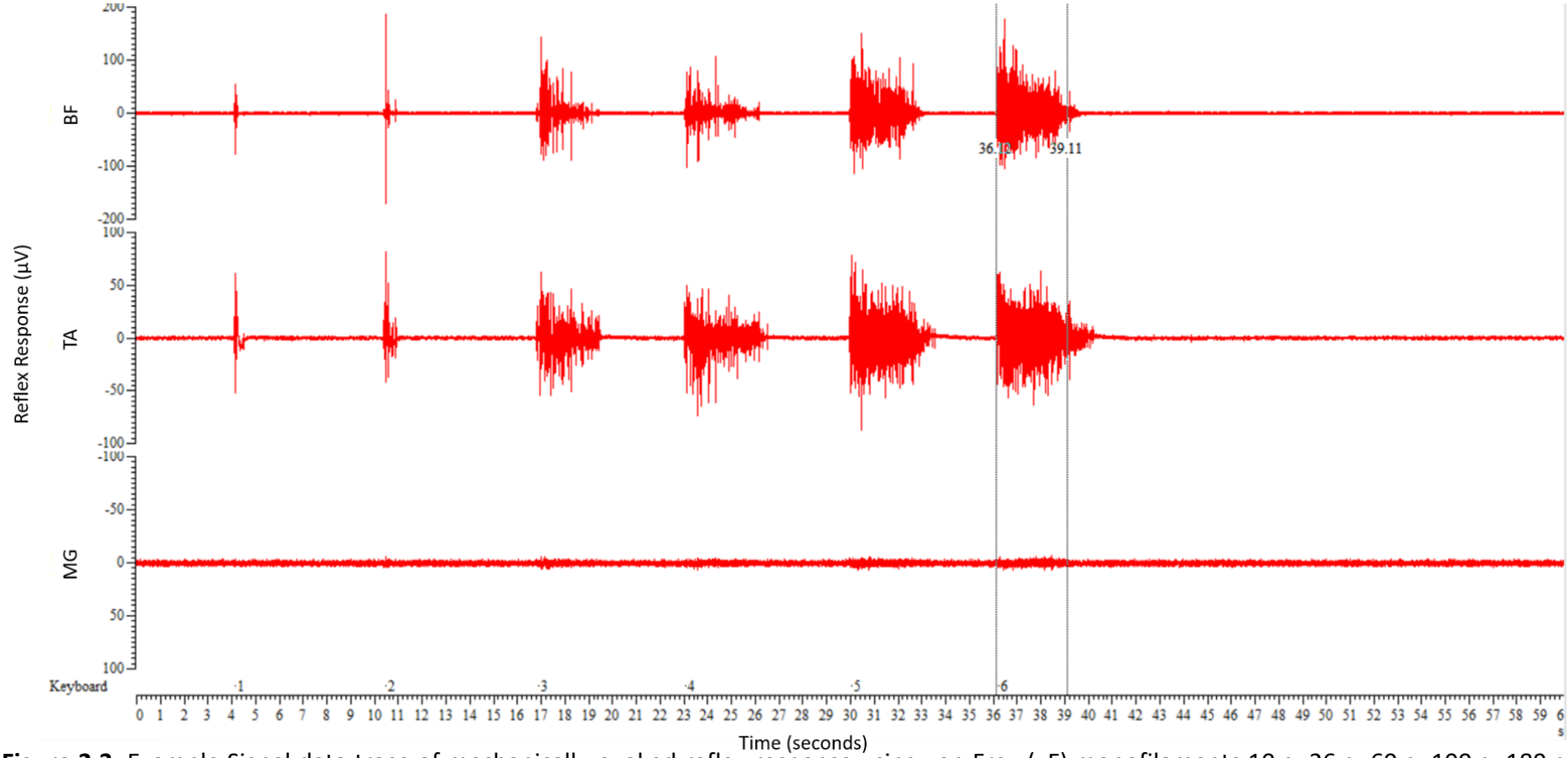

Figure 2.3. Example Signal data trace of mechanically-evoked reflex response using von Frey (vF) monofilaments 10 g, 26 g, 60 g, 100 g, 180 g and 300 g (represented by 1-6) recorded in a naïve rat after stimulation to the toes. Responses are observed in biceps femoris (BF) and tibialis anterior (TA) but not medial gastrocnemius (MG).

2.2.3. Conditioning stimulus

After measuring stable reflex responses for at least 30 minutes following the switch to alfaxalone anaesthesia (section 2.2.1.5), three control reflex responses were recorded and a conditioning (DNIC) stimulus was applied to one of two stimulus sites; the contralateral carpi radialis muscle (forelimb injection) or contralateral MG muscle (hindlimb injection) see section 3.2.1 for full details on the capsaicin conditioning stimulus.

Reflex responses were then measured for a minimum of 60 minutes to determine the effect of the conditioning stimulus on reflexes. Following stabilization of responses, a second injection of capsaicin was given to the site not previously stimulated and reflexes were again measured for at least one hour. The order of the site receiving the first capsaicin injection was alternated between experiments.

Subsequently, after recording had been completed, animals were euthanised by overdose of pentobarbital sodium anaesthesia administered via the jugular vein cannula. Death was confirmed by cessation of heart rate using carotid artery cannula connected to blood pressure meter, heart rate meter and by cervical dislocation.

2.3. Statistical analyses

Prior to any analysis, all data was tested for adherence to a normal distribution using the Kolmogorov-Smirnov normality test. Data was tabularised using Excel® for Office 365 (version 1908; Microsoft®, Washington, USA) and all statistical analyses were performed in Prism® software (version 7.05; GraphPad Software Inc, California, USA).

2.3.1. Control parameters for electrophysiology

Weight, anaesthetic and reflex response threshold and stimulation (for electrical stimulation) parameters were all found to be not normally distributed, therefore were analysed using a non-parametric Mann-Whitney or Kruskal-Wallis with Dunn's multiple comparisons test for comparisons between groups. Data for weight and anaesthetic parameters are expressed as mean and errors are standard error of means (SEMs). Reflex response threshold and stimulation values are expressed as medians and errors are interquartile ranges (IQRs).

Control reflex responses were calculated as an average of the 3 responses directly before any capsaicin was applied and found to be not normally distributed, therefore were analysed using a non-parametric Mann-Whitney or Kruskal-Wallis test with Dunn's multiple comparisons test for comparisons

between groups. Control reflex responses are expressed as medians and errors are IQRs.

2.3.2. Effect of capsaicin

Reflex response data was found to be not normally distributed, therefore, in all experiments, reflex responses were normalised to produce the mean of the pre-capsaicin control (3 readings prior to hindlimb or forelimb capsaicin application) and the control levels were expressed as 100%. In each experimental group, data are presented as medians and the scatter of responses are indicated by the IQRs of the median values. In individual groups, effect of capsaicin on each reflex response over the post-injection time period was analysed using Friedman's ANOVA with Dunn's multiple comparisons test, citing values for inhibition of heel-MG and toes-BF or TA reflexes at 17 min and 19 min post-capsaicin time points respectively.

Median duration of inhibition or facilitation were calculated by determining 2 standard deviations (SDs) above and below each time point for individual experiments to ascertain when responses were outside this range. These were then analysed using a non-parametric Mann-Whitney or Kruskal-Wallis test with Dunn's multiple comparisons test.

At individual time points significance between groups was established by using multiple pairwise, non-parametric Mann-Whitney or Kruskal-Wallis test with Dunn's multiple comparisons test, which were cited on graphical figures.

Area under the curve (AUC) values were calculated in Prism using a baseline value of 100% and as the region of interest was inhibition of reflex responses only negative peaks were evaluated in this analysis. Area of negative peaks was found to be normally distributed therefore were analysed between groups using a parametric unpaired t-test, one-way ANOVA with Tukey's multiple comparisons test or RM one-way ANOVA with Holm-Sidak's multiple comparisons test.

Chapter Three

Factors influencing diffuse noxious inhibitory controls of nociceptive withdrawal reflexes in naïve animals

3.1. Introduction

DNIC is an endogenous spino-bulbospinal pain modulatory pathway occurring when a response from one noxious (test) stimulus is inhibited by another distant noxious (conditioning) stimulus (Le Bars et al., 1979a); studying DNIC can therefore give an important insight into the integrity of these endogenous descending analgesic pathways. However the degree and longevity of DNIC can be affected by gender, age, species, levels of physical activity and sleep patterns (Edwards et al., 2003; Baad-Hansen et al., 2005; Edwards et al., 2009; Naugle and Riley, 2014), and experimentally, DNIC is similarly dependent on a number of factors - the test/conditioning stimuli, spinal cord integrity and anaesthesia - which have therefore been investigated in the following studies.

DNIC relies heavily on the relationship between the test and conditioning stimuli. Previous studies have therefore used a variety of conditioning stimulus modalities to evoke DNIC including mechanical pinch, noxious heat or cold, and chemicals such as bradykinin (Le Bars et al., 1979a), often versus thermal, electrical and mechanical evoked test responses measured in single dorsal horn neurons or in the trigeminal nucleus caudalis of the brain (Le Bars et al., 1979a; Dickenson et al., 1980; Schouenborg and Dickenson, 1985). Where reflexes have been used as the test response they have been evoked using a mechanical pressure applicator to the surface of the hind paw coupled with a capsaicin injection to the fore paw (Da Silva et al., 2018) or by electrical stimulation using ice water as the conditioning stimulus (Biurrun Manresa et al., 2014). For the

following studies it was important that the effect of the DNIC conditioning stimulus was significant and not transient hence there is a great deal of evidence to suggest that chemical stimuli evoke a greater degree and longer-lasting inhibition (Le Bars et al., 1979a; Dickenson et al., 1980; Gjerstad et al., 1999). To this end intramuscular injection of the noxious irritant capsaicin (8-methyl-*N*-vanillyl-6-nonenamide) is a direct method of delivering a powerful inhibitory agent and a dose of 200 μg has been previously shown to induce maximal inhibition within 15 minutes of injection with the effects lasting up to and beyond 1 hour (Gjerstad et al., 1999). With respect to the test stimulus, electrical stimulation evokes clear reflex responses and allows quantitative measurement of the strength of stimulation (Danziger et al., 1999). However electrical impulses to the skin recruit all nerve fibre types simultaneously which is not the normal physiological response. Mechanical stimulation of the skin surface using graded von Frey monofilaments give a more physiologically natural stimulation with A-fibres being initially activated followed by the slower C-fibre response (Bishop, 1946).

Anatomically, it is believed DNIC originates in the brainstem and higher brain (see section 1.3.1) centres (Bouhassira et al., 1990, 1992a, 1992b, 1993) as sectioning the spinal cord has been found to completely abolish the inhibitory effects of DNIC (Le Bars et al., 1979b). However some studies have suggested there is also a segmental spinal component to DNIC as some inhibition of test responses was still observed in spinalized animals following the conditioning

stimulus (Fitzgerald, 1982; Cadden et al., 1983). The SRD is believed to be the primary region of DNIC action however other regions which are not located in the brainstem have also been evaluated. One such region is the infralimbic cortex (ILC) located in the pre-fontal cortex which can exert pronociceptive facilitation via the SRD which is increased during pain states however whilst it is clearly involved in DNIC it is unlikely to be a direct involvement (Patel and Dickenson, 2019). Experiments conducted in decerebrated animals therefore allow the contribution to DNIC of areas rostral to the colliculi to be assessed and spinalization will determine any segmental component to DNIC of spinal reflexes.

Pre-clinical neurological studies aim to aid understanding of mechanisms underlying chronic pain and are frequently carried out in whole animal models, therefore often with the requirement of anaesthesia. However high levels of anaesthesia are known to inhibit spinal, hence reflex, excitability as well as affecting DNIC (Cervero et al., 1991; Jinks et al., 2003a, 2003b; Arendt-Nielsen et al., 2008). Alfaxalone is a neuroactive steroid anaesthetic that heightens the effects of the endogenous inhibitory neurotransmitter GABA by binding to its ionotropic $GABA_A$ receptors (Harrison and Simmonds, 1984). Alfaxalone is an excellent choice of anaesthesia for its safety, reduced cardiopulmonary depression, lack of pain on injection and very few side effects (Child et al., 1972; Michou et al., 2012; Knotek et al., 2013; Santos González et al., 2013; Warne et al., 2015). Whilst alfaxalone gives an excellent depth of anaesthesia it also

permits reflex responses making it an ideal anaesthesia for electrophysiological studies and as such has been used previously for reflex measurements (Clarke and Matthews, 1985; Kelly et al., 2013b; Hunt et al., 2016). However, the effect of alfaxalone anaesthesia on DNIC is unknown.

3.2. Methods

Experiments were performed on a total of 66 naïve male Sprague-Dawley rats (mean weight 366 g, range 269 – 496 g) housed as previously described (section 2.1). Under isoflurane in N_2O/O_2, animals were prepared for electrophysiological recording of reflex responses using surgical procedures described in section 2.2.1, although some animals also underwent additional procedures (decerebration, spinalization) which are described in detail below. After switching to alfaxalone anaesthesia (see section 2.2.1.5), reflex recording of heel-MG, toes-BF and toes-TA responses to either electrical or mechanical (test) stimuli was performed as described in section 2.2.2.1.

3.2.1. Study 1: Effect of capsaicin concentration on DNIC of reflexes

Initial experiments investigated the optimum concentration of capsaicin to use as the conditioning stimulus in order to cause consistent inhibition that was of a large enough amplitude to measure but that also showed a certain degree of recovery over the hour-long post-capsaicin measurement period. Based on

previous studies (Kelly et al., 2013a), a dose of 500 µg was chosen for one group (n = 9) whilst 10-fold lower and higher concentrations were used in two other experimental groups i.e. 50 µg (n = 10) and 5mg (n = 6) capsaicin.

The three necessary capsaicin stock solutions were prepared by diluting 250 mg, 25 mg and 2.5 mg (E)-Capsaicin (Tocris, Bristol, UK) in Tween80 and absolute ethanol (1:1, 0.25 ml: 0.25 ml) to produce concentrations of 500 mg ml^{-1}, 50 mg ml^{-1} or 5 mg ml^{-1} respectively. The chosen stock solution was then diluted 10-fold with Ringer's solution just prior to injecting 100 µl intramuscularly into either the contralateral forelimb or the contralateral hindlimb using a 25-gauge needle (see section 2.2.3).

3.2.2. Study 2: Effect of capsaicin in decerebrated or spinalized animals

Based on the findings of Study 1, 500 µg was chosen as the capsaicin dose for subsequent experiments in naïve animals due to consistency of inhibition following hind- or forelimb injection as well as recovery of reflexes over the 60 minute recording period (section 3.3.1.2).

3.2.2.1. Spinalization

In order to spinalize animals (n = 10) a laminectomy was performed as follows. The hair was removed over the lower thoracic vertebrae and, after swabbing with dilute Virusolve+ Concentrate solution, an incision was made along the

midline approximately 1-2 cm in length. Blunt dissection of the superficial fascia exposed the latissimi dorsi muscles, which were cut away from the spinous processes using a scalpel. Rongeurs were used to remove muscle from the vertebral bones between T8 and T10 and then the T8 and T9 vertebrae were removed to expose the spinal cord. Using sharp surgical scissors, a small incision was made in the dura mater which was extended to further expose the spinal cord. A small amount of local anaesthetic (200 µl of 5% EMLA) was applied prior to a transverse cut to section the spinal cord. Spongostan soaked in lidocaine was then inserted into the gap in the spinal cord to ensure a complete section was maintained and cotton wool soaked in Ringer's solution was placed on and around the spinal cord to keep exposed surfaces moist. The muscle and skin overlying the laminectomy were then sutured together.

3.2.2.2. Decerebration

A subset of naïve animals were decerebrated (n = 9) using the methodology of Dobson and Harris (2012) which is outlined below. Firstly, as an additional step during neck surgery (see section 2.2.1.2), the right carotid artery was exposed in the same way as the left, but rather than being ligated, it was reversibly occluded using an artery clip; this was to temporarily reduce blood flow to the head during the decerebration process hence reduce bleeding.

Decerebration itself consisted of shaving most of the scalp, performing a midline incision and scraping back the pericranium to expose the coronal,

sagittal and transverse sutures of the skull. Two 3 mm holes were bored in the cranium either side of the sagittal suture and midway between the coronal and transverse sutures using a micro-drill (Minicraft MB150; Electron Electronics, Betchwork, UK). These initial holes were extended using rongeurs up to the transverse suture, leaving the sagittal suture intact. Rostral and caudal ligatures (size 3-0; Harvard Apparatus, Kent, UK) were inserted around the parietal bones to occlude the superior sagittal sinus, and the parietal bone region between the ligatures was then removed using rongeurs. The dura mater was cut using sharp scissors and retracted to expose the cerebral hemispheres. Aspiration of the dorsal cerebral cortex was performed using a 1.65 mm (outer diameter) cannula attached to a vacuum pump (New Askir 20 electric surgical suction pump; CA-MI, Pilastro, Italy) in a caudal to rostral stroking motion until the rostral edge of the colliculi were visible. Rapid and complete aspiration of brain tissue rostral to the colliculi was then performed. With suction still in place to cope with any bleeding from the basilar artery and/or cavernous sinus, a cuboidal piece of Spongostan soaked in tissue adhesive (3M Vetbond; Animal Care Products, York, UK) was pressed firmly downwards at the rostral edge of the colliculi to occlude any ruptured vessels and prevent further bleeding. Further Spongostan soaked in tissue adhesive was then inserted into the remaining cavity to encourage haemostasis. Pre-warmed to 37 °C, paraffin oil (Sigma-Aldrich, Dorset, UK) was then poured into the cranial cavity to prevent dehydration of the exposed brain tissue and the skin overlying the skull was clipped together. The vessel clip was removed from the right carotid artery to allow blood flow back to the head.

3.2.3. Study 3: Effect of alfaxalone level on DNIC of reflexes

Experiments were performed in animals decerebrated using the protocol outlined above (section 3.2.2.2). Alfaxalone anaesthesia was maintained using a 10-fold lower concentration than normal of 1 mg mL^{-1} by diluting with Ringer's solution (n = 13).

3.2.4. Study 4: Effect of DNIC on mechanically-evoked reflexes

In naïve intact animals (n = 9) mechanical stimuli were used to evoke reflex responses via application of a range of vF monofilaments. These are applied to the skin surface until the fibre starts to bend, and once this occurs, the force applied stays almost constant even if the fibre is bent further (Fruhstorfer et al., 2001). Individual monofilaments (10 g, 26 g, 60 g, 100 g, 180 g and 300 g) were applied in succession for 3 seconds each alternately to either the skin at the heel or the lateral toe at 2 min intervals. In accordance with previous studies using electrical stimuli, MG was recorded in response to stimulation of the heel and BF and TA in response to stimulation of the toes (Harris and Clarke, 2003).

3.3. Results

3.3.1. Study 1: Effect of capsaicin concentration on DNIC of reflexes

3.3.1.1. Control parameters for electrophysiology

3.3.1.1.1. Weight and anaesthetic levels

Weights of animals were taken on the day of electrophysiology with mean values being 350 ± 11 g (n = 10), 369 ± 5 g (n = 9) and 380 ± 18 g (n = 6) for 50 µg, 500 µg and 5 mg treatment groups respectively; no significant difference was found between the three groups (p = 0.3383, Kruskal-Wallis test). Following an initial bolus dose (see section 2.2.1.5), alfaxalone anaesthesia was maintained using a CRI which for 50 µg, 500 µg and 5 mg groups was at a mean rate of 51.81 ± 1.76 mg kg^{-1} hr^{-1}, 48.523 ± 1.94 mg kg^{-1} hr^{-1} and 50.08 ± 0.57 mg kg^{-1} hr^{-1} respectively; again there was no significant difference between the three groups (p = 0.2108, Kruskal-Wallis test).

3.3.1.1.2. Electrical threshold and stimulation strength

Capsaicin dose	Median threshold (mA)		Median stimulation strength (mA)	
	Heel-MG	Toes-BF/TA	Heel-MG†	Toes-BF/TA
50 µg (n = 10)	4.15 (2.50 – 5.15)	0.50 (0.40 – 0.94)	9.00 (8.13 – 9.63)	7.50 (5.50 – 8.25)
500 µg (n = 9)	5.30 (3.35 – 7.80)	0.50 (0.28 – 1.45)	10.00 (10.00 – 10.00)	4.00 (1.70 – 7.00)
5 mg (n = 6)	3.45 (3.08 – 3.78)	0.40 (0.28 – 0.65)	8.50* (6.60 – 9.00)	8.00 (5.38 – 8.25)

Table 3.1. Median electrical stimulation parameters for heel-medial gastrocnemius (MG) and toes-biceps femoris (BF) or tibialis anterior (TA) reflexes for groups subsequently injected with 50 µg, 500 µg or 5 mg capsaicin. Values in brackets are interquartile ranges. †$p < 0.05$ denotes significant difference between groups (Kruskal-Wallis test). *$p < 0.05$ compared to 500 µg dose (Dunn's multiple comparisons test).

No significant differences were found in the electrical threshold values for toes-BF/TA or heel-MG responses between the three capsaicin groups ($p > 0.05$, Kruskal-Wallis test; Table 3.1). Similarly no significant group differences were found for toes-BF/TA stimulation strengths ($p > 0.05$, Kruskal-Wallis test), however there was a significant difference regarding the stimulation strength for evoking heel-MG reflexes ($p = 0.0161$, Kruskal-Wallis test) with animals to be injected with 500 µg being stimulated at a higher strength than those to be given 5 mg ($p = 0.0146$, Dunn's multiple comparisons test).

When pooled across the three dosage groups, median electrical stimulation threshold values were significantly higher for heel-MG compared to toes-BF/TA, responses being 3.85 mA (IQR 2.93 – 5.7 mA) and 0.40 mA (IQR 0.40 – 0.95 mA) respectively ($p < 0.0001$, Mann-Whitney test). Consequently, the median stimulation strength for evoking measurable heel-MG reflexes was also significantly higher than for toes-BF/TA at 9.0 mA (IQR 8.13 – 10.0 mA) compared to 6.0 mA (IQR 4.0 – 8.0 mA) respectively ($p < 0.0001$, Mann-Whitney test).

3.3.1.1.3. Control reflex responses

Median control responses prior to capsaicin injection for each of the three reflexes were compared between groups and no significant differences were found ($p > 0.05$, Kruskal-Wallis test; Table 3.2).

Capsaicin dose	Median control reflex response (μV.ms)		
	Heel-MG	Toes-BF	Toes-TA
50 μg (n = 10)	92 (59 – 155)	171 (97 – 310)	52 (35 – 104)
500 μg (n = 9)	74 (34 – 121)	259 (111 – 484)	102 (61 – 206)
5 mg (n = 6)	68 (34 – 101)	99 (51 – 189)	86 (51 – 208)

Table 3.2. Median control responses to electrical stimulation for heel-medial gastrocnemius (MG), toes-biceps femoris (BF) and toes-tibialis anterior (TA) reflexes prior to administration of 50 μg, 500 μg or 5 mg capsaicin. Values in brackets are interquartile ranges. Between groups there was no significant difference in the size of control responses for each reflex ($p > 0.05$, Kruskal-Wallis test).

3.3.1.2. Effect of capsaicin

3.3.1.2.1. Injection into the contralateral hindlimb

Within the group of animals to receive the 500 μg dose of capsaicin, one animal had small and inconsistent heel-MG responses, therefore these data were not included in the following analysis of this reflex. Significant inhibition to a median of 72% (IQR 61 – 77%) of pre-capsaicin controls and for a median duration of 61 min (IQR 37 – 61 min) was induced in heel-MG responses using the largest 5 mg (n = 6) capsaicin dose ($p = 0.0088$, Friedman's ANOVA; Figure 3.1A), however no significant inhibition was apparent using lower 50 μg (n = 10) and 500 μg (n = 8) doses ($p = 0.6116$ and $p = 0.3347$ respectively, Friedman's ANOVA). Further comparison of the dose-dependence of inhibition using negative AUC analysis did not further reveal any significant difference between the groups ($p = 0.7178$, one-way ANOVA; Figure 3.2A).

Significant inhibition was produced in toes-BF responses to a median of 64% (IQR 45 – 76%) and 8% (IQR 6 – 50%) of controls by 50 μg (n = 10) and 500 μg (n = 9) capsaicin injections respectively ($p = 0.0005$ and $p < 0.0001$ respectively, Friedman's ANOVA; Figure 3.1B), however, although a decrease in responses appeared to be present following the largest 5 mg (n = 6) dose, this was not statistically significant ($p = 0.1078$, Friedman's ANOVA). Median duration of inhibition was 55 min (IQR 32 – 63 min) and 63 min (IQR 41 – 63 min) for 50 μg and 500 μg capsaicin respectively which was not significantly different ($p = 0.3938$, Mann-Whitney test). Analysis of negative AUC values also supported a

significant difference in overall inhibition between 50 µg, 500 µg and 5 mg doses (p = 0.0382, one-way ANOVA; Figure 3.2B).

Significant inhibition was induced in toes-TA responses by 50 µg (n = 10) and 500 µg (n = 9) capsaicin doses to a median of 66% (IQR 51 – 77%) and 13% (IQR 0 – 63%) of controls respectively (p = 0.0016 and p = 0.0003 respectively, Friedman's ANOVA; Figure 3.1C); however again, even though median responses appeared to be reduced following the largest 5 mg (n = 6) dose, this was not significant (p = 0.1218, Friedman's ANOVA). Median duration of inhibition was not significantly different between 50 µg and 500 µg doses being 49 min (IQR 6 – 57 min) and 63 min (IQR 36 – 63 min) respectively (p = 0.1227, Mann-Whitney test). Analysis of negative AUC values further supported a significant difference in overall inhibition between groups (p = 0.0126, one-way ANOVA; Figure 3.2C).

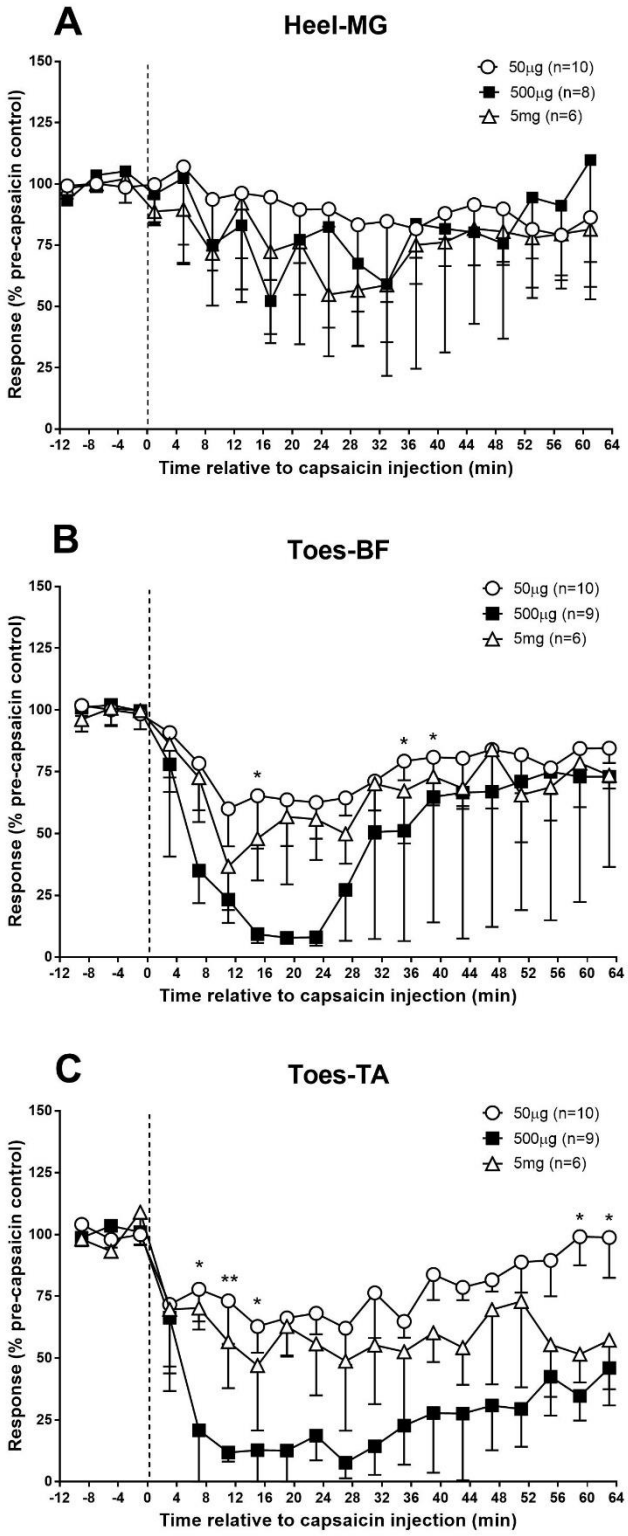

Figure 3.1. Effect of intramuscular injection of 50 µg, 500 µg or 5 mg capsaicin into the contralateral hindlimb on electrically evoked (A) heel-medial gastrocnemius (MG), (B) toes-biceps femoris (BF) and (C) toes-tibialis anterior (TA) reflexes. Values plotted are medians and errors are interquartile ranges. *$p < 0.05$ or **$p < 0.01$ denotes significant difference in inhibition between 50 µg and 500 µg (Dunn's multiple comparisons test).

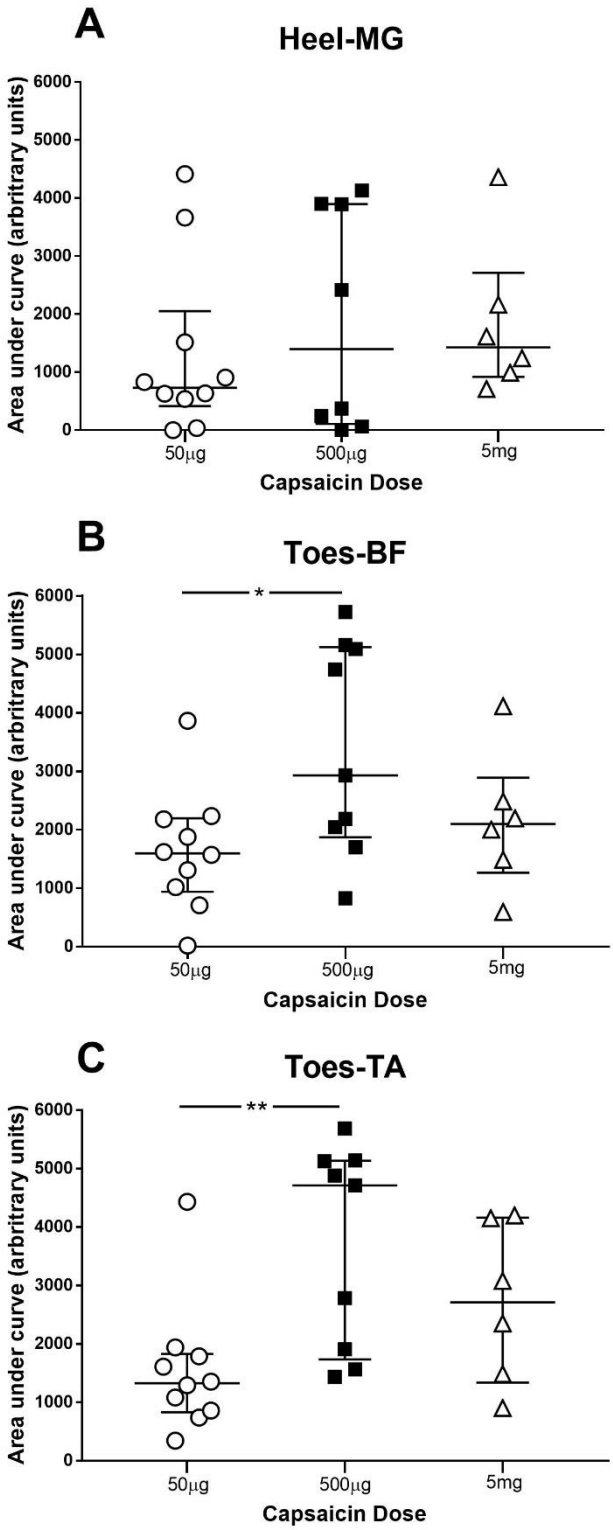

Figure 3.2. Effect of intramuscular injection of 50 µg (n = 10), 500 µg (n = 9) or 5 mg (n = 6) capsaicin into the contralateral hindlimb on electrically evoked (A) heel-medial gastrocnemius (MG), (B) toes-biceps femoris (BF) and (C) toes-tibialis anterior (TA) reflexes. Values plotted are area under curve (AUC) determinations for each animal, with horizontal bars indicating medians and interquartile ranges. *$p < 0.05$ or **$p < 0.01$ denotes significant difference in inhibition between capsaicin doses (Tukey's multiple comparisons test).

3.3.1.2.2. Injection into the contralateral forelimb

Significant inhibition to a median of 72% (IQR 70 – 83%) of pre-capsaicin controls and for a median duration of 55 min (IQR 4 – 61 min) was induced in heel-MG responses using the largest 5 mg (n = 6) dose ($p = 0.0327$, Friedman's ANOVA; Figure 3.3A). However, no inhibition was induced at 50 µg (n = 10) and 500 µg (n = 9) doses ($p = 0.1730$ and $p = 0.2357$ respectively, Friedman's ANOVA). Further comparison using negative AUC also indicated a significance difference in overall inhibition between the three doses ($p = 0.0403$, one-way ANOVA; Figure 3.4A).

Significant inhibition was induced in toes-BF responses using 50 µg (n = 10), 500 µg (n = 9) and 5 mg (n = 6) capsaicin doses to medians of 76% (IQR 42 – 92%), 14% (IQR 7 – 29%) and 39% (IQR 6 – 70%) of controls respectively ($p = 0.0001$, $p < 0.0001$ and $p = 0.0001$ respectively, Friedman's ANOVA; Figure 3.3B). Median duration of inhibition was significantly different across the three groups being 29 min (IQR 16 – 44 min), 63 min (IQR 63 – 63 min) and 51 min (IQR 20 – 63 min) for 50 µg, 500 µg and 5 mg respectively ($p = 0.0066$, Kruskal-Wallis test) with specific differences indicated between 50 µg and 500 µg ($p = 0.0046$, Dunn's multiple comparisons test). Analysis of negative AUC values also supported this significance difference in overall inhibition between doses ($p = 0.0004$, one-way ANOVA; Figure 3.4B).

Significant inhibition was induced in toes-TA responses using 50 µg (n= 10), 500 µg (n = 9) and 5 mg (n = 6) capsaicin concentrations to medians of 74% (IQR 52 – 91%), 14% (IQR 11 – 16%) and 40% (IQR 7 – 68%) of controls respectively ($p = 0.0197$, $p < 0.0001$ and $p = 0.0001$ respectively, Friedman's ANOVA; Figure 3.3C). Median duration of inhibition following 50 µg, 500 µg and 50 mg capsaicin was 33 min (IQR 0 – 63 min), 63 min (IQR 47 – 63 min) and 57 min (IQR 29 – 63 min) respectively but these values were not significantly different between the three dosages ($p = 0.1001$, Kruskal-Wallis test). Similarly analysis of negative AUC values supported a significant difference in overall inhibition between doses ($p = 0.0012$, one-way ANOVA; Figure 3.4C).

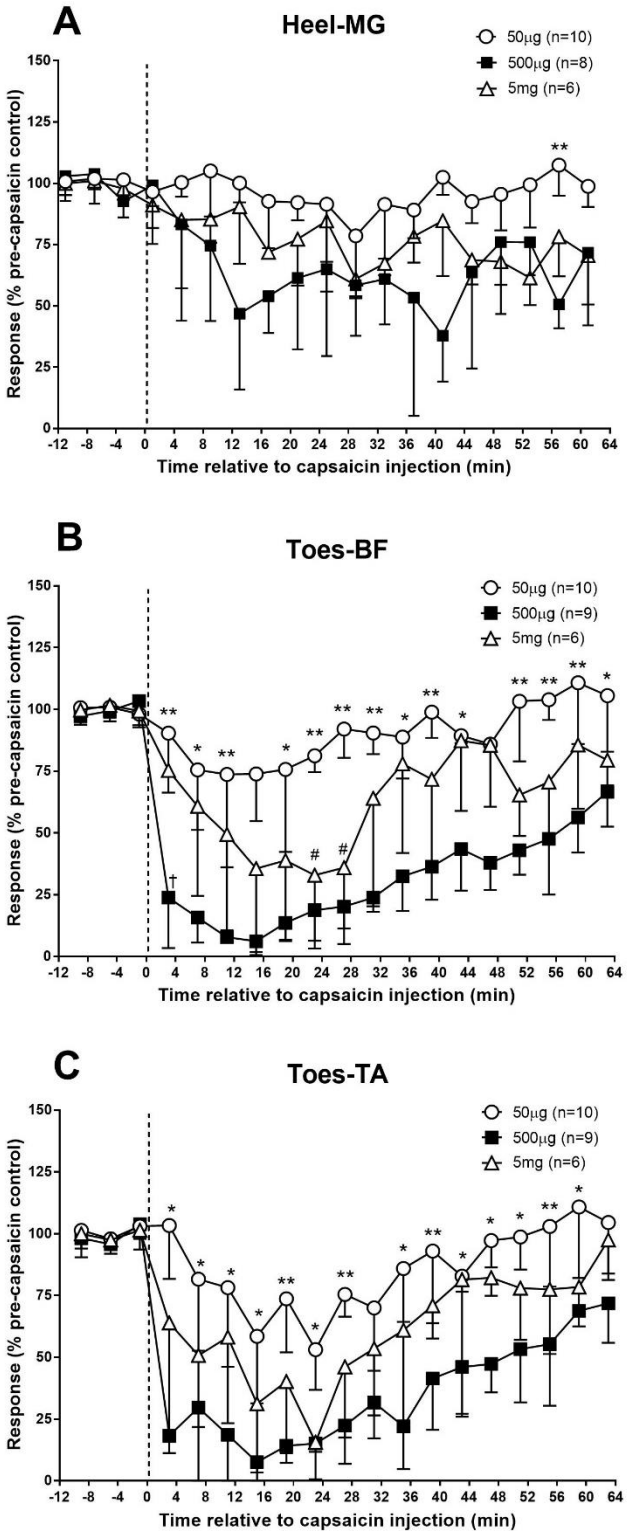

Figure 3.3. Effect of intramuscular injection of 50 µg, 500 µg or 5 mg capsaicin into the contralateral forelimb on electrically evoked (A) heel-medial gastrocnemius (MG), (B) toes-biceps femoris (BF) and (C) toes-tibialis anterior (TA) reflexes. Values plotted are medians and errors are interquartile ranges. *$p < 0.05$ or **$p < 0.01$ denotes significant difference in inhibition between 50 µg and 500 µg; #$p < 0.05$ between 50 µg and 5mg and †$p < 0.05$ between 500 µg and 5mg (Dunn's multiple comparisons test).

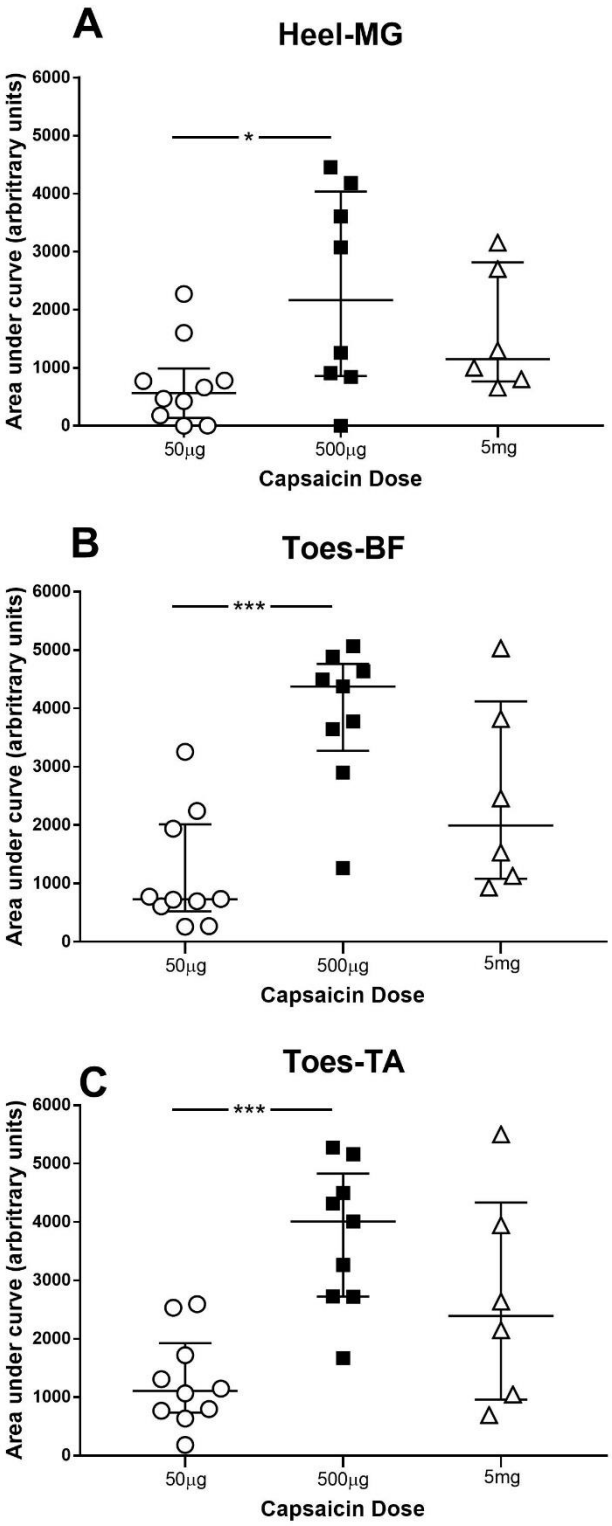

Figure 3.4. Effect of intramuscular injection of 50 µg (n = 10), 500 µg (n = 9) or 5 mg (n = 6) capsaicin into the contralateral forelimb on electrically evoked (A) heel-medial gastrocnemius (MG), (B) toes-biceps femoris (BF) and (C) toes-tibialis anterior (TA) reflexes. Values plotted are area under curve (AUC) determinations for each animal, with horizontal bars indicating medians and interquartile ranges. *$p < 0.05$, or ***$p < 0.001$ denotes significant difference in inhibition between doses (Tukey's multiple comparisons test).

3.3.1.2.3. Effect of capsaicin injection site

Comparison of inhibition of heel-MG, toes-BF or toes-TA responses due to hindlimb or forelimb injections at each capsaicin dosage indicated no significant differences between these sites in terms of depth of inhibition, duration (in each case $p > 0.05$, Mann-Whitney test) or overall inhibition (i.e. AUC analysis; $p > 0.05$, unpaired t-test).

3.3.2. Study 2: Effect of capsaicin in decerebrated or spinalized animals

Note that throughout this section, data will be compared to that obtained in intact animals administered 500 µg capsaicin in Study 1.

3.3.2.1. Control parameters

3.3.2.1.1. Weight and anaesthetic levels

Weights of animals were measured on the day of electrophysiology and mean values were 371 ± 7 g (n = 10) and 345 ± 19 g (n = 9) for spinalized and decerebrate animals respectively; in comparison, the mean weight of intact animals was 369 ± 5 g (n = 9). No significant difference was found between groups (p = 0.2745, Kruskal-Wallis test). Following an initial bolus dose (see section 2.2.1.5), alfaxalone anaesthesia was maintained using a CRI which for spinalized and decerebrate animals was at a mean rate of 45.10 ± 1.76 mg kg^{-1} hr^{-1} and 43.58 ± 0.78 mg kg^{-1} hr^{-1} respectively and again when compared to intact animals (48.23 ± 1.94 mg kg^{-1} hr^{-1}), there was no significant difference between groups (p = 0.1935, Kruskal-Wallis test).

3.3.2.1.2. Electrical threshold and stimulation strength

Preparation	Median threshold (mA)		Median stimulation strength (mA)	
	Heel-MG†	Toes-BF/TA	Heel-MG †	Toes-BF/TA
Intact (n = 9)	4.60 (3.55 – 7.60)	0.50 (0.28 – 1.45)	10.00 (10.00 – 10.00)	4.00 (1.70 – 7.00)
Spinalized (n = 10)	1.10** (0.78 – 2.28)	0.80 (0.50 – 0.98)	6.50 (4.75 – 8.50)	7.00 (4.35 – 9.25)
Decerebrate (n = 9)	1.10** (0.53 – 1.45)	0.60 (0.53 – 0.70)	4.00** (3.00 – 5.00)	7.00 (3.50 – 8.00)

Table 3.3. Median electrical stimulation parameters for the heel-medial gastrocnemius (MG) and toes-biceps femoris (BF) or tibialis anterior (TA) reflexes for intact, spinalized and decerebrate animal preparations. Values in brackets are interquartile ranges. †$p < 0.05$ denotes significant difference between groups (Kruskal-Wallis test). **$p < 0.01$ denotes significant difference compared to intact animals (Dunn's multiple comparisons test).

Median electrical threshold values were significantly different between the three groups for heel-MG reflexes (p = 0.0005, Kruskal-Wallis test), with both spinalized and decerebrate animals indicated as having significantly lower thresholds than intact animals (p = 0.0042 and p = 0.0010 respectively, Dunn's multiple comparisons test; Table 3.3). In contrast, no significant difference was found between preparations for toes-BF/TA thresholds (p = 0.3011, Kruskal-Wallis test). Consequently, significant differences in heel-MG stimulation strengths were evident between the three preparations (p = 0.0017, Kruskal-Wallis test) with lower stimulation strengths used in decerebrated compared to intact animals (p = 0.0011, Dunn's multiple comparisons test). Stimulation strengths used to evoke toes-BF/TA reflexes were not significantly different between the three groups (p = 0.1097, Kruskal-Wallis test).

3.3.2.1.3. Control reflex responses

Control reflex responses for heel-MG were significantly different between the three preparations (p = 0.0370, Kruskal-Wallis test; Table 3.4); although no specific differences were indicated by the post-test, decerebrate animals had considerably higher control responses than intact and spinalized animals. Similarly control reflexes for toes-BF were significantly different between the three preparations (p = 0.0207, Kruskal-Wallis test), but in contrast to heel-MG responses, smaller responses were present in decerebrate and spinalized groups compared to intact animals, with only the latter indicating a significant difference (p = 0.0232, Dunn's multiple comparisons test). This pattern also

seemed to be seen for toes-TA control reflex responses although no significant difference was identified between preparations ($p = 0.2306$, Kruskal-Wallis test).

Preparation	Median control reflex responses (µV.ms)		
	Heel-MG†	Toes-BF†	Toes-TA
Intact (n = 9)	74 (34 – 121)	259 (111 – 484)	102 (61 – 206)
Spinalized (n = 10)	79 (53 – 183)	79* (41 – 108)	52 (44 – 95)
Decerebrate (n = 9)	173 (105 – 367)	87 (57 – 125)	75 (45 – 112)

Table 3.4. Median control responses to electrical stimulation for heel-medial gastrocnemius (MG), toes-biceps femoris (BF) and toes-tibialis anterior (TA) reflexes prior to administration of capsaicin in intact, spinalized or decerebrate animals. Values in brackets are interquartile ranges. †$p < 0.05$ denotes significant difference between groups (Kruskal-Wallis test). *$p < 0.05$ denotes significant difference compared to intact animals (Dunn's multiple comparisons test).

3.3.2.2. Effect of capsaicin

3.3.2.2.1. Injection into the contralateral hindlimb

Similar to heel-MG reflex responses in intact (n = 8) animals (section 3.3.1.2.1), 500 µg capsaicin produced no significant inhibition in spinalized (n = 10) or decerebrate (n = 9) animals (p = 0.7032 and p = 0.6192 respectively, Friedman's ANOVA; Figure 3.5A). Further comparison of preparations using negative AUC analysis confirmed no significant difference between the groups (p = 0.1672, one-way ANOVA; Figure 3.6A).

For toes-BF responses, decerebrate (n = 9) animals were significantly inhibited (p < 0.0001, Friedman's ANOVA; Figure 3.5B) by 500 µg capsaicin to a median of 33% (IQR 8 – 46%) of controls with inhibition lasting for a median duration of 63 min (IQR 63 – 63 min); this compares to values of 8% (IQR 6 – 50%) and 63 min (IQR 41 – 63 min) in intact (n = 9) animals, with duration of inhibition not being significantly different between these two groups (p = 0.2941, Mann-Whitney test). In contrast, no significant capsaicin-induced change in responses was observed in spinalized (n = 10) animals (p = 0.7521, Friedman's ANOVA). Analysis of negative AUC values supported a significant difference in overall inhibition between intact, spinalized and decerebrate groups (p = 0.0002, one-way ANOVA; Figure 3.6B) with significance indicated between spinalized animals and both intact and decerebrate groups (p = 0.0007 and p = 0.0011 respectively, Tukey's multiple comparisons test).

Following capsaicin injection, significant inhibition was observed in toes-TA responses in decerebrate (n = 9) animals to a median of 23% (IQR 15 – 50%) of controls ($p < 0.0001$, Friedman's ANOVA; Figure 3.5C) and inhibition was maintained for a median duration of 63 min (IQR 49 – 63 min); this compares to intact animals (n = 9) in which these reflexes were inhibited to 13% (IQR 0 – 63%) of controls and for a median duration of 63 min (IQR 35 – 63 min) which was not significantly different ($p = 0.9240$, Mann-Whitney test) to decerebrates. Again, no significant inhibition was observed in spinalized (n = 10) animals ($p = 0.0730$, Friedman's ANOVA). Analysis of negative AUC values also indicated a significant difference in overall inhibition between the intact, spinalized and decerebrate groups ($p = 0.0010$, one-way ANOVA; Figure 3.6C) with these differences again indicated between spinalized animals and both intact and decerebrate groups ($p = 0.0015$ and $p = 0.0065$ respectively, Tukey's multiple comparisons test).

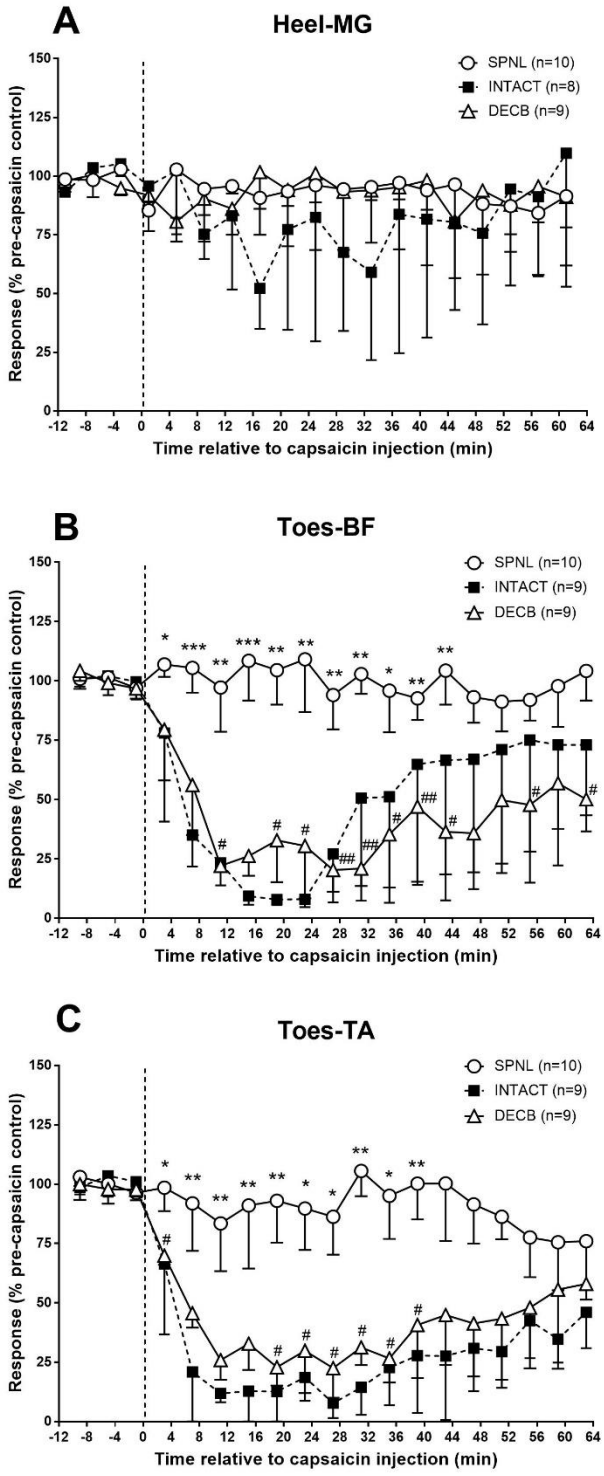

Figure 3.5. Effect of intramuscular injection of 500 µg capsaicin into the contralateral hindlimb on electrically evoked (A) heel-medial gastrocnemius (MG), (B) toes-biceps femoris (BF) and (C) and toes-tibialis anterior (TA) reflexes in intact, spinalized and decerebrate animals. Values plotted are medians and errors are interquartile ranges. Dashed line indicates intact data from Study 1. *p < 0.05, **p < 0.01 or ***p < 0.001 denotes a significant difference in inhibition between spinal and intact and #p < 0.05 between spinal and decerebrate (Dunn's multiple comparisons test).

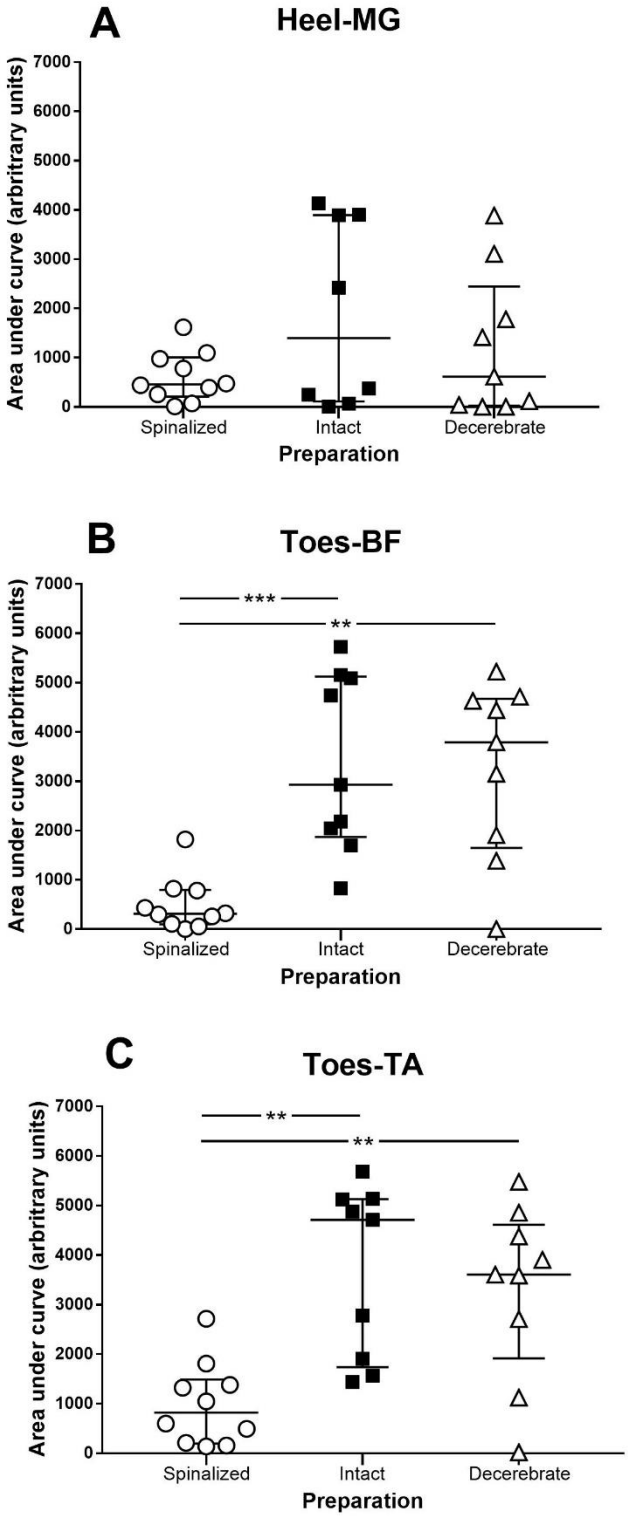

Figure 3.6. Effect of intramuscular injection of 500 µg capsaicin into the contralateral hindlimb on electrically evoked (A) heel-medial gastrocnemius (MG), (B) toes-biceps femoris (BF) and (C) and toes-tibialis anterior (TA) reflexes in intact (n = 9), spinalized (n = 10) and decerebrate (n = 9) animals. Values plotted are area under curve (AUC) determinations for each animal, with horizontal bars indicating medians and interquartile ranges. **p < 0.01 or ***p < 0.001 denotes significant difference in inhibition between preparations (Tukey's multiple comparisons test).

3.3.2.2.2. Injection into the contralateral forelimb

No significant inhibition of heel-MG reflexes was induced by capsaicin in decerebrate (n = 9) animals (p = 0.5815, Friedman's ANOVA; Figure 3.7A); although responses had appeared to be reduced by this capsaicin dose in intact animals (section 3.3.1.2.2), again this was not significant. In contrast significant facilitation of MG responses was induced by capsaicin in spinalized (n = 10) animals to a median of 121% (IQR 107 – 184%) of controls (p = 0.0009, Friedman's ANOVA). Further comparison of preparations using negative AUC analysis indicated a significant difference in overall inhibition between intact, spinalized and decerebrate animals (p = 0.0002, one-way ANOVA; Figure 3.8A) with these differences indicated between intact and both spinalized and decerebrate groups (p = 0.0004 and p = 0.0008 respectively, Tukey's multiple comparisons test).

After capsaicin injection into the contralateral forelimb, significant inhibition was observed in toes-BF responses in decerebrate (n = 9) animals to a median of 33% (IQR 28 – 73%) of controls (p < 0.0001, Friedman's ANOVA; Figure 3.7B) and for a median duration of 51 min (IQR 33 – 63 min); in intact animals, inhibition had been to 14% (IQR 7 – 29%) of controls and duration was 63 min (IQR 63 – 63 min) and this was not significantly different to decerebrates (p = 0.0701, Mann-Whitney test). In contrast capsaicin caused significant facilitation of toes-BF reflexes in spinalized (n = 10) animals to a median of 121% (IQR 117 – 147%) of controls (p = 0.0010, Friedman's ANOVA). Similarly analysis of

negative AUC supported an overall significant difference between intact, spinalized and decerebrate groups ($p < 0.0001$, one-way ANOVA; Figure 3.8B) with differences indicated between intact and decerebrate, spinalized and decerebrate as well as spinalized and intact groups ($p = 0.0347$, $p = 0.0008$ and $p < 0.0001$ respectively, Tukey's multiple comparisons test).

For toes-TA responses, significant inhibition was caused by capsaicin in decerebrate (n = 9) animals to a median of 29% (IQR 19 – 39%) of controls ($p < 0.0001$, Friedman's ANOVA; Figure 3.7C) and for a median duration of 51 min (IQR 25 – 61 min); corresponding values in intact animals were 8% (IQR 0 – 23%) and 63 min (IQR 47 – 63 min) which were not significantly different to decerebrates ($p = 0.2081$, Mann-Whitney test). No significant inhibition was caused by capsaicin in spinalized (n = 10) animals ($p = 0.5864$, Friedman's ANOVA). Analysis of negative AUC also indicated a significant overall difference in inhibition between intact, spinalized and decerebrate groups ($p < 0.0001$, one-way ANOVA; Figure 3.8C) with post-tests indicating the differences between spinalized and both intact and decerebrate groups ($p < 0.0001$ and $p = 0.0006$ respectively, Tukey's multiple comparisons test).

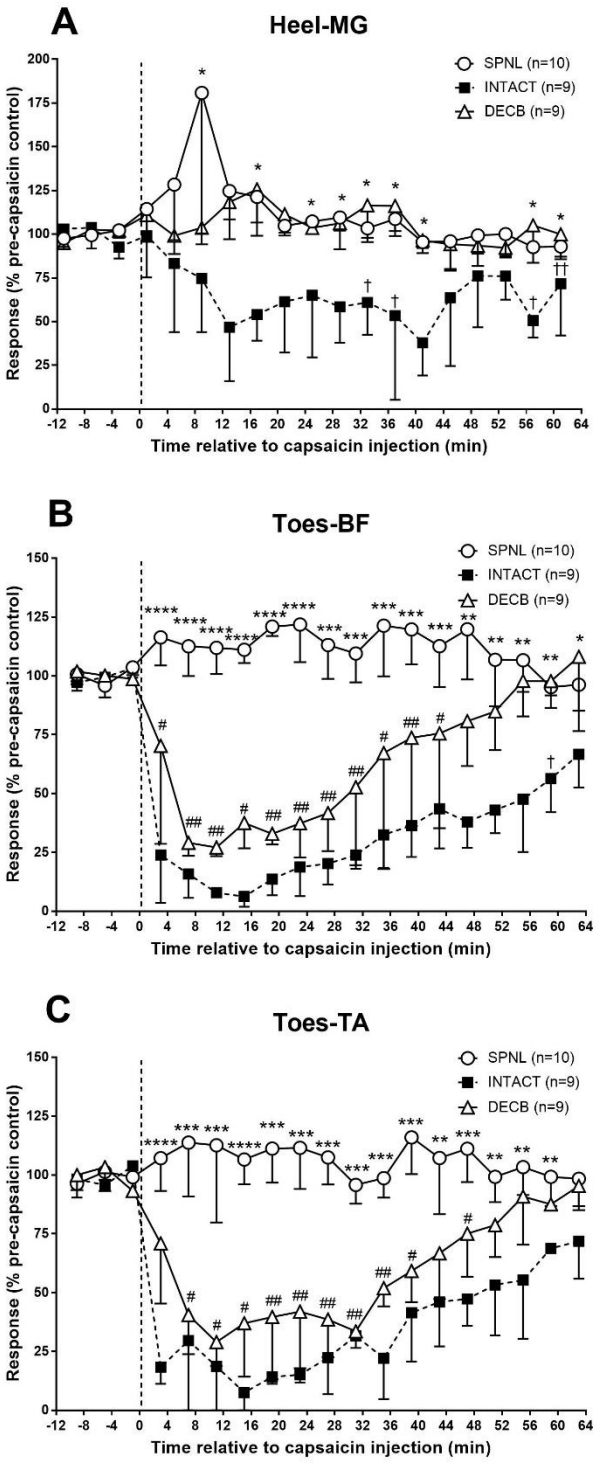

Figure 3.7. Effect of intramuscular injection of 500 µg capsaicin into the contralateral forelimb on electrically evoked (A) heel-medial gastrocnemius (MG), (B) toes-biceps femoris (BF) and (C) toes-tibialis anterior (TA) reflexes in intact, spinalized and decerebrate animals. Values plotted are medians and errors are interquartile ranges. Dashed line indicates intact data from Study 1. *p < 0.05, **p < 0.01, ***p < 0.001 or ****p < 0.0001 denotes a significant difference in inhibition between spinal and intact; #p < 0.05 or ##p < 0.01 between spinal and decerebrate and †p < 0.05 or ††p < 0.01 between intact and decerebrate (Dunn's multiple comparisons test).

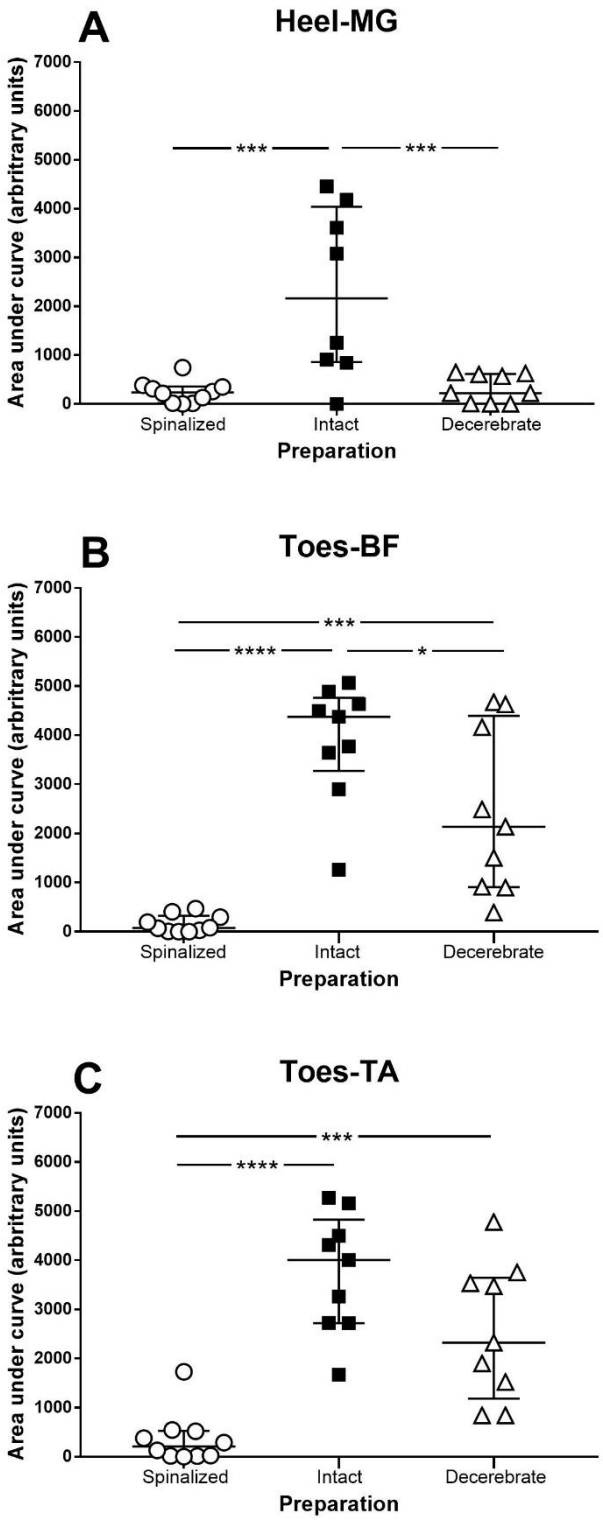

Figure 3.8. Effect of intramuscular injection of 500 µg capsaicin into the contralateral forelimb on electrically evoked (A) heel-medial gastrocnemius (MG), (B) toes-biceps femoris (BF) and (C) and toes-tibialis anterior (TA) reflexes in intact (n = 9), spinalized (n = 10) and decerebrate (n = 9) animals. Values plotted are area under curve (AUC) determinations for each animal, with horizontal bars indicating medians and interquartile ranges. *$p < 0.05$, ***$p < 0.001$ or ****$p < 0.0001$ denotes significant difference in inhibition between preparations (Tukey's multiple comparisons test).

3.3.2.2.3. Effect of capsaicin injection site

Comparison of the effect of hindlimb and forelimb capsaicin injection sites for inducing inhibition of heel-MG and toes-BF reflexes indicated a significant difference between sites in spinalized preparation ($p = 0.0089$ and $p = 0.0115$ respectively, Mann-Whitney test) due to the forelimb injection causing significant facilitation; for heel-MG responses this disparity between injection sites was supported by a significant difference in overall 'inhibition' when comparing negative AUC values ($p = 0.0499$, unpaired t-test). However, no difference between injection sites was found for inhibition of toes-TA reflexes (depth, duration or overall level) in spinalized animals or for any reflex in decerebrates ($p > 0.05$, Mann-Whitney or unpaired t-test).

3.3.3. Study 3: Effect of alfaxalone level on DNIC of reflexes

Throughout this section, data will be compared to that obtained in decerebrate animals administered 500 µg capsaicin under 10-fold higher 'normal' levels of alfaxalone in Study 2.

3.3.3.1. Control parameters

3.3.3.1.1. Weight and anaesthetic levels

Decerebrate animals maintained under low (~10 fold lower) alfaxalone levels had mean weights of 366 ± 10 g (n = 13), which compared to decerebrate animals exposed to normal alfaxalone levels (345 ± 19 g; n = 9), were not significantly different between groups (p = 0.2998, Mann-Whitney test). Following an initial bolus dose (see section 2.2.1.5), alfaxalone anaesthesia was administered at a mean rate of 43.58 ± 0.78 mg kg^{-1} hr^{-1} and 4.86 ± 0.07 mg kg^{-1} hr^{-1} for normal and low alfaxalone decerebrate groups respectively which, as expected, was significantly different between the groups (p < 0.0001, Mann-Whitney test).

3.3.3.1.2. Electrical threshold and stimulation strength

Alfaxalone dose	Median threshold (mA)		Median stimulation strength (mA)	
	Heel-MG	Toes-BF/TA	Heel-MG	Toes-BF/TA
Normal alfaxalone (n = 9)	1.10 (0.53 – 1.45)	0.60 (0.53 – 0.70)	4.00 (3.00 – 5.00)	7.00 (3.50 – 8.00)
Low alfaxalone (n = 13)	0.40*** (0.30 – 0.50)	0.30**** (0.20 – 0.40)	1.00*** (0.80 – 1.35)	1.00**** (0.70 – 1.35)

Table 3.5. Median electrical stimulation parameters for the heel-medial gastrocnemius (MG) and toes-biceps femoris (BF) or tibialis anterior (TA) reflexes for normal and low alfaxalone groups. Values in brackets are interquartile ranges. ***p < 0.001 or ****p < 0.0001 compared to normal alfaxalone group (Mann-Whitney test).

Median electrical threshold values were significantly different between groups for heel-MG ($p = 0.0003$, Mann-Whitney test; Table 3.5) and toes-BF/TA ($p < 0.0001$, Mann-Whitney test) reflexes with normal alfaxalone animals having significantly higher thresholds than low alfaxalone animals. Consequently, significantly higher stimulation strengths were required under normal alfaxalone conditions in order to evoke measurable reflexes in heel-MG ($p = 0.0001$, Mann-Whitney test) and toes-BF/TA ($p < 0.0001$, Mann-Whitney test).

3.3.3.1.3. Control reflex responses

The size of heel-MG control reflexes prior to capsaicin injection was not significantly different between normal and low alfaxalone groups despite the median response seeming to be larger in the latter group ($p = 0.5123$, Mann-Whitney test; Table 3.6). In contrast, toes-BF and toes-TA control responses were both significantly larger in the low alfaxalone group compared to animals under normal alfaxalone conditions ($p < 0.0001$, Mann-Whitney test).

Alfaxalone dose	Median control reflex responses (μV.ms)		
	Heel-MG	Toes-BF	Toes-TA
Normal alfaxalone (n = 9)	173 (105 – 367)	87 (57 – 125)	75 (45 – 112)
Low alfaxalone (n = 13)	261 (119 – 542)	299**** (250 – 748)	219**** (154 – 798)

Table 3.6. Median control responses to electrical stimulation for heel-medial gastrocnemius (MG), toes-biceps femoris (BF) and toes-tibialis anterior (TA) reflexes prior to administration of 500 μg capsaicin in normal and low alfaxalone groups. Values in brackets are interquartile ranges. ****$p < 0.0001$ compared to normal alfaxalone group (Mann-Whitney test).

3.3.3.2. Effect of capsaicin

3.3.3.2.1. Injection into the contralateral hindlimb

Although no significant inhibition of heel-MG responses occurred under normal levels of alfaxalone (n = 9; section 3.3.2.2.1), significant inhibition to a median of 28% (IQR 9 - 104%) of controls was seen in the low alfaxalone group (n = 11; $p < 0.0001$, Friedman's ANOVA; Figure 3.9A). Median duration of inhibition was 57 mins (IQR 5 – 61 mins). Direct comparison of the degree of inhibition at the same post-capsaicin time points for the normal and low alfaxalone groups did not quite reach significance at any point ($p > 0.05$, Mann-Whitney test). Although negative AUC values also suggested a sizable disparity in overall inhibition between normal and low alfaxalone groups this did not reach significance ($p = 0.1472$, unpaired t-test; Figure 3.10A).

Significant inhibition was induced by capsaicin in toes-BF responses to a median of 5% (IQR 1 – 17%) of controls under low alfaxalone (n = 11; $p < 0.0001$, Friedman's ANOVA; Figure 3.9B) which lasted a median duration of 63 min (IQR 63 – 63 min). This compared to a median inhibition of 33% (IQR 15 – 51%) and duration of 63 min (IQR 63 – 63 min) under normal (n = 9) alfaxalone conditions (section 3.3.2.2.1). Between these two alfaxalone levels no significant differences were found in median duration of inhibition ($p > 0.9999$, Mann-Whitney test). Analysis of negative AUC values also found no significant difference in overall inhibition between the normal and low alfaxalone groups ($p = 0.1625$, unpaired t-test; Figure 3.10B).

Significant inhibition was observed in toes-TA responses under low (n = 11) alfaxalone conditions to a median of 11% (0 – 33%) of pre-capsaicin controls ($p < 0.0001$, Friedman's ANOVA; Figure 3.9C) which lasted for a median duration of 63 min (IQR 63 – 63 min). Compared to data obtained under normal alfaxalone levels (inhibition to 23% (IQR 15 – 50%) of controls lasting for 63 min (IQR 49 – 63 min) there was no significant difference ($p = 0.5573$, Mann-Whitney test). Comparison of inhibition at the same time points also found no significant differences ($p > 0.05$, Mann-Whitney test) as was the case when comparing negative AUC values ($p = 0.4462$, unpaired t-test; Figure 3.10C).

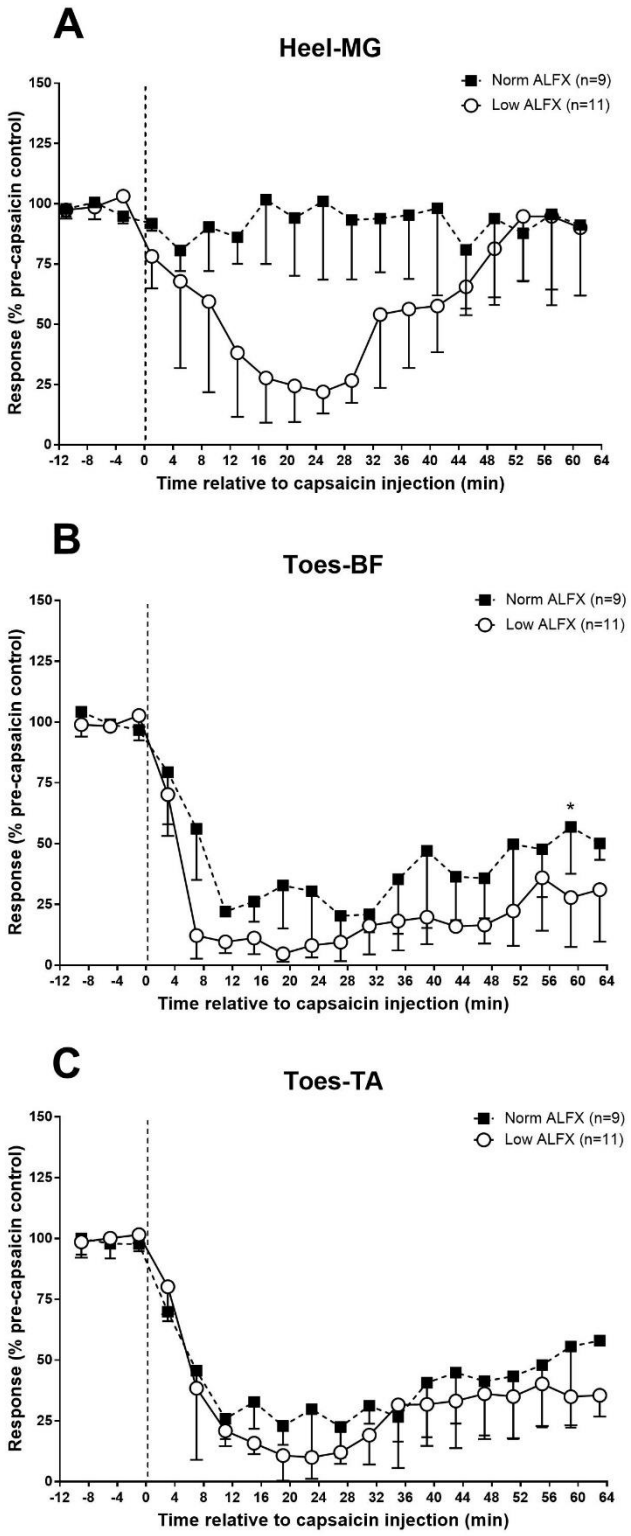

Figure 3.9. Effect of intramuscular injection of 500 µg capsaicin into the contralateral hindlimb on electrically evoked (A) heel-medial gastrocnemius (MG), (B) toes-biceps femoris (BF) and (C) toes-tibialis anterior (TA) reflexes in normal and low alfaxalone groups. Values plotted are medians and errors are interquartile ranges. Dashed line indicates normal alfaxalone data from Study 2. *$p < 0.05$ denotes significant difference in inhibition between alfaxalone levels (Mann-Whitney test).

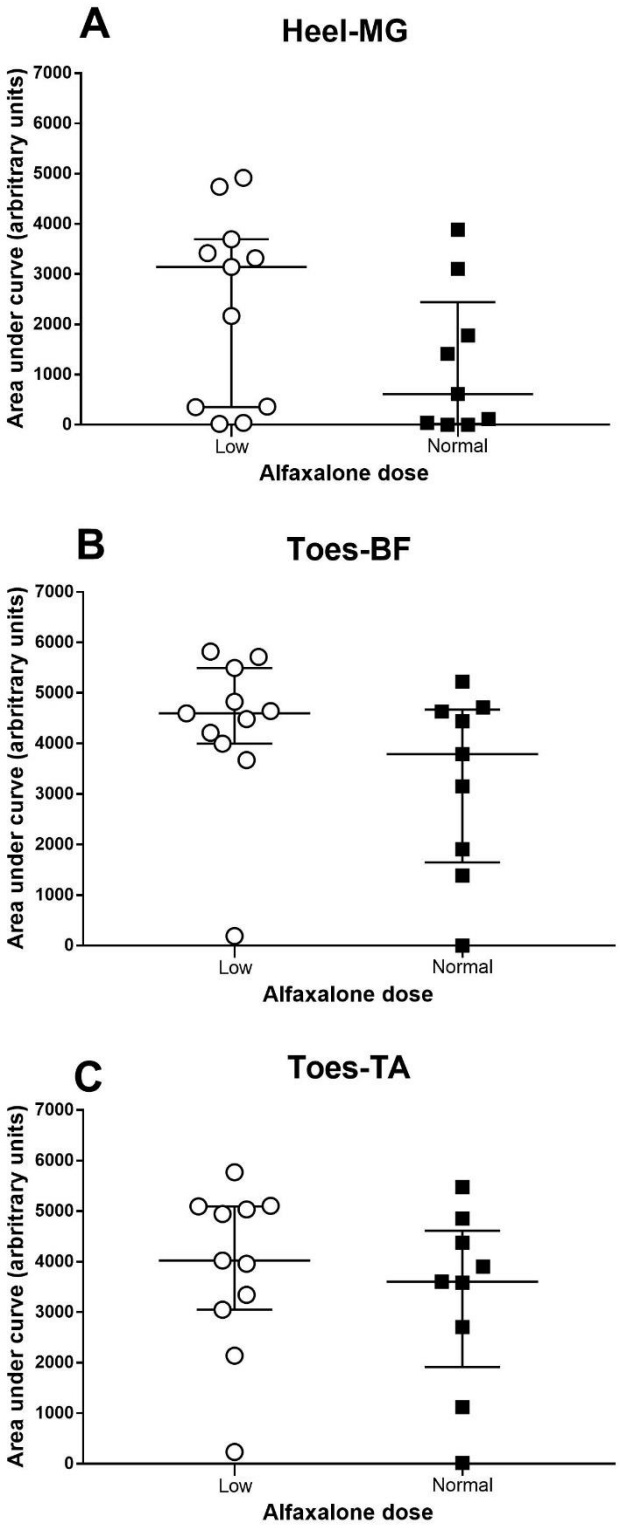

Figure 3.10. Effect of intramuscular injection of 500 µg capsaicin into the contralateral hindlimb on electrically evoked (A) heel-medial gastrocnemius (MG), (B) toes-biceps femoris (BF) and (C) and toes-tibialis anterior (TA) reflexes in normal (n = 9) and low alfaxalone (n = 11) animals. Values plotted are area under curve (AUC) determinations for each animal, with horizontal bars indicating medians and interquartile ranges.

3.3.3.2.2. Injection into the contralateral forelimb

Similar to the effect of capsaicin in decerebrates under normal alfaxalone levels (section 3.3.2.2.2), no significant inhibition of heel-MG reflexes was induced under low alfaxalone (n = 10) conditions (p = 0.1372, Friedman's ANOVA; Figure 3.11A). Similarly, analysis of negative AUC values indicated a significant difference in overall inhibition between the normal and low alfaxalone groups (p = 0.0101, unpaired t-test; Figure 3.12A).

Significant inhibition of toes-BF responses following capsaicin injection was observed under low (n = 10) alfaxalone conditions to a median of 11% (IQR 6–43%) of controls (p = 0.0111, Friedman's ANOVA; Figure 3.11B) and the median duration of inhibition was 63 min (IQR 63 – 63min). This compares a median inhibition of 33% (IQR 28 – 73%) and duration of 51 min (IQR 33 – 63 min) under normal alfaxalone conditions (section 3.3.3.2.2). Although duration of inhibition was not significantly different (p = 0.0851, Mann-Whitney test). Analysis of negative AUC values further supported a significant alfaxalone-dependent difference in overall inhibition (p = 0.0473, unpaired t-test; Figure 3.12B).

Similar to toes-BF responses, significant capsaicin-induced inhibition in toes-TA reflexes occurred under low (n = 10) alfaxalone conditions to a median of 22% (IQR 6 – 57%) of controls (p = 0.0009, Friedman's ANOVA; Figure 3.11C), with inhibition lasting for a median duration of 63 min (IQR 58 – 63 min). Under

normal alfaxalone levels, inhibition had been to 40% (IQR 13 – 68%) of controls and for a median duration of 51 min (IQR 25 – 61 min; section 3.3.2.2.2); comparison of duration of inhibition found a significant difference between normal and low alfaxalone groups ($p = 0.0409$, Mann-Whitney test). Analysis of negative AUC values however was not able to detect a significant difference between the two groups ($p = 0.1456$, unpaired t-test; Figure 3.12C).

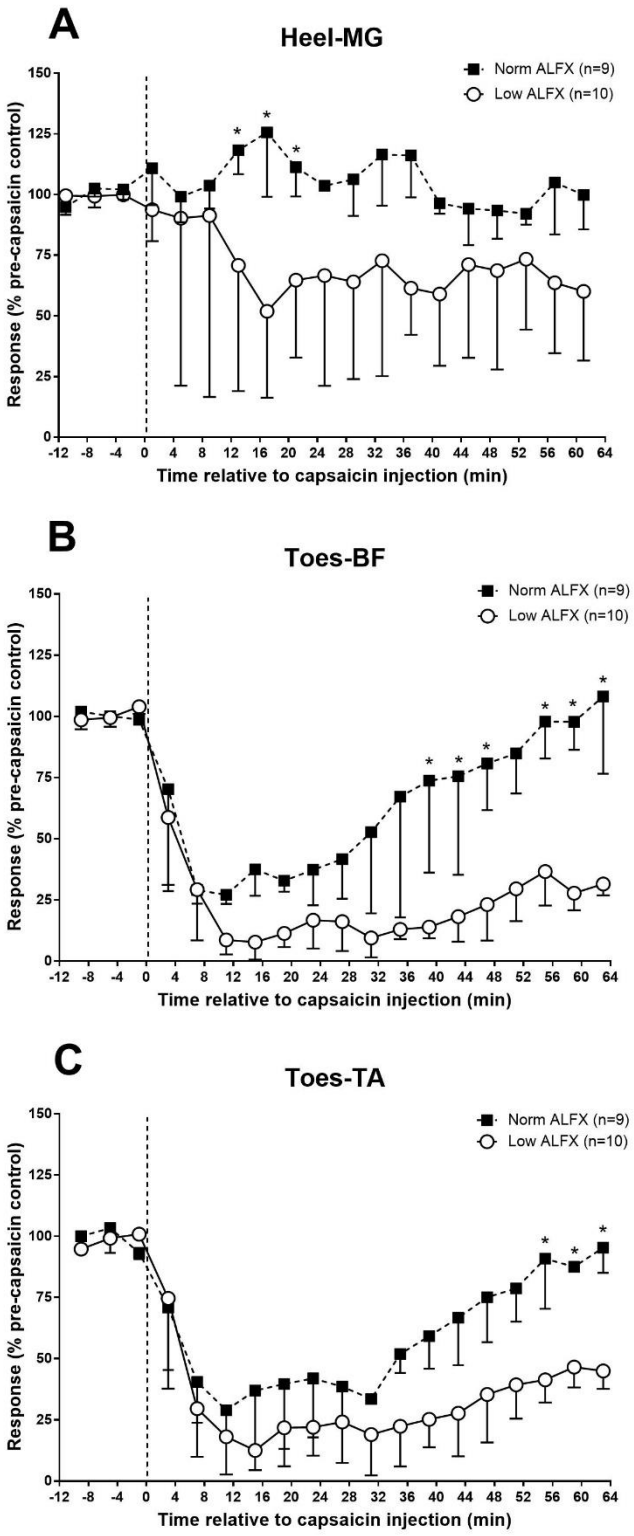

Figure 3.11. Effect of intramuscular injection of 500 µg capsaicin into the contralateral forelimb on electrically evoked (A) heel-medial gastrocnemius (MG), (B) toes-biceps femoris (BF) and (C) toes-tibialis anterior (TA) reflexes in normal and low alfaxalone animals. Values plotted are medians and errors are interquartile ranges. Dashed line indicates normal alfaxalone data from Study 2. *$p < 0.05$ denotes significant difference in inhibition between alfaxalone levels (Mann-Whitney test).

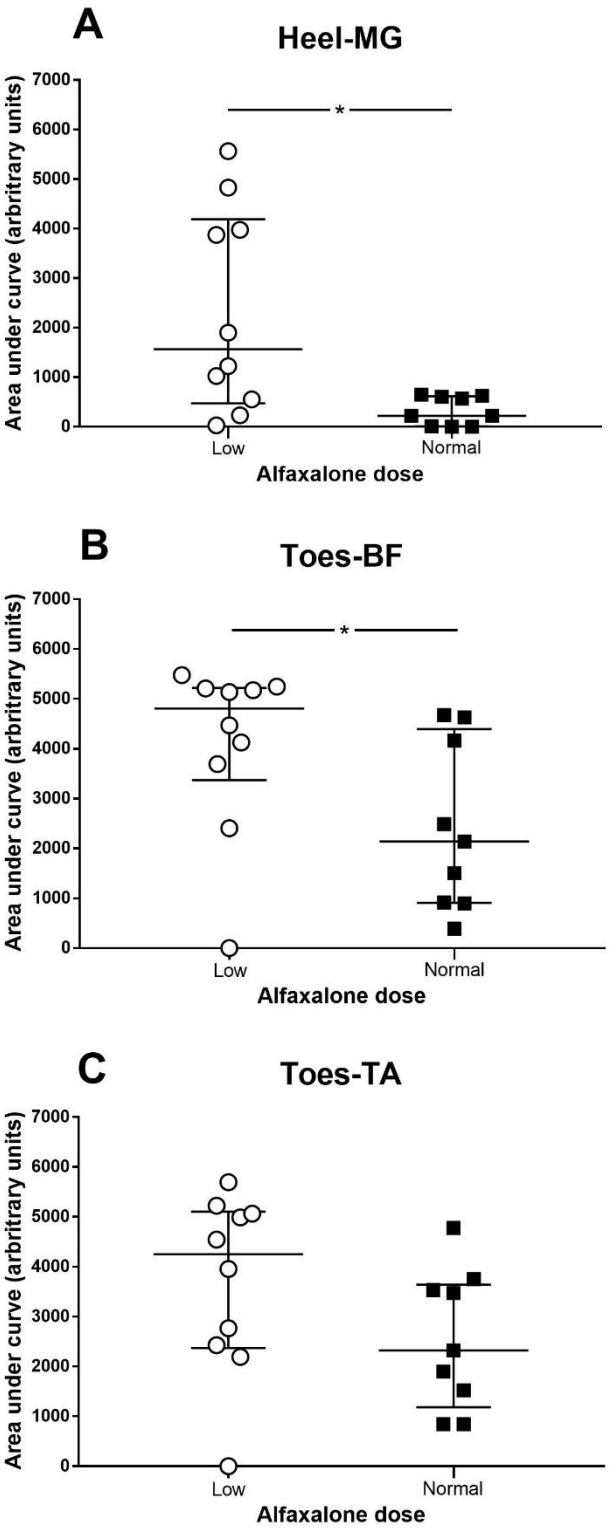

Figure 3.12. Effect of intramuscular injection of 500 μg capsaicin into the contralateral forelimb on electrically evoked (A) heel-medial gastrocnemius (MG), (B) toes-biceps femoris (BF) and (C) and toes-tibialis anterior (TA) reflexes in normal (n = 9) and low alfaxalone (n = 10) animals. Values plotted are area under curve (AUC) determinations for each animal, with horizontal bars indicating medians and interquartile ranges. *$p < 0.05$ denotes significant difference in inhibition between alfaxalone levels (unpaired t-test).

3.3.3.2.3. Effect of capsaicin injection site

Comparison of inhibition of heel-MG, toes-BF or toes-TA responses due to hindlimb or forelimb injections in low alfaxalone experiments found no significant differences between these sites in terms of the depth, duration (in each case $p > 0.05$, Mann-Whitney test) or overall inhibition (i.e. AUC analysis; $p > 0.05$, unpaired t-test) produced.

3.3.4. Study 4: Effect of DNIC on mechanically-evoked reflexes

In this section, data will be compared to responses obtained in Study 1 in intact animals using electrical (test) stimuli and administered 500 µg capsaicin as a conditioning stimulus.

3.3.4.1. Control parameters

3.3.4.1.1. Weight and anaesthetic levels

Animals used in experiments where responses were mechanically-evoked had a mean weight of 389 ± 17 g (n = 9) which was not significantly different to rats where electrical stimuli were used (369 ± 5 g (n = 9); p = 0.3283, Mann-Whitney test; see section 3.3.1.1.1). Following an initial bolus dose (see section 2.2.1.5), animals were infused with alfaxalone at a mean rate of 48.78 ± 2.26 mg kg^{-1} hr^{-1} which again was not statistically different compared to the electrically-stimulated group (48.23 ± 1.94 mg kg^{-1} hr^{-1} (n = 9); p = 0.7962, Mann-Whitney test).

3.3.4.1.2. Mechanical thresholds

Median vF filament threshold values for evoking a response in heel-MG, toes-BF and toes-TA were 60 g (IQR 18 – 80 g), 26 g (IQR 10 – 26 g) and 26 g (IQR 10 – 60 g) respectively, which were not significantly different ($p = 0.2547$, Kruskal-Wallis test).

3.3.4.1.3. Control reflex responses

As would be expected, as vF weight increased median control reflex responses significantly increased in heel-MG, toes-BF and toes-TA ($p < 0.0001$, Kruskal-Wallis test; Table 3.7). No significant differences were found in the size of the three reflex responses at each vF weight ($p > 0.05$, Kruskal-Wallis test).

von Frey (vF) weight (g)	Median control reflex responses (µV.ms)		
	Heel-MG†	Toes-BF†	Toes-TA†
10	31 (12 – 89)	39 (15 – 79)	40 (3 – 77)
26	48 (19 – 188)	87 (61 – 488)	275 (20 – 782)
60	731 (86 – 1057)	664 (523 – 3049)	1497* (536 – 4281)
100	1012 (93 – 6877)	1671* (927 – 5436)	2213* (735 – 5244)
180	1471** (644 – 6048)	2687* (1592 – 6921)	1923* (1365 – 6464)
300	1333** (999 – 6708)	3096* (1510 – 9731)	2905* (1250 – 5988)

Table 3.7. Median control responses in heel-medial gastrocnemius (MG), toes-biceps femoris (BF) and toes-tibialis anterior (TA) to mechanical stimulation (n = 9) using increasing von Frey (vF) filaments prior to administration of 500 µg capsaicin. Values in brackets are interquartile ranges. †$p < 0.05$ denotes significant difference between filaments for a given reflex (Kruskal-Wallis test). *$p < 0.05$ or **$p < 0.01$ denotes significant difference compared to 10 g vF weight for a given reflex (Dunn's multiple comparisons test).

3.3.4.2. Effect of capsaicin

Responses evoked by 10 g and 26 g vF monofilaments were found to be too variable and sometimes absent before and after capsaicin, therefore these responses have been omitted from results.

3.3.4.2.1. Injection into the contralateral hindlimb

Following injection of capsaicin, no significant inhibition of heel-MG responses (n = 9) to 60 g vF monofilaments was found (p = 0.1171, Friedman's ANOVA; Figure 3.13A). However significant inhibition of these reflexes to 100 g, 180 g and 300 g vF weights did occur to a median of 15% (IQR 3 – 61%), 10% (IQR 0 – 21%) and 27% (IQR 6 – 46%) of controls respectively (p = 0.0029, p = 0.0055 and p = 0.0011 respectively, Friedman's ANOVA). Median duration of inhibition was 13 min (IQR 0 – 41 min), 17 min (IQR 0 – 55 min) and 25 min (IQR 7 – 49 min) for 100 g, 180 g and 300 g vF weights respectively which was not significantly different between filaments (p = 0.6771, Kruskal-Wallis test). Analysis of negative AUC values did not reveal any significant difference between overall capsaicin-induced inhibition of heel-MG responses evoked by the 60 – 300 g von Frey weights (p = 0.0806, RM one-way ANOVA; Figure 3.14A).

Significant capsaicin-induced inhibition of toes-BF reflexes (n = 9) evoked by 60 g, 100 g, 180 g and 300 g monofilaments was found to medians of 19% (IQR 0 – 30%), 6% (IQR 0 – 17%), 5% (IQR 3 – 40%) and 6% (IQR 3 – 23%) of controls

respectively ($p < 0.0001$, $p < 0.0001$, $p = 0.0005$ and $p = 0.0012$ respectively, Friedman's ANOVA; Figure 3.13B) and median duration of inhibition was 39 min (IQR 0 – 63 min), 47 min (IQR 8 – 63 min), 47 min (IQR 21 – 63 min) and 47 min (IQR 23 – 59 min) respectively, which was not significantly different between weights ($p = 0.8968$, Kruskal-Wallis test). Negative AUC analysis did not indicate any significant difference in the overall inhibition of the toes-BF response between the 60 – 300 g vF weights ($p = 0.4588$, RM one-way ANOVA; Figure 3.14B).

Capsaicin injected into the contralateral hindlimb caused a reduction in toes-TA responses (n = 9) evoked by 60 g, 100 g, 180 g and 300 g monofilaments to medians of 49% (IQR 20 – 55%), 28% (IQR 17 – 33%), 34% (IQR 16 – 90%) and 33% (IQR 6 – 99%) of controls respectively, however the inhibitory effect for responses evoked by the 180 g vF filament was not found to be significant ($p = 0.0002$, $p = 0.0012$, $p = 0.2578$ and $p = 0.0340$ respectively, Friedman's ANOVA; Figure 3.13C). Median duration of inhibition of the toes-TA response was 27 min (IQR 2 – 49 min), 31 min (IQR 13 – 59 min) and 31 min (IQR 9 – 43 min) for 60 g, 100 g and 300 g vF weights respectively which was not significantly different between filaments ($p = 0.6068$, Kruskal-Wallis test). Further comparison using negative AUC analysis found overall inhibition of toes-TA reflexes by capsaicin was not significantly different for the 60 – 300 g weights ($p = 0.2383$, RM one-way ANOVA; Figure 3.14C).

3.3.4.2.2. Mechanically versus electrically evoked reflex responses

Comparison of mechanically evoked responses using 60 – 300 g vF monofilaments and electrically evoked responses indicated that the level of inhibition induced by capsaicin was similar between groups for heel-MG, toes-BF and toes-TA reflexes ($p = 0.5251$, $p = 0.8931$ and $p = 0.6014$ respectively, Kruskal-Wallis test; Figure 3.13). Similarly, comparison of negative AUC values indicated no significant differences between groups for heel-MG, toes-BF and toes-TA reflexes ($p = 0.9731$, $p = 0.8879$, and $p = 0.2685$, one-way ANOVA).

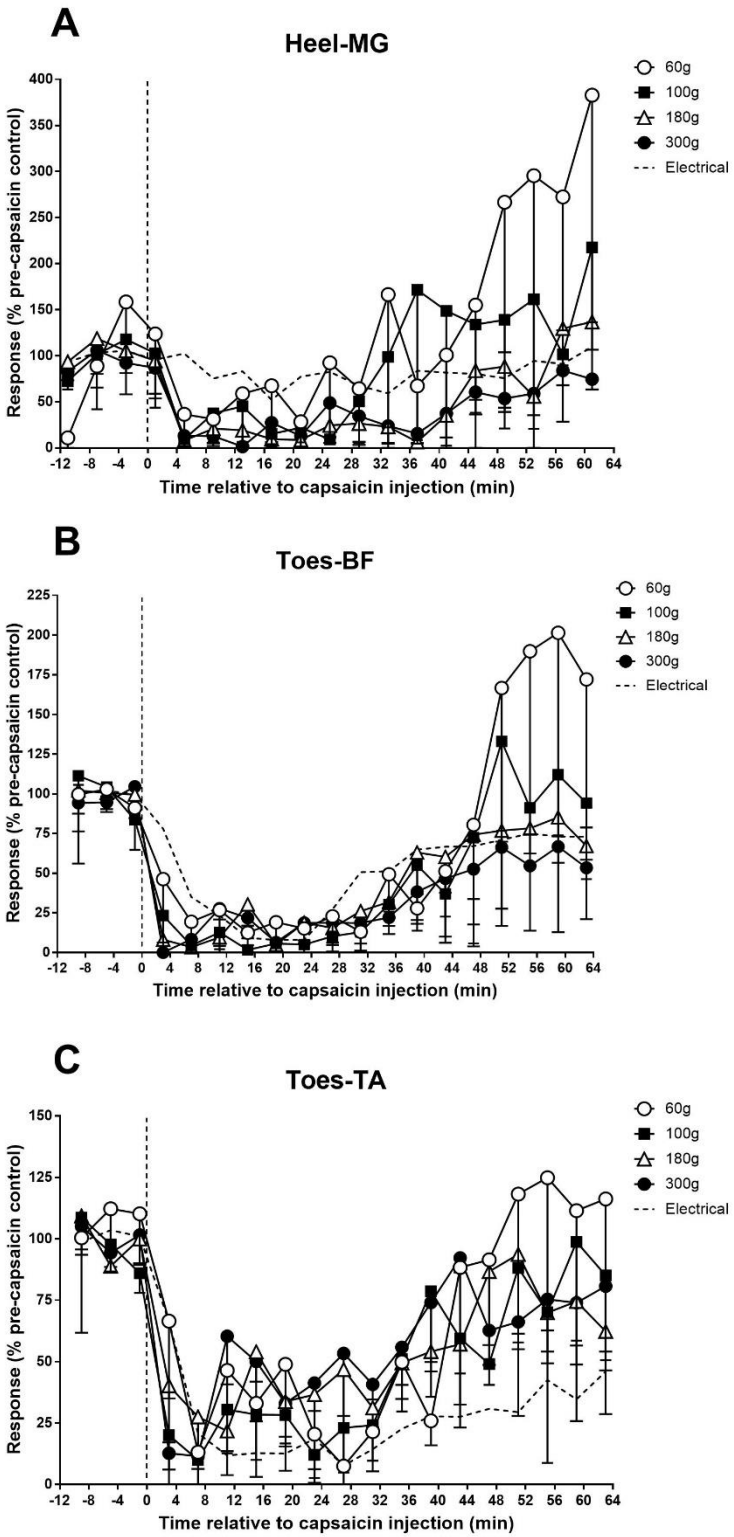

Figure 3.13. Effect of intramuscular injection of 500 µg capsaicin into the contralateral hindlimb on mechanically evoked (n = 9) (A) heel-medial gastrocnemius (MG), (B) toes-biceps femoris (BF) and (C) toes-tibialis anterior (TA) reflexes using 60 g, 100 g, 180 g and 300 g von Frey (vF) monofilaments. Values plotted are medians and errors are interquartile ranges. Electrically evoked responses are shown as a reference only.

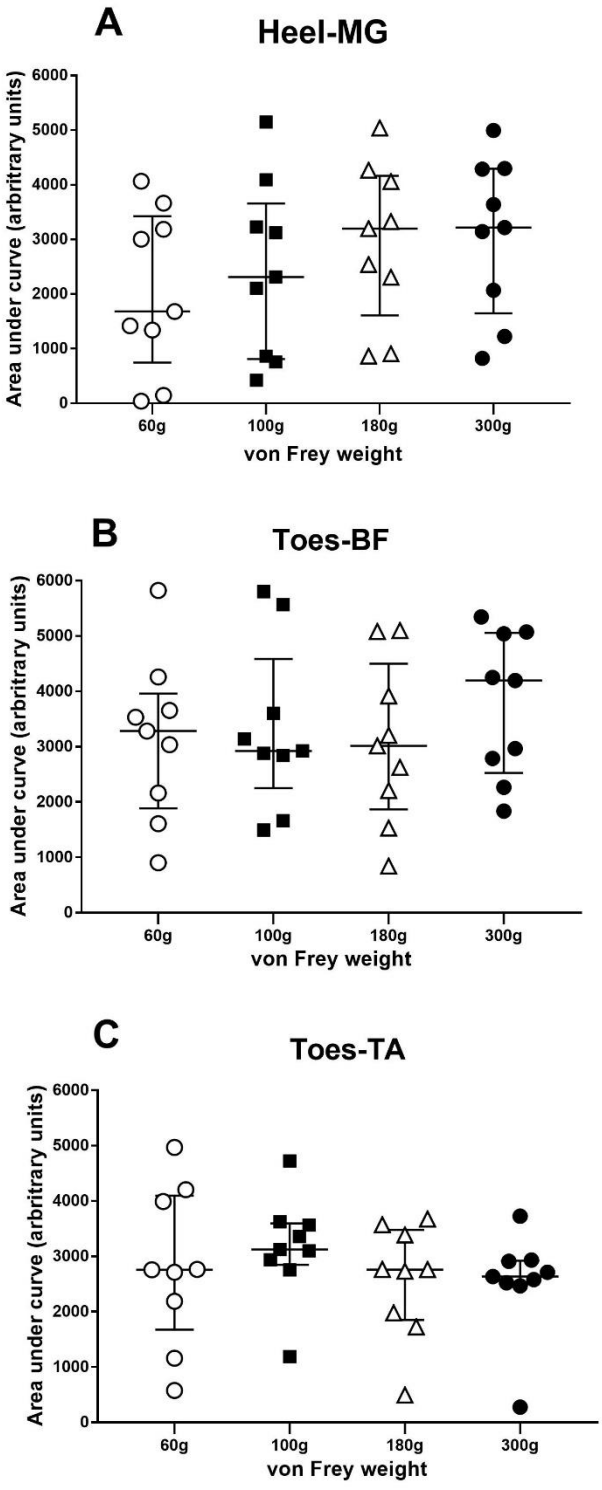

Figure 3.14. Effect of intramuscular injection of 500 µg capsaicin into the contralateral hindlimb on mechanically evoked (n = 9) (A) heel-medial gastrocnemius (MG), (B) toes-biceps femoris (BF) and (C) toes-tibialis anterior (TA) reflexes using 60 – 300 g von Frey (vF) monofilaments. Values plotted are area under curve (AUC) determinations for each animal with horizontal bars indicating medians and interquartile ranges.

3.3.4.2.3. Injection into the contralateral forelimb

Injection of capsaicin into the contralateral forelimb caused a marked reduction in heel-MG reflexes (n = 9) evoked by 60 g, 100 g, 180 g and 300 g vF monofilaments to medians of 11% (IQR 4 – 37%), 17% (IQR 5 – 27%), 5% (IQR 3 – 29%) and 23% (IQR 4 – 43%) of controls respectively, although inhibition of responses evoked by the 60 g vF filament was not quite significant ($p = 0.0533$, $p = 0.0006$, $p = 0.0001$ and $p < 0.0001$ respectively, Friedman's ANOVA; Figure 3.15A). Median duration of inhibition was 41 min (IQR 5 – 61 min), 57 min (IQR 43 – 61 min) and 49 min (IQR 43 – 61 min) for 100 g, 180 g and 300 g vF filaments respectively which was not significantly different ($p = 0.7139$, Kruskal-Wallis test). Similarly analysis of negative AUC values showed no significant difference in overall capsaicin-induced inhibition for 60 g, 100 g, 180 g and 300 g vF monofilaments ($p = 0.6271$, RM one-way ANOVA; Figure 3.16A).

Significant capsaicin-induced inhibition of toes-BF responses (n = 9) evoked by 60 g, 100 g, 180 g and 300 g monofilaments occurred to a median of 3% (IQR 0 – 12%), 10% (IQR 4 – 30%), 4% (IQR 1 – 32%) and 14% (IQR 0 – 21%) respectively ($p < 0.0001$, $p < 0.0001$, $p < 0.0001$ and $p < 0.0001$ respectively, Friedman's ANOVA; Figure 3.15B) with median duration of inhibition being 47 min (IQR 20 – 61 min), 39 min (IQR 16 – 61 min), 55 min (IQR 45 – 63 min) and 39 min (IQR 31 – 61 min) respectively which was not significantly different ($p = 0.5478$, Kruskal-Wallis test). Further analysis using negative AUC found overall

inhibition was not significantly different between the vF weights (p = 0.2465, RM one-way ANOVA; Figure 3.16B).

Significant inhibition of toes-TA responses (n = 9) using 60 g, 100 g, 180 g and 300 g vF filaments was caused by capsaicin to a median of 2% (IQR 0 – 21%), 4% (IQR 0 – 19%), 13% (IQR 0 – 17%) and 19% (IQR 1 – 37%) of controls respectively (p = 0.0001, p < 0.0001, p < 0.0001 and p < 0.0001 respectively, Friedman's ANOVA; Figure 3.15C) For a median duration of 35 min (IQR 10 – 51 min), 39 min (IQR 12 – 63 min), 47 min (IQR 18 – 57 min) and 39 min (IQR 14 – 43 min) respectively, which was not significantly different between filaments (p = 0.7942, Kruskal-Wallis test). Further comparison by analysis of negative AUC values found no significant differences in overall inhibition (p = 0.4265, RM one-way ANOVA; Figure 3.16C).

3.3.4.2.4. Mechanically versus electrically evoked reflex responses

Comparing mechanically evoked reflex responses elicited by 60 – 300 g vF monofilaments with electrically evoked responses indicated no significant differences in the depth of capsaicin-evoked inhibition for the heel-MG, toes-BF and toes-TA responses between the groups (p = 0.1955, p = 0.5872 and p = 0.8912 respectively, Kruskal-Wallis test; Figure 3.15). Negative AUC analysis also indicated no significant differences between overall inhibition of heel-MG, toes-BF and toes-TA reflex responses (p = 0.1209, p = 0.6973 and p = 0.5718 respectively, one-way ANOVA).

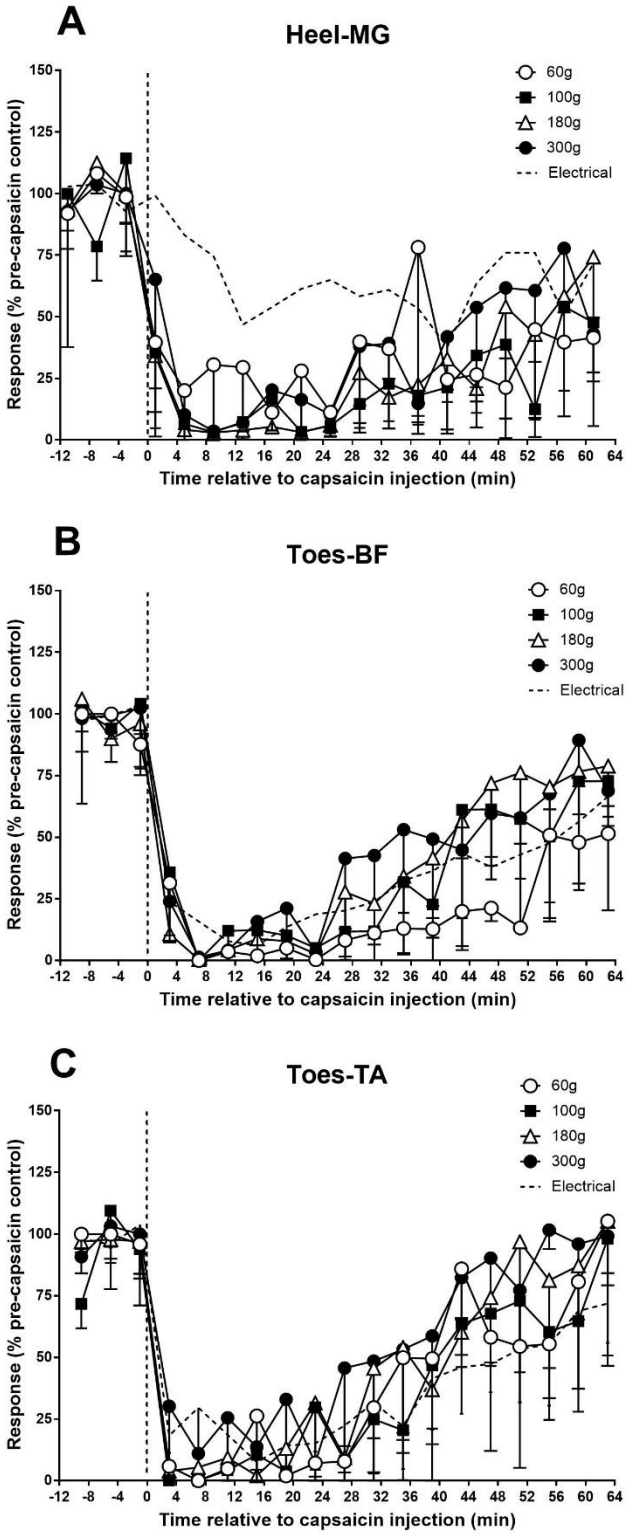

Figure 3.15. Effect of intramuscular injection of 500 µg capsaicin into the contralateral forelimb on mechanically evoked (n = 9) (A) heel-medial gastrocnemius (MG), (B) toes-biceps femoris (BF) and (C) toes-tibialis anterior (TA) reflexes using 60 – 300 g von Frey (vF) monofilaments. Values plotted are medians and errors are interquartile ranges. Electrically evoked responses are shown as a reference only.

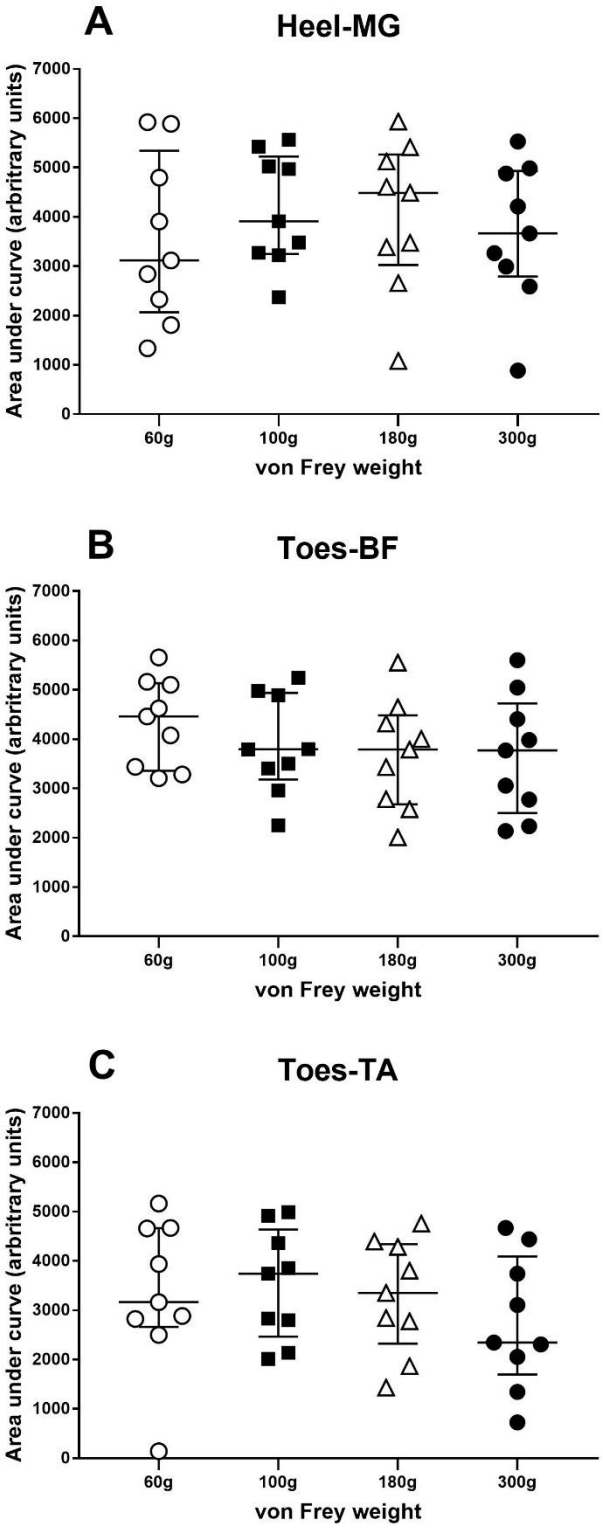

Figure 3.16. Effect of intramuscular injection of 500 µg capsaicin into the contralateral forelimb on mechanically evoked (n = 9) (A) heel-medial gastrocnemius (MG), (B) toes-biceps femoris (BF) and (C) toes-tibialis anterior (TA) reflexes using 60 – 300 g von Frey (vF) monofilaments. Values plotted are area under curve (AUC) determinations for each animal, with horizontal bars indicating medians and interquartile ranges.

3.3.4.2.5. Effect of capsaicin injection site

Comparison of the degree of inhibition of heel-MG responses between hindlimb and forelimb capsaicin injection sites indicated no significant differences using 60 – 300 g filaments ($p > 0.05$, Mann-Whitney test) although duration of inhibition was found to be significantly shorter after the hindlimb injection using 60 g or 300 g vF monofilaments with medians of 0 min (IQR 0 – 0 min) and 25 min (IQR 7 – 49 min) respectively compared to 33 min (IQR 0 – 61 min) and 49 min (IQR 43 – 61 min)($p = 0.009$ and $p = 0.0409$ respectively, Mann-Whitney test). In addition, analysis of negative AUC values suggested overall inhibition was significantly less for the hindlimb compared to the forelimb injection site for the 100 g weight ($p = 0.0203$, unpaired t-test).

For toes-BF and toes-TA reflexes, there was no significant difference between hindlimb and forelimb capsaicin injection sites with respect to depth, duration or overall inhibition of mechanically-evoked responses evoked by any vF filament ($p > 0.05$, Mann-Whitney or unpaired t-test).

3.4. Discussion

DNIC has been proposed as a form of 'counter-irritation' and was first described in spinal convergent neurons after the application of a nociceptive conditioning stimulus outside of their RFs (Le Bars et al., 1979a, 1991). In fact much of the pre-clinical work undertaken on DNIC has been from single cells in the dorsal horn or the trigeminal nucleus caudalis, with only a few studies using reflexes, which did not include the variety of functional responses considered in the present investigation (Cadden et al., 1983; Villanueva et al., 1984; Gjerstad et al., 1999; Danziger et al., 2001). The present studies have therefore shown that reflex responses are inhibited by capsaicin in a dose-related manner and this inhibition is abolished in spinalized animals, altered by decerebration and is dependent on the modality of the test stimulus.

Le Bars and co-workers first outlined that DNIC could be evoked using a variety of noxious conditioning stimulus modalities including pinch using serrated forceps, radiant heat, electrical stimulation and bradykinin (Le Bars et al., 1979a). In fact noxious chemical stimulation has in many studies produced potent inhibitory effects when compared against noxious pinch, heat and electrical impulses, indicating it is an excellent conditioning stimulus for a sustained inhibitory effect (Le Bars et al., 1979a; Gjerstad et al., 1999; Tambeli et al., 2003). In this respect bradykinin exerted large inhibitory effects on dorsal horn responses and trigeminal nucleus caudalis cells for several minutes when injected i.p. and a strong depression (80 – 90%) was also observed when

investigating glutamate-evoked activity which have been due to spatial summation induced by recruitment of a large number of visceral nociceptors (Le Bars et al., 1979a; Dickenson et al., 1980; Villanueva et al., 1984). Other effective noxious chemical conditioning stimuli have included the selective C-fibre irritant mustard oil (Young et al., 1995), which strongly inhibited spinal reflexes in rabbits for over 1 hour when applied to heterotopic skin sites (Harris and Clarke, 2003), and formalin, which produced profound inhibition of the tail-flick response when injected into the hindlimb in rats within the first 10 minutes after injection (Wen et al., 2010).

The present studies employed capsaicin as the chemical DNIC-inducing conditioning stimulus and have shown potent, long lasting inhibition of spinal 'test' reflex responses following its intramuscular injection into the contralateral fore- or hindlimb in intact naïve animals, with responses inhibited to 8% of controls for periods up to and over 60 minutes. Capsaicin is an alkylamide found in Capsicum fruits and is an irritant responsible for the pungency of hot chilli peppers (National Center for Biotechnology Information, 2019). It acts as a prototypic vanilloid receptor agonist and activates TRPV1 channels to transduce pain in the form of a burning sensation (Bevan and Szolcsányi, 1990). That capsaicin produces inhibition of neural responses is not new. Capsaicin administered via intramuscular, subdermal and intracutaneous routes or applied to soft tissue (gingiva) of the mouth produced inhibitory effects to the perception of pain (Dallel et al., 1999; Gjerstad et al., 1999;

Tambeli et al., 2003; Baad-Hansen et al., 2005). Dallel and co-workers reported that 0.1% capsaicin given intracutaneously into the RF of spinal trigeminal nucleus oralis WDR neurons had minimal effects on electrically evoked A-fibre responses but inhibited C-fibre responses to 23% of baseline which did not recover for 60 minutes post-capsaicin (Dallel et al., 1999). Similarly, C-fibre evoked recordings from individual WDR neurons in the lumbar dorsal horn were reduced to 62% of baseline responses after a 200 µg intramuscular injection of capsaicin into the contralateral gastrocnemius soleus muscle (Gjerstad et al., 1999). Noxious stimulus-induced antinociception (NSIA) is a similar inhibitory pain modulation system to DNIC and when the effect of NSIA on the nociceptive trigeminal jaw-opening reflex (JOR) was tested using 250 µg subdermal capsaicin injection to the hindpaw, the JOR was attenuated for 60 minutes with some inhibitions lasting for 2.5 hours (Tambeli et al., 2003).

Capsaicin-induced inhibition in the present studies was shown to be dose-related with 50 µg evoking weaker inhibition and 500 µg showing a stronger inhibitory effect in terms of depth and duration. Clear inhibitory effects appear to require a certain degree of recruitment of peripheral nociceptors whether this is through increased spatial input from a larger area exposed to the conditioning stimulus or via increased temporal input from a stronger stimulus (Le Bars et al., 1979a). As the volume of capsaicin was kept constant for the different doses (100 µl per site), the spatial distribution of the injectate would essentially be the same, therefore a difference in inhibitory effect would likely

be due to the increased activation of TRPV1 receptors within a consistent area. This stimulation of TRPV1 receptors either increased the number of C-fibres activated and/or caused an increased firing rate within these fibres to induce DNIC (i.e. a greater afferent barrage), resulting in a strong relationship between intensity of the conditioning stimulus and the strength of the resulting inhibition (Danziger et al., 2001; Le Bars and Willer, 2010). It would be expected that the 5 mg dose would have a greater inhibitory effect on reflex responses compared to the 500 µg dose, however this was not observed. This lack of increased inhibition for the higher dose may be due to saturation of the TRPV1 receptor population whereby there were no more receptors to be activated or due to desensitization of the TRPV1 receptor which can occur after prolonged exposure to capsaicin (Caterina et al., 2000). As the levels of inhibition often seemed to be reduced at this higher dose, it seems the latter was the most likely cause.

Similar to conditioning stimuli a wide selection of stimulus modalities have been used to evoke test responses such as noxious sustained pinch, tactile stimulation, radiant heat or electrical stimulation (Le Bars et al., 1979a). Few studies however have investigated in any detail the relationship between the test and conditioning stimuli in determining the level of DNIC produced, even though it is evident that they are interdependent (Le Bars et al., 1979a; Arendt-Nielsen et al., 2008; Pud et al., 2009). For instance when using an electrical test stimulus, employing mechanical pressure, thermal heat or electrical

stimulation for the conditioning stimulus led to differing degrees of DNIC (Danziger et al., 2001). Similarly, Dickenson and colleagues demonstrated that electrical test stimuli combined with bradykinin as the conditioning stimulus resulted in 89% inhibition, however when sustained pinch was combined with bradykinin, heat or pinch as the conditioning stimulus a maximal inhibition of 60% was observed (Dickenson et al., 1980). This would indicate electrical test stimulation combined with bradykinin results in greater inhibition than a sustained pinch as the test stimulus. In addition, previous research has indicated that threshold current electrical test stimulation results in greater DNIC induced inhibition of up to 90% when compared to suprathreshold test stimulation suggesting that the effect of DNIC is greater when using reduced electrical test stimulation (Le Bars et al., 1979a; Dickenson et al., 1980). In the present studies, evoking reflex responses mechanically using graded vF filaments offered a more natural approach compared to electrical stimuli for evoking withdrawal reflexes, as afferent fibres of different diameter and state of myelination would be progressively activated in accordance to the pressure applied rather than simultaneously as caused by electrical means (Schaible and Grubb, 1993); it also allowed the effect of the same capsaicin conditioning stimulus to be investigated against six different test stimulus strengths in a short time frame. Consequently, it was found that in naïve animals, the level of DNIC was in fact similar for reflexes evoked by vF filaments in the 60 – 300 g range (unfortunately responses at lower weights were too inconsistent to be useful). Comparing modalities used to evoke reflex responses is difficult but the median level of capsaicin-induced inhibition achieved versus electrically-

evoked responses also seemed generally comparable to that of mechanically-evoked responses. Although 500 µg capsaicin was chosen for its profile in terms of depth and duration of induced inhibition, it could be that this conditioning stimulus was overly effective and did not allow subtle differences against the graded test stimuli to be teased out; further studies could therefore look at lower capsaicin doses for comparison.

It has been shown that DNIC of nervous system excitability at lower spinal cord levels can be evoked by noxious stimuli applied to widespread areas of the body such as the tail, the hind and forelimbs, the ears, the muzzle and the viscera; the extent of evoked inhibition was found to be not only dependent on the strength of the stimulus but also on the location of the conditioning stimulus (Le Bars et al., 1979a). Thus, electrically-evoked responses in dorsal horn neurons were inhibited by noxious pinch to the tail and muzzle by 88% and 85% of controls respectively however to a lesser degree from the contralateral hindlimb, ears and forepaws (70%, 62% and 70% of controls respectively). It was suggested that these differences may be due to a higher degree of central representation from the tail and muzzle as they are important in the behaviour of rats (Le Bars et al., 1979a). Similarly, other studies have found that mustard oil applied to the snout and contralateral MG muscle in rabbits produced different degrees of inhibition of electrically-evoked reflex responses in MG, semitendinosus (ST) and TA (Harris and Clarke, 2003; Harris, 2016). However, in the current study no obvious difference in DNIC was found between capsaicin

injected into the contralateral hindlimb or contralateral forelimb in the intact animal which is similar to that found by Le Bars et al. (1979a) from these two locations.

In contrast, spinalization (complete transection of the thoracic spinal cord) led to complete abolition of capsaicin-induced inhibition for all reflex responses at either injection site, and in fact heel-MG and toes-BF reflex responses showed significant facilitation following capsaicin injection into the contralateral forelimb. This shows that capsaicin-induced DNIC of these reflexes is mediated by supraspinal inhibitory pathways (see section 1.2.5) as has been shown previously for individual dorsal horn neurons using spinalization (Le Bars et al., 1979b; Cadden et al., 1983) or reversible cold block of descending influences (Hall et al., 1982; Dickhaus et al., 1985; Gjerstad et al., 1999). Inhibition of dorsal horn responses has been observed in spinalized animals after noxious stimulation to widespread areas outside their RF (Gerhart et al., 1981; Cadden et al., 1983; Sandkühler et al., 1993) indicating that mechanisms within the spinal cord are also antinociceptive, particularly in studies with high cervical spinalization, therefore propriospinal mechanisms could also contribute to DNIC (Fitzgerald, 1982). However, the complete reversal of DNIC in the present studies suggests no contribution of segmental mechanisms below the thoracic region, particularly in respect of the hindlimb capsaicin injection given its location caudal to the spinal section. Facilitation of withdrawal reflex responses has previously been shown, but in intact rats from the extensor interossei

muscles where facilitation was induced by noxious pinch of the nose (Kalliomäki et al., 1992). Also tail flick withdrawal latency was facilitated by placing the hindpaw in hot water in intact animals as well as spinal (T6 - T7) preparations which was suggested to be aiding an escape reaction in rats where pain can be reduced by widespread noxious stimuli, however reflexes are differentially affected as part of an escape reaction (Morgan et al., 1994). However, the facilitation in the current study was observed in spinalized, not in intact, animals and from the forelimb therefore is not likely of direct neural origin.

Decerebration is a technique to remove higher brain structures or sever sensory centres of the brain from peripheral inputs and can be achieved by mechanical removal or destruction of specific neural tissues (Sapru and Krieger, 1978). Removal of the cerebral cortex and thalamus results in an insensate animal, therefore limits or completely eradicates the need for a continuous anaesthetic regime (Dobson and Harris, 2012; see below). What it also allowed was the contribution of forebrain structures to DNIC of reflexes to be studied. Removal of forebrain structures appeared to affect DNIC of reflexes in the current study with decerebrated animals showing a significantly reduced level and shorter duration of inhibition when capsaicin was injected into the forelimb as well as it appearing reduced after capsaicin injection into the hindlimb. This contrasts to previous electrophysiological studies which indicated that noxious heat immersion of the contralateral hindpaw did not alter pinch-evoked dorsal horn neuronal discharges of the ipsilateral hindpaw in intact decerebrate

animals compared to intact anaesthetised animals (McGaraughty and Henry, 1997) as well as early lesioning studies by Le Bars and co-workers. They found that DNIC was subserved by a supraspinal loop with the ascending parts of the loop contained within the ventrolateral quadrant of the cervical spinal cord where lesions were found to decrease DNIC (Villanueva et al., 1986b) and the descending loop located in the dorsolateral funiculus of the spinal cord (Basbaum and Fields, 1979; Villanueva et al., 1986a). Lesions of brainstem structures including the locus coeruleus/subcoeruleus (Bouhassira et al., 1992a) and RVM (Bouhassira et al., 1993) were found to have no effect of the efficacy of DNIC . Similarly, thalamic lesions were found to have no effects on DNIC induced inhibition (Villanueva et al., 1986b; De Broucker et al., 1990) and neither were lesions to PAG, CNF and PB which are directly involved in pain modulation (Bouhassira et al., 1990). However, lesions to the SRD did produce a marked reduction, but not complete abolition, in the efficacy of DNIC (Bouhassira et al., 1992b). However, in contrast to the above findings, other studies using lidocaine injections into the MRF and medullary NRM were found to abolish or partially block spinal inhibition produced by DNIC (Morton et al., 1987), so these areas may also be involved as well. A more recent study has suggested that the PB neurons, whilst not directly involved in DNIC induced inhibition, are key components to the supraspinal ascending-descending loop (Lapirot et al., 2009).

In addition to effects on DNIC, there were also differences between anaesthetised intact, decerebrated or spinalized animals on reflexes per se suggesting that these muscles are differentially controlled. In intact animals, heel-MG reflexes had significantly higher electrical thresholds when compared to toes-BF/TA and subsequently higher stimulation strengths were used to evoke the reflex response. This is similar to previous studies in the rat whereby thresholds for evoking reflexes in MG from the heel were significantly greater than those for evoking responses in TA and ST from the toes (Schouenborg and Kalliomäki, 1990). However, mean electrical thresholds for evoking the heel-MG reflex were decreased in spinalized and decerebrate animals compared to intact animals, whereas thresholds for evoking flexor reflexes from the toes were not significantly different for the three preparations. This suggests that this extensor response in rats is tonically inhibited by descending pathways involving structures rostral to the colliculi which thereby set the gain of the reflex, whereas threshold values for flexors are consistently low and not modulated by descending pathways, allowing them to be the dominant responders. Decerebrate spinal preparations in rabbits are found to have significantly lower thresholds from evoking reflex responses from the heel, however are not altered in decerebrate non-spinal preparations (Harris and Clarke, 2003). Similarly, reflex responses evoked from the toes were found to be higher in decerebrate non-spinal rabbits but remain unaltered in decerebrate spinal rabbits indicating that thresholds are altered by various preparations (Harris and Clarke, 2003). Other studies have shown thresholds for multiple reflex responses are all reduced following spinalization in

unanaesthetised decerebrate rats for periods of up to 8 hours (Schouenborg et al., 1992). Reduction in thresholds after spinalization is an indication of hyper-excitability of reflex responses caused by disruption of tonic descending inhibitory pathways (Dickhaus et al., 1985; Cervero et al., 1991; Gjerstad et al., 1999) and as such reflex responses in previous studies from various muscles are found to be hyper-excitable (Dickhaus et al., 1985; Schouenborg et al., 1992; Harris and Clarke, 2003). Similarly, heel-MG and toes-BF/TA responded differently to noxious capsaicin injection with toes-BF/TA responses appearing to be more susceptible to DNIC than heel-MG responses which would suggest these reflexes are differentially modulated via descending controls. When evoked using electrical stimulation heel-MG reflex responses were often not inhibited by the DNIC conditioning stimulus, however toes BF/TA were inhibited to varying degrees in intact preparations. Previous studies have indicated in rabbit that reflex responses in MG, TA and ST could all be inhibited for over 1 hour after the application of mustard oil to the snout or contralateral MG muscle (Harris and Clarke, 2003).

Alfaxalone is a neuroactive steroid that enhances the interaction of the inhibitory neurotransmitter GABA with its ionotropic $GABA_A$ receptors by moving chloride into the cell, hyperpolarising the neuron and inhibiting action potential propagation thereby causing modulation of this ligand-gated chloride channel resulting in anaesthesia and muscle relaxation (Harrison and Simmonds, 1984; Lambert et al., 2003; White et al., 2017). Alfaxalone used in

electrophysiology recordings increased nociceptive thresholds and decreased response magnitude, however maintained the ability to increase responses with increased stimulus strength (Hunt et al., 2016). This makes it an excellent and stable anaesthesia to use in reflex response studies (White et al., 2017). The present studies have shown that altering the level of alfaxalone anaesthesia had a significant effect on reflex parameters (lower median electrical thresholds and stimulation strengths when levels were reduced). These observations would be easily predicted in animals which are given a reduced anaesthesia rate as anaesthesia is known to impact on pain responses (Stamford, 1995). Intravenously administered alfaxalone has been found to cause complete loss of a toe-pinch reflex in iguanas after just over 2 minutes of a 5mg kg^{-1} dose suggesting that alfaxalone has strong depressive influences on reflexes (Knotek et al., 2013).

However, the anaesthetic regime implemented in DNIC studies is often overlooked but could play a key role on the efficacy of DNIC (Jinks et al., 2003a). The use of decerebrate animals therefore also allows different levels of anaesthesia to be employed with the possibility of pain or distress fully removed (Silverman et al., 2005). Consequently, in the current studies, under low levels of alfaxalone there appeared to be greater DNIC efficacy than under high alfaxalone conditions indicating a stable level of anaesthesia is important. Although alfaxalone has not been previously studied, published literature indicates that other anaesthetics affect DNIC, with increased levels of

isoflurane depressing DNIC induced by tail or hindpaw clamp on dorsal horn recordings evoked by noxious thermal stimulation to the hindpaw (Jinks et al., 2003a). Similarly, mechanically evoked dorsal horn recordings (noxious pinch to the hindpaw) were strongly inhibited by noxious pinch to the muzzle, however this DNIC induced inhibition was lost when halothane anaesthesia was increased from 1.3% to 2.5% but was able to be restored by reducing halothane to previous levels (Tomlinson et al., 1983). When DNIC induced by noxious heat and bradykinin were compared in sodium pentobarbitone or halothane anaesthesia regimes, dorsal horn recordings evoked by electrical stimulation were inhibited in both regimes to varying degrees (Alarcón and Cervero, 1989). Using barbiturate anaesthesia the majority of neurons were inhibited in response to noxious heat and bradykinin by 40% and 46% respectively (Alarcón and Cervero, 1989). Contrastingly, using halothane anaesthesia caused inhibition of nearly all neurons in response to noxious heat and bradykinin by 71% and 78% respectively indicating halothane anaesthesia inhibits more cells and to a higher magnitude than barbiturate regimes (Alarcón and Cervero, 1989).

Finally, another consideration is the manifestation of DNIC in different species of animal. In this study Sprague-Dawley rats have been used, however other studies have used many other species including the mouse (Fleischmann and Urca, 1989), cat (Morton et al., 1987, 1988; Alarcón and Cervero, 1989; Wen et al., 2010), rabbit (Harris and Clarke, 2003; Harris, 2016), dog (Hunt et al., 2018)

and primate (Gerhart et al., 1981; Brennan et al., 1998). In the current studies preliminary experiments (results not shown) using a conditioning stimulus consisting of a noxious pinch to the contralateral forelimb or muzzle, or mustard oil to the muzzle, had no effect on electrically-evoked reflex responses in the rat. However noxious pinch to the muzzle has been found to be very potent in rats in other studies and has therefore elicited strong DNIC (Le Bars et al., 1979a; Schouenborg and Dickenson, 1985). Similarly, mustard oil is also considered to be a strong noxious stimulus capable of evoking DNIC in rabbits when applied to the snout (Harris and Clarke, 2003; Harris, 2016). Experiments in dogs found DNIC difficult to evoke using cold water to the paw (Hunt et al., 2018), however other studies in humans have shown that noxious cold induces a good level of measurable DNIC inhibition (Gehling et al., 2016; Granovsky et al., 2016).

Chapter Four

Diffuse noxious inhibitory controls of nociceptive withdrawal reflexes in the monosodium iodoacetate model of osteoarthritis (28-35 days post-induction)

4.1. Introduction

OA is a type of joint disease affecting articular cartilage, subchondral bone, synovium, the capsule and ligaments causing cartilage degeneration, fibrillation, fissures and complete loss of the joint surface leading to damage of the underlying bone (Cooper et al., 2015)(see section 1.1). In chronic pain states, such as OA, continued nociceptive input from the affected joint peripherally leads to central sensitization, part of which may result from altered descending pathways (Danziger et al., 1999)(see section 1.2.5). Modification of descending inhibitory pathways, including those involved in DNIC, potentially causes a reduction in their efficacy resulting in maintenance of chronic pain (Danziger et al., 1999). As spinally organised withdrawal reflexes are modulated by descending inhibitory pathways, which set an appropriate threshold for excitability as well as the dimensions of the reflex's RF (Schouenborg et al., 1992), OA-induced alterations in these pathways should be reflected in changes in reflex responses.

Pre-clinical animal models are an important tool for investigating changes which occur during OA (see section 1.5.6). As previously discussed, there is no one animal model of OA that is perfect, each having its advantages and disadvantages. For the following studies the MIA model (see section 1.5.7) was chosen as the most appropriate due to its ease of induction, the rapid timeframe over which the model develops and, as peripheral and central sensation are of interest to this study, these pain mechanisms are known to

occur and have been partially characterised in this model (Sagar et al., 2010, 2011; Kelly et al., 2012, 2013a, 2013b). The MIA model mimics behavioural, pathogenic and pharmacologic features associated with human OA including synovial inflammation, chondropathy and osteophytosis (Bove et al., 2003; Mapp et al., 2013). At 14 days post-MIA injection, the MIA model is considered to be a neuropathic pain model, with extensive damage observed in the subchondral bone marrow and these areas are replaced by loose spindle fibres and separated from the normal trabecular bone and marrow areas (Guzman et al., 2003). Chondrocyte clusters (chondrones) are also observed between normal and necrotic cartilage (Guzman et al., 2003). Proteoglycan loss is widespread throughout the cartilage as well as signs of stresses in the cartilage with bone reabsorption continuing and the beginnings of osteophytes (Mapp et al., 2013). Between 21-28 days post injection the cartilage layer is extensively thinned, subchondral bone is thickened and osteophytes are continuing to grow (Fernihough et al., 2004). Throughout this period animals show significant pain behaviour in both weight bearing asymmetry, tactile allodynia and mechanical hyperalgesia (Fernihough et al., 2004).

4.2. Methods

Experiments were performed on a total of 84 male Sprague-Dawley rats (mean weight 150 g, range 133 – 188 g) housed as previously described (see section 2.1). Prior to electrophysiology, all animals underwent the following procedure to either induce the MIA model (n = 43) or to be part of the saline control group (n = 41).

4.2.1. Induction of monosodium iodoacetate (MIA) model

The MIA model was induced following a protocol outlined in previous studies (Guingamp et al., 1997; Kelly et al., 2013b; Mapp et al., 2013; Sagar et al., 2014). Asepsis was maintained throughout the procedure in accordance with a standard operating procedure (SOP) approved by the Named Veterinary Surgeon (NVS). Each animal was placed into a transparent induction chamber and anaesthetised using 3% isoflurane in 2 L min^{-1} oxygen until the animal lost its righting reflex. The rat was then transferred to a nose cone where the isoflurane was reduced to 2% in 2 L min^{-1} oxygen, with a pinch to the hindpaw ensuring the animal was areflexic and appropriately anaesthetised. The left hindlimb was shaved from the ankle joint to midway between the knee and hip joints and cleaned with Virusan gel (Clinipath Equipment Limited, Hull, UK) on a sterile swab. The animal was then placed on a sterile drape where the shaved area was again cleaned with Virusan gel. Using sterile gloves, and with the knee joint at a 90° angle, the joint space was injected with 1 mg sodium iodoacetate ≥ 98% (MIA, Sigma-Aldrich, Dorset, UK) in 50 µl of sterile saline via the patella

tendon using a 12 mm, 29-gauge needle fixed to a 0.5 ml insulin syringe (VWR International Ltd, Leicestershire, UK) which was filled prior to surgery from a freshly prepared stock solution of 20 mg MIA in 1 ml sterile saline (a separate Eppendorf of stock solution was made for each rat). Control animals received the same surgical procedure but only 50 µl sterile saline was injected. Following injection, animals were placed in a recovery cage heated to 37 °C until they were upright and fully recovered, before being returned to a clean home cage (up to four rats per cage). Following injection animals were monitored closely, with twice daily weight checks and gait scoring as well as checks for normal activity, hunched posture, starey coat, discharge from the eyes/nose, dehydration, a satisfactory wound, the presence of swelling or limping for the first 4 days post-injection and every other day thereafter for the duration of the study.

4.2.2. Assessment of pain behaviour

The MIA model is known for its association with mild pain-like behaviour (Ogbonna et al., 2013; Sagar et al., 2014). At least 1 day prior to injection animals were habituated to the behavioural testing equipment to reduce stress. Animals were assessed immediately before knee joint injection (baseline; day 0) and every 7 days during the 28-35 day post-injection period. Behavioural testing was performed at a similar time on each given day for consistency and to reduce the effect of circadian rhythms on pain (Konecka and Sroczynska, 1998; Christina et al., 2004).

4.2.2.1. Weight bearing analysis

Pain arising from the injected joint can be measured indirectly by assessing the weight borne on each leg, or on hindlimbs, in OA patients and pre-clinical animal studies respectively and used as a measure of pain and discomfort (Swagerty and Hellinger, 2001; Bove et al., 2003; Combe et al., 2004; Bove et al., 2006; Kelly et al., 2013b; Mapp et al., 2013; Ogbonna et al., 2013; Moilanen et al., 2015). Weight bearing asymmetry was assessed using an incapacitance tester (Linton Instruments, Norfolk, UK) to measure weight distribution between the ipsilateral (injected) and contralateral (non-injected) hindlimb of each rat. This comprised of a Perspex box which was angled to allow the rat to place its forelimbs freely, whilst each hindlimb rested in the centre of two separate transducer pads which recorded the weight exerted by each one (Figure 4.1). Once a rat was settled in this position, recordings were taken over a three second period and averaged by the incapacitance tester. Readings were taken in triplicate and averaged for analysis. Results are presented as the gram weight difference between the ipsilateral and contralateral hindlimbs with respect to the ipsilateral limb, such that equal weight distribution is represented by 0 g, increased weight on the contralateral hindlimb is a positive gram value and increased weight on the ipsilateral hindlimb is a negative gram value.

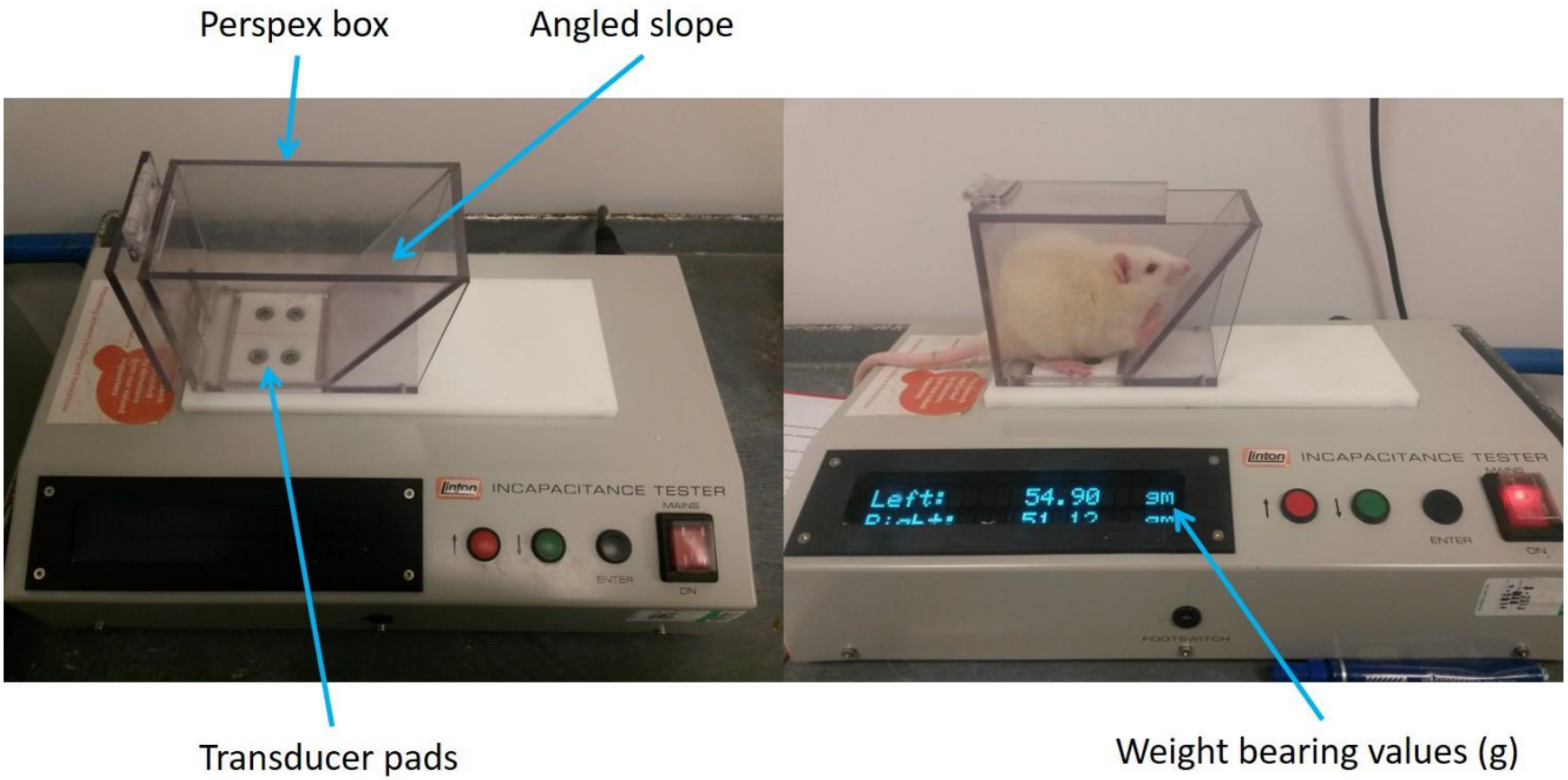

Figure 4.1. Incapacitance tester for weight bearing analysis.

4.2.2.2. Assessment of mechanical paw withdrawal thresholds

Mechanical allodynia and hyperalgesia are key features of pain in OA (Schaible et al., 2002). These can be tested using vF monofilaments applied to the plantar surface of each hindpaw; a method which is regularly utilised in preclinical pain studies (Mapp et al., 2013; Ogbonna et al., 2013; Nwosu et al., 2016b). The methodology used was adapted from the up-down method (Chaplan et al., 1994), by which animals were placed into Perspex boxes over a metal cross-grid floor, therefore allowing access to the plantar surface of each hindpaw (Figure 4.2). Hindpaw withdrawal thresholds were then measured by applying each vF monofilament perpendicular to the skin in the mid-plantar region (just proximal to the less sensitive footpad) for 3 seconds. The range of vF monofilaments used were 0.16, 0.4, 0.6, 1.0, 2.0, 4.0, 6.0, 8.0, 15.0 and 26.0 g. Testing began by applying the 2.0 g monofilament, and if there was no response, successively higher filaments were applied until a rapid withdrawal occurred. At this point the next lower vF monofilament was reapplied, and if no response occurred the next higher force was again used; hence the up-down method. A total of 6 withdrawal responses were recorded with the lowest consistent force required to evoke a withdrawal response classified as the PWT. To avoid lifting the paw during testing, and to prevent sensitization of the plantar surface, the 26.0 g monofilament was the maximum force used to assess PWTs.

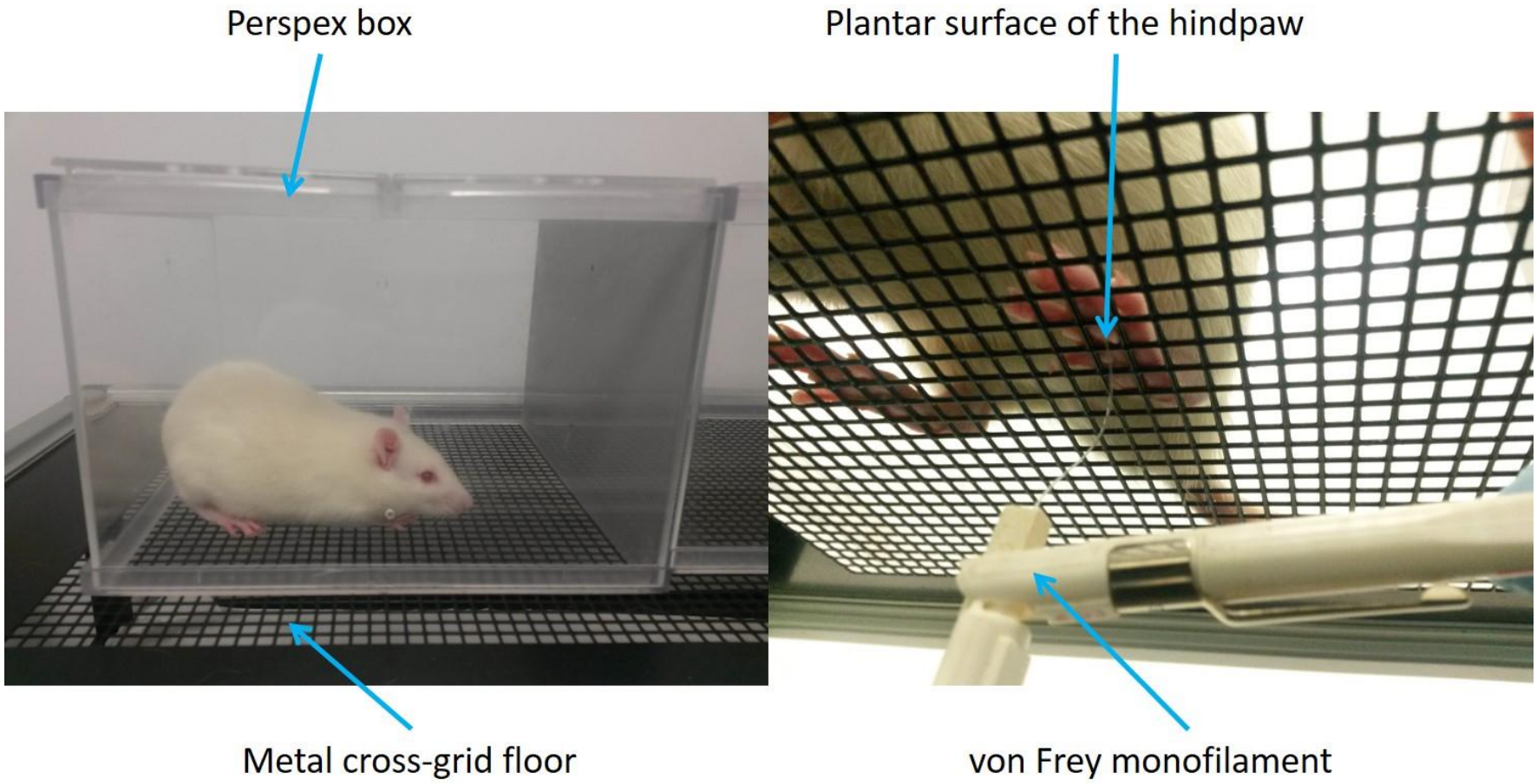

Figure 4.2. Paw withdrawal threshold (PWT) assessment via application of von Frey (vF) monofilaments.

4.2.3. Assessment of knee joint damage

Following electrophysiological recordings (see below) and euthanasia by anaesthetic overdose, both hindlimbs were immediately removed just below the hip bone in a number of MIA and saline-injected animals. The skin was removed and hindlimbs were frozen at -20 °C for joint damage assessment at a later time point.

Knee joint damage was subsequently quantified using a macroscopic photographic chondropathy score (PCS) methodology based on the appearance of the articular surfaces (Walsh et al., 2009). Following overnight thawing at -4 °C, overlying muscle was removed from around the joint and the MCL and LCL cut followed by the ACL and PCL until the tibiofemoral joint could be separated to expose the cartilage on each surface. The femoral condyle and tibial plateau were then individually photographed and the severity and extent of loss of surface integrity of articular cartilage were recorded on a joint scoring sheet (Figure 4.3A)(Dougados et al., 1994). Joints were then annotated with approximate area of damage and severity and these areas graded according to Walsh et al. (2009)(Figure 4.3B). In addition, the photographs were used to separately assess joints using ImageJ software (version 1.51k; National Institutes of Health, Maryland, USA) to mark out areas with damage, hence calculate the percentage area with each category of surface damage for the medial and lateral portions of the tibial plateau and femoral condyle. Using

these graded percentage data joint OA severity was then calculated and classified using the following three systems:

i) Collin's classification tree scoring (Figure 4.4A) which grades OA at the articular surface based on the presence, extent and severity of OA changes (Collins, 1949). Severity is allocated based on the appearance of the joint using the previously referred to grading system (Figure 4.3B), and results range from grade 0 to grade IV, with 0 representing limited damage.

ii) Original Système Française D'Arthroscopie (SFA) scoring (Figure 4.4B) was derived by combining two formulas by Dougados et al. (1994) which depend on whether the compartment was medial or lateral and on the percentage of articular surface allocated to each severity grade (Figure 4.3B). Scores for joint damage can range from -9.2 to +2650.8 which results in joints with no damage as -9.2.

iii) Revised SFA scoring (Figure 4.4C) derived using modifications of the original SFA scoring formulae (Ayral et al., 1994) where the medial and lateral sections of the tibial plateau and femoral condyle are graded based on the percentage of articular surface damage (Figure 4.3B). Scores are 0 to +400 which allows a joint with no damage to be classified as 0 rather than give negative scores.

A

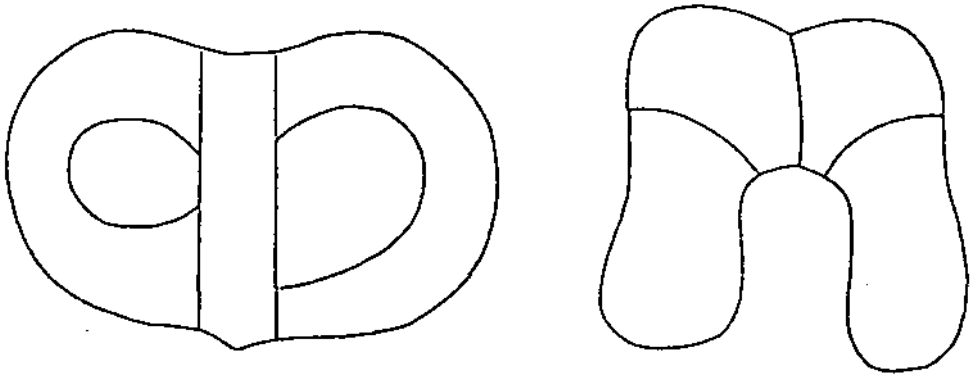

B

Grade	Surface Appearance
0	Normal – smooth, unbroken surface, homogenous white to off-white colour
1	Swelling and softening – a little brown homogeneous colouration
2	Superficial fibrillation – lightly broken surface, white to off-white/light brown in colour
3	Deep fibrillation – coarsely broken cartilage surface, dark brown, grey or red colour
4	Subchondral bone exposed – stippled white and dark brown/red in colour

Figure 4.3. Grading of severity and extent of loss of surface integrity of articular cartilage. (A) Joint scoring sheet for the tibial plateau (left) and femoral condyle (right)(Dougados et al., 1994). (B) Graded scoring system based on the surface appearance of the joint (Walsh et al., 2009).

A

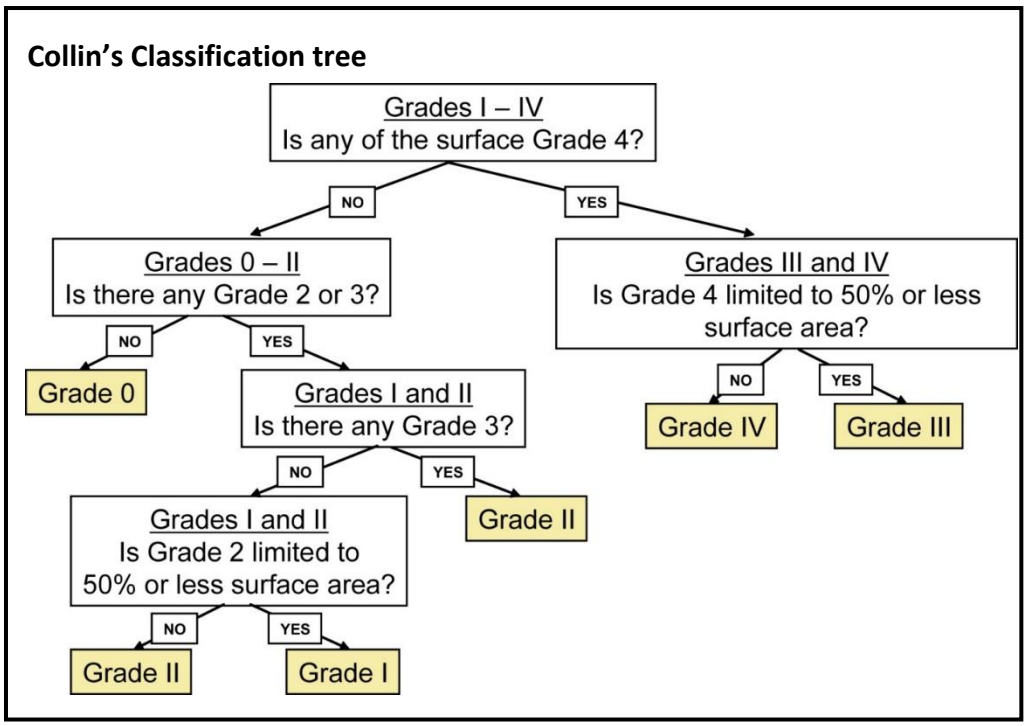

B

Original SFA Score

Medial surface = −2.2 + (Grade1 × 1.3) + (Grade2 × 2.2) + (Grade3 × 3.4) + (Grade4 × 7.2)

Lateral surface = −2.4 + (Grade1 × 0.8) + (Grade2 × 2.3) + (Grade3 × 5.0) + (Grade4 × 6.1)

Total Joint = sum of the lateral/medial femoral condyle and tibial plateau

C

Revised SFA Score

Score = (Grade1 × 0.14) + (Grade2 × 0.34) + (Grade3 × 0.65) + Grade4

Figure 4.4. (A) Classification tree for Collin's grading of osteoarthritic (OA) changes at the articular surface (Collins, 1949). (B) Original Système Française D'Arthroscopie (SFA) score based on a global assessment of OA changes in the articular surfaces (Dougados et al., 1994). (C) Revised SFA score which is a modified version of the original SFA system allowing normal joints to be scored as 0 (Ayral et al., 1994).

4.2.4. Electrophysiological studies

Animals were surgically prepared for electrophysiological studies as described in section 2.2.1. Reflexes were evoked using electrical or mechanical stimulation of the heel and toes and recorded in MG or BF and TA respectively, as previously detailed (section 2.2.2). Stock capsaicin solution was prepared to 5 or 0.5 mg ml^{-1} injection concentrations (section 3.2.1) and injected as a conditioning stimulus into contralateral forelimb and hindlimb locations as previously described (section 2.2.3).

The first set of experiments comprised four groups: MIA-injected (n = 9) or saline-injected (n = 10) with reflexes evoked electrically and MIA-injected (n = 11) or saline-injected (n = 10) with reflexes evoked mechanically. For all groups 100 µl of 5 mg ml^{-1} capsaicin (i.e. 500 µg) was used as the DNIC-inducing stimulus.

Due to the strong relationship between the test and conditioning stimulus when investigating DNIC, a lower capsaicin dose (100 µl of 0.5 mg ml^{-1} i.e. 50 µg) was used to induce inhibition in MIA and saline-injected animals to allow possible subtle differences in DNIC between groups to be detected. This lower conditioning stimulus was again tested in 4 groups: MIA (n = 10) and saline-injected (n = 10) animals with reflexes evoked electrically and MIA (n = 13) or saline-injected (n = 11) animals using mechanically-evoked reflex responses.

4.3. Results

4.3.1. Joint severity scoring

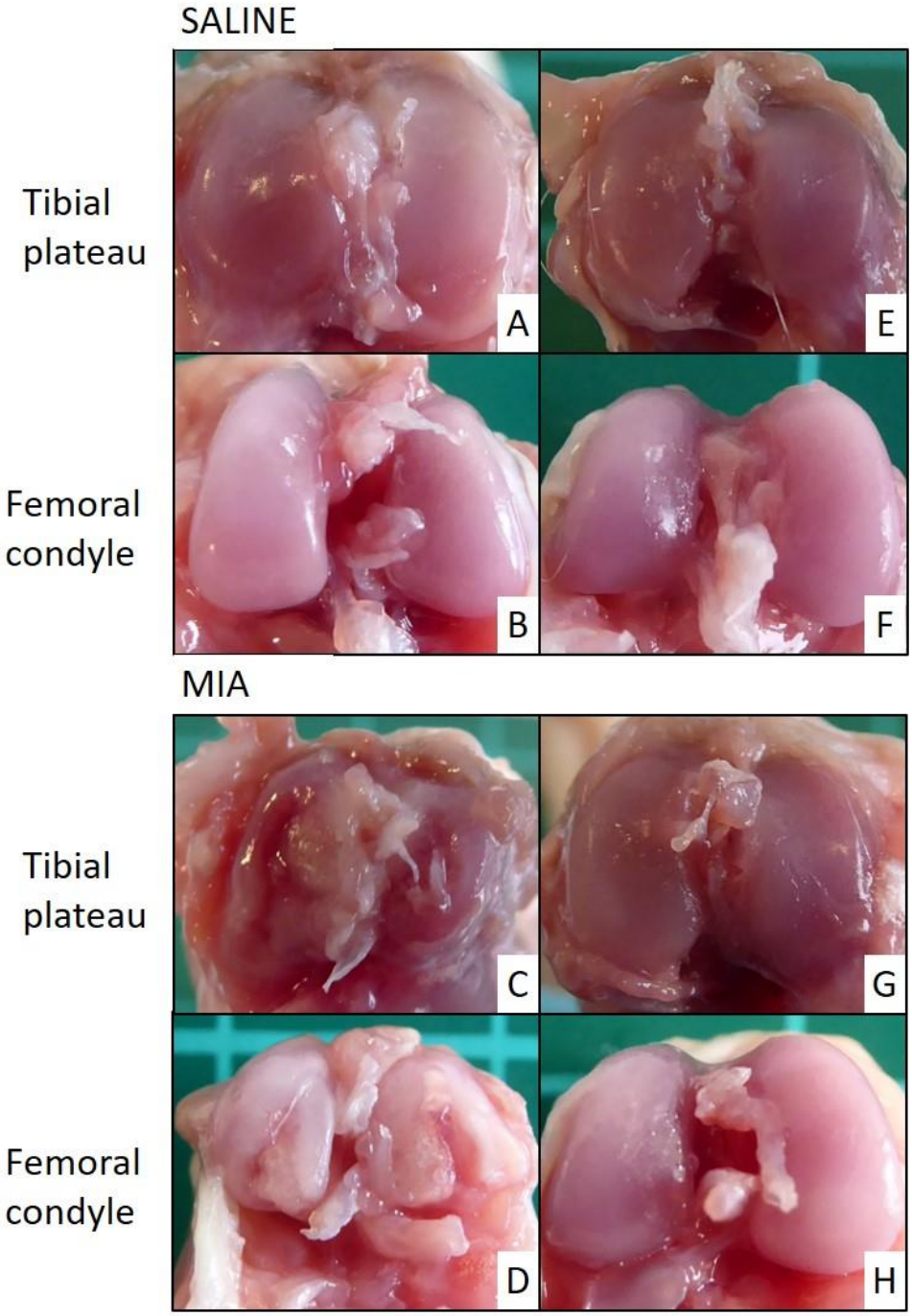

Figure 4.5. Examples of joint damage severity 28-35 days after saline (A, B) or MIA (C, D) injection into the knee joint of the left hindlimb. Images are of ipsilateral tibial plateaus (A, C) or femoral condyles (B, D). Images E – H are corresponding structures in the contralateral (i.e. non-injected) right hindlimb of the same animals.

Treatment	Hindlimb	Mean joint score		
		Collins††††	SFA††††	Revised SFA††††
Saline	Contralateral (n = 12)	0 ± 0****	-9.2 ± 0****	0 ± 0****
	Ipsilateral (n = 5)	0 ± 0****	-9.2 ± 0****	0 ± 0****
MIA	Contralateral (n = 15)	0 ± 0****	18.3 ± 5.1****	3.8 ± 0.7****
	Ipsilateral (n = 15)	11.7 ± 0.2	756.4 ± 53.2	117.1 ± 8.3

Table 4.1. Scoring of ipsilateral and contralateral hindlimb knee joints 28-35 days post-saline or MIA injection using three different methods. Values are means and errors are standard error of means. ††††$p < 0.0001$ denotes significant difference between joints for a given scoring method (one-way ANOVA). ****$p < 0.0001$ denotes significance compared to MIA-injected ipsilateral hindlimb (Tukey's multiple comparisons test). SFA = Système Française D'Arthroscopie.

Mean joint scores were significantly different using either the Collins, SFA or revised SFA methods of joint scoring ($p < 0.0001$ for all, one-way ANOVA; Table 4.1) with the ipsilateral MIA-injected hindlimb showing significantly greater damage than the three other joints by all three scoring methods ($p < 0.0001$, Tukey's multiple comparisons test; Figure 4.5).

4.3.2. Pain behaviour

4.3.2.1. Weight bearing asymmetry

The weight bearing data was tested across saline-injected animals that were later given either 500 µg or 50 µg capsaicin with electrically and mechanically-evoked responses and found there was a significant difference between the 4 groups but no differences between time points ($p = 0.0009$ and $p = 0.1166$ respectively, two-way ANOVA). These differences were found to be between the 50 µg capsaicin dose animals with electrically-evoked responses due to some animals showing slightly larger differences between the hindlimbs. The same groups were tested across the MIA-injected animals and found to have no significant differences between groups however as expected had significant differences over time ($p = 0.1203$ and $p < 0.0001$ respectively, two-way ANOVA).

The weight bearing data was therefore pooled across all groups to show any differences between saline and MIA-injected animal and indicated the difference between the ipsilateral and contralateral hindlimb was significantly larger in MIA compared to saline-injected animals ($p < 0.0001$, two-way ANOVA; Figure 4.6A) with mean values of 57.1 ± 2.7 g (n = 41) and 3.2 ± 0.5 g (n = 43) respectively, at day 28-35 post-injection.

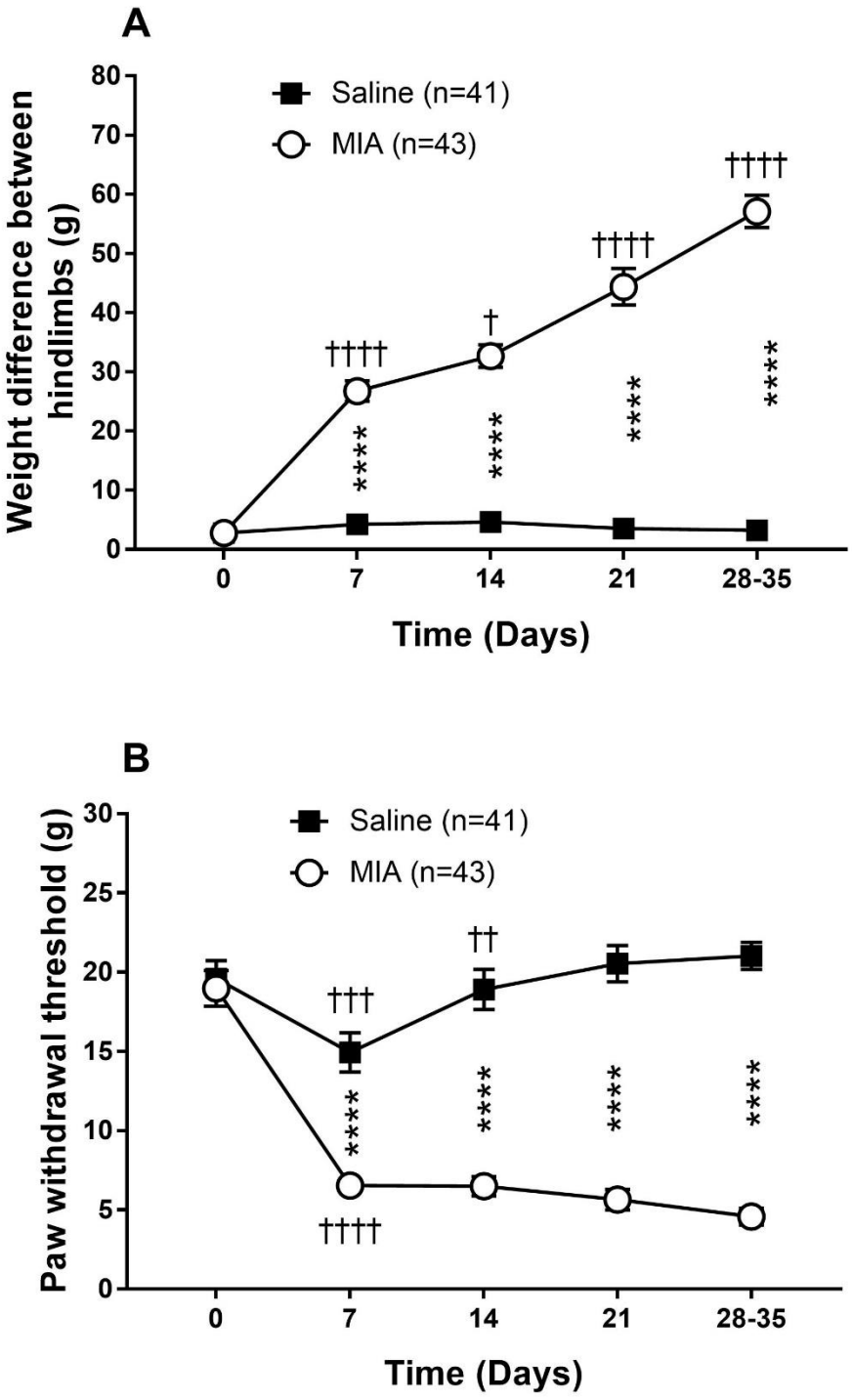

Figure 4.6. Pain behaviour post saline or MIA injection with (A) weight bearing asymmetry or (B) paw withdrawal thresholds. Values plotted are means and errors are standard error of means. ****p < 0.0001 denotes significant difference between saline and MIA-injected animals. †p < 0.05, ††p < 0.01, †††p < 0.001 or ††††p < 0.0001 denotes significant difference to previous time point in saline or MIA-injected animals (Sidak's multiple comparisons test).

4.3.2.2. Paw withdrawal thresholds

PWTs were tested across the 4 saline-injected groups (both capsaicin doses and electrically and mechanically-evoked reflex responses) and found that there was a significant difference between groups as well as between time points ($p = 0.0023$ and $p < 0.0001$ respectively, two-way ANOVA). These differences were indicated between the animals which had electrically-evoked responses and received a 500 μg capsaicin dose and the other 3 groups, with some animals in this group showing lower than expected thresholds for the earlier time points. The same groups were tested across the MIA-injected animals and found no significant differences between groups but again as expected differences between time points ($p = 0.3507$ and $p < 0.0001$ respectively, two-way ANOVA).

The PWT data was therefore pooled across the 4 groups to show the overall effects between saline and MIA-injected animals and indicated that PWTs were significantly reduced in MIA-injected hindlimbs ($p < 0.0001$, two-way ANOVA; Figure 4.6B) to a mean of 4.6 ± 0.5 g (n = 43) at day 28-35 post-injection, compared to 21.0 ± 0.8 g (n = 41) in saline-injected hindlimbs.

4.3.3. Control parameters for electrophysiology

4.3.3.1. Weight and anaesthetic parameters

Animals whose reflexes were later electrically-evoked and given either 500 µg or 50 µg capsaicin dose had mean weights of 152 ± 5 g (n = 10) and 145 ± 2 g (n = 10) at the point of saline induction and 151 ± 1 g (n = 9) and 148 ± 2 g (n = 10) at the point of MIA induction respectively. Similarly, animals whose reflexes were later mechanically-evoked and given either 500 µg or 50 µg capsaicin dose had mean weights of 148 ± 5 g (n = 10) and 149 ± 3 g (n = 11) at the point of saline induction and 157 ± 4 g (n = 11) and 150 ± 2 g (n = 13) at the point of MIA induction respectively which were not significantly different across the 8 groups (p = 0.3613, one-way ANOVA).

At the time of electrophysiology mean weights of animals whose reflexes were later electrically-evoked and given 500 µg or 50 µg capsaicin injection were 380 ± 14 g and 361 ± 8 g in saline-injected animals and 383 ± 7 g and 358 ± 8 g in MIA-injected animals respectively. Animals whose reflexes were later mechanically-evoked and given 500 µg or 50 µg capsaicin injection were 364 ± 11 g and 379 ± 9 g in saline-injected animals and 361 ± 9 g and 370 ± 8 g in MIA-injected animals respectively which again were not significantly different between the 8 groups (p = 0.4124, one-way ANOVA).

Following an initial bolus dose (see section 2.2.1.5), alfaxalone anaesthesia was maintained using a CRI at mean rates of 47.67 ± 1.19 mg kg^{-1} hr^{-1} and 45.8 ± 0.83 mg kg^{-1} hr^{-1} for saline-injected animals whose reflexes were electrically evoked and given 500 µg or 50 µg capsaicin injection and at 47.34 ± 0.48 mg kg^{-1} hr^{-1} and 44.23 ± 0.90 mg kg^{-1} hr^{-1} in MIA-injected animals respectively. Similarly, alfaxalone anaesthesia was maintained at mean rates of 46.34 ± 0.70 mg kg^{-1} hr^{-1} and 44.36 ± 0.43 mg kg^{-1} hr^{-1} for saline-injected animals whose reflexes were later mechanically-evoked and given 500 µg or 50 µg capsaicin injection and at 51.28 ± 3.30 mg kg^{-1} hr^{-1} and 45.03 ± 0.52 mg kg^{-1} hr^{-1} in MIA-injected animals respectively which were significantly different between the 8 groups ($p = 0.0125$, one-way ANOVA) with differences shown between MIA-injected animals that were later given 500 µg capsaicin and had mechanically-evoked responses and the lower dose capsaicin injection groups; saline and MIA-injected mechanically-evoked groups and the MIA-injected electrically-evoked group ($p = 0.0146$, $p = 0.0272$ and $p = 0.0154$ respectively, Tukey's multiple comparisons test).

4.3.3.2. Electrical threshold and stimulation strength

Treatment	Capsaicin dose (µg)	Median threshold (mA)		Median stimulation strength (mA)	
		Heel-MG	Toes-BF/TA	Heel-MG††	Toes-BF/TA
Saline (n = 10)	500	1.60 (0.88 – 2.33)	0.60 (0.48 – 0.83)	6.75 (6.00 – 7.00)	8.00 (6.75 – 9.00)
MIA (n = 8)	500	0.85 (0.65 – 1.20)	0.75 (0.40 – 0.88)	6.00 (4.25 – 6.75)	7.50 (6.25 – 8.00)
Saline (n = 10)	50	0.75 (0.58 – 1.70)	0.55 (0.30 – 6.50)	3.50 (1.35 – 6.00)	6.00 (3.90 – 6.50)
MIA (n = 10)	50	0.85 (0.55 – 1.28)	3.3 (0.40 – 7.25)	3.10 (0.53 – 4.13)	6.50 (4.00 – 9.00)

Table 4.2. Median electrical stimulation parameters for heel-medial gastrocnemius (MG) and toes-biceps femoris (BF) or tibialis anterior (TA) reflexes in saline and MIA-injected animals later injected with 500 µg or 50 µg capsaicin respectively. Values in brackets are interquartile ranges. ††$p < 0.01$ denotes significant difference between groups (Kruskal-Wallis test).

Median electrical threshold values were not significantly different between groups for the heel-MG or toes-BF/TA reflex responses ($p = 0.1983$ and $p = 0.6574$ respectively, Kruskal-Wallis test; Table 4.2). Similarly, no significance was indicated between saline and MIA-injected animals in the toes-BF/TA median electrical stimulation strengths ($p = 0.1045$, Kruskal-Wallis test). However, significant differences were indicated between groups for heel-MG median electrical stimulation strengths ($p = 0.0056$, Kruskal-Wallis test) with this difference indicated between the saline-injected animals given 500 µg capsaicin and the MIA-injected group given 50 µg capsaicin ($p = 0.0068$, Dunn's multiple comparisons test).

When data were pooled for all animals across saline and MIA-injected groups, no significant difference was observed in median electrical thresholds between heel-MG and toes-BF/TA ($p = 0.0716$, Mann-Whitney test) with medians of 0.9 mA (IQR 0.68 – 1.68 mA) and 0.65 mA (IQR 0.40 – 1.34 mA) respectively. However, median stimulation strengths were significantly smaller for heel-MG reflexes compared to toes-BF/TA reflexes ($p = 0.0002$, Mann-Whitney test) with values of 5.00 mA (IQR 3.00 – 6.63 mA) and 7.00 mA (IQR 5.75 – 8.00 mA) respectively.

4.3.3.3. Electrical control reflex responses

Treatment	Capsaicin dose (µg)	Median control reflex responses (µV.ms)		
		Heel-MG	Toes-BF	Toes-TA
Saline (n = 10)	500	114 (79 – 226)	94 (76 – 211)	63 (55 – 99)
MIA (n = 9)	500	117 (78 – 165)	104 (62 – 200)	95 (63 – 105)
Saline (n = 10)	50	198 (88 – 318)	141 (118 – 330)	95 (63 – 281)
MIA (n = 10)	50	116 (95 – 162)	162 (53 – 197)	55 (46 – 129)

Table 4.3. Median control responses to electrical stimulation for heel-medial gastrocnemius (MG), toes-biceps femoris (BF) and toes-tibialis anterior (TA) reflexes prior to administration of 500 µg or 50 µg capsaicin in saline and MIA-injected animals. Values in brackets are interquartile ranges.

The size of heel-MG, toes-BF and toes-TA reflex responses prior to 500 µg or 50 µg capsaicin injection were not significantly different between saline (n = 10 and n = 10) and MIA-injected (n = 9 and n = 10) animals for electrically-evoked reflex responses (p = 0.7480, p = 0.4230 and p = 0.4231, Kruskal-Wallis test; Table 4.3). For saline-injected animals there was a significant difference between the three reflex responses across both capsaicin doses (p = 0.0149, Kruskal-Wallis test) with toes-BF responses in the 50 µg capsaicin dose significantly larger than toes-TA responses prior to a 500 µg capsaicin dose (p = 0.0062, Dunn's multiple comparisons test). However, MIA-injected animals showed no significant differences between heel-MG, toes-BF and toes-TA reflex responses (p = 0.3190, Kruskal-Wallis test).

4.3.3.4. Mechanical thresholds

Treatment	Capsaicin dose (µg)	Median mechanical threshold (von Frey (vF) weight, g)		
		Heel-MG	Toes-BF	Toes-TA
Saline (n = 10)	500	43 (26 – 60)	26 (26 – 35)	18 (10 – 60)
MIA (n = 10)	500	26 (22 – 60)	26 (10 – 26)	26 (10 – 26)
Saline (n = 11)	50	26 (10 – 60)	26 (10 – 60)	10 (10 –26)
MIA (n = 13)	50	26 (26 – 60)	26 (18 – 60)	26 (18 – 26)

Table 4.4. Median mechanical threshold parameters for the heel-medial gastrocnemius (MG), toes-biceps femoris (BF) and toes-tibialis anterior (TA) reflexes for saline and MIA-injected animals later injected with 500 µg or 50 µg capsaicin respectively. Values in brackets are interquartile ranges.

Median mechanical threshold values were not significantly different between heel-MG, toes-BF and toes-TA in saline or MIA-injected animals which were given either 500 μg or 50 μg capsaicin ($p = 0.1163$ and $p = 0.0911$ respectively, Kruskal-Wallis test; Table 4.4). Similarly, there was no significant differences in the thresholds between saline and MIA-injected animals given either 500 μg or 50 μg capsaicin in heel-MG, toes-BF and toes-TA reflex responses ($p = 0.1498$, $p = 0.7223$ and $p = 0.7115$, Kruskal-Wallis test).

4.3.3.5. Mechanical control reflex responses

Treatment and von Frey weight (g)		Median control reflex responses (μV)					
		Heel-MG		Toes-BF		Toes-TA	
Capsaicin dose (μg)		500	50	500	50	500	50
Saline	10	0.016 (0.005 – 0.021)	0.043 (0.012 – 0.149)	0.016 (0.007 – 0.040)	0.032 (0.014 – 0.093)	0.048 (0.013 – 0.146)	0.062 (0.013 – 0.107)
	26	0.071 (0.004 –0.607)	0.065 (0.015 –0.391)	0.252 (0.073 – 0.641)	0.097 (0.023 – 0.536)	0.509 (0.036 – 1.092)	0.259 (0.108 – 0.517)
	60	3.222 (0.505 – 13.630)	4.167 (0.155 – 6.589)	1.513 (0.520 – 2.469)	1.106 (0.337 – 3.125)	1.673 (0.850 – 3.901)	1.361 (0.873 – 1.891)
	100	6.186 (1.412 – 20.637)	12.626 (3.371 – 21.600)	3.461 (1.585 – 4.068)	2.621 (1.785 – 6.091)	2.923 (1.450 – 5.875)	2.147 (1.331 – 3.376)
	180	8.103 (3.335 – 20.737)	9.843 (5.581 – 30.650)	5.173 (3.002 – 8.742)	9.704 (2.960 – 12.084)	4.568 (2.759 – 7.111)	2.960 (2.209 – 3.918)
	300	10.477 (3.945 – 21.924)	12.570 (6.762 – 44.222)	5.835 (2.444 – 12.195)	9.710 (2.837 – 15.728)	4.642 (2.370 – 8.113)	3.324 (2.231 – 4.125)

MIA	10	0.018 (0.010 – 0.055)	0.016 (0.007 – 0.035)	0.029 (0.015 – 0.111)	0.009 (0.003 – 0.048)	0.036 (0.007 – 0.219)	0.029 (0.018 – 0.060)
	26	0.072 (0.036 – 0.254)	0.048 (0.025 – 0.109)	0.165 (0.062 – 1.113)	0.091 (0.027 – 0.490)	0.615 (0.098 – 1.103)	1.83 (0.134 – 0.873)
	60	7.019 (1.291 – 16.016)	4.461 (3.376 – 7.153)	1.780 (1.126 – 3.566)	0.703 (0.197 – 3.317)	2.790 (1.846 – 4.849)	1.461 (0.853 – 2.730)
	100	13.501 (5.167– 18.194)	9.289 (5.563– 13.602)	2.836 (1.483 – 6.513)	3.872 (2.268 – 8.363)	3.892 (2.676 – 5.609)	3.180 (2.054 – 4.591)
	180	12.598 (5.299 – 24.438)	9.881 (6.663 – 14.932)	4.053 (2.505 – 10.540)	7.482 (4.501 – 10.739)	5.180 (3.159 – 5.945)	3.008 (2.137 – 4.623)
	300	14.879 (5.700 – 21.587)	9.471 (5.863 – 15.471)	6.004 (1.829 – 11.455)	8.769 (6.553 – 13.297)	5.737 (3.760 – 6.547)	3.398 (2.409 – 5.734)

Table 4.5. Median control responses to mechanical stimulation for heel-medial gastrocnemius (MG), toes-biceps femoris (BF) and toes-tibialis anterior (TA) reflexes prior to administration of 500 µg or 50 µg capsaicin in saline (n = 10 and n = 11) and MIA-injected (n = 11 and n = 13) animals. Values in brackets are interquartile ranges.

As vF weight (10 – 300 g) increased, median control reflex responses significantly increased for heel-MG, toes-BF and toes-TA reflex responses for animals injected with 500 μg or 50 μg capsaicin in saline (n = 10 and n = 11) and MIA-injected (n = 11 and n = 13) animals ($p < 0.0001$, Kruskal-Wallis test). Comparison of responses prior to capsaicin injection indicated control responses were not significantly different between MIA and saline-injected animals in any reflex response ($p > 0.05$, two-way ANOVA; Figure 4.7). Similarly no significant differences were observed in any reflex response evoked by vF filaments (10 – 300g) between MIA and saline-injected animals using direct pairwise analysis ($p > 0.05$, Kruskal-Wallis test; Table 4.5).

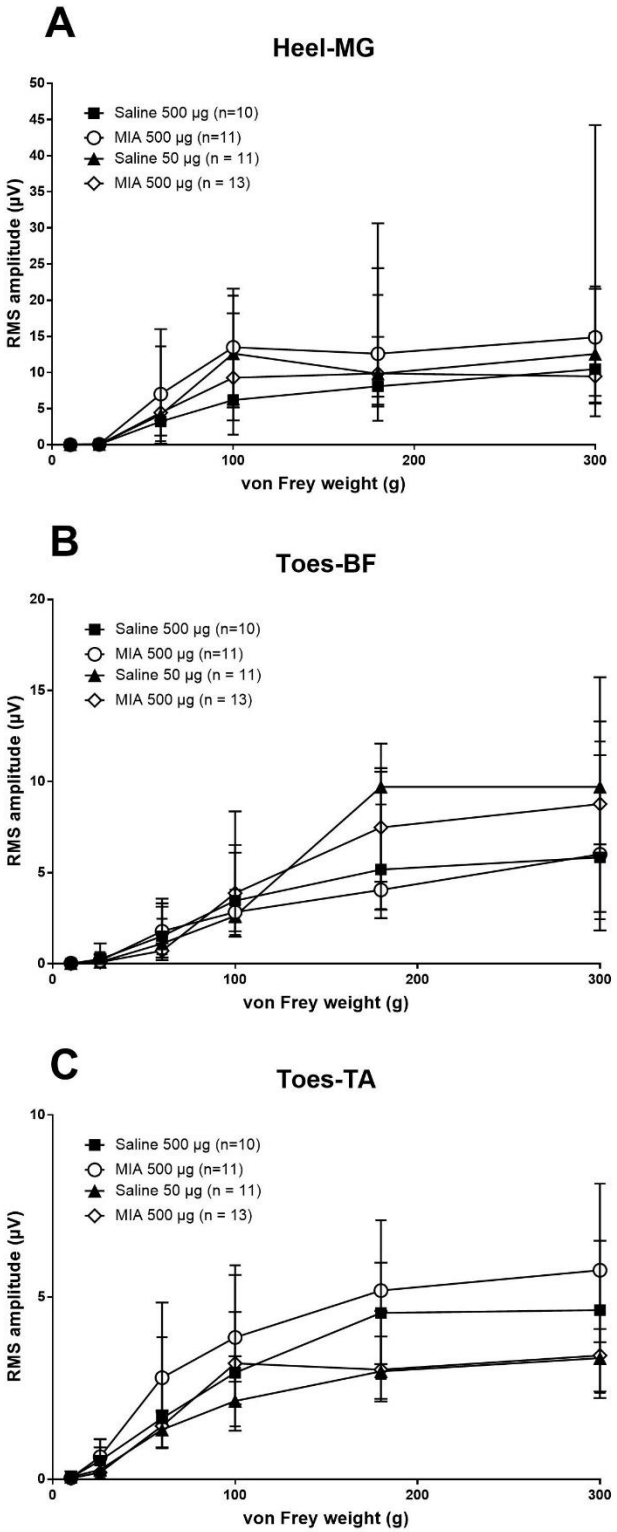

Figure 4.7. Control responses prior to injection of 500 µg or 50 µg capsaicin for (A) heel-medial gastrocnemius (MG), (B) toes-biceps femoris (BF) and (C) toes-tibialis anterior (TA) reflexes evoked using 10 g, 26 g, 60 g, 100 g, 180 g and 300 g von Frey (vF) monofilaments in saline and MIA animals 28-35 days post-injection. Values plotted are medians and errors are interquartile ranges.

4.3.4. Effect of 500 µg capsaicin on electrically-evoked responses

4.3.4.1. Injection into the contralateral hindlimb

Significant inhibition was induced in heel-MG responses by 500 µg capsaicin in saline-injected (n = 10) animals to a median of 81% (IQR 71 – 88%) of controls with a median duration of inhibition of 61 min (IQR 34 – 61 min), however no significant inhibition was found in MIA-injected (n = 9) animals ($p = 0.0162$ and $p = 0.5428$ respectively, Friedman's ANOVA; Figure 4.8A). Analysis of negative AUC values did not indicate any significant difference in overall inhibition between saline and MIA groups ($p = 0.7057$, unpaired t-test; Figure 4.9A).

Significant inhibition by capsaicin was induced in toes-BF to a median of 23% (IQR 9 – 34%) and 28% (IQR 3 – 32%) of controls in saline (n = 10) and MIA-injected (n = 9) animals respectively ($p > 0.0001$ for both, Friedman's ANOVA; Figure 4.8B). Median duration of inhibition was calculated as 63 min (IQR 63 – 63 min) and 63 min (IQR 47 – 63 min) for saline and MIA-injected animals respectively which was significantly different between groups ($p = 0.0325$, Mann-Whitney test). Equally, analysis of negative AUC values indicated no significant difference in overall inhibition between the saline and MIA-injected groups ($p = 0.3401$, unpaired t-test; Figure 4.9B).

Data for one toes-TA response were excluded from analysis for one saline-injected animal due to excessive variability hence unreliability. Significant

capsaicin-induced inhibition was observed in toes-TA responses in saline (n = 9) and MIA-injected (n = 9) animals to medians of 28% (IQR 8 – 34%) and 26% (IQR 8 – 39%) of controls respectively ($p < 0.0001$ for both, Friedman's ANOVA; Figure 4.8C). Median duration of inhibition was 63 min (IQR 47 – 63 min) and 63 min (IQR 47 – 63 min) in saline and MIA-injected animals respectively which was not significantly different between groups ($p = 0.6199$, Mann-Whitney test). Similarly, negative AUC values were not significantly different between saline and MIA-injected groups ($p = 0.4181$, unpaired t-test; Figure 4.9C).

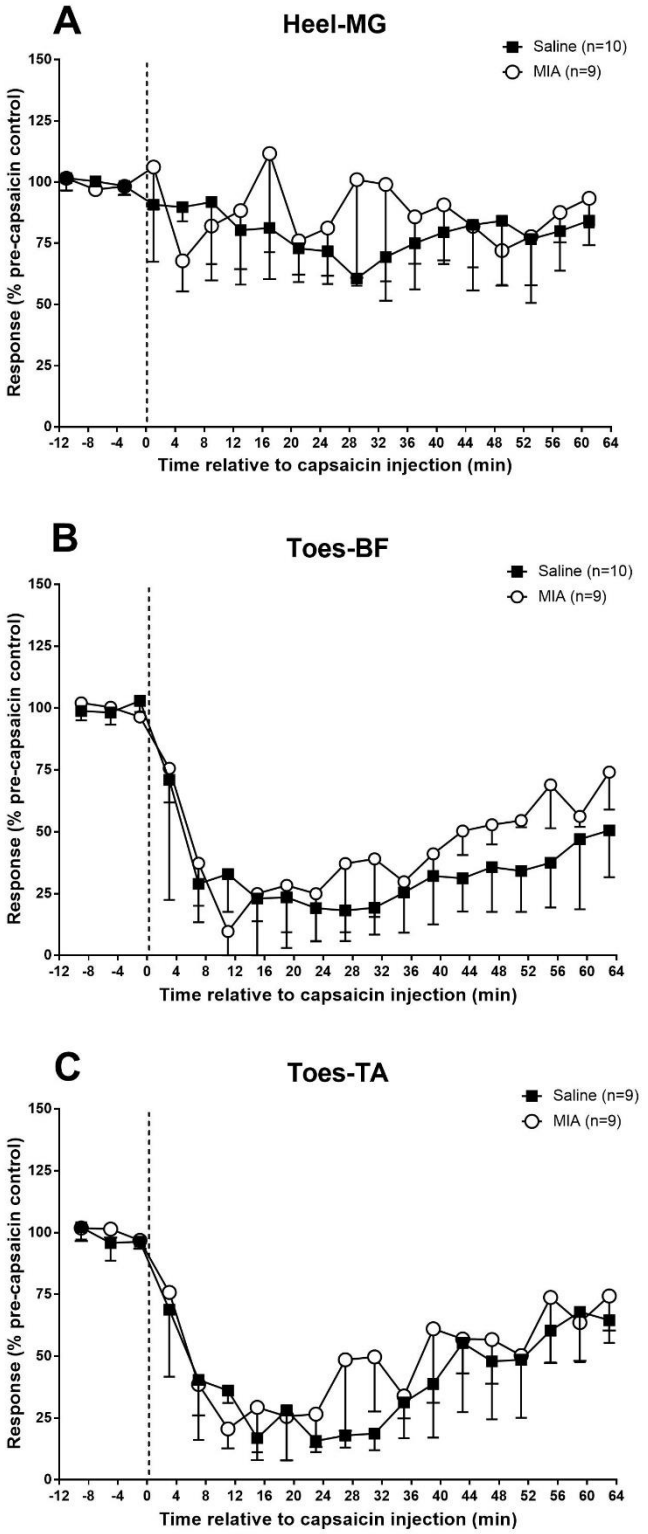

Figure 4.8. Effect of intramuscular injection of 500 µg capsaicin into the contralateral hindlimb on electrically evoked (A) heel-medial gastrocnemius (MG), (B) toes-biceps femoris (BF) and (C) toes-tibialis anterior (TA) reflexes in 28-35 day saline and MIA-injected animals. Values plotted are medians and errors are interquartile ranges.

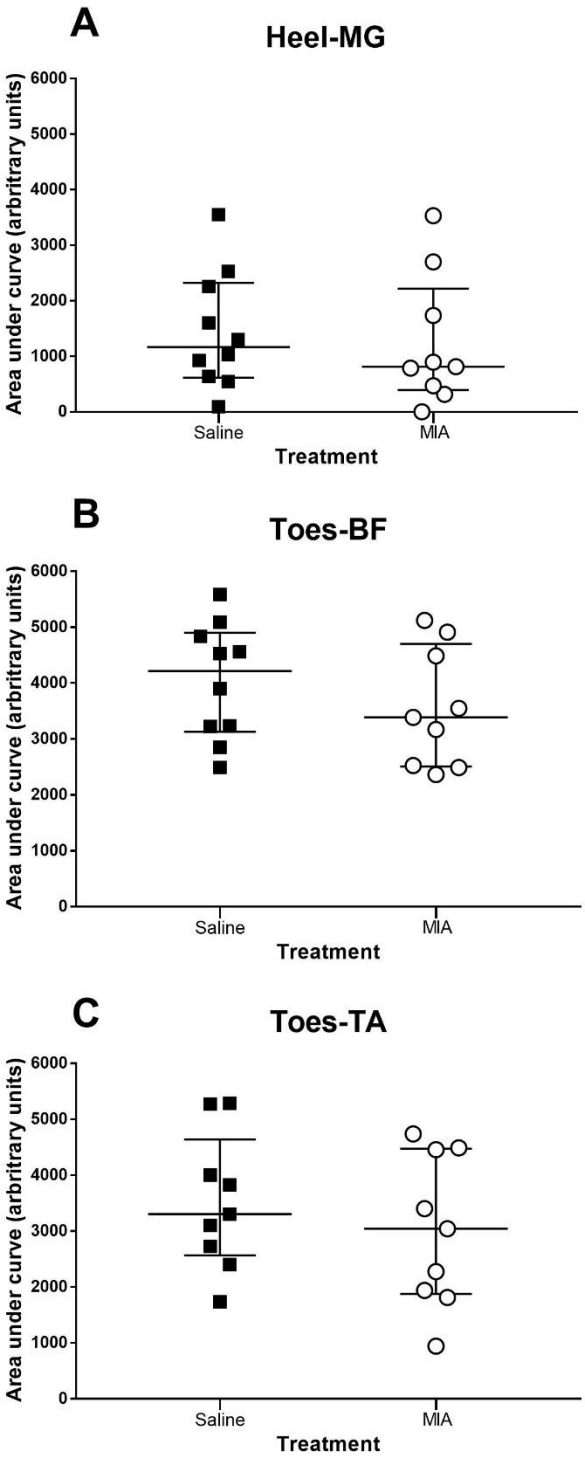

Figure 4.9. Effect of intramuscular injection of 500 µg capsaicin into the contralateral hindlimb on electrically evoked (A) heel-medial gastrocnemius (MG), (B) toes-biceps femoris (BF) and (C) toes-tibialis anterior (TA) reflexes in 28-35 day saline (n = 10; 10; 9, respectively) and MIA-injected (n = 9) animals. Values plotted are area under curve (AUC) determinations for each animal, with horizontal bars indicating medians and interquartile ranges.

4.3.4.2. Injection into the contralateral forelimb

Significant inhibition of heel-MG responses was induced in both saline (n = 10) and MIA-injected (n = 9) animals (p = 0.0070 and p = 0.0005 respectively, Friedman's ANOVA; Figure 4.10A) to a median of 92% (IQR 80 – 109%) and 79% (IQR 60 – 87%) of controls respectively. Median duration of inhibition was also similar between saline and MIA-injected animals (p = 0.6171, Mann-Whitney test) lasting for a median of 39 min (IQR 28 – 61 min) and 57 min (IQR 39 – 59 min) respectively. Similarly, analysis of overall inhibition using negative AUC values indicated no significant difference between the saline and MIA groups (p = 0.1686, unpaired t-test; Figure 4.11A).

Significant inhibition following capsaicin injection was observed in toes-BF responses in saline (n = 10) and MIA (n = 9) groups to medians of 31% (IQR 19 – 37%) and 25% (IQR 16 – 64%) of controls respectively (p < 0.0001, Friedman's ANOVA; Figure 4.10B); median duration of inhibition was 63 min (IQR 43 – 63 min) and 47 min (IQR 41 – 63min) respectively which was not significantly different (p = 0.2539, Mann-Whitney test). Analysis of negative AUC values indicated no significant difference in overall inhibition between saline and MIA groups (p = 0.4479, unpaired t-test; Figure 4.11B).

Significant inhibition of toes-TA reflexes was produced by 500 μg capsaicin in saline (n = 10) and MIA-injected (n = 9) animals to medians of 27% (IQR 11 – 34%) and 31% (IQR 20 – 60%) of controls respectively (p < 0.0001, Friedman's

ANOVA; Figure 4.10C). Median duration of inhibition was not significantly different between saline and MIA groups ($p = 0.7058$, Mann-Whitney test) with medians of 43 min (IQR 31 – 60 min) and 51 min (IQR 27 – 63 min) respectively. Similarly, analysis of negative AUC values also indicated no significant difference between the two groups ($p = 0.5934$, unpaired t-test; Figure 4.11C).

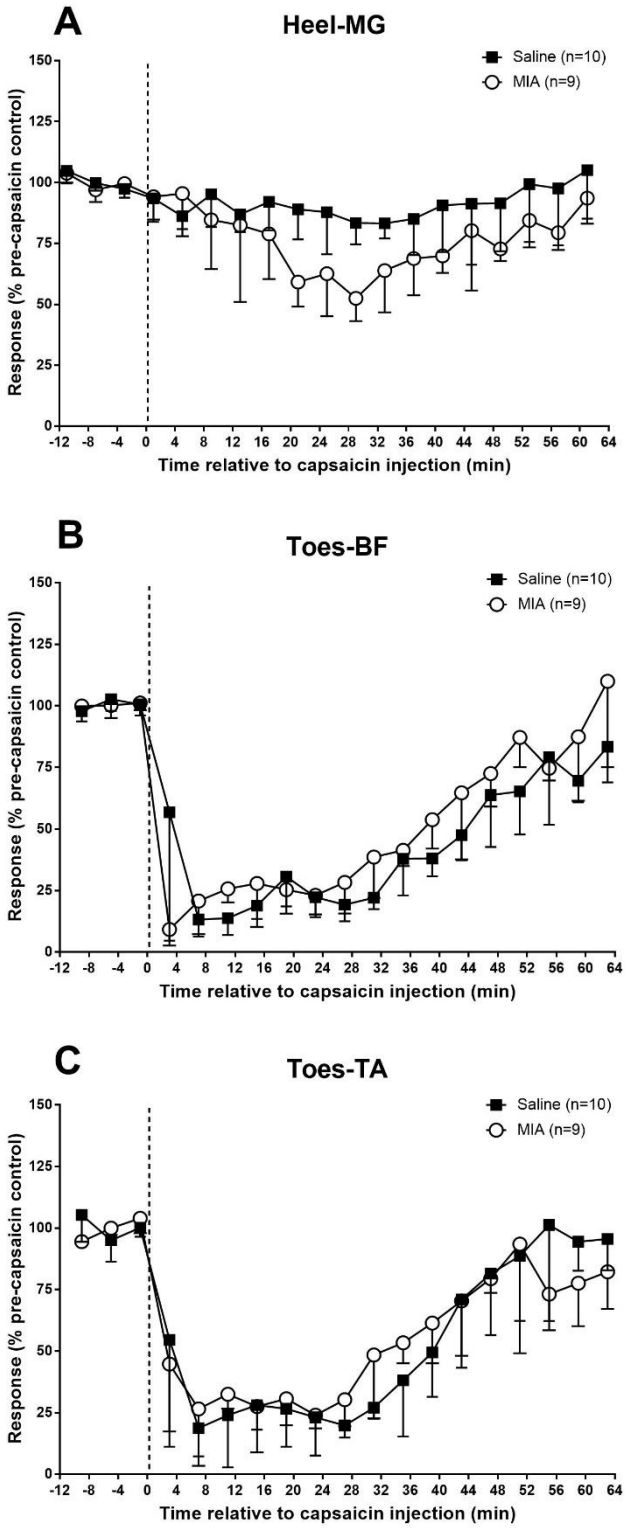

Figure 4.10. Effect of intramuscular injection of 500 µg capsaicin into the contralateral forelimb on electrically evoked (A) heel-medial gastrocnemius (MG), (B) toes-biceps femoris (BF) and (C) toes-tibialis anterior (TA) reflexes in 28-35 day saline and MIA-injected animals. Values plotted are medians and errors are interquartile ranges.

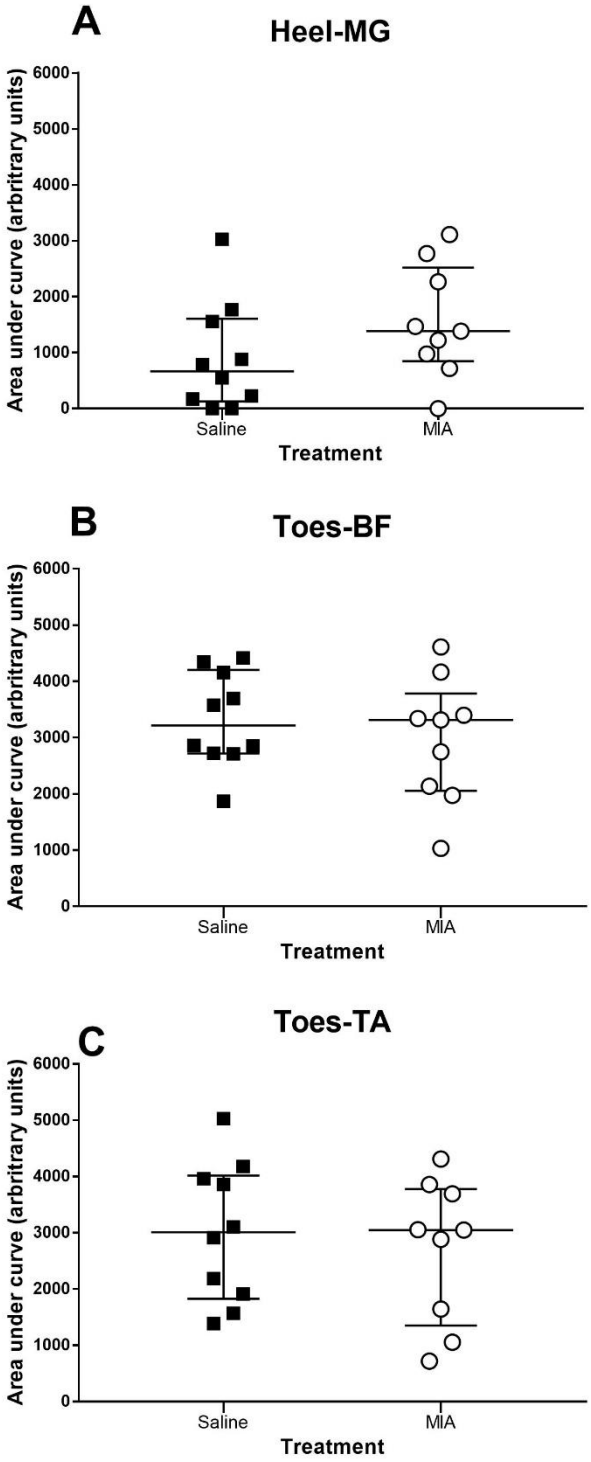

Figure 4.11. Effect of intramuscular injection of 500 µg capsaicin into the contralateral forelimb on electrically evoked (A) heel-medial gastrocnemius (MG), (B) toes-biceps femoris (BF) and (C) toes-tibialis anterior (TA) reflexes in 28-35 day saline (n = 10) and MIA-injected (n = 9) animals. Values plotted are area under curve (AUC) determinations for each animal, with horizontal bars indicating medians and interquartile ranges.

4.3.4.3. Effect of capsaicin injection site

Comparison of heel-MG responses between hindlimb and forelimb capsaicin injection sites for saline or MIA animals indicated no significant differences in the degree of inhibition ($p = 0.2176$ and $p = 0.3401$ respectively, Mann-Whitney test), inhibition duration ($p = 0.2455$ and $p = 0.3008$ respectively, Mann Whitney test) or overall (AUC) inhibition ($p = 0.2419$ and $p = 0.5705$ respectively, unpaired t-test).

Degree of inhibition of toes-BF responses post-capsaicin was not significantly different between conditioning sites for saline or MIA-injected animals ($p = 0.4359$ and $p = 0.3388$ respectively, Mann-Whitney test), as was duration of inhibition ($p = 0.2105$ and $p = 0.2433$ respectively, Mann-Whitney test) and overall inhibition ($p = 0.1126$ and $p = 0.2713$ respectively, unpaired t-test). Toes-TA responses were also similarly inhibited from both hindlimb and forelimb capsaicin injections for saline or MIA groups in terms of depth ($p = 0.8421$ and $p = 0.3996$ respectively, Mann-Whitney test), duration ($p = 0.0737$ and $p = 0.1325$ respectively, Mann-Whitney test) and overall inhibition ($p = 0.3805$ and $p = 0.6202$ respectively, unpaired t-test).

4.3.5. Effect of 50 µg capsaicin on electrically-evoked responses

4.3.5.1. Injection into the contralateral hindlimb

No significant inhibition was found in heel-MG responses by 50 µg capsaicin in saline-injected (n = 10) animals (p = 0.5509, Friedman's ANOVA; Figure 4.12A), however significant inhibition was induced in MIA-injected (n = 10) animals (p = 0.0139, Friedman's ANOVA) to a median of 69% (IQR 55 – 93%) of controls with a median duration of inhibition of 61 min (IQR 0 – 61 min). Analysis of negative AUC values did not indicate any significant difference (p = 0.3804, unpaired t-test; Figure 4.13A) in overall inhibition between the saline and MIA-injected animals.

Significant inhibition following capsaicin injection was observed in toes-BF responses in saline (n = 10) and MIA-injected animals (n = 10) to medians of 80% (IQR 77 – 83%) and 68% (IQR 53 – 88%) of controls respectively (p < 0.0001 and p = 0.0002 respectively, Friedman's ANOVA; Figure 4.12B). Median duration of inhibition was 61 min (IQR 17 – 63 min) and 29 min (IQR 17 – 56 min) for saline and MIA-injected animals respectively, which was not significantly different between groups (p = 0.2290, Mann-Whitney test). Similarly, analysis of negative AUC values indicated no significant difference in overall inhibition between saline and MIA-injected animals (p = 0.2637, unpaired t-test; Figure 4.13B).

No significant inhibition was observed in saline-injected (n = 10) animals in toes-TA responses ($p = 0.0780$, Friedman's ANOVA; Figure 4.12C). However, significant inhibition ($p < 0.0001$, Friedman's ANOVA) was induced in MIA-injected (n = 10) animals in toes-TA responses to medians of 88% (IQR 64 – 93%) of controls with a median duration of inhibition of 21 min (IQR 11 – 27 min). Analysis of negative AUC values did not reveal any significant differences in overall inhibition between the saline and MIA-injected animals ($p = 0.4884$, unpaired t-test; Figure 4.13C).

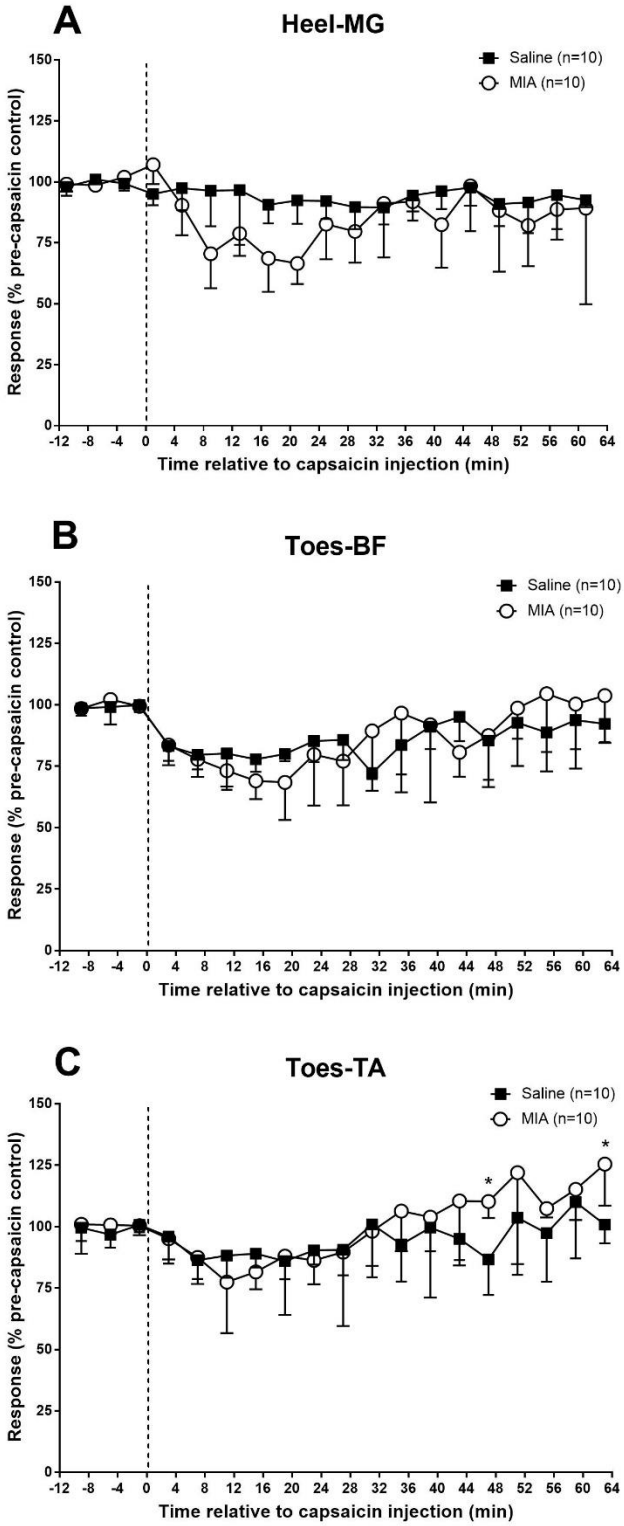

Figure 4.12. Effect of intramuscular injection of 50 µg capsaicin into the contralateral hindlimb on electrically evoked (A) heel-medial gastrocnemius (MG), (B) toes-biceps femoris (BF) and (C) toes-tibialis anterior (TA) reflexes in 28-35 day saline and MIA-injected animals. Values plotted are medians and errors are interquartile ranges. *$p < 0.05$ denotes significant difference between saline and MIA-injected animals (Mann-Whitney test).

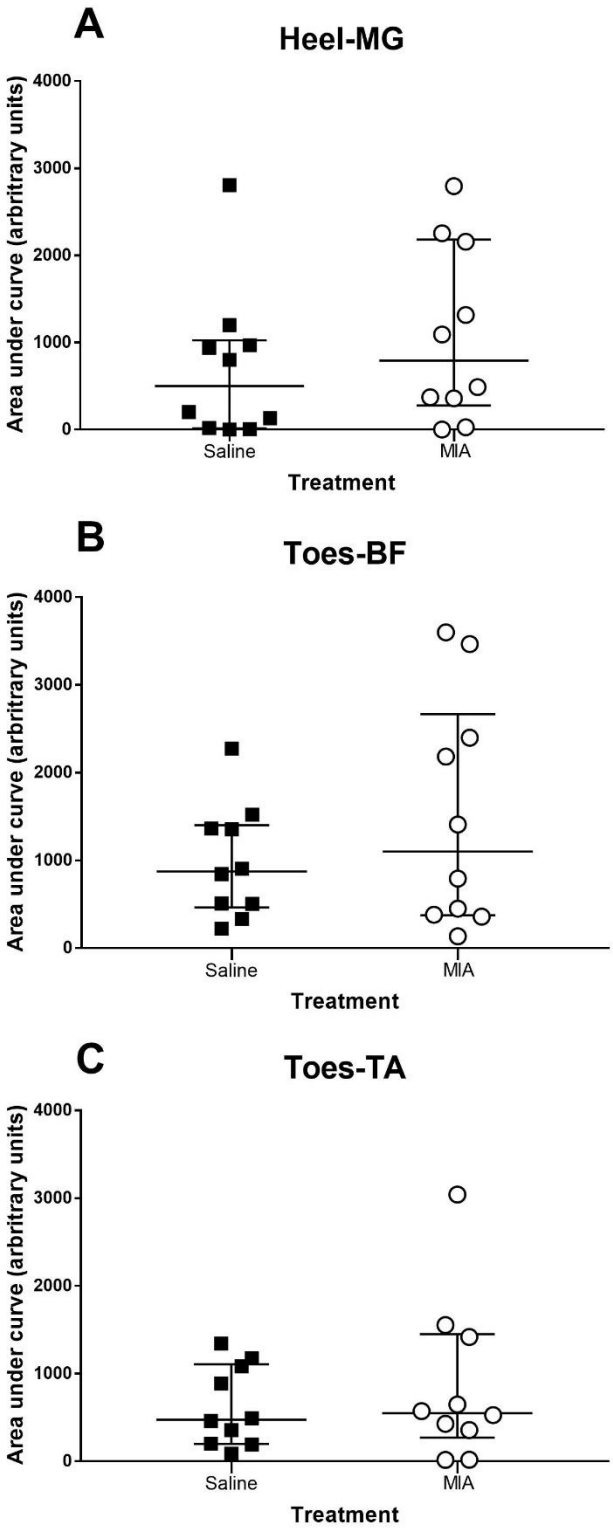

Figure 4.13. Effect of intramuscular injection of 50 µg capsaicin into the contralateral hindlimb on electrically evoked (A) heel-medial gastrocnemius (MG), (B) toes-biceps femoris (BF) and (C) toes-tibialis anterior (TA) reflexes in 28-35 day saline (n = 10) and MIA-injected (n = 10) animals. Values plotted are area under curve (AUC) determinations for each animal, with horizontal bars indicating medians and interquartile ranges.

4.3.5.2. Injection into the contralateral forelimb

Significant inhibition was induced in heel-MG responses by 50 µg capsaicin in saline-injected (n = 10) animals (p = 0.0137, Friedman's ANOVA; Figure 4.14A) to a median of 86% (IQR 77 – 102%) of controls with a median duration of inhibition of 13 min (IQR 0 – 61 min). However, no significant inhibition (p = 0.9902, Friedman's ANOVA) was observed in MIA-injected (n = 10) animals. Similarly, analysis of negative AUC values indicated no significant difference in overall inhibition between the saline and MIA-injected animals (p = 0.8377, unpaired t-test; Figure 4.15A).

Significant inhibition following capsaicin injection was observed in toes-BF responses in saline (n = 10) and MIA-injected (n = 10) animals to a median of 70% (IQR 58 – 85%) and 65% (IQR 51 – 77%) of controls respectively (p < 0.0001, Friedman's ANOVA; Figure 4.14B); median duration of inhibition was 27 min (IQR 20 – 60 min) and 23 min (IQR 17 – 57 min) respectively which was not significantly different (p = 0.5408, Mann-Whitney test). Further analysis using negative AUC values indicated no significant difference in overall inhibition between saline and MIA-injected animals (p = 0.4996, unpaired t-test; Figure 4.15B).

Significant inhibition of toes-TA responses was produced by capsaicin injection in saline (n = 10) and MIA-injected (n = 10) animals (p < 0.0001, Friedman's ANOVA; Figure 4.14C) to medians of 81% (IQR 70 – 88%) and 80% (IQR 77 –

84%) of controls respectively. Median duration of inhibition was not significantly different between saline and MIA groups ($p = 0.3922$, Mann-Whitney test) with medians of 25 min (IQR 17 – 36 min) and 19 min (IQR 8 – 33 min) respectively. Further analysis using negative AUC values also indicated no significant difference in overall inhibition between saline and MIA-injected animals ($p = 0.6612$, unpaired t-test; Figure 4.15C).

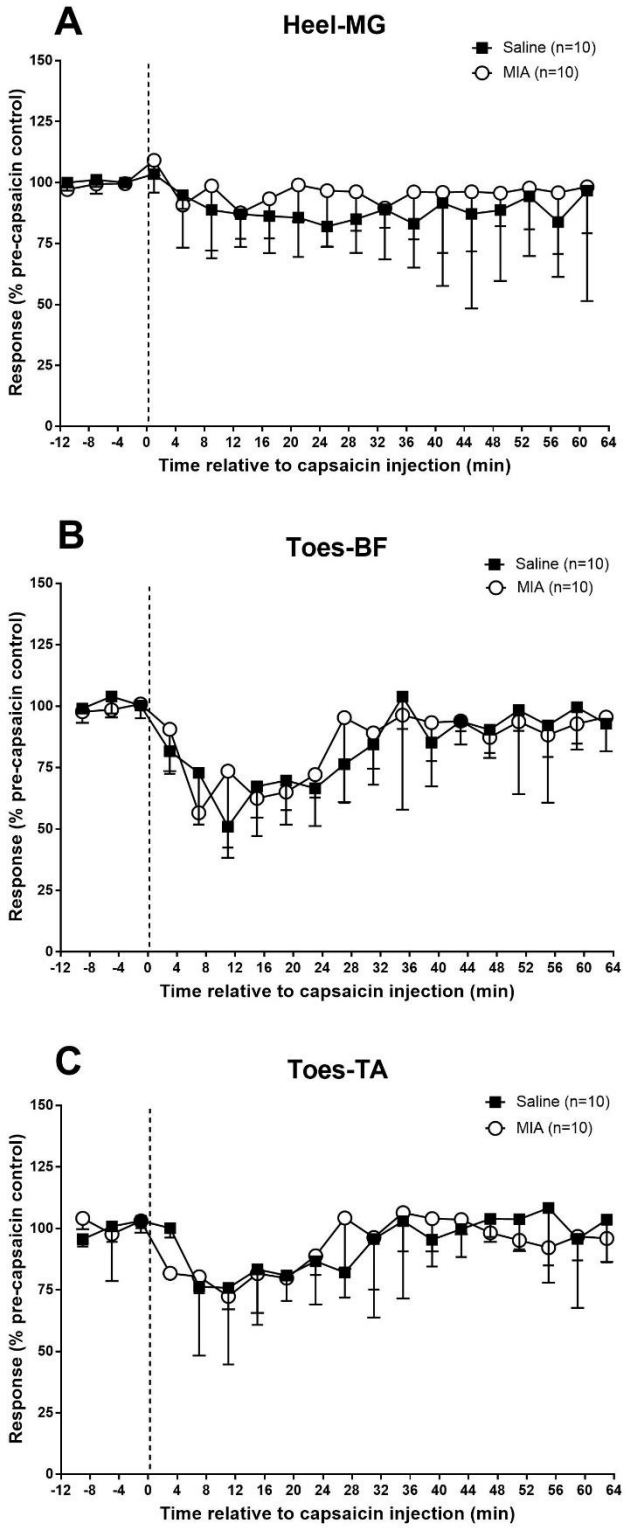

Figure 4.14. Effect of intramuscular injection of 50 µg capsaicin into the contralateral forelimb on electrically evoked (A) heel-medial gastrocnemius (MG), (B) toes-biceps femoris (BF) and (C) toes-tibialis anterior (TA) reflexes in 28-35 day saline and MIA-injected animals. Values plotted are medians and errors are interquartile ranges.

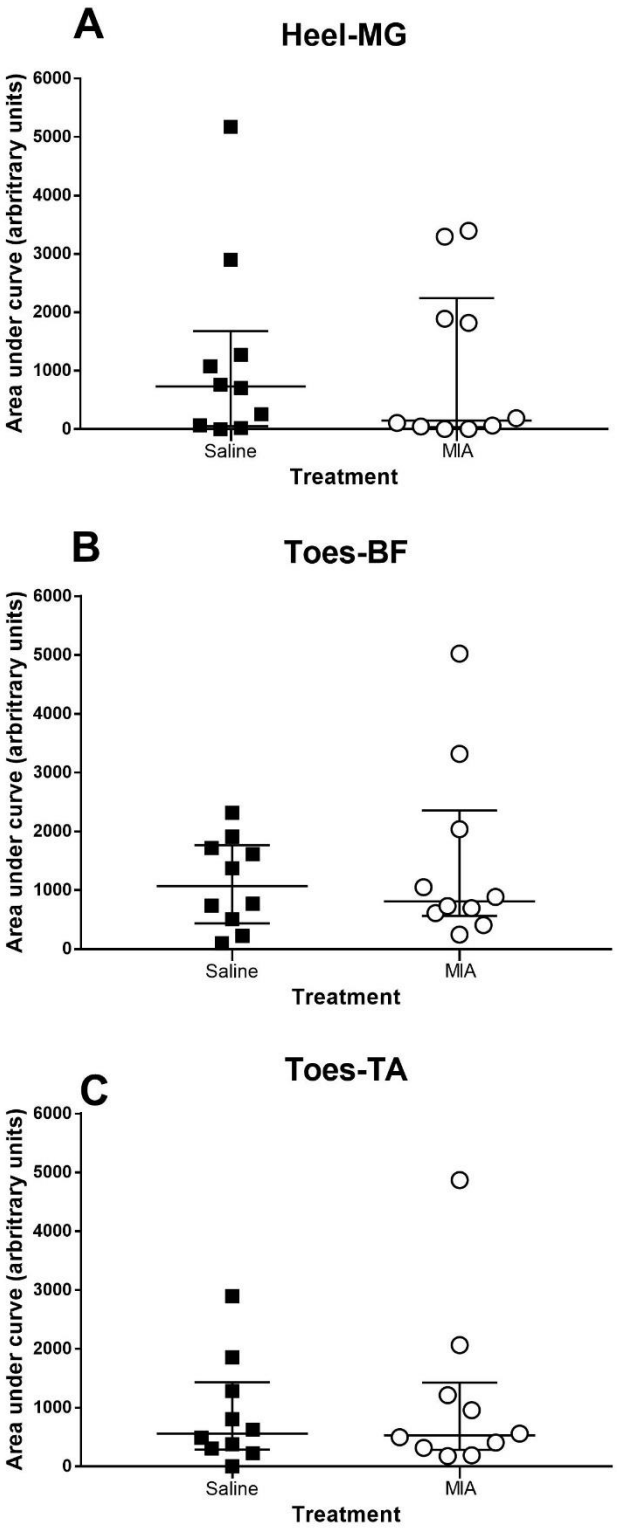

Figure 4.15. Effect of intramuscular injection of 50 µg capsaicin into the contralateral forelimb on electrically evoked (A) heel-medial gastrocnemius (MG), (B) toes-biceps femoris (BF) and (C) toes-tibialis anterior (TA) reflexes in 28-35 day saline and MIA-injected animals. Values plotted are area under curve (AUC) determinations for each animal, with horizontal bars indicating medians and interquartile ranges.

4.3.5.3. Effect of capsaicin injection site

Comparisons of heel-MG responses between hindlimb and forelimb capsaicin injection sites for saline or MIA animals indicated no significant differences in the degree of inhibition ($p = 3930$ and $p = 0.4359$ respectively, Mann-Whitney test), inhibition duration ($p = 0.9157$ and $p = 0.4844$ respectively, Mann Whitney test) or overall (AUC) inhibition ($p = 0.3908$ and $p = 0.9925$ respectively, unpaired t-test).

No significant differences were observed in toes-BF responses post-capsaicin between the conditioning sites for saline or MIA-injected animals in terms of degree of inhibition ($p = 0.4937$ and $p = 0.6842$ respectively, Mann-Whitney test), duration of inhibition ($p = 0.3755$ and $p = 0.7243$ respectively, Mann-Whitney test) or overall (AUC) inhibition ($p = 0.6516$ and 0.9818 respectively, unpaired t-test).

Toes-TA reflexes were also similarly inhibited from both hindlimb and forelimb capsaicin injections for saline or MIA animals in terms of depth ($p = 0.3630$ and $p = 0.9705$ respectively, Mann-Whitney test), duration ($p = 0.8502$ and $p = 0.7494$ respectively, Mann-Whitney test) and overall (AUC) inhibition ($p = 0.4196$ and $p = 0.6228$ respectively, unpaired t-test).

4.3.6. Effect of 500 µg capsaicin on mechanically-evoked responses

Responses evoked by 10 g and 26 g vF monofilaments were found to be variable and sometimes absent before and after capsaicin, therefore these responses have been omitted from analysis.

4.3.6.1. Injection into the contralateral hindlimb

In the saline group (n = 10), significant inhibition of heel-MG responses evoked by 60 g, 100 g, 180 g and 300 g vF weights was caused by contralateral hindlimb injection of capsaicin ($p < 0.0001$, $p < 0.0001$, $p = 0.0001$ and $p < 0.0001$ respectively, Friedman's ANOVA) to a median of 13% (IQR 1 – 35%), 5% (IQR 0 – 18%), 22% (IQR 5 – 38%) and 34% (IQR 11 – 47%) of controls respectively (Figures 4.16A, 4.17A, 4.18A and 4.19A). The corresponding level of inhibition in MIA-injected animals (n = 10) was to a median of 2% (IQR 1 – 21%), 1% (IQR 1 – 14%), 21% (IQR 17 – 42%) and 40% (IQR 27 – 65%) of controls respectively ($p = 0.0007$, $p < 0.0001$, $p = 0.0010$ and $p = 0.0055$ respectively, Friedman's ANOVA). Median duration of inhibition was 49 min (IQR 27 – 61 min), 57 min (IQR 30 – 61 min), 47 min (IQR 33 – 61 min) and 39 min (IQR 31 – 61 min) for 60 g, 100 g, 180 g and 300 g vF weights respectively in saline-injected animals and 51 min (IQR 0 – 61 min), 53 min (IQR 0 – 58 min), 59 min (IQR 35 – 61 min) and 45 min (IQR 27 – 61 min) for the corresponding vF weights in MIA-injected animals; which were not significant between groups ($p = 0.8960$, $p = 0.4901$, $p = 0.5306$ and $p = 0.9242$ respectively, Mann-Whitney test). Analysis of negative AUC values indicated no significant difference in overall inhibition of heel-MG

reflexes to 60 – 300 g vF filaments between saline and MIA-injected animals ($p = 0.4452$, $p = 0.1203$, $p = 0.7774$ and $p = 0.7924$ respectively, unpaired t-test; Figure 4.20A).

Following capsaicin administration, toes-BF reflexes evoked by 60 g, 100 g, 180 g and 300 g monofilaments were significantly inhibited ($p < 0.0001$, Friedman's ANOVA) to medians of 6% (IQR 1 – 15%), 12% (IQR 3 – 30%), 22% (IQR 12 – 36%) and 32% (IQR 25 – 49%) of controls respectively in saline-injected animals ($n = 10$; Figures 4.16B, 4.17B, 4.18B and 4.19B). These reflexes in MIA-injected animals ($n = 10$) were significantly inhibited ($p < 0.0001$, Friedman's ANOVA) to a median of 12% (IQR 2 – 26%), 25% (IQR 5 – 43%), 33% (IQR 12 – 37%) and 46% (IQR 10 – 56%) of controls at the corresponding vF weights. Median duration of inhibition was 47 min (IQR 35 – 63 min), 51 min (IQR 27 – 63 min), 53 min (IQR 29 – 63 min) and 63 min (IQR 58 – 63 min) for 60 g, 100 g, 180 g and 300 g vF weights respectively in saline-injected animals and 33 min (IQR 0 – 63 min), 59 min (IQR 26 – 63 min), 59 min (IQR 48 – 63 min) and 63 min (IQR 25 – 63 min) in MIA-injected animals; these durations were not significant between groups ($p = 0.4551$, $p = 0.4781$, $p = 0.4467$ and $p = 0.3870$ respectively, Mann-Whitney test). Analysis of negative AUC values indicated no significant difference in overall inhibition of responses to 60 – 300 g vF filaments between treatment groups ($p = 0.1822$, $p = 0.1033$, $p = 0.3018$ and $p = 0.9034$ respectively, unpaired t-test; Figure 4.20B).

For toes-TA reflexes in saline-injected animals (n = 10), responses to 60 g, 100 g, 180 g and 300 g monofilaments were significantly inhibited ($p < 0.0001$, Friedman's ANOVA) to medians of 8% (IQR 4 – 35%), 11% (IQR 4 – 54%), 33% (IQR 19 – 58%) and 51% (IQR 42 – 63%) of controls respectively (Figures 4.16C, 4.17C, 4.18C and 4.19C); for MIA-injected animals (n = 10), significant inhibition ($p < 0.0001$, $p < 0.0001$, $p = 0.0001$ and $p = 0.0004$ respectively, Friedman's ANOVA) to medians of 6% (IQR 2 – 16%), 22% (IQR 3 – 39%), 32% (IQR 21 – 42%) and 39% (IQR 27 – 70%) of controls was produced in TA reflexes evoked by these same respective vF filaments. Median duration of inhibition was 41 min (IQR 17 – 63 min), 37 min (IQR 29 – 63 min), 35 min (IQR 27 – 44 min) and 63 min (IQR 58 – 63 min) for 60 g, 100 g, 180g and 300 g vF weights respectively in saline-injected animals and correspondingly 61 min (IQR 0 – 63 min), 59 min (IQR 38 – 63 min), 63 min (IQR 48 – 63 min) and 53 min (IQR 8 – 63 min) in MIA-injected animals which indicated significance in responses evoked using the 180 g vF weight ($p = 0.7416$, $p = 0.3860$, $p = 0.0332$ and $p = 0.6176$ respectively, Mann-Whitney test). Comparison of negative AUC values similarly found that overall inhibition of toes-TA responses was not significantly different between saline and MIA-injected animals for any vF weight ($p = 0.2296$, $p = 0.1607$, $p = 0.2199$ and $p = 0.3749$ respectively, unpaired t-test; Figure 4.20C).

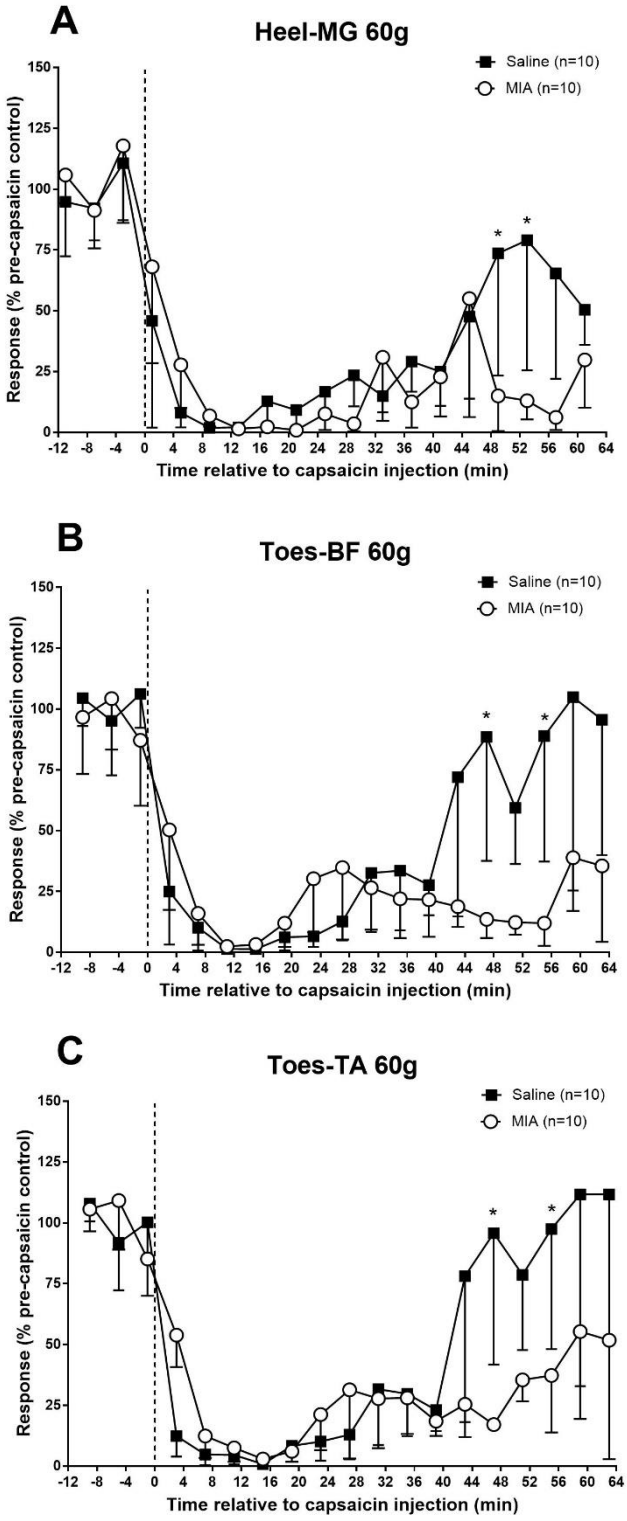

Figure 4.16. Effect of intramuscular injection of 500 µg capsaicin into the contralateral hindlimb on mechanically evoked (A) heel-medial gastrocnemius (MG), (B) toes-biceps femoris (BF) and (C) toes-tibialis anterior (TA) reflexes using a 60 g von Frey (vF) monofilament in 28-35 day saline and MIA-injected animals. Values plotted are medians and errors are interquartile ranges. *$p < 0.05$ denotes significant difference between saline and MIA-injected animals at the same post-capsaicin time points (Mann-Whitney test).

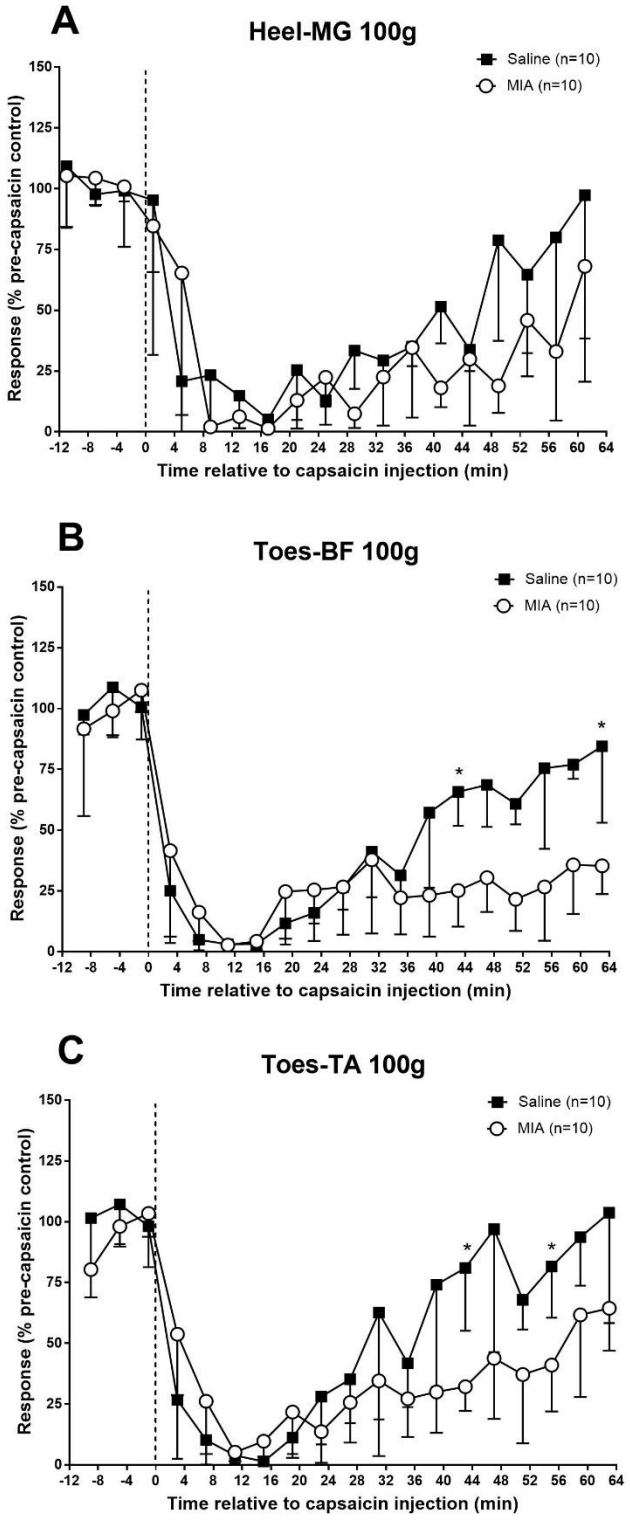

Figure 4.17. Effect of intramuscular injection of 500 µg capsaicin into the contralateral hindlimb on mechanically evoked (A) heel-medial gastrocnemius (MG), (B) toes-biceps femoris (BF) and (C) toes-tibialis anterior (TA) reflexes using a 100 g von Frey (vF) monofilament in 28-35 day saline and MIA-injected animals. Values plotted are medians and errors are interquartile ranges. *p < 0.05 denotes significant difference between saline and MIA-injected animals at the same post-capsaicin time points (Mann-Whitney test).

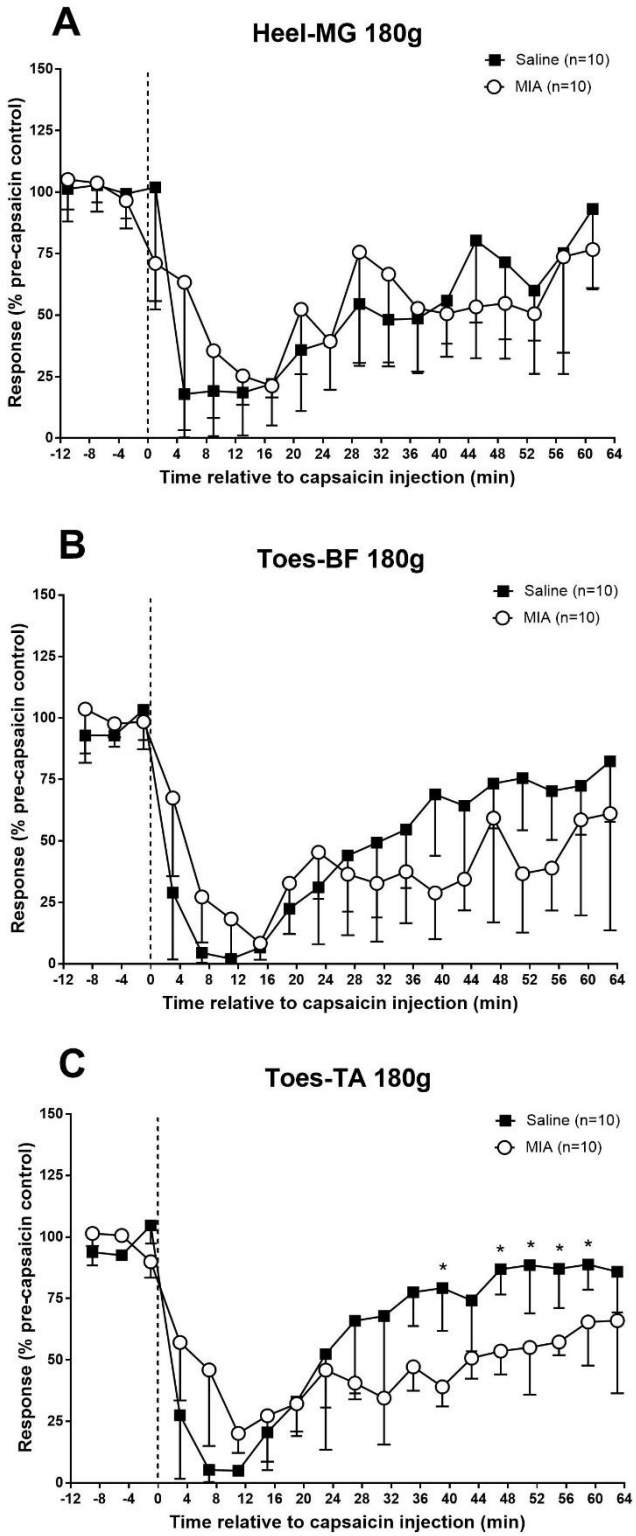

Figure 4.18. Effect of intramuscular injection of 500 µg capsaicin into the contralateral hindlimb on mechanically evoked (A) heel-medial gastrocnemius (MG), (B) toes-biceps femoris (BF) and (C) toes-tibialis anterior (TA) reflexes using a 180 g von Frey (vF) monofilament in 28-35 day saline and MIA-injected animals. Values plotted are medians and errors are interquartile ranges. *p < 0.05 denotes significant difference between saline and MIA-injected animals at the same post-capsaicin time points (Mann-Whitney test).

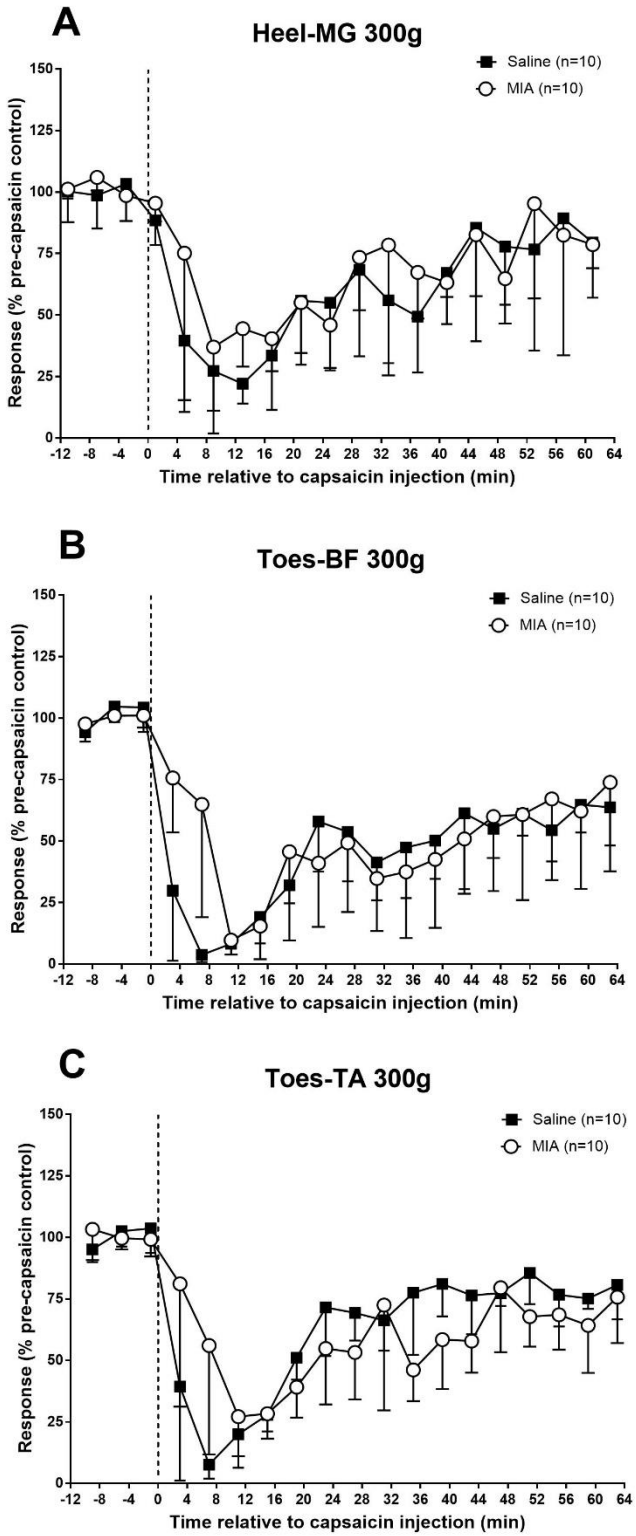

Figure 4.19. Effect of intramuscular injection of 500 µg capsaicin into the contralateral hindlimb on mechanically evoked (A) heel-medial gastrocnemius (MG), (B) toes-biceps femoris (BF) and (C) toes-tibialis anterior (TA) reflexes using a 300 g von Frey (vF) monofilament in 28-35 day saline and MIA-injected animals. Values plotted are medians and errors are interquartile ranges.

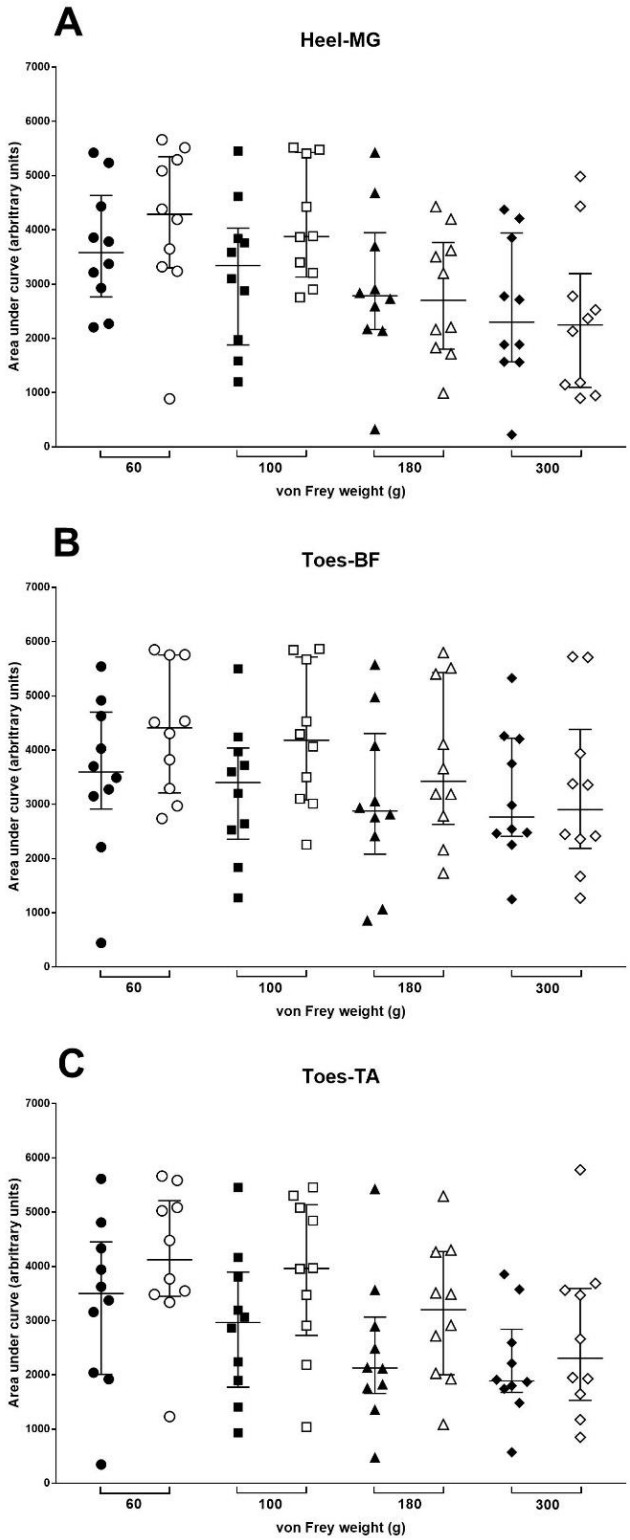

Figure 4.20. Effect of intramuscular injection of 500 µg capsaicin into the contralateral hindlimb on mechanically evoked (A) heel-medial gastrocnemius (MG), (B) toes-biceps femoris (BF) and (C) toes-tibialis anterior (TA) reflexes using 60 – 300 g von Frey (vF) monofilaments in 28-35 day saline (n = 10, closed symbols) and MIA-injected (n = 10, open symbols) animals. Values plotted are area under curve (AUC) determinations for each animal with horizontal bars indicating medians and interquartile ranges.

4.3.6.2. Injection into the contralateral forelimb

Significant inhibition ($p < 0.0001$, Friedman's ANOVA; Figures 4.21A, 4.22A, 4.23A and 4.24A) was induced in heel-MG using 60 g, 100 g, 180 g and 300 g monofilaments to medians of 7% (IQR 2 – 12%), 1% (IQR 0 – 11%), 10% (IQR 3 – 34%) and 30% (IQR 15 – 36%) of controls respectively in saline-injected animals (n = 10). These reflexes in MIA-injected animals (n = 9) were significantly inhibited ($p < 0.0001$, Friedman's ANOVA) to medians of 1% (IQR 1 – 4%), 6% (IQR 1 – 24%), 30% (IQR 17 – 55%) and 56% (IQR 52 – 63%) of controls at the corresponding vF weights. Median duration of inhibition was 35 min (IQR 0 – 42 min), 29 min (IQR 0 – 41 min), 33 min (IQR 19 – 53 min) and 35 min (IQR 25 – 57 min) for 60 g, 100 g, 180 g and 300 g vF weights respectively in saline-injected animals and 57 min (IQR 23 – 61 min), 53 min (IQR 37 – 59 min), 45 min (IQR 19 – 61 min) and 29 min (IQR 11 – 59 min) in MIA-injected animals which indicated significance between groups in responses evoked by the 100 g vF weight ($p = 0.1238$, $p = 0.0254$, $p = 0.4529$ and $p = 0.7037$ respectively, Mann-Whitney test). Further analysis using negative AUC values indicated that overall inhibition was significantly different between saline and MIA-injected animals in responses evoked using the 60 g filament, however reflexes evoked by 100 g, 180 g and 300 g showed no significant differences between treatment groups ($p = 0.0338$, $p = 0.3838$, $p = 0.8719$ and $p = 0.2048$ respectively, unpaired t-test; Figure 4.25A).

In the saline group (n = 10), significant inhibition of toes-BF reflexes evoked by 60 g, 100 g, 180 g and 300 g vF weights was induced by contralateral hindlimb injection of capsaicin ($p < 0.0001$, Friedman's ANOVA; Figures 4.21B, 4.22B, 4.23B and 4.24B) to medians of 3% (IQR 0 – 31%), 5% (IQR 1 – 31%), 16% (IQR 2 – 54%) and 34% (IQR 5 – 64%). The corresponding level of inhibition in the MIA-injected group (n = 9) was to a median of 15% (IQR 12 – 24%), 23% (IQR 4 – 35%), 29% (IQR 17 – 64%) and 45% (IQR 24 – 68%) of controls respectively ($p < 0.0001$, Friedman's ANOVA). Median duration of inhibition was 25 min (IQR 0 – 63 min), 53 min (IQR 25 – 63 min), 43 min (IQR 27 – 63 min) and 41 min (IQR 15 – 63 min) for 60 g, 100 g, 180 g and 300 g vF filaments respectively in saline-injected animals and 55 min (IQR 10 – 63 min), 47 min (IQR 23 – 61 min), 31 min (IQR 13 – 63 min) and 63 min (IQR 45 – 63 min) for the corresponding vF weights in MIA-injected animals; which were not significant between groups ($p = 0.6372$, $p = 0.7603$, $p = 0.6970$ and $p = 0.1990$ respectively, Mann-Whitney test). Analysis of negative AUC values found no significant difference in overall inhibition of toes-BF responses between saline and MIA-injected animals ($p = 0.7144$, $p = 0.9687$, $p = 0.9365$ and $p = 0.8000$ respectively, unpaired t-test; Figure 4.25B).

Following capsaicin injection toes-TA responses evoked by 60 g, 100 g, 180 g and 300 g monofilaments were significantly inhibited ($p < 0.0001$, Friedman's ANOVA; Figures 4.21C, 4.22C, 4.23C and 4.24C) to medians of 7% (IQR 2 – 32%), 13% (IQR 2 – 43%), 27% (IQR 18 – 60%) and 44% (IQR 35 – 73%) of controls in

saline-injected animals (n = 10); for MIA-injected animals (n = 9), significant inhibition ($p < 0.0001$ Friedman's ANOVA) to medians of 16% (IQR 11 – 39%), 27% (IQR 10 – 44%), 43% (IQR 37 – 60%) and 77% (IQR 65 – 97%) of controls was produced in toes-TA reflexes by these same respective vF filaments. Median duration of inhibition was 53 min (IQR 26 – 63 min), 49 min (IQR 27 – 63 min), 51 min (IQR 27 – 63 min) and 39 min (IQR 23 – 60 min) for 60 g, 100 g, 180 g and 300 g vF weights respectively in saline-injected animals and correspondingly 55 min (IQR 19 – 63 min), 59 min (IQR 29 – 63 min), 35 min (IQR 27 – 63 min) and 19 min (IQR 9 – 63 min) in MIA-injected animals which were not significantly different between groups ($p = 0.7940$, $p = 0.8218$, $p = 0.6640$ and $p = 0.3614$ respectively, Mann-Whitney test). Comparison of negative AUC values found that overall inhibition of toes-TA responses was not significantly different between saline and MIA-injected animals for any vF weight ($p = 0.7320$, $p = 0.6973$, $p = 0.5141$ and $p = 0.2954$ respectively, unpaired t-test; Figure 4.25C).

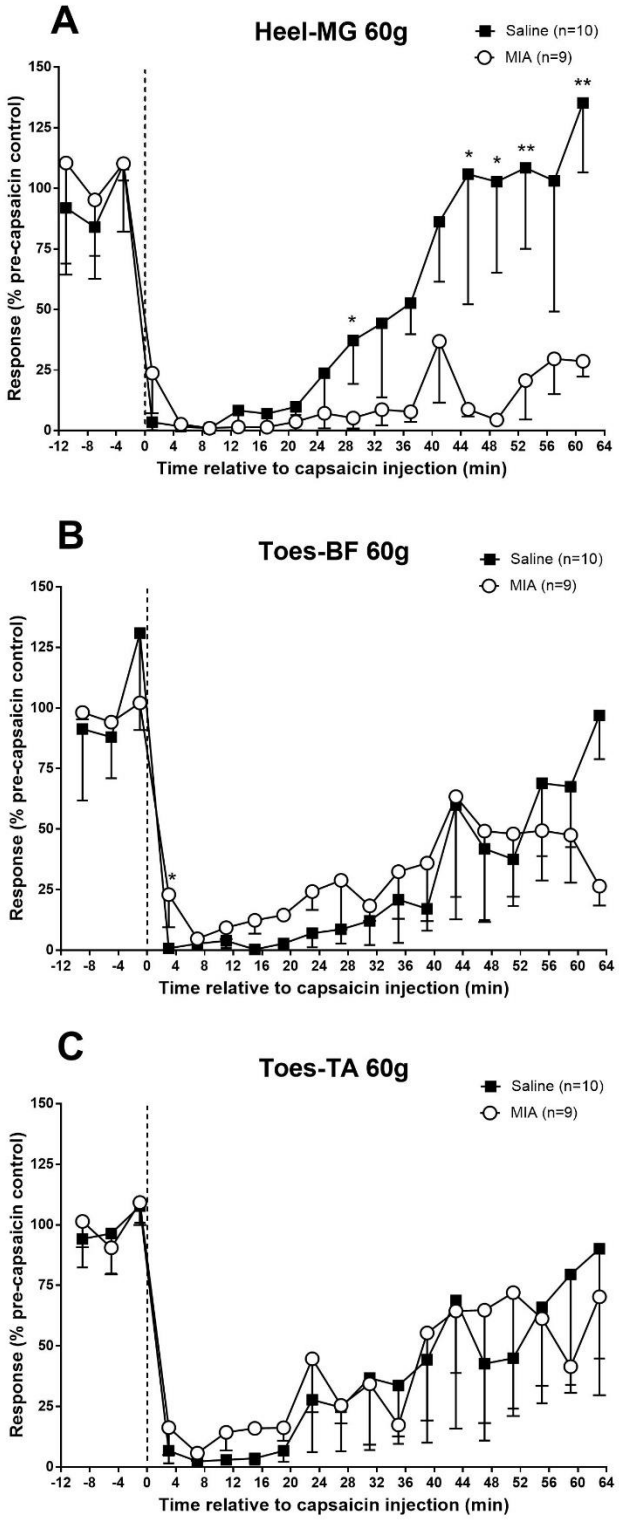

Figure 4.21. Effect of intramuscular injection of 500 µg capsaicin into the contralateral forelimb on mechanically evoked (A) heel-medial gastrocnemius (MG), (B) toes-biceps femoris (BF) and (C) toes-tibialis anterior (TA) reflexes using a 60 g von Frey (vF) monofilament in 28-day in saline and MIA-injected animals. Values plotted are medians and errors are interquartile ranges. *$p < 0.05$ denotes significant difference between saline and MIA-injected animals (Mann-Whitney test).

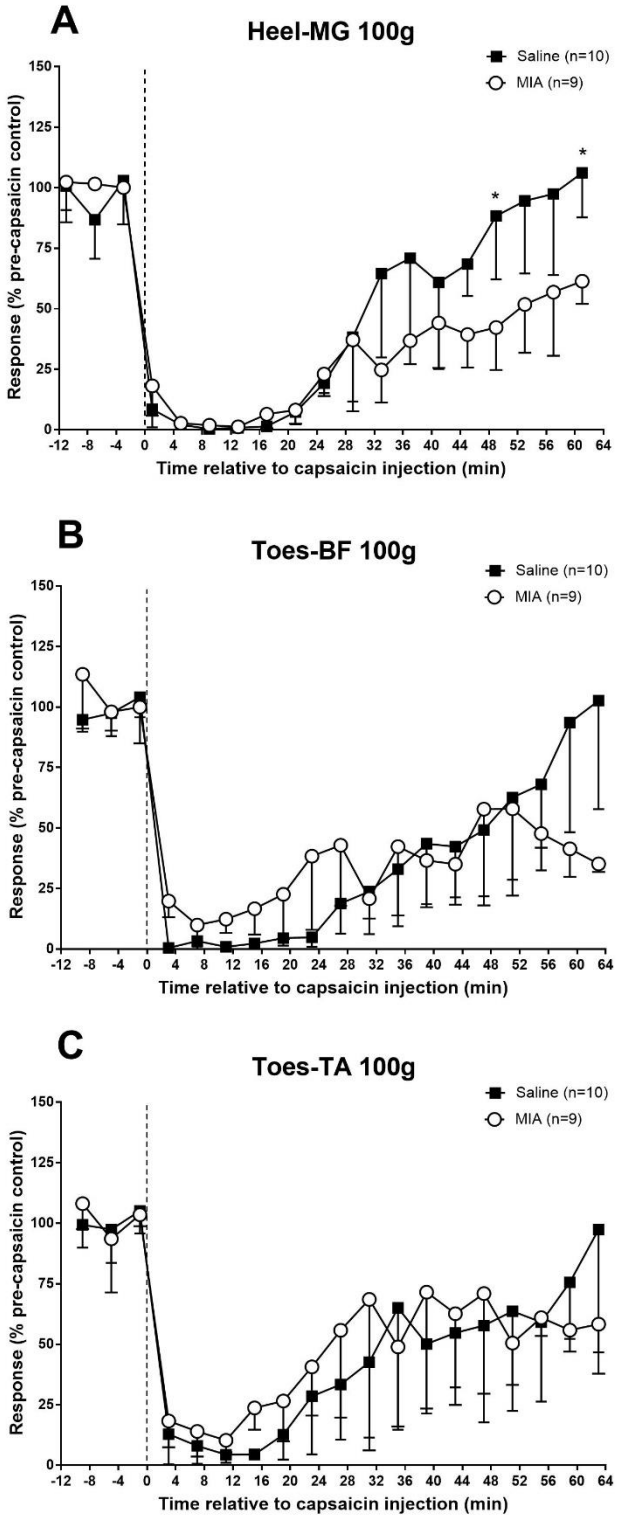

Figure 4.22. Effect of intramuscular injection of 500 µg capsaicin into the contralateral forelimb on mechanically evoked (A) heel-medial gastrocnemius (MG), (B) toes-biceps femoris (BF) and (C) toes-tibialis anterior (TA) reflexes using a 100 g von Frey (vF) monofilament in 28-day in saline and MIA-injected animals. Values plotted are medians and errors are interquartile ranges. *$p < 0.05$ denotes significant difference between saline and MIA-injected animals (Mann-Whitney test).

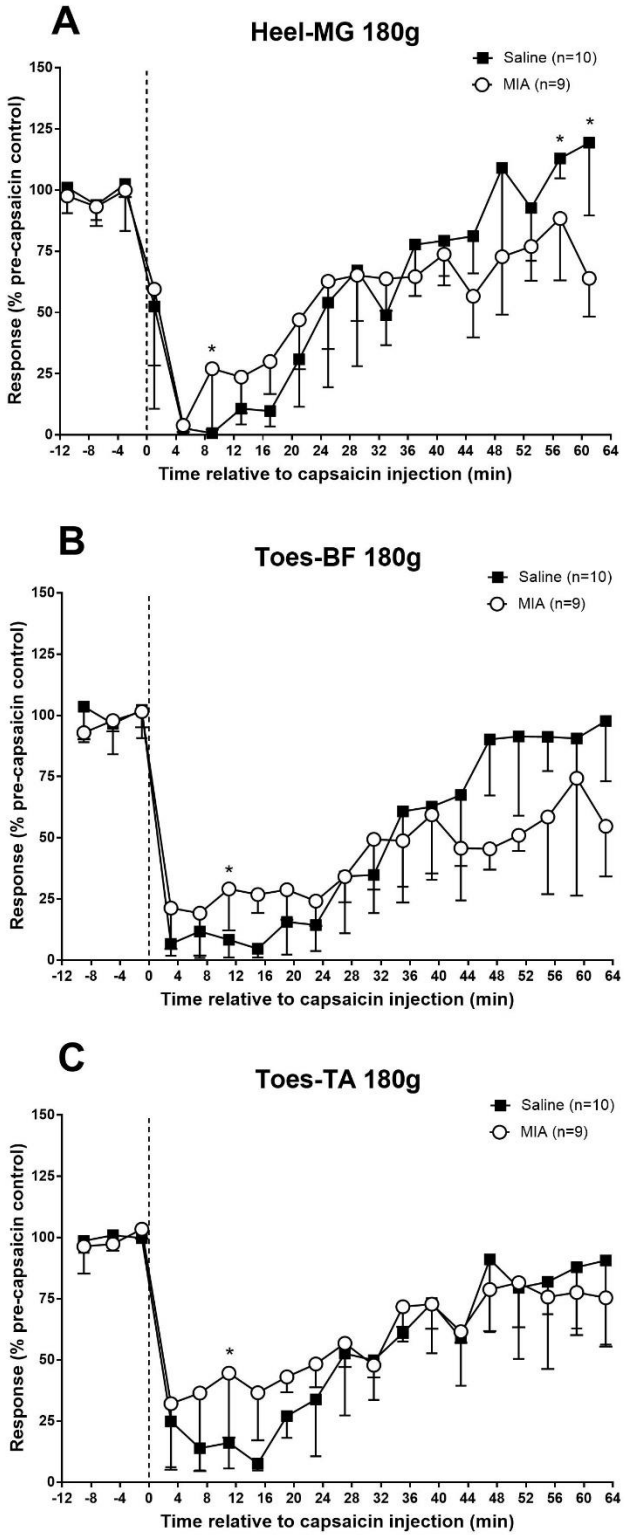

Figure 4.23. Effect of intramuscular injection of 500 µg capsaicin into the contralateral forelimb on mechanically evoked (A) heel-medial gastrocnemius (MG), (B) toes-biceps femoris (BF) and (C) toes-tibialis anterior (TA) reflexes using a 180 g von Frey (vF) monofilament in 28-day in saline and MIA-injected animals. Values plotted are medians and errors are interquartile ranges. *$p < 0.05$ denotes significant difference between saline and MIA-injected animals (Mann-Whitney test).

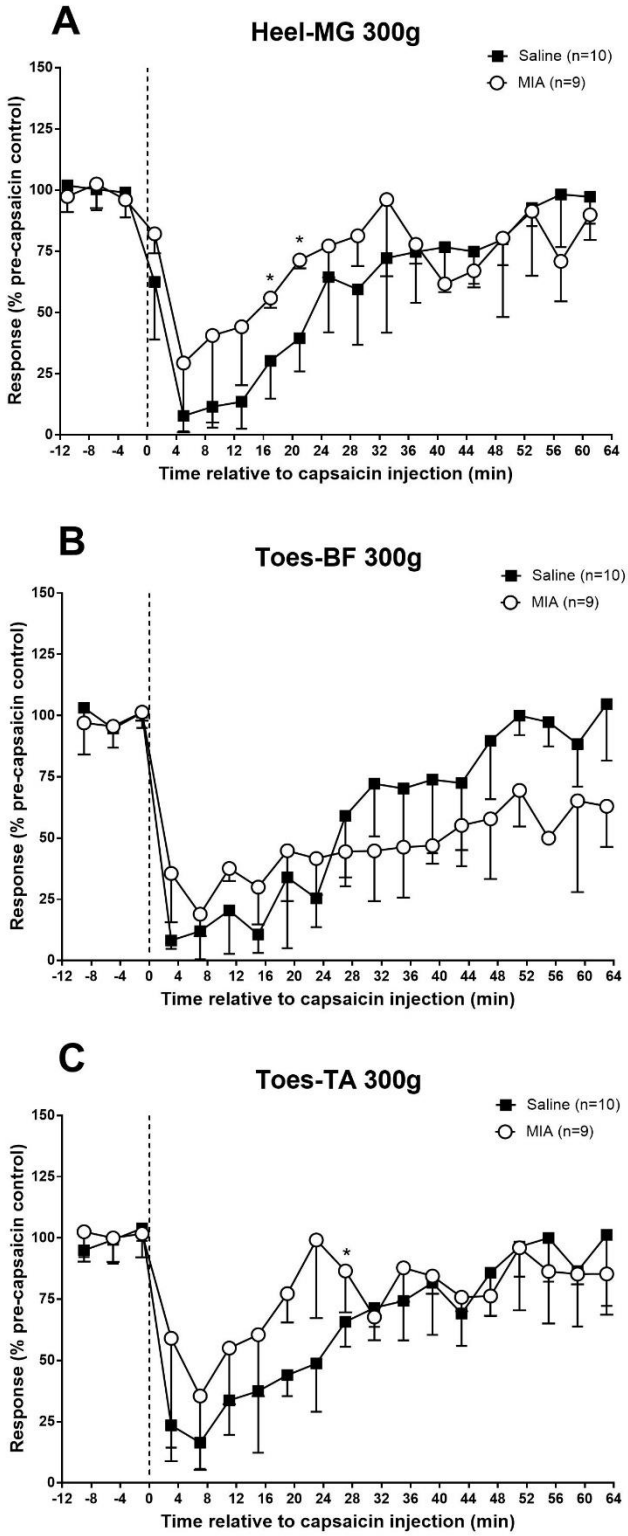

Figure 4.24. Effect of intramuscular injection of 500 µg capsaicin into the contralateral forelimb on mechanically evoked (A) heel-medial gastrocnemius (MG), (B) toes-biceps femoris (BF) and (C) toes-tibialis anterior (TA) reflexes using a 300 g von Frey (vF) monofilament in 28-day in saline and MIA-injected animals. Values plotted are medians and errors are interquartile ranges. *p < 0.05 denotes significant difference between saline and MIA-injected animals (Mann-Whitney test).

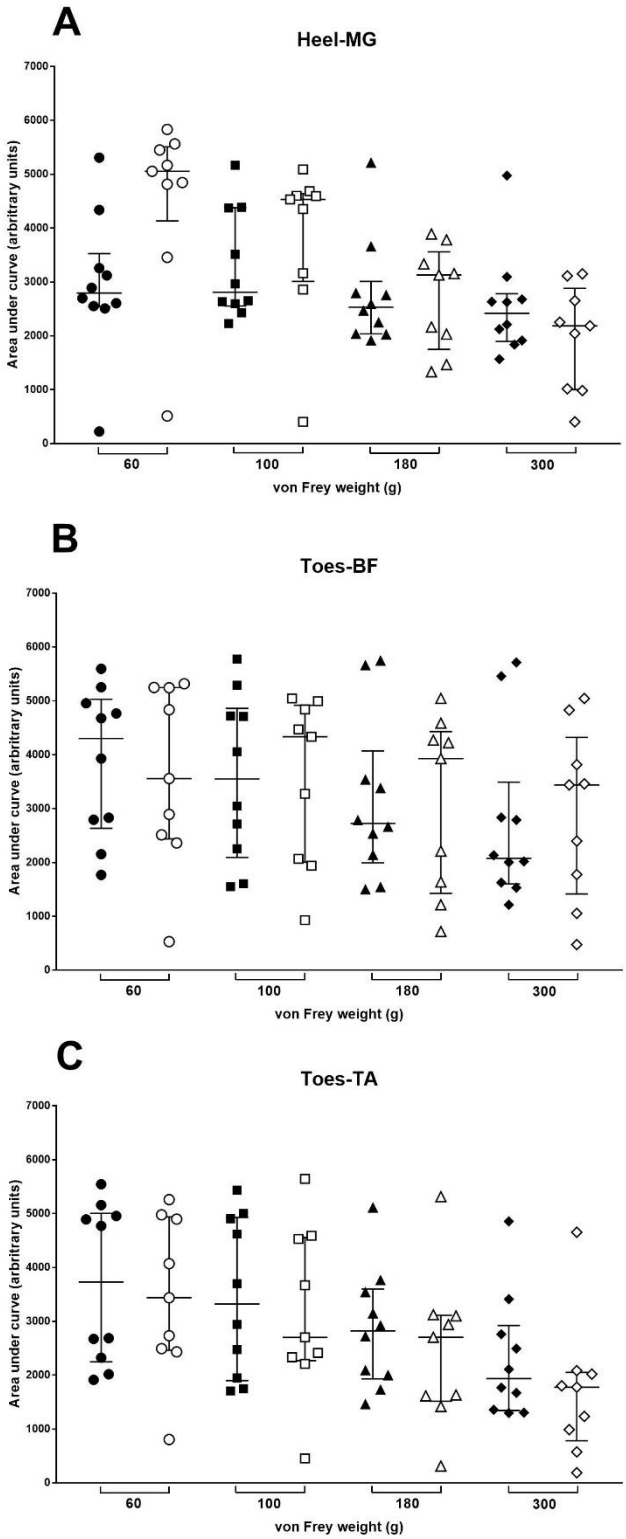

Figure 4.25. Effect of intramuscular injection of 500 µg capsaicin into the contralateral forelimb on mechanically evoked (A) heel-medial gastrocnemius (MG), (B) toes-biceps femoris (BF) and (C) toes-tibialis anterior (TA) reflexes using 60 – 300 g von Frey (vF) monofilaments in 28-day saline (n = 10, closed symbols) and MIA-injected (n = 9, open symbols) animals. Values plotted are area under curve (AUC) determinations for each animal with horizontal bars indicating medians and interquartile ranges.

4.3.6.3. Effect of capsaicin injection site

In nearly all cases, comparison of heel-MG, toes-BF and toes-TA responses between hindlimb and forelimb capsaicin injection sites indicated no significant difference in the degree, duration or overall inhibition between saline or MIA-injected animals ($p > 0.05$, Mann-Whitney or unpaired t-test). The one exception being that duration of inhibition was significantly shorter after forelimb compared to hindlimb injection for heel-MG reflexes evoked by the 100 g monofilament in saline-injected animals with medians of 29 min (IQR 0 – 41 min) and 57 min (IQR 30 – 61 min) respectively ($p = 0.0366$, Mann-Whitney test).

4.3.7. Effect of 50 μg capsaicin on mechanically-evoked responses

Responses evoked by 10 g and 26 g vF monofilaments were found to be variable and sometimes absent before and after capsaicin, therefore these responses have been omitted from results.

4.3.7.1. Injection into the contralateral hindlimb

In the saline group (n = 10), no significant inhibition was induced in heel-MG by 60 g, 100 g, 180 g or 300 g vF weights ($p = 0.5695$, $p = 0.3639$, $p = 0.1898$ and $p = 0.4784$ respectively, Friedman's ANOVA) or in MIA-injected animals (n = 11) evoked by 180 g and 300 g vF weights ($p = 0.4981$ and $p = 0.6085$ respectively, Friedman's ANOVA; Figures 4.26A, 4.27A, 4.28A and 4.29A). However, significant inhibition was induced in responses evoked by 60 g and 100 g vF weights in MIA-injected animals ($p = 0.0003$ and $p = 0.0081$ respectively, Friedman's ANOVA) to medians of 55% (IQR 23 – 98%) and 65% (IQR 54 – 101%) respectively. Median duration of inhibition was calculated as 13 min (IQR 0 – 61 min) and 17 min (IQR 0 – 21 min) for 60 g and 100 g vF weights respectively in MIA-injected animals which was not significant between groups ($p = 0.6802$, Mann-Whitney test). Analysis of negative AUC values indicated no significant differences in overall inhibition of heel-MG reflexes between saline and MIA-injected animals ($p = 0.3757$, $p = 0.8095$, $p = 0.4907$ and $p = 0.4978$ respectively, Mann-Whitney test; Figure 4.30A).

Toes-BF responses evoked by 60 g, 100 g, 180 g and 300 g monofilaments were inhibited by 50 μg capsaicin into the contralateral hindlimb to medians of 56% (IQR 36 – 82%), 51% (IQR 42 – 70%), 82% (IQR 60 – 89%) and 80% (IQR 69 – 95%) of controls respectively in saline-injected animals (n = 10), however the inhibitory effect for responses evoked by the 300 g vF filament was not found to be significant ($p = 0.0009$, $p = 0.0002$, $p = 0.0418$ and $p = 0.1243$ respectively, Friedman's ANOVA; Figures 4.26B, 4.27B, 4.28B and 4.29B). These reflexes in MIA-injected animals (n = 11) were significantly inhibited ($p = 0.0046$, $p < 0.0001$, $p = 0.0038$ and $p = 0.0002$ respectively, Friedman's ANOVA) to a median of 56% (IQR 6 – 117%), 26% (IQR 5 – 96%), 51% (IQR 26 – 79%) and 65% (IQR 16 – 87%) of controls at the corresponding vF weights. Median duration of inhibition was calculated as 0 min (IQR 0 – 17 min), 7 min (IQR 0 – 23 min), 17 min (IQR 8 – 38 min) and 15 min (IQR 6 – 30 min) for 60 g, 100 g, 180 g and 300 g vF weights respectively in saline-injected animals and 0 min (IQR 0 – 15 min), 51 min (IQR 0 – 63 min), 23 min (IQR 11 – 43 min) and 31 min (IQR 11 – 47 min) in MIA-injected animals which was significant between groups ($p = 0.7178$, $p = 0.1018$, $p = 0.4959$ and $p = 0.3568$ respectively, Mann-Whitney test). Analysis of negative AUC values revealed significant differences in overall inhibition between saline and MIA-injected animals of responses to the 100 g vF weight in the toes-BF reflex response ($p = 0.0305$, unpaired t-test; Figure 4.30B), however did not reveal any significant differences in responses to any other filaments (60 g, 180 g and 300 g)($p = 0.6508$, $p = 0.1616$ and $p = 0.1579$ respectively, unpaired t-test).

For toes-TA reflexes in saline-injected animals (n = 10), responses to 60 g, 100 g, 180 g and 300 g vF filaments were inhibited to medians of 63% (IQR 41 – 93%), 78% (IQR 52 – 101%), 95% (IQR 84 – 98%) and 87% (IQR 70 – 99%) of controls respectively, however the inhibitory effect for responses evoked by the 300 g vF filament was not found to be significant ($p = 0.0368$ $p = 0.0005$, $p = 0.0303$ and $p = 0.0681$ respectively, Friedman's ANOVA; Figures 4.26C, 4.27C, 4.28C and 4.29C). Similarly, for MIA-injected animals (n = 11) significant inhibition ($p = 0.0018$, $p < 0.0001$, $p = 0.0004$ and $p = 0.0018$ respectively, Friedman's ANOVA) to medians of 50% (IQR 11 – 92%), 58% (IQR 27 – 92%), 77% (IQR 69 – 89%) and 84% (IQR 66 – 88%) of controls was produced in toes-TA reflexes evoked by these same respective vF filaments. Median duration of inhibition was calculated as 9 min (IQR 0 – 17 min), 11 min (IQR 0 – 24 min), 19 min (IQR 7 – 48 min) and 10 min (IQR 0 – 30 min) for 60 g, 100 g,180 g and 300 g vF weights respectively in saline-injected animals and correspondingly 15 min (IQR 0 – 43 min), 23 min (IQR 7 – 63 min), 23 min (IQR 11 – 35 min) and 43 min (IQR 23 – 63 min) in MIA-injected animals which was not significant between groups ($p = 0.5523$, $p = 0.02520$, $p = 0.9063$ and $p = 0.0513$ respectively, Mann-Whitney test). Comparison of negative AUC values found significant differences in overall inhibition of toes-TA responses evoked by the 100 g vF filament ($p = 0.0335$, unpaired t-test; Figure 4.30C), however, responses evoked by 60 g, 180 g and 300 g vF filaments did not indicate any significant differences ($p = 0.6738$, $p = 0.2986$ and $p = 0.2007$ respectively, unpaired t-test).

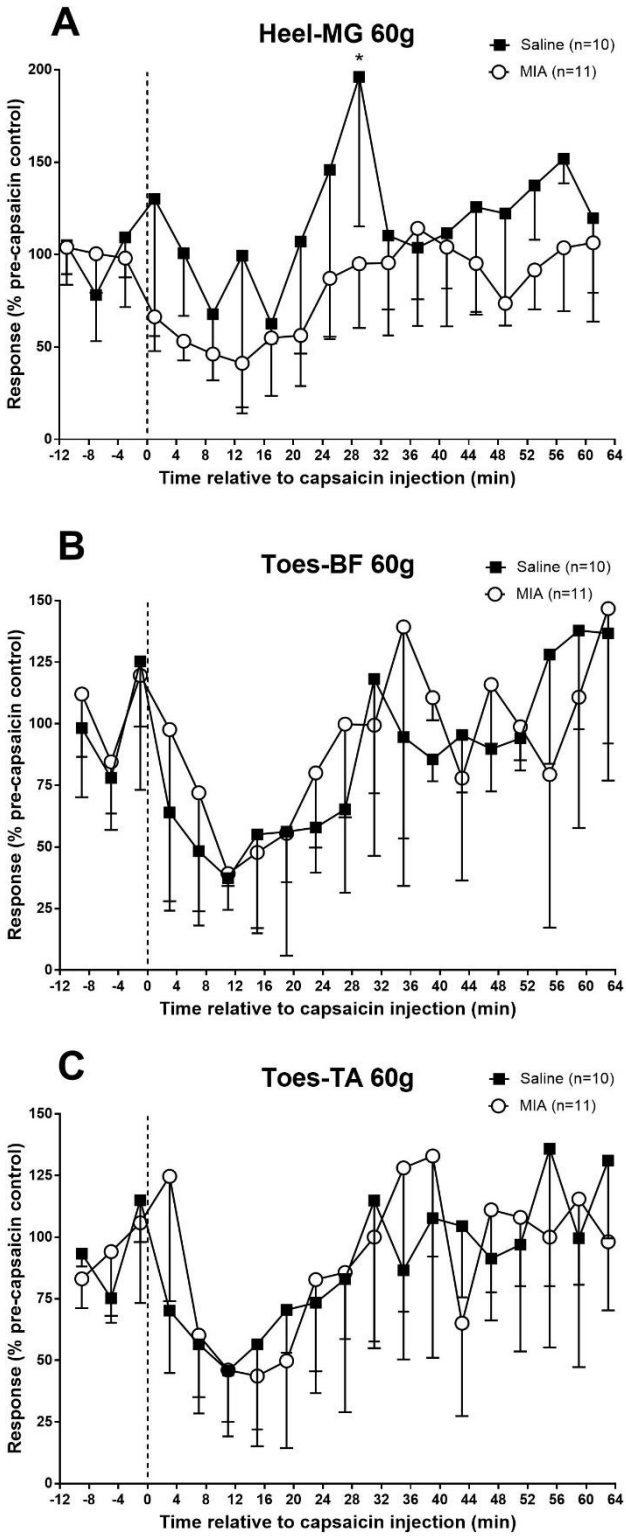

Figure 4.26. Effect of intramuscular injection of 50 µg capsaicin into the contralateral hindlimb on mechanically evoked (A) heel-medial gastrocnemius (MG), (B) toes-biceps femoris (BF) and (C) toes-tibialis anterior (TA) reflexes using a 60 g von Frey (vF) monofilament in 28-35 day saline and MIA-injected animals. Values plotted are medians and errors are interquartile ranges. *$p < 0.05$ denotes significant difference between saline and MIA-injected animals at the same post-capsaicin time points (Mann-Whitney test).

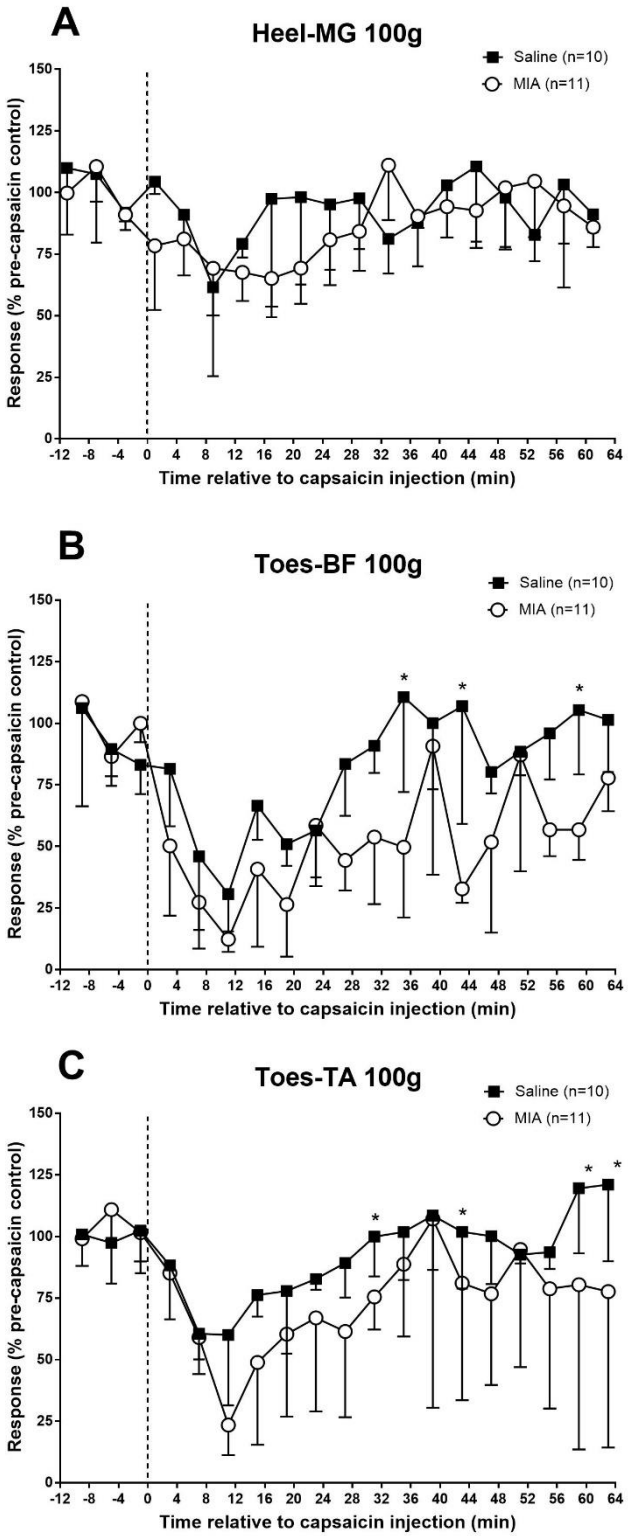

Figure 4.27. Effect of intramuscular injection of 50 µg capsaicin into the contralateral hindlimb on mechanically evoked (A) heel-medial gastrocnemius (MG), (B) toes-biceps femoris (BF) and (C) toes-tibialis anterior (TA) reflexes using a 100 g von Frey (vF) monofilament in 28-35 day saline and MIA-injected animals. Values plotted are medians and errors are interquartile ranges. *p < 0.05 denotes significant difference between saline and MIA-injected animals at the same post-capsaicin time points (Mann-Whitney test).

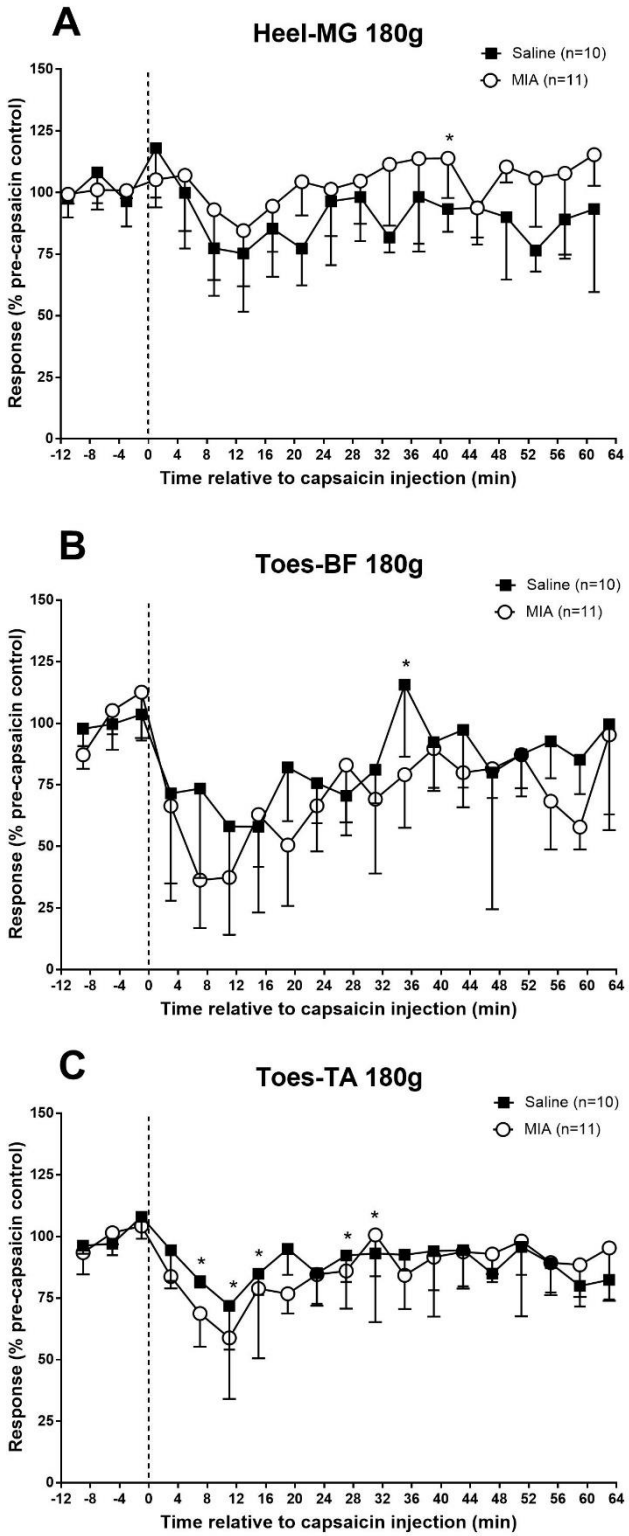

Figure 4.28. Effect of intramuscular injection of 50 µg capsaicin into the contralateral hindlimb on mechanically evoked (A) heel-medial gastrocnemius (MG), (B) toes-biceps femoris (BF) and (C) toes-tibialis anterior (TA) reflexes using a 180 g von Frey (vF) monofilament in 28-35 day saline and MIA-injected animals. Values plotted are medians and errors are interquartile ranges. *p < 0.05 denotes significant difference between saline and MIA-injected animals at the same post-capsaicin time points (Mann-Whitney test).

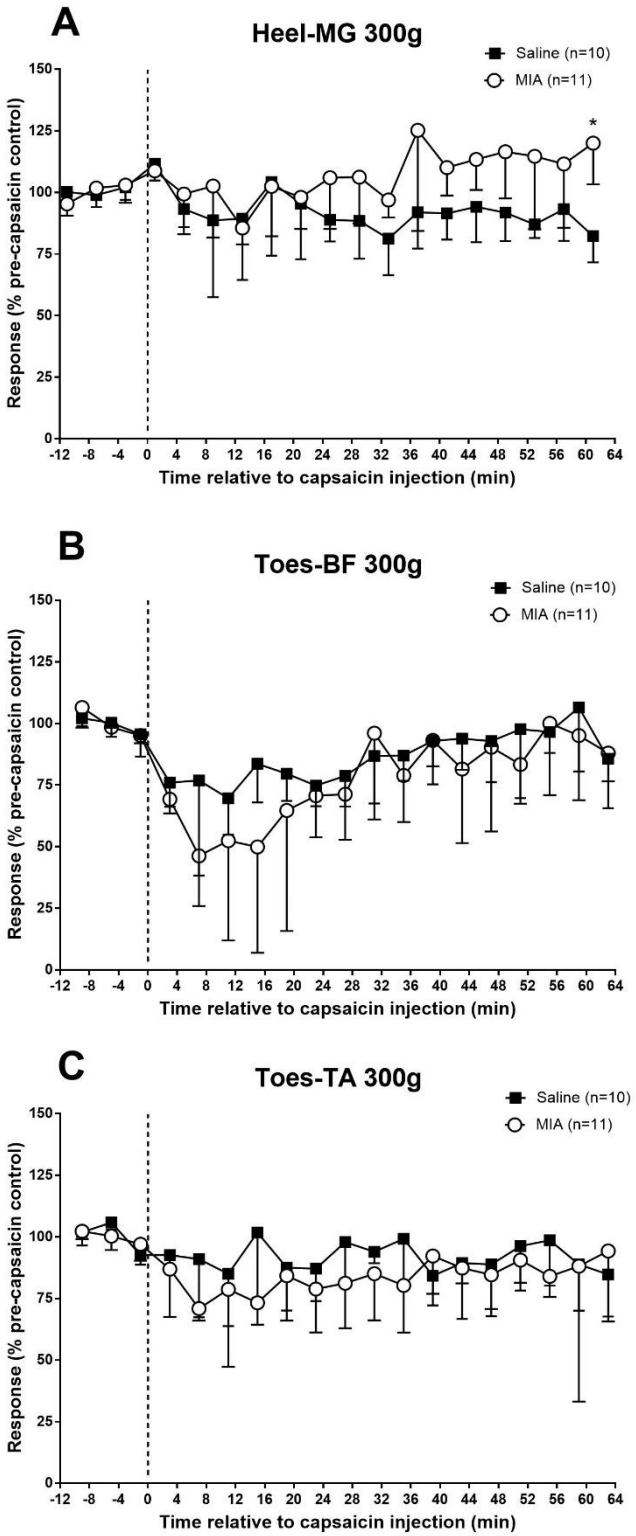

Figure 4.29. Effect of intramuscular injection of 500 µg capsaicin into the contralateral hindlimb on mechanically evoked (A) heel-medial gastrocnemius (MG), (B) toes-biceps femoris (BF) and (C) toes-tibialis anterior (TA) reflexes using a 300 g von Frey (vF) monofilament in 28-35 day saline and MIA-injected animals. Values plotted are medians and errors are interquartile ranges. *$p < 0.05$ denotes significant difference between saline and MIA-injected animals at the same post-capsaicin time points (Mann-Whitney test).

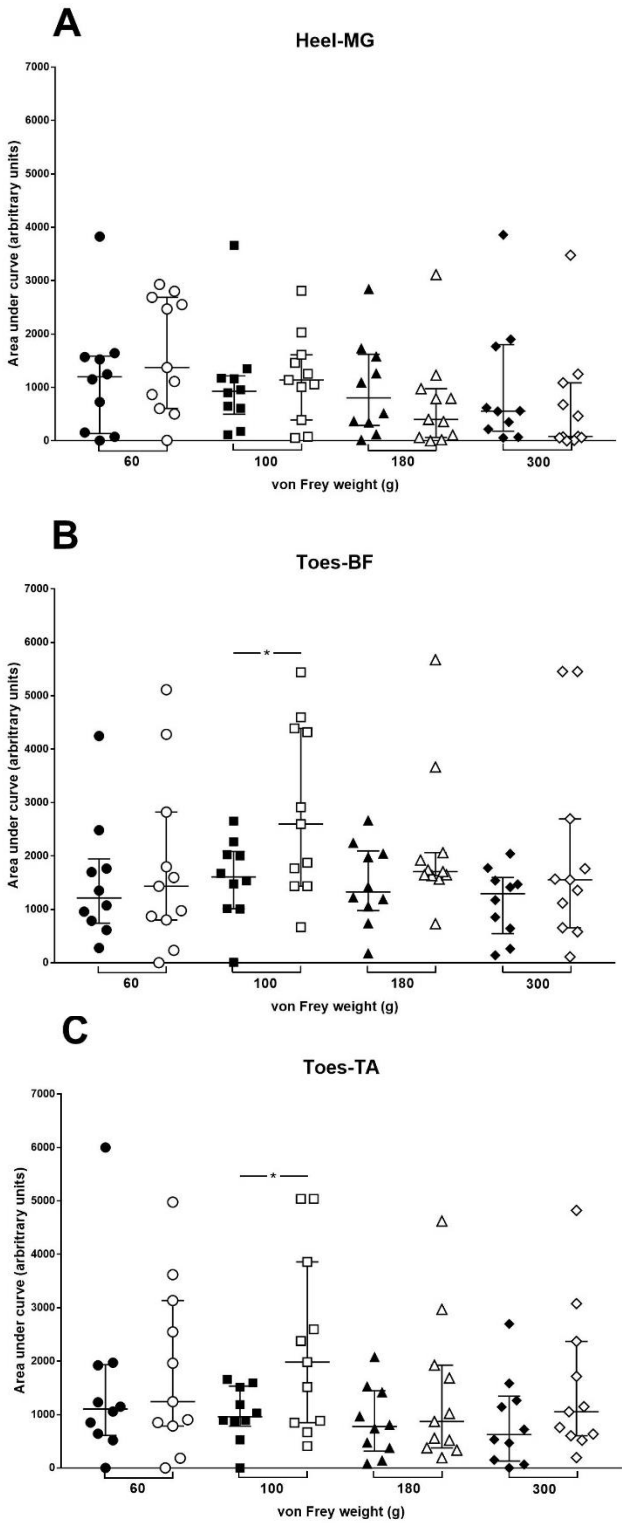

Figure 4.30. Effect of intramuscular injection of 50 µg capsaicin into the contralateral hindlimb on mechanically evoked (A) heel-medial gastrocnemius (MG), (B) toes-biceps femoris (BF) and (C) toes-tibialis anterior (TA) reflexes using 60 – 300 g von Frey (vF) monofilaments in 28-35 day saline (n = 10, closed symbols) and MIA-injected (n = 11, open symbols) animals. Values plotted are area under curve (AUC) determinations for each animal with horizontal bars indicating medians and interquartile ranges. *p < 0.05 denotes significant difference between saline and MIA-injected animals (unpaired t-test).

4.3.7.2. Injection into the contralateral forelimb

Following 50 µg capsaicin to the contralateral forelimb, heel-MG responses evoked by 60 g, 100 g, 180 g and 300 g vF filaments were inhibited to medians of 73% (IQR 62 – 136%), 62% (IQR 41 – 85%), 83% (IQR 62 – 86%) and 83% (IQR 76 – 90%) of controls respectively in saline-injected animals (n = 9), however the inhibitory effect for responses evoked by the 300 g vF filament was not found to be significant ($p = 0.0011$, $p < 0.0001$, $p = 0.0005$ and $p = 0.0615$ respectively, Friedman's ANOVA; Figures 4.31A, 4.32A, 4.33A and 4.34A). Similarly, in MIA-injected animals (n = 11), heel-MG responses evoked by the corresponding vF weights were inhibited to medians of 64% (IQR 51 – 93%), 97% (IQR 68 – 100%), 99% (IQR 77 – 104%) and 94% (IQR 84 – 110%) of controls, however responses evoked by 100 g and 300 g were not found to be significant ($p = 0.0006$, $p = 0.0622$, $p = 0.0407$ and $p = 0.1229$ respectively, Friedman's ANOVA). Median duration of inhibition in saline-injected animals was 0 min (IQR 0 – 3 min), 9 min (IQR 0 – 33 min), 53 min (IQR 13 – 59 min) and 61 min (IQR 13 – 61 min) for 60 g, 100 g, 180 g and 300 g vF weights respectively and 1 min (IQR 0 – 61 min), 1 min (IQR 0 – 61 min), 9 min (IQR 0 – 61 min) and 0 min (IQR 0 – 61 min) in MIA-injected animals; these durations were not significantly different between groups ($p = 0.1968$, $p = 0.8913$, $p = 0.2768$ and $p = 0.0650$, Mann-Whitney test). Furthermore, analysis of negative AUC values revealed no significant differences in overall inhibition of responses to 60 – 300 g vF filaments between groups ($p = 0.7835$, $p = 0.7281$, $p = 0.8554$ and $p = 0.4589$ respectively, unpaired t-test; Figure 4.35A).

In saline-injected animals (n = 9), significant inhibition of toes-BF responses evoked by 60 g, 100 g, 180 g and 300 g monofilaments was induced ($p = 0.0001$, $p = 0.0153$, $p < 0.0001$ and $p = 0.0001$ respectively, Friedman's ANOVA; Figures 4.31B, 4.32B 4.33B and 4.34B) to medians of 15% (IQR 9 – 47%), 65% (IQR 33 – 82%), 75% (IQR 70 – 92%) and 87% (IQR 68 – 107%) of controls respectively. The corresponding level of significant inhibition in MIA-injected animals (n = 11) was to medians of 53% (IQR 17 – 81%), 28% (IQR 21 – 56%), 54% (IQR 29 – 69%) and 63% (IQR 44 – 73%) of controls respectively ($p < 0.0001$, Friedman's ANOVA). Median duration of inhibition was calculated as 11 min (IQR 0 – 47 min), 0 min (IQR 0 – 31 min), 15 min (IQR 0 – 43 min) and 11 min (IQR 0 – 25 min) for 60 g, 100 g, 180 g and 300 g vF weights respectively in saline-injected animals and 0 min (IQR 0 – 7 min), 23 min (IQR 0 – 31 min), 35 min (IQR 11 – 55 min) and 35 min (IQR 15 – 63 min) for the corresponding vF weights in MIA-injected animals; these durations were significantly different for the 300 g vF weight, however no other differences were found ($p = 0.0928$, $p = 0.3448$, $p = 0.2356$ and $p = 0.0286$, Mann-Whitney test). Analysis of negative AUC values revealed significant differences in overall inhibition of toes-BF responses to 180 g and 300 g vF filaments ($p = 0.0204$ and $p = 0.0220$ respectively, unpaired t-test; Figure 4.35B), however, no other differences between groups were observed ($p = 0.1944$ and $p = 0.1304$ respectively, unpaired t-test).

Following capsaicin administration, toes-TA reflex responses evoked by 60 g, 100 g, 180 g and 300 g vF filaments were inhibited to medians of 40% (IQR 22 – 62%), 86% (IQR 74 – 100%), 82% (IQR 74 – 99%) and 80% (IQR 76 – 94%) of controls respectively in saline-injected animals (n = 9), however the inhibition evoked using 180 g was not significant ($p < 0.0001$, $p = 0.0088$, $p = 0.6771$ and $p = 0.0411$ respectively, Friedman's ANOVA; Figures 4.31C, 4.32C, 4.33C and 4.34C). Similarly, these reflexes in MIA-injected animals (n = 11) were inhibited to medians of 52% (IQR 23 – 64%), 60% (IQR 56 – 73%), 105% (IQR 92 – 120%) and 101% (IQR 82 – 104%) of controls at the corresponding vF weights, however the inhibition evoked using 300 g was not significant ($p = 0.0001$, $p < 0.0001$, $p = 0.0016$ and $p = 0.0557$ respectively, Friedman's ANOVA). Median duration of inhibition was calculated as 7 min (IQR 0 – 39 min), 7 min (IQR 0 – 17 min), 11 min (IQR 0 – 27 min) and 19 min (IQR 0 – 43 min) for 60 g, 100 g, 180 g and 300 g vF weights respectively in saline-injected animals and 23 min (IQR 0 – 47 min), 19 min (IQR 0 – 51 min), 15 min (IQR 0 – 39 min) and 15 min (IQR 0 – 39 min) in MIA-injected animals, which was not significantly different between groups ($p = 0.5208$, $p = 0.1481$, $p = 0.4525$ and $p = 0.9175$ respectively, Mann-Whitney test). Analysis of negative AUC values revealed no significant differences in overall inhibition of responses to 60 – 300 g vF filaments ($p = 0.2175$, $p = 0.5542$, $p = 0.9637$ and $p = 0.7412$, unpaired t-test; Figure 4.35C).

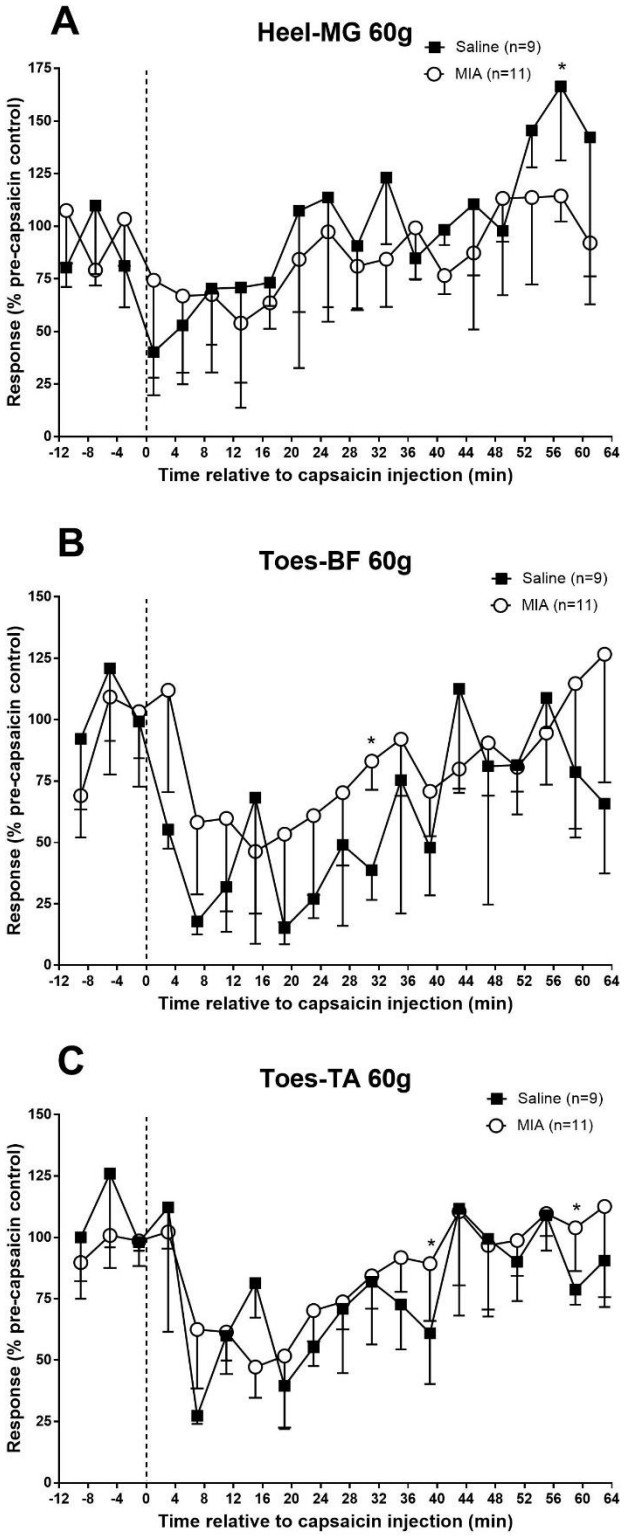

Figure 4.31. Effect of intramuscular injection of 50 µg capsaicin into the contralateral forelimb on mechanically evoked (A) heel-medial gastrocnemius (MG), (B) toes-biceps femoris (BF) and (C) toes-tibialis anterior (TA) reflexes using a 60 g von Frey (vF) monofilament in 28-35 day saline and MIA-injected animals. Values plotted are medians and errors are interquartile ranges. *$p < 0.05$ denotes significant difference between saline and MIA-injected animals at the same post-capsaicin time points (Mann-Whitney test).

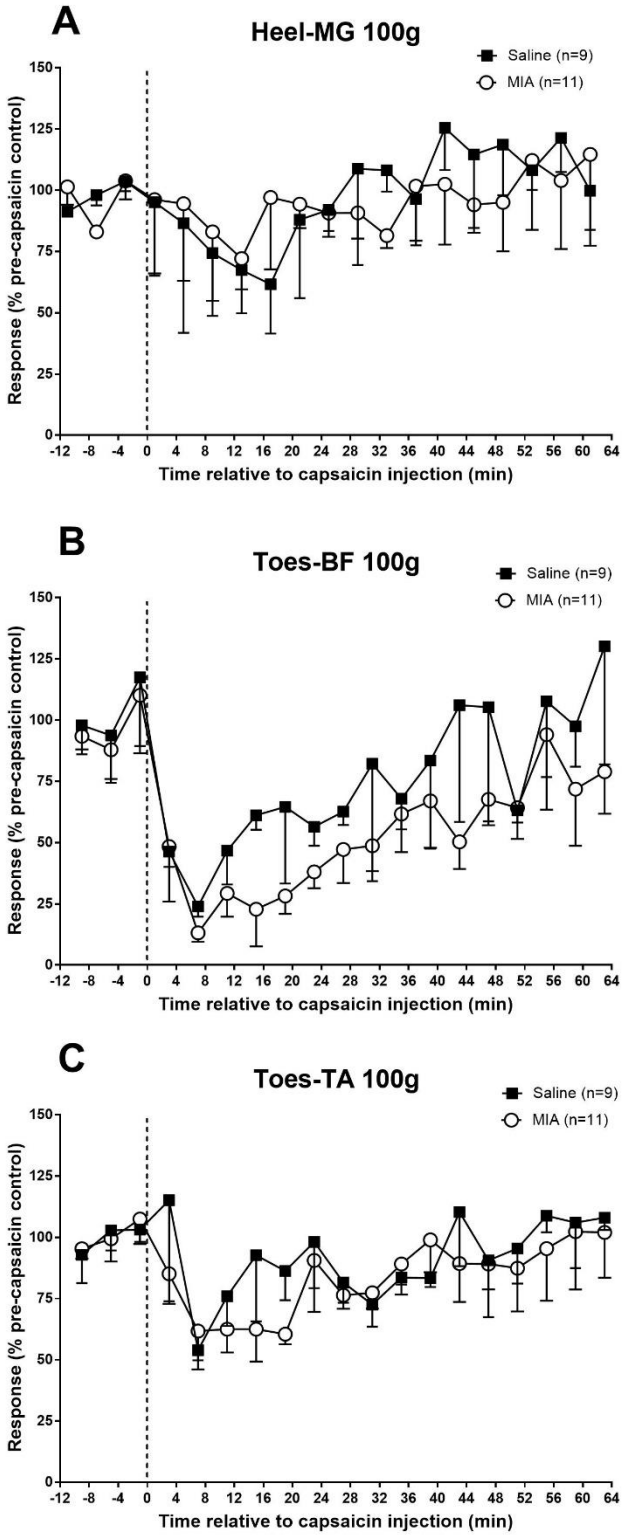

Figure 4.32. Effect of intramuscular injection of 50 µg capsaicin into the contralateral forelimb on mechanically evoked (A) heel-medial gastrocnemius (MG), (B) toes-biceps femoris (BF) and (C) toes-tibialis anterior (TA) reflexes using a 100 g von Frey (vF) monofilament in 28-35 day saline and MIA-injected animals. Values plotted are medians and errors are interquartile ranges.

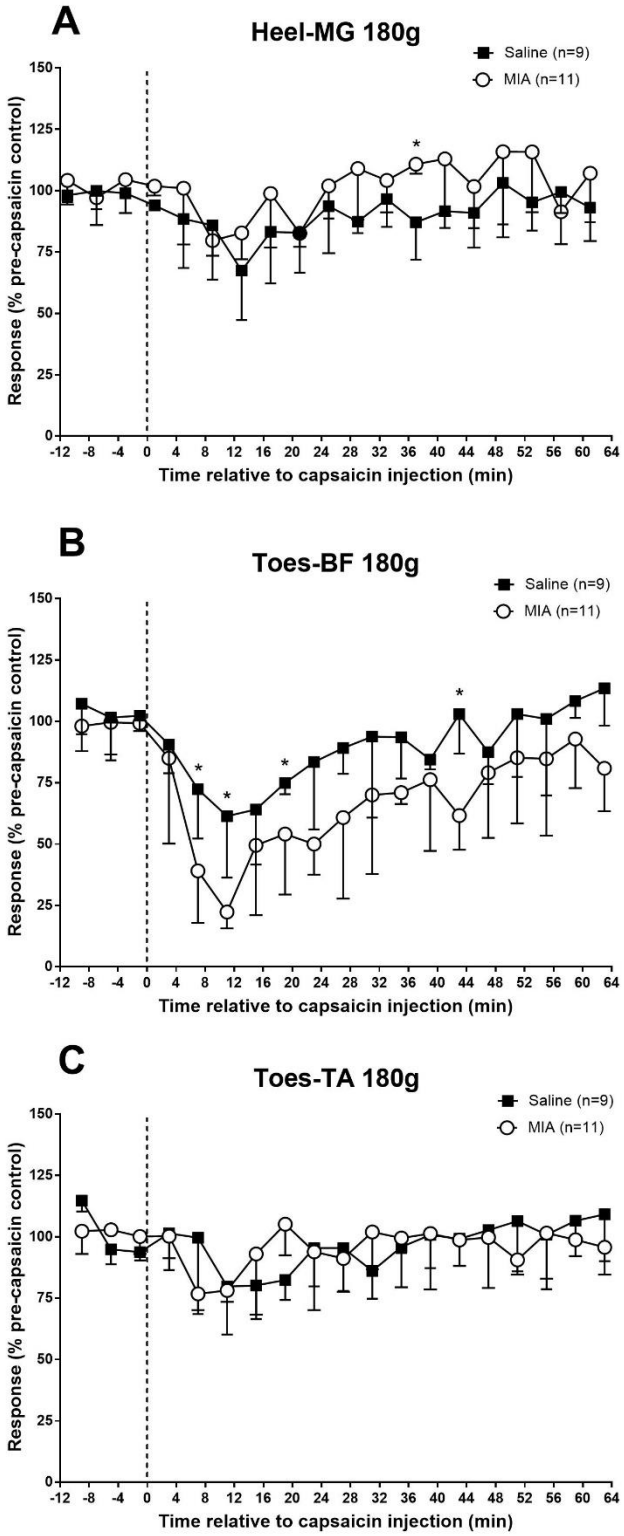

Figure 4.33. Effect of intramuscular injection of 50 µg capsaicin into the contralateral forelimb on mechanically evoked (A) heel-medial gastrocnemius (MG), (B) toes-biceps femoris (BF) and (C) toes-tibialis anterior (TA) reflexes using a 180 g von Frey (vF) monofilament in 28-35 day saline and MIA-injected animals. Values plotted are medians and errors are interquartile ranges. *$p < 0.05$ denotes significant difference between saline and MIA-injected animals at the same post-capsaicin time points (Mann-Whitney test).

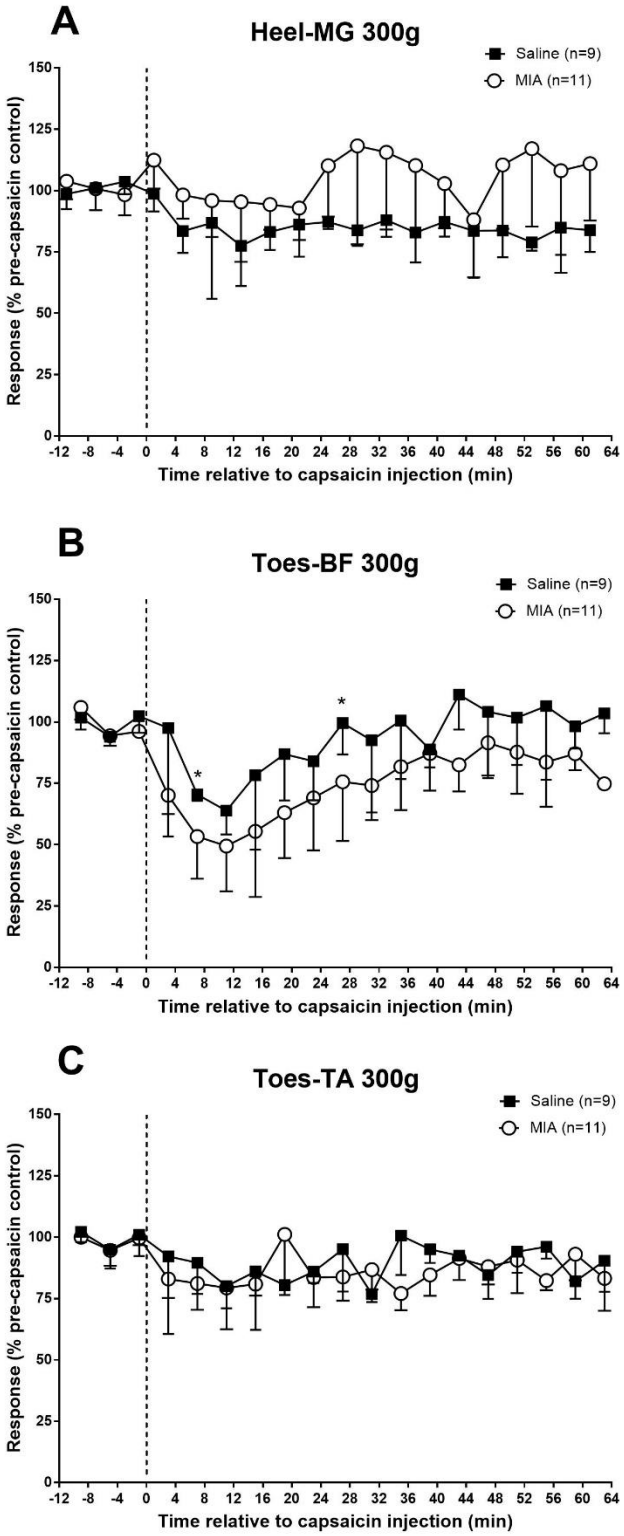

Figure 4.34. Effect of intramuscular injection of 50 µg capsaicin into the contralateral forelimb on mechanically evoked (A) heel-medial gastrocnemius (MG), (B) toes-biceps femoris (BF) and (C) toes-tibialis anterior (TA) reflexes using a 300 g von Frey (vF) monofilament in 28-35 day saline and MIA-injected animals. Values plotted are medians and errors are interquartile ranges. *$p < 0.05$ denotes significant difference between saline and MIA-injected animals at the same post-capsaicin time points (Mann-Whitney test).

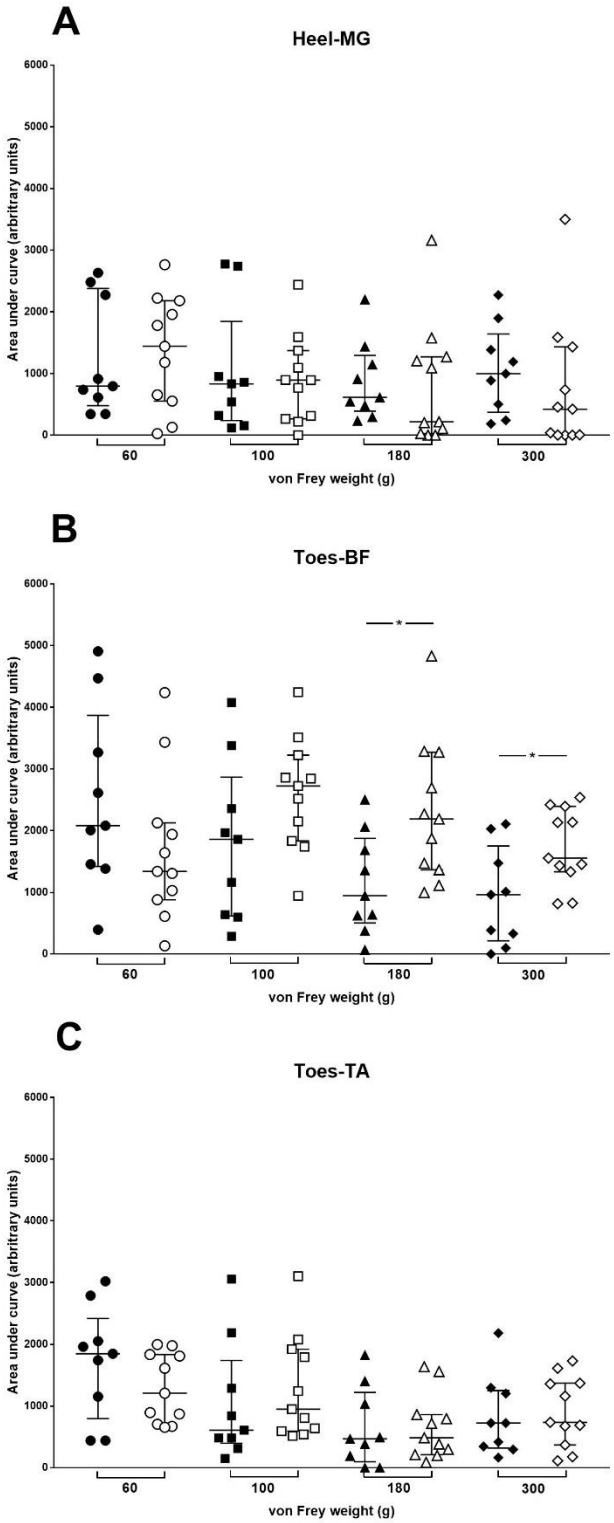

Figure 4.35. Effect of intramuscular injection of 50 µg capsaicin into the contralateral forelimb on mechanically evoked (A) heel-medial gastrocnemius (MG), (B) toes-biceps femoris (BF) and (C) toes-tibialis anterior (TA) reflexes using 60 – 300 g von Frey (vF) monofilaments in 28-35 day saline (n = 9, closed symbols) and MIA-injected (n = 11, open symbols) animals. Values plotted are area under curve (AUC) determinations for each animal with horizontal bars indicating medians and interquartile ranges. *$p < 0.05$ denotes significant difference between saline and MIA-injected animals (unpaired t-test).

4.3.7.3. Effect of capsaicin injection site

Comparison of heel-MG, toes-BF and toes-TA responses between hindlimb and forelimb capsaicin injection sites indicated no significant differences in the degree, duration or overall (AUC) inhibition between saline or MIA-injected animals ($p > 0.05$, Mann-Whitney or unpaired t-test).

4.4. Discussion

OA is a degenerative joint disease which can be investigated in animals using various animal models (see section 1.5.6). After 28-35 days the MIA model has been shown to have severe cartilage lesions across the whole articular surface (0.3 mg and 3.0 mg dose) with chondral erosions and exposing the subchondral bone on both the tibial plateau and femoral condyle (Guingamp et al., 1997). The non load-bearing regions of the joint such as the patella and femoral groove have been shown to be much less affected, however large osteophytes can be observed in the periphery of the femoral condyles and tibial plateaus after 30 days (0.3 mg and 3.0 mg dose) and still persist after 49 days (1 mg dose)(Guingamp et al., 1997; Mapp et al., 2013). Macroscopic chondropathy scores were shown to be significantly increased after 21 days in MIA-injected animals (1 mg dose) characterised by cartilage damage in both the medial and lateral tibiofemoral compartments (Nwosu et al., 2016a). In the present study MIA animals had severe cartilage damage 28-35 days post-injection with the majority of cartilage on both the tibial plateaus and femoral condyles completely destroyed. The surface of the joint indicated deep fibrillation as well as large “stippled white” areas where the underlying subchondral bone was exposed. In some of the scored MIA joints, the presence of osteophytes in the periphery of the joint could be observed and although this was not taken into account in the scoring of joints it is a key feature of the development and severity of OA. Although the present study did not investigate the histology of the joint there is extensive literature supporting the histological damage

observed in animals injected with MIA (Guingamp et al., 1997; Guzman et al., 2003; Fernihough et al., 2004; Pomonis et al., 2005; Ferland et al., 2011; Mapp et al., 2013; Nwosu et al., 2016a, 2016b). Histology at 22 days post MIA injection (1 mg dose) revealed chondrocyte necrosis with loss of the matrix which results in a significant decrease in the thickness of the cartilage. This marked change in the cartilage often leads to separation of the necrotic cartilage from the subchondral bone resulting in fibrillation and ulceration of the cartilage, eventually exposing the underlying subchondral bone (van der Kraan et al., 1989; Guingamp et al., 1997; Guzman et al., 2003; Pomonis et al., 2005). After 14 days, synovial inflammation has been observed in the MIA model (1 mg dose) which, persisting for the duration of the disease, is associated with increased osteophyte formation in both human and mouse OA (Dieppe and Lohmander, 2005). Additionally, assessing radiographs of MIA-injected joints (1 mg) after 29 days indicated obvious joint degeneration which was characterised by osteolysis and swelling as well as displacement of the patella, along with significant reductions in bone marrow density (BMD) and bone mineral content (BMC) at 24 days using the same concentration (Pomonis et al., 2005). In the present studies, the MIA model led to significantly increased joint severity scores in the ipsilateral hindlimb compared to saline injected controls and contralateral hindlimbs after the 28-35 day post injection period. All 3 scoring methods indicated the same differences that the MIA-injected ipsilateral hindlimb was significantly altered from the ipsilateral saline-injected limb as well as both contralateral groups, however the SFA scoring and revised SFA scoring both showed a greater spread of the data compared to the Collins

method. Other studies have assessed joint scoring based on damage characterised by cartilage thinning, loss of proteoglycan staining and cleft formation, indicating a 2 mg MIA model had significant joint damage scores at 28 days post injection (Fernihough et al., 2004). What is clear from previous macroscopic and histological investigations is that the MIA model is strongly related to the concentration of MIA injected, with dosages ranging from 0.01 mg to 3.0 mg, however 1 mg and 2 mg are more commonly used to produce measurable pathological changes associated with human OA. This is evidenced by the injection of 0.03 mg and 0.1 mg doses of MIA which had significantly less severe cartilage lesions with cartilage in load-bearing areas showing signs of thinning when compared to 0.3 mg and 3.0 mg doses and doses of 0.01 mg showed no macroscopic changes at all after 30 days (Guingamp et al., 1997). The efficacy of the MIA animal model in producing pain behaviour was measured in the form of PWTs to assess mechanical allodynia and hyperalgesia as an induced stimulus response, and weight bearing to assess any deficit in the OA limb. As expected, weight bearing and PWTs were found to be significantly reduced in the MIA injected limb, with this increased sensitivity being apparent at the latest by day 7 (the first post-injection behavioural testing point in these particular studies). Previous studies using the same MIA dose have shown that a reduction in ipsilateral weight bearing is present at 7 days post-injection (Bove et al., 2003). These authors also found that increasing the amount of MIA injected (to 3 mg) produced no greater pain behaviour than 1 mg. Studies using 2 mg MIA showed animals had weight bearing asymmetry at day 5 which was then generally maintained at the same level over the 28-35 day post injection

period, as were deficits in the current studies (Bove et al., 2003; Fernihough et al., 2004). Similarly, PWTs using vF monofilaments were found to dramatically decrease post-injection and stay at a similar level for the duration of the 28 day post injection period (Fernihough et al., 2004; Ferland et al., 2011). The pathological and behavioural changes measured indicate that the OA model was established in the present studies and produced consistent quantifiable pain behaviour that was maintained until the period of electrophysiology testing.

There is evidence to suggest that in OA, a change in descending controls occurs and this may be reflected in a change in the efficacy of DNIC which is believed to contribute significantly to enhanced pain responses and the spread of pain in OA (Arendt-Nielsen et al., 2010). However, the present electrophysiological studies investigating the efficacy of DNIC in saline and MIA-injected animals indicated there were no significant differences observed in animals at day 28-35 post-injection. Previous studies investigating DNIC in animal models of chronic pain conditions indicate DNIC inhibition is abolished in moderate to severe chronic pain models after 14 days (Danziger et al., 1999, 2001; Okada-Ogawa et al., 2009; Bannister et al., 2015; Lockwood et al., 2019b). In a 2 mg MIA model, DNIC investigated in single cell responses in the dorsal horn 14-20 days post-injection were not altered after application of a noxious pinch conditioning stimulus showing that DNIC in chronic OA has been eliminated (Lockwood et al., 2019b). In chronic monoarthritic rats (50 µl complete Freund's

adjuvant (CFA) to the ankle) electrically-stimulated extracellular recordings from neurons in the nucleus caudalis were subjected to mechanical and thermal stimulation 3-4 weeks post injection and it was found that DNIC was reduced in these animals compared to the control (Danziger et al., 1999). This lack of inhibition is also observed in spinal nerve ligation (SNL) injured animals, 14-18 days post surgery, where mechanically-evoked deep dorsal horn neurons were inhibited by noxious ear pinch in sham surgery animals but this DNIC inhibition was not present in operated animals (Bannister et al., 2015). The MIA and CFA models are both considered to have a neuropathic component in their later stages, comparably SNL nerve injury is a model of neuropathic pain, therefore the alteration of DNIC in both studies show that descending pathways are altered in neuropathic pain models. Similarly, in chronic morphine treated animals, a model to represent medication overuse which can produce chronic daily headache in humans, DNIC of medullary dorsal horn neurons induced by thermal conditioning stimulation was again abolished compared to controls (Okada-Ogawa et al., 2009).

The current study investigated the effect of two doses of capsaicin on DNIC of NWRs and did not find any difference between the saline and MIA-injected animals at either dose. DNIC investigated after 14-20 days in animals given 2 mg MIA to the knee joint found extracellular single unit responses from the deep dorsal horn WDR neurons in laminae V – VI were inhibited using concurrent noxious ipsilateral knee pinch but not ipsilateral ear pinch

(Lockwood et al., 2019b). This would suggest that chemical capsaicin stimulation is potentially still too noxious to observe subtle differences between saline and MIA animals and that mechanical conditioning stimulation may be more suited for investigating these changes. This has been observed previously whereby after noxious ear pinch there was a consistent lack of reduction in evoked responses, however after noxious ipsilateral knee pinch some inhibition was observed indicating that inhibition was possible to induce if the conditioning stimulus was highly noxious (Lockwood et al., 2019b). This difference between noxious ear pinch and noxious ipsilateral knee pinch may also be due to the conditioning stimulus site in that pinch to the knee may have been more efficacious in inducing inhibition in evoked responses compared to ear pinch (Lockwood et al., 2019b). In the current study inhibition differences are observed between the two conditioning stimulus sites (hindlimb and forelimb) in both saline and MIA-injected animals suggesting that the site of stimulation is a key factor in inducing DNIC inhibition.

In the current study both electrical and mechanical test stimulus modalities were utilised to further investigate the test and conditioning stimulus relationship. No significant differences between saline and MIA-injected animals were determined using either electrical or mechanical test stimulation, however these results would suggest that mechanically-evoked reflex responses are more useful as they allowed a range of stimulation intensities to be tested. Although no differences in DNIC were found between MIA and

saline-injected animals it did allow a test versus conditioning effect to be observed with results indicating that as vF weight was increased the DNIC induced inhibition was reduced at both doses of capsaicin. In previous studies, electrically-evoked single convergent neurons in the nucleus caudalis were subjected to graded mechanical and electrical conditioning stimulation of the hindpaw in nerve-injured rats and it was found that in response to both graded mechanical and electrical stimulation DNIC inhibition was significantly larger as the stimulus intensity increased (Danziger et al., 2001). However, DNIC inhibition triggered by mechanical stimulation was significantly increased when applied to the operated hindpaw compared to the non-operated hindpaw in nerve injured rats, but this was not the case for electrical stimulation, whereby DNIC induced inhibitions were similar regardless of the stimulation site (Danziger et al., 2001). These differences in DNIC induced inhibitions clearly indicate the importance of the test stimulus.

It is important to note that all the previously mentioned studies investigating DNIC in chronic pain models are undertaken in responses from extracellular recordings of the dorsal horn or the nucleus caudalis whereas the present study has uniquely recorded from reflex responses in hindlimb muscles. It is therefore an important consideration that the lack of difference between saline and MIA animals in the present study may be due to the site of the recorded response and that reflexes do not exhibit any change in the DNIC response.

Chapter Five

Diffuse noxious inhibitory controls of nociceptive withdrawal reflexes in the monosodium iodoacetate model of osteoarthritis (3-4 days post injection)

5.1. Introduction

Previous investigations of the MIA (1 mg dose) model of OA pain have established a biphasic response in pain behaviour assessment, where day 1 after injection animals display significant deficit in weight-bearing, which peaks at day 3-4 after which the deficit reduces slightly and by day 7 a steady level of weight bearing pain behaviour is established for the duration of the study (Bove et al., 2003; Pomonis et al., 2005). Contrastingly, PWTs in the MIA (2 mg dose) model reduce by day 5 post injection and this was maintained for the duration of the study (31 days)(Fernihough et al., 2004). This initial pain behaviour is associated with inflammation present in the joint immediately after the MIA (1 mg dose) injection, and after this has dissipated, pain behaviour lessens slightly (Bove et al., 2003; Fernihough et al., 2004). Inflammation is maximal on day 1 followed by a subsidence of inflammation at day 3 which largely resolves by day 7 (Bove et al., 2003). Histologically, from day 1 after 1 mg MIA injection chondrocytes appear shrunken and show fragmented nuclei in the entire thickness of articular cartilage in both the tibial plateau and femoral condyle (Guzman et al., 2003; Schaible, 2013). The synovial membrane is expanded by proteinaceous fibrin and oedema fluid as well as infiltrating macrophages, neutrophils, plasma cells and lymphocytes which indicates an inflammatory response (Bove et al., 2003; Guzman et al., 2003; Schaible, 2013). By day 7, chondrocytes have marked loss of cellular detail with collapse of the cartilage matrix and loss of proteoglycan, as well as damage to the subchondral bone, with increased osteoclasts along the junction between the damaged cartilage

and subchondral bone, indicating the beginning of changes in the subchondral bone and bone reabsorption (Guzman et al., 2003; Mapp et al., 2013). The confirmation of inflammation indicates an established initial inflammatory pain phase in the early MIA model (Thakur et al., 2012).

Previous studies in chronic pain models have indicated that DNIC are affected, likely due to a change in the balance of descending inhibitory and facilitatory pathways, which therefore contributes to the maintenance of chronic pain (Bannister et al., 2015, 2017). However, the point at which these changes occur during the disease progression of animal models is unknown. As previous studies (Chapter 4) did not detect a difference in DNIC of reflexes at later stages of the model (i.e. where the model has a neuropathic component), the present studies have therefore targeted this early inflammatory phase.

5.2. Methods

Experiments were performed on a total of 17 male Sprague-Dawley rats (mean weight 307 g, range 289 – 331 g) housed as previously described (see section 2.1). Prior to electrophysiology all animals in this chapter underwent the procedure to induce the MIA model (n = 9) or saline control (n = 8)(see section 4.2.1). Pain behaviour was assessed as previously described (see section 4.2.2) but was performed daily post MIA or saline-injection up until day 3 or 4, prior to electrophysiological recording of reflexes responses (heel-MG, toes-BF, toes-TA)(section 2.2) evoked using mechanical stimuli (see section 2.2.2). Mechanical stimulation was chosen for the test stimulation based on findings in the previous chapter in that it gave a range of test stimulus intensities which were more natural and therefore presented a 'more sensitive' means by which a difference between the two groups may be found. Joints from 3-day MIA and saline-injected animals were collected and scored using the previously described method (see section 4.2.3).

Efficacy of DNIC on reflexes in MIA and saline-injected animals on day 3-4 post injection was assessed using a 50 µg capsaicin injection (100 µl of 500 µg ml^{-1}) into the contralateral fore- or hindlimb (see section 3.2.1). The lower strength of conditioning stimulus was chosen for the following experiments to increase the sensitivity and detect a change in DNIC between the two groups.

5.3. Results

5.3.1. Joint severity scoring

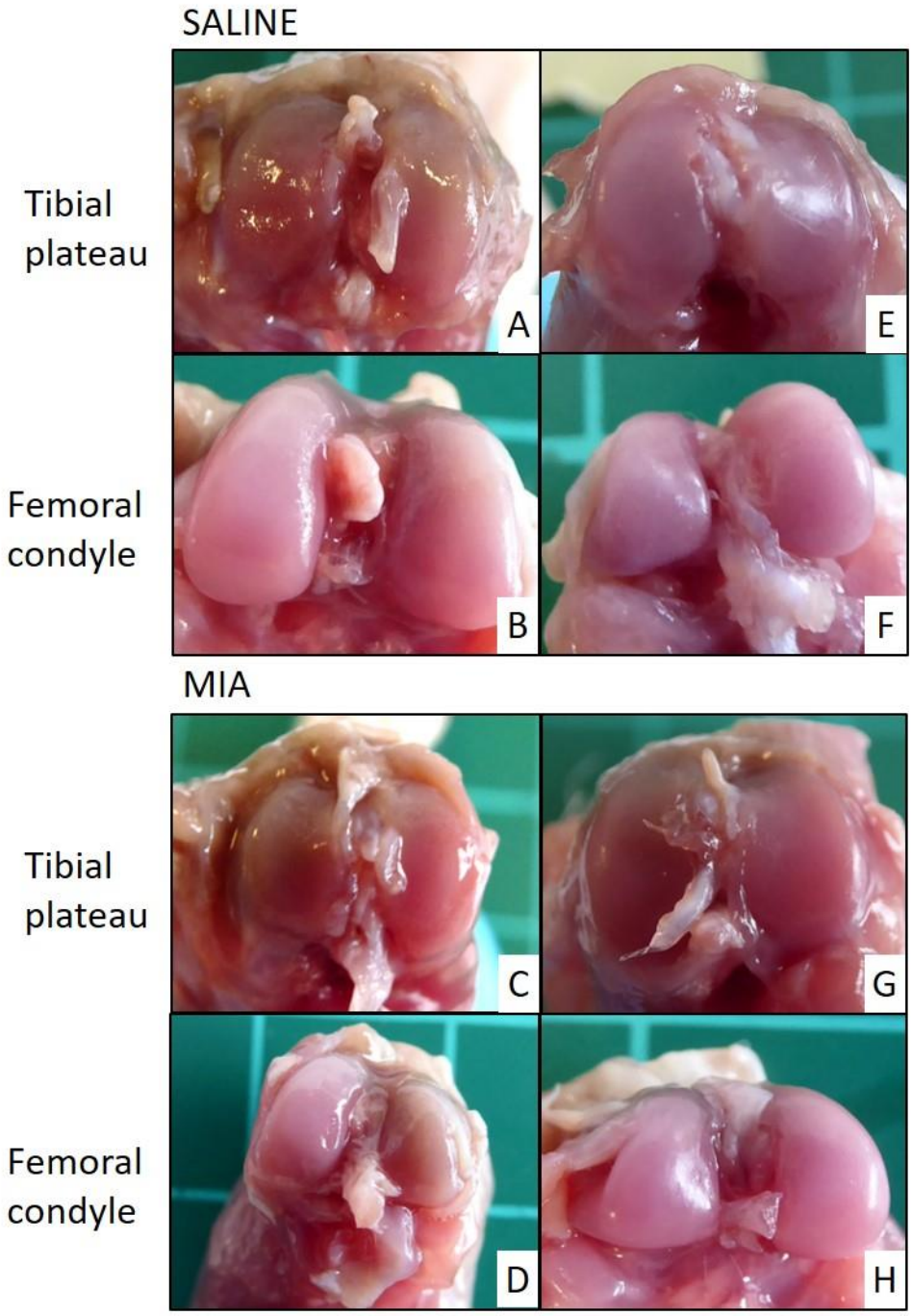

Figure 5.1. Examples of joint damage severity 3-4 days after saline (A, B) or MIA (C, D) injection into the knee joint of the left hindlimb. Images are of ipsilateral tibial plateaus (A, C) or femoral condyles (B, D). Images E – H are corresponding structures in the contralateral (i.e. non-injected) right hindlimb of the same animals.

Treatment	Hindlimb	Mean joint score		
		Collins†	SFA††	Revised SFA††
Saline	Contralateral (n = 2)	0 ± 0	-9.2 ± 0*	0 ± 0*
	Ipsilateral (n = 2)	0 ± 0	-9.2 ± 0*	0 ± 0*
MIA	Contralateral (n = 4)	0 ± 0	-9.2 ± 0**	0 ± 0**
	Ipsilateral (n = 6)	1.3 ± 0.4	62.8 ± 12.8	10.7 ± 2.0

Table 5.1. Scoring of ipsilateral and contralateral hindlimb knee joints 3-4 days post-saline or MIA injection using three different methods. Values are means and errors are standard error of means. †$p < 0.05$ or ††$p < 0.01$ denotes significant difference between joints for a given scoring method (one-way ANOVA). *$p < 0.05$ or **$p < 0.01$ denotes significance compared to MIA-injected ipsilateral hindlimb (Tukey's multiple comparisons test). SFA = Système Française D'Arthroscopie.

Mean joint scores were significantly different using either the Collins, SFA or revised SFA methods of joint scoring ($p = 0.0468$, $p = 0.0012$ and $p = 0.0018$, one-way ANOVA; Table 5.1), with the ipsilateral MIA-injected hindlimb showing significantly greater damage than the SFA and revised SFA scoring methods ($p < 0.05$, Tukey's multiple comparisons test; Figure 5.1).

5.3.2. Pain behaviour

5.3.2.1. Weight bearing asymmetry

The difference in weight bearing between the ipsilateral and contralateral hindlimb was significantly larger in MIA-injected animals compared to saline-injected controls ($p < 0.0001$, two-way ANOVA; Figure 5.2A) with mean values of 43.8 ± 7.4 g ($n = 9$) and 3.9 ± 0.7 g ($n = 8$) respectively at day 3-4 post-injection, with significant differences shown from day 1 to day 3-4 between groups ($p = 0.0037$, $p < 0.0001$ and $p < 0.0001$ respectively, Sidak's multiple comparisons test). Over the 3-4 day post injection period, difference in weight bearing between the hindlimbs was not significantly altered in saline-injected animals ($p > 0.05$, Sidak's multiple comparisons test). Weight bearing difference between the hindlimbs was significantly increased on day 1 compared to day 0 post-MIA injection however, did not significantly increase between day 1 and 2 or day 2 and day 3-4 ($p = 0.0018$, $p = 0.0882$ and $p = 0.4457$ respectively, Sidak's multiple comparisons test).

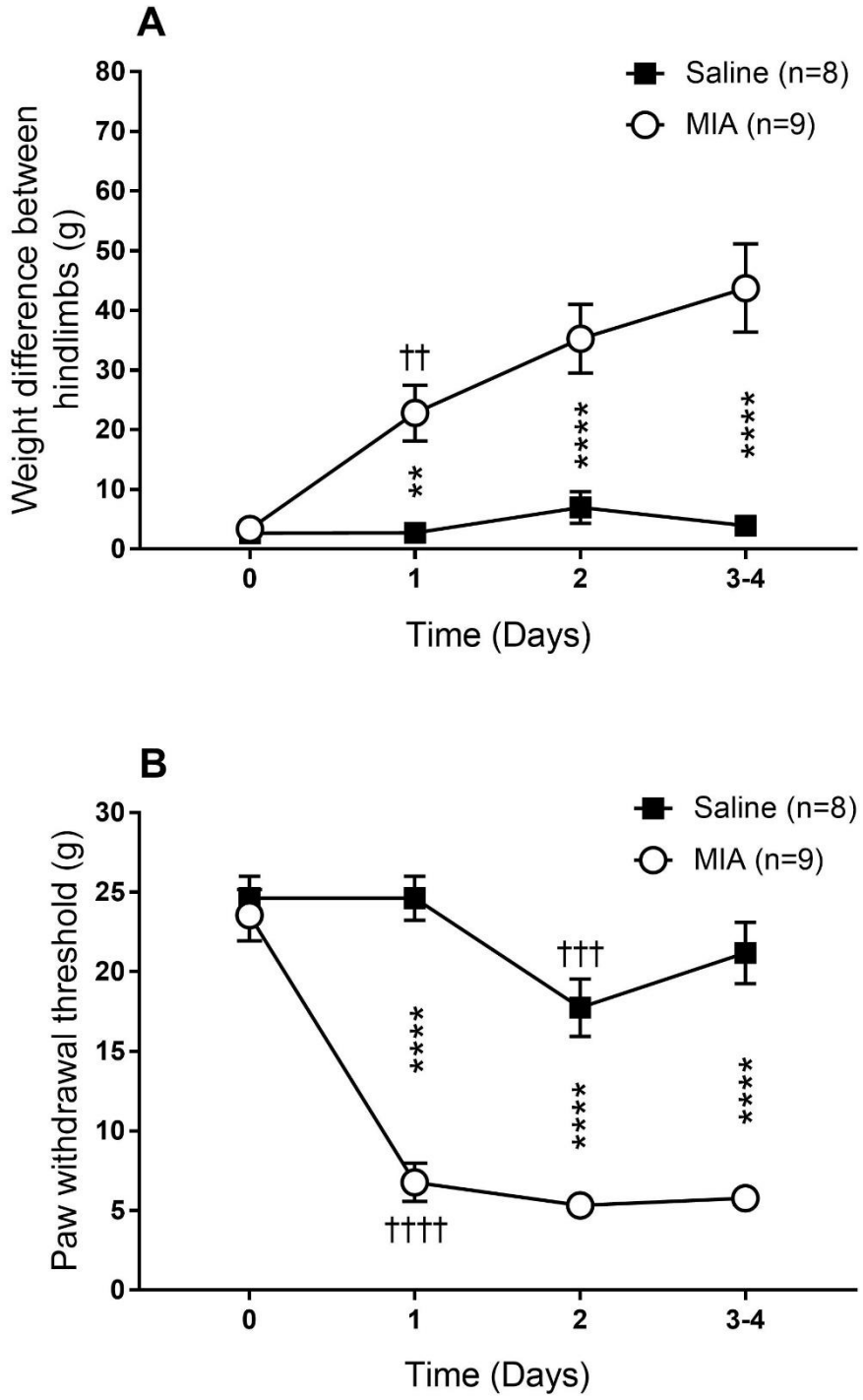

Figure 5.2. Pain behaviour post-saline or MIA injection by measuring (A) weight bearing asymmetry or (B) paw withdrawal thresholds. Values plotted are means and errors are standard error of means. **p < 0.01 or ****p < 0.0001 denotes significant difference between saline and MIA-injected animals and ††p < 0.01, †††p < 0.001 or ††††p < 0.0001 denotes significant difference to previous time point in saline or MIA-injected animals (Sidak's multiple comparisons test).

5.3.2.2. Paw withdrawal thresholds

PWTs were significantly reduced in MIA-injected animals compared to saline-injected animals ($p < 0.0001$, two-way ANOVA; Figure 5.2B) to means of 5.8 ± 0.3 g ($n = 9$) and 21.2 ± 1.9 g ($n = 8$) respectively at day 3-4 post-injection, with significant differences shown from day 1 to day 3-4 between groups ($p < 0.0001$, Sidak's multiple comparisons test). Over the 3-4 day post injection period, PWTs were significantly lower on day 2 compared to day 1 in saline-injected animals ($p = 0.0009$, Sidak's multiple comparisons test). Similarly, PWTs were significantly lower on day 1 compared to day 0 post MIA-injection ($p < 0.0001$, Sidak's multiple comparisons test).

5.3.3. Control parameters for electrophysiology

5.3.3.1. Weight and anaesthetic levels

Mean weights of animals on the day of injection were 306 ± 5 g (n = 8) and 307 ± 4 g (n = 9) for saline and MIA groups respectively; no significant differences were found between groups (p = 0.9066, Mann-Whitney test). On the day of electrophysiology (day 3-4) mean weights of animals in saline and MIA groups were 323 ± 5 g and 324 ± 5 g respectively; again, not significantly different (p > 0.9999, Mann-Whitney test).

Following an initial bolus dose (see section 2.2.1.5), alfaxalone anaesthesia was maintained using a CRI at a mean rate of 47.25 ± 2.28 mg kg^{-1} hr^{-1} and 46.53 ± 0.92 mg kg^{-1} hr^{-1} saline and MIA-injected animals respectively, which was not significant between groups (p = 0.7430, Mann-Whitney test).

5.3.3.2. Mechanical thresholds

Treatment	Median mechanical threshold (vF weight)		
	Heel-MG	Toes-BF	Toes-TA
Saline (n = 8)	60 (26 – 60)	10 (10 – 26)	10 (10 –26)
MIA (n = 9)	26 (18 – 60)	10 (10 – 26)	10 (10 – 26)

Table 5.2. Median mechanical threshold parameters for the heel-medial gastrocnemius (MG), toes-biceps femoris (BF) and tibialis anterior (TA) reflexes for saline and MIA animals 3-4 days post-injection. Values in brackets are interquartile ranges.

Median mechanical thresholds were found to be significantly higher between the three reflex responses in saline-injected animals but not MIA-injected animals ($p = 0.0248$ and $p = 0.1383$ respectively, Kruskal-Wallis test; Table 5.2). Comparison between saline and MIA-injected animals for heel-MG, toes-BF or toes-TA responses indicated no significant differences ($p = 0.2248$, $p = 0.8100$ and $p > 0.9999$ respectively, Mann-Whitney test).

5.3.3.3. Control reflex responses

Treatment	von Frey (vF) weight (g)	Median control reflex responses (μV)		
		Heel-MG	Toes-BF	Toes-TA
Saline (n = 8)	10	0.018 (0.004 – 0.029)	0.073 (0.005 – 0.386)	0.073 (0.005 – 0.627)
	26	0.025 (0.010 – 0.126)	0.334 (0.088 – 0.536)	0.344 (0.162 – 1.498)
	60	6.541 (1.507 – 12.784)	2.084 (0.800 – 4.407)	2..346 (1.173 – 3.807)
	100	12.715 (6.447 – 25.781)	6.920 (3.541 – 10.899)	4.575 (2.685 – 4.954)
	180	18.975 (13.317 – 30.214)	11.714 (4.569 – 19.548)	4.531 (3.918 – 5.858)
	300	21.618 (13.172 – 30.333)	13.315 (4.795 – 21.225)	5.239 (4.676 – 6.448)
MIA (n = 9)	10	0.014 (0.012 – 0.023)	0.083 (0.010 – 0.197)	0.179 (0.011 – 0.298)
	26	0.086 (0.037 – 0.534)	0.154 (0.093 – 1.012)	0.605 (0.077 – 1.399)
	60	3.726 (2.129 – 5.278)	2.228 (1.025 – 2.793)	2.117 (1.435 – 3.595)
	100	4.761* (3.570– 11.712)	3.050 (1.866 – 4.921)	4.032 (2.208 – 6.683)
	180	4.993** (4.062 – 11.806)	5.201 (2.992 – 9.139)	4.528 (2.955 – 7.620)
	300	4.406** (4.113 – 12.070)	8.787 (4.280 – 10.657)	4.316 (3.311 – 7.145)

Table 5.3. Median control responses to mechanical stimulation for heel-medial gastrocnemius (MG), toes-biceps femoris (BF) and toes-tibialis anterior (TA) reflexes prior to administration of 50 μg capsaicin in 3-4 day saline and MIA-injected animals. Values in brackets are interquartile ranges. *$p < 0.05$ or **$p < 0.01$ denotes significance compared to equivalent saline control (Mann-Whitney test).

As expected, as vF weight (10 – 300 g) increased, median control reflex responses significantly increased for heel-MG, toes-BF and toes-TA responses in both saline (n = 8) and MIA-injected (n = 9) animals ($p < 0.0001$, Kruskal-Wallis test). Comparison of responses prior to capsaicin injection indicated heel-MG control responses were significantly smaller in MIA-injected animals compared to saline-injected animals ($p < 0.0001$, two-way ANOVA) with responses evoked by 100 g, 180 g and 300 g vF filaments indicated as significantly smaller in MIA-injected animals compared to saline-injected animals ($p = 0.0363$, $p = 0.0001$ and $p = 0.0003$ respectively, Sidak's multiple comparison test; Figure 5.3). Toes-BF responses also exhibited similar results with MIA-injected animals indicting smaller responses that saline-injected animals ($p = 0.0032$, two-way ANOVA) and again with the larger 180g and 300g vF filaments ($p = 0.0337$ and $p = 0.0484$, Sidak's multiple comparisons test). Direct pairwise comparison also indicted the same results for heel-MG responses evoked from the same vF filaments (100g, 180g and 300g, $p = 0.0464$, $p = 0.0025$ and $p = 0.0055$ respectively, Mann-Whitney test; Table 5.3) , however no significant differences in toes-BF and toes-TA responses were found between MIA and saline groups for each (10 – 300 g) vF filaments using pairwise analysis ($p > 0.05$, Mann-Whitney test).

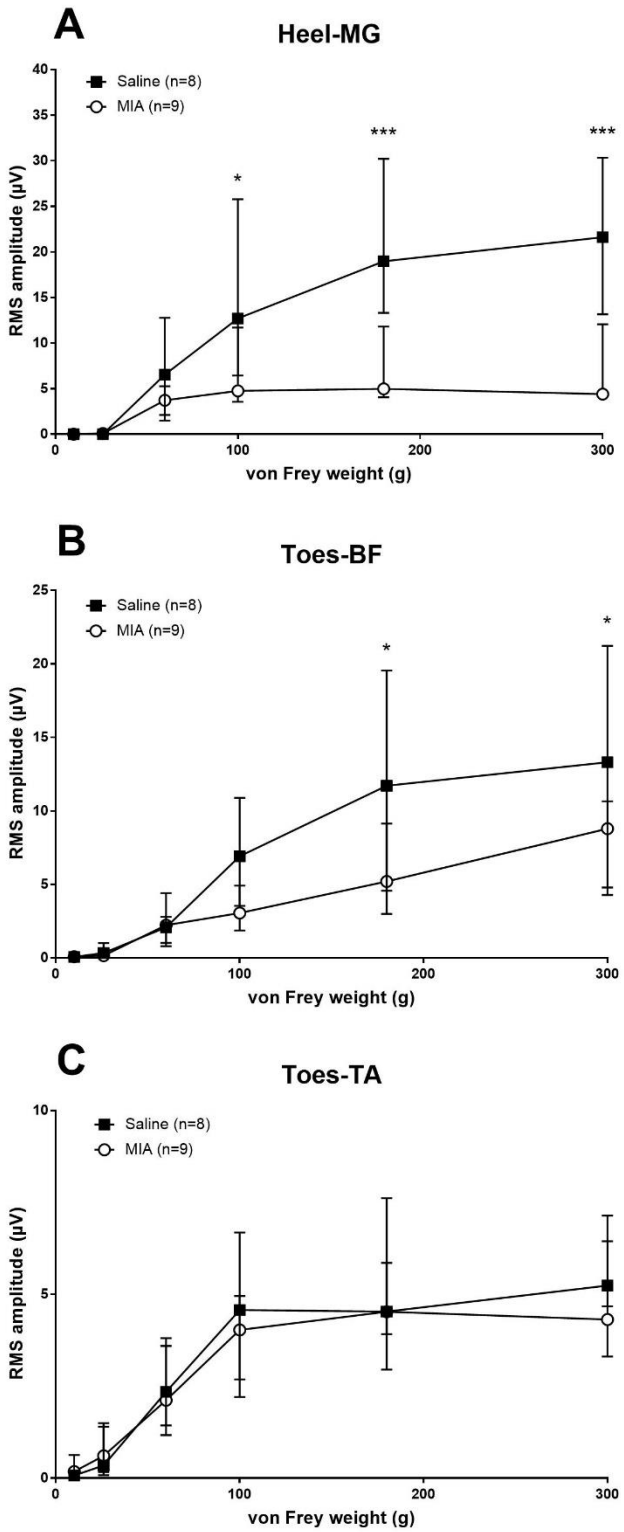

Figure 5.3. Control responses for (A) heel-medial gastrocnemius (MG), (B) toes-biceps femoris (BF) and (C) toes-tibialis anterior (TA) reflexes evoked using 10 g, 26 g, 60 g, 100 g, 180 g and 300 g von Frey (vF) monofilaments in saline and MIA animals 3-4 days post-injected. Values plotted are medians and errors are interquartile ranges. *$p < 0.05$ or ***$p < 0.001$ denotes significant difference between saline and MIA-injected animals (Sidak's multiple comparisons test).

5.3.4. Effect of 50 μg capsaicin in 3-4 day saline and MIA-injected animals

Responses evoked by 10 g and 26 g vF monofilaments were found to be variable and sometimes absent before and after capsaicin, therefore these responses have been excluded.

5.3.4.1. Injection into the contralateral hindlimb

In the saline group (n = 6), significant inhibition of heel-MG responses evoked by 60 g, 100 g, 180 g and 300 g vF filaments was caused by contralateral hindlimb injection of capsaicin ($p < 0.0001$, $p < 0.0001$, $p = 0.0063$ and $p = 0.0430$ respectively, Friedman's ANOVA) to a median of 16% (IQR 7 – 39%), 44% (IQR 42 – 62%), 56% (IQR 41 – 75%) and 61% (IQR 48 – 90%) of controls respectively (Figures 5.4A, 5.5A, 5.6A and 5.7A). The corresponding level of inhibition in MIA-injected animals (n = 8) was to a median of 71% (IQR 51 – 89%), 67% (IQR 34 – 91%), 75% (IQR 65 – 101%) and 96% (IQR 77 – 101%) of controls respectively ($p = 0.0243$, $p = 0.0004$, $p = 0.0008$ and $p = 0.0378$ respectively, Friedman's ANOVA). Median duration of inhibition was 17 min (IQR 1 – 26 min), 39 min (IQR 22 – 49 min), 21 min (IQR 0 – 25 min) and 23 min (IQR 8 – 40 min) for 60 g, 100 g, 180 g and 300 g vF weights respectively in saline-injected animals and 9 min (IQR 1 – 19 min), 11 min (IQR 0 – 51 min), 17 min (IQR 3 – 54 min) and 9 min (IQR 0 – 28 min) for the corresponding vF weights in MIA-injected animals; which were not significant between groups ($p = 0.4895$, $p = 0.5035$, $p = 0.8162$ and $p = 0.2371$ respectively, Mann-Whitney test). Analysis of negative AUC values indicated a significant difference in

overall inhibition of heel-MG reflexes evoked using the 60 g vF weight between saline and MIA-injected animals ($p = 0.0335$, unpaired t-test; Figure 5.8A). However, no significant differences were observed between saline and MIA-injected animals in heel-MG responses evoked by 100 g, 180 g or 300 g vF weights ($p = 0.1449$, $p = 0.3149$ and $p = 0.5415$ respectively, unpaired t-test).

Following capsaicin administration, toes-BF reflexes evoked by 60 g, 100 g, 180 g and 300 g monofilaments were significantly inhibited ($p = 0.0037$, $p < 0.0001$, $p = 0.0008$ and $p < 0.0001$ respectively, Friedman's ANOVA) to medians of 21% (IQR 14 – 51%), 26% (IQR 12 – 63%), 15% (IQR 10 – 58) and 46% (IQR 26 – 70%) of controls respectively in saline-injected animals ($n = 8$; Figures 5.4B, 5.5B, 5.6B and 5.7B). These reflexes in MIA-injected animals ($n = 6$) were significantly inhibited ($p = 0.0128$, $p = 0.0004$, $p = 0.0019$ and $p = 0.0001$ respectively, Friedman's ANOVA) to a median of 85% (IQR 63 – 108%), 57% (IQR 48 – 82%), 58% (IQR 38 – 80%) and 67% (IQR 42 – 83%) of controls at the corresponding vF weights. Median duration of inhibition was 35 min (IQR 0 – 63 min), 45 min (IQR 14 – 63 min), 63 min (IQR 44 – 63 min) and 51 min (IQR 38 – 63 min) for 60 g, 100 g, 180 g and 300 g vF filaments respectively in saline-injected animals and 12 min (IQR 0 – 23 min), 5 min (IQR 0 – 44 min), 31 min (IQR 16 – 63 min) and 35 min (IQR 24 – 57 min) in MIA-injected animals; these were not significantly different between groups ($p = 0.2984$, $p = 0.1645$, $p = 0.1608$ and $p = 0.1605$ respectively, Mann-Whitney test). Analysis of negative AUC values indicated a significant difference in overall inhibition of responses evoked by

the 180 g vF weight (p = 0.0229, unpaired t-test; Figure 5.8B). However, no significant differences were observed between saline and MIA-injected animals in heel-MG responses evoked by 60 g, 100 g or 300 g vF weights (p = 0.0983, p = 0.0564 and p = 0.2217 respectively, unpaired t-test).

For toes-TA reflexes in saline-injected animals (n = 8), responses to 60 g, 100 g, 180 g and 300 g monofilaments were significantly inhibited (p = 0.0039, p < 0.0001, p = 0.0006 and p < 0.0001 respectively, Friedman's ANOVA) to medians of 32% (IQR 18 – 65%), 58% (IQR 40 – 77%), 74% (IQR 64 – 83%) and 66% (IQR 62 – 71%) of controls respectively (Figures 5.4C, 5.5C, 5.6C and 5.7C) and MIA-injected animals (n = 6) evoked by the 60 g vF weight (p = 0.0328, Friedman's ANOVA) to a median of 97% (IQR 79 – 108%) of controls. However, no significant inhibition was induced in toes-TA by 100 g, 180 g or 300 g vF weights (p = 0.0865, p = 0.2361 and p = 0.1601 respectively, Friedman's ANOVA). Median duration of inhibition was 24 min (IQR 0 – 50 min), 27 min (IQR 11 – 54 min), 27 min (IQR 18 – 42 min) and 29 min (IQR 15 – 42 min) for 60 g, 100 g, 180 g and 300 g vF weights respectively in saline-injected animals and 8 min (IQR 0 – 29 min) for MIA-injected animals using the 60 g vF weight, which was not significant between groups (p = 0.6107, p = 0.5005, p = 0.2368 and p = 0.4049 respectively, Mann-Whitney test). Analysis of negative AUC revealed significant differences in overall inhibition between saline and MIA-injected animals of responses to the 300 g vF weight in the toes-TA reflex response (p = 0. 0094, unpaired t-test; Figure 5.8C), however did not reveal any significant

differences of responses to any other filaments ($p = 0.1894$; 60 g, $p = 0.2051$; 100 g and $p = 0.1668$; 180 g, unpaired t-test).

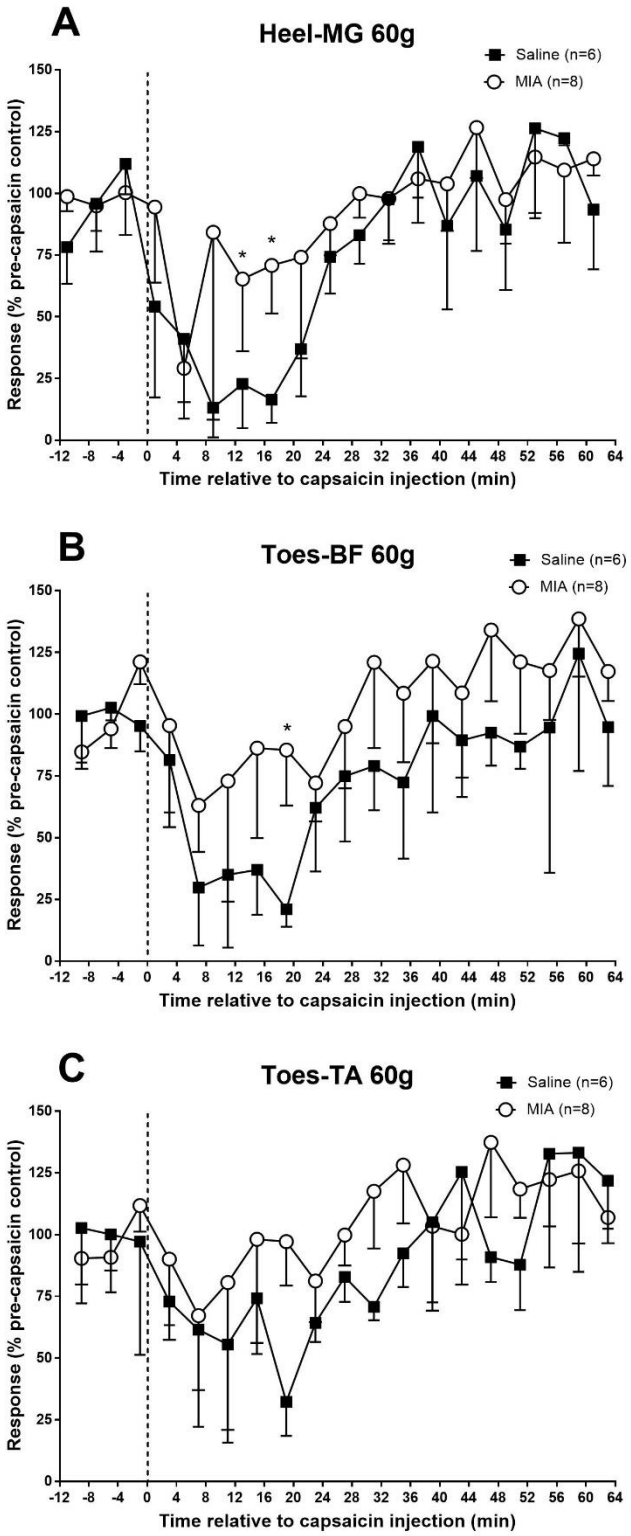

Figure 5.4. Effect of intramuscular injection of 50 µg capsaicin into the contralateral hindlimb on mechanically evoked (A) heel-medial gastrocnemius (MG), (B) toes-biceps femoris (BF) and (C) toes-tibialis anterior (TA) reflexes using a 60 g von Frey (vF) monofilament in 3-4 day saline and MIA-injected animals. Values plotted are medians and errors are interquartile ranges. *p < 0.05 denotes significant difference between saline and MIA-injected animals at the same post-capsaicin time points (Mann-Whitney test).

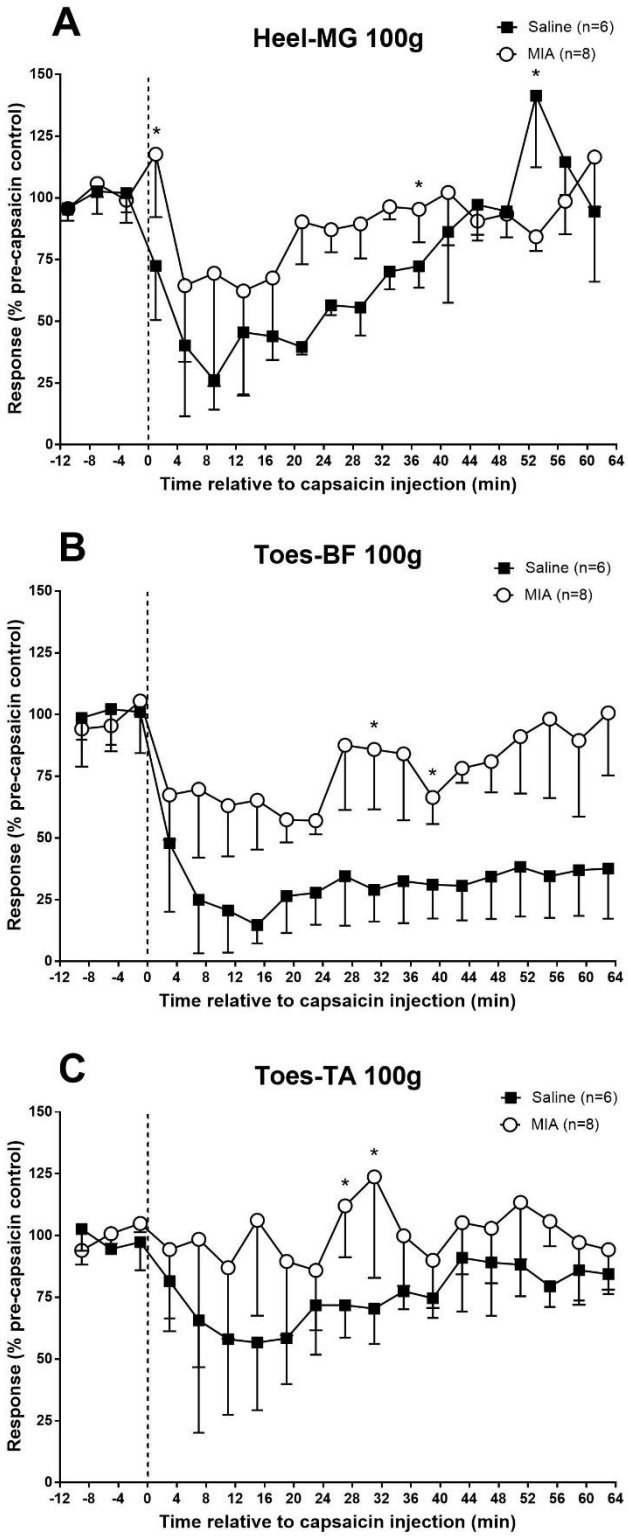

Figure 5.5. Effect of intramuscular injection of 50 µg capsaicin into the contralateral hindlimb on mechanically evoked (A) heel-medial gastrocnemius (MG), (B) toes-biceps femoris (BF) and (C) toes-tibialis anterior (TA) reflexes using a 100 g von Frey (vF) monofilament in 3-4 day saline and MIA-injected animals. Values plotted are medians and errors are interquartile ranges. *$p < 0.05$ denotes significant difference between saline and MIA-injected animals at the same post-capsaicin time points (Mann-Whitney test).

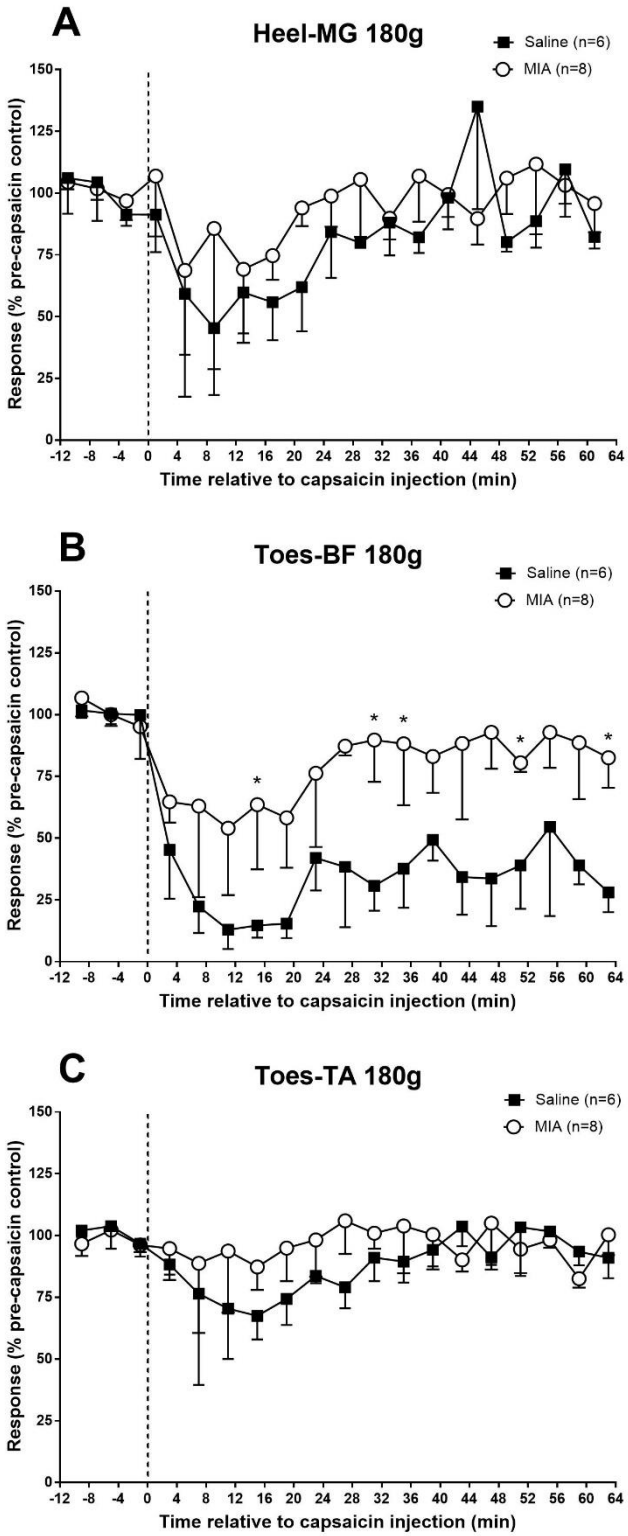

Figure 5.6. Effect of intramuscular injection of 50 µg capsaicin into the contralateral hindlimb on mechanically evoked (A) heel-medial gastrocnemius (MG), (B) toes-biceps femoris (BF) and (C) toes-tibialis anterior (TA) reflexes using a 180 g von Frey (vF) monofilament in 3-4 day saline and MIA-injected animals. Values plotted are medians and errors are interquartile ranges. *p < 0.05 denotes significant difference between saline and MIA-injected animals at the same post-capsaicin time points (Mann-Whitney test).

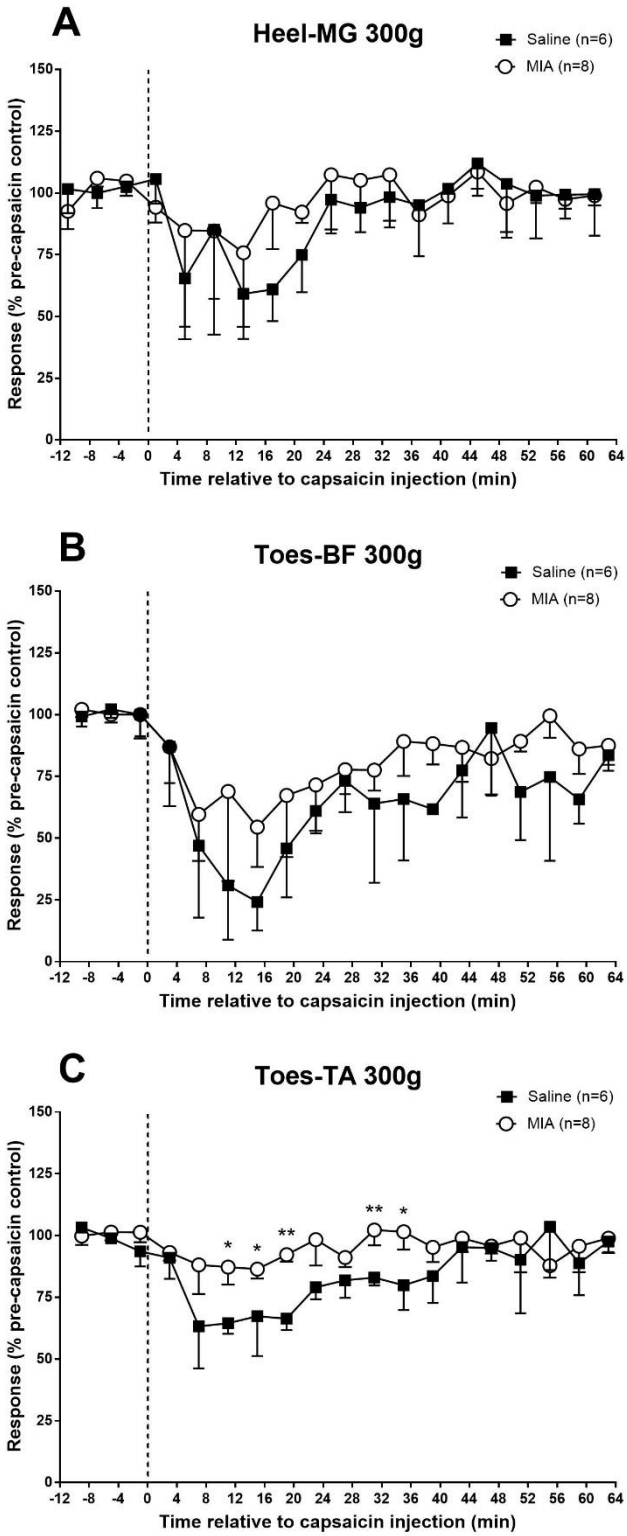

Figure 5.7. Effect of intramuscular injection of 50 µg capsaicin into the contralateral hindlimb on mechanically evoked (A) heel-medial gastrocnemius (MG), (B) toes-biceps femoris (BF) and (C) toes-tibialis anterior (TA) reflexes using a 300 g von Frey (vF) monofilament in 3-4 day saline and MIA-injected animals. Values plotted are medians and errors are interquartile ranges. *p < 0.05 denotes significant difference between saline and MIA-injected animals at the same post-capsaicin time points (Mann-Whitney test).

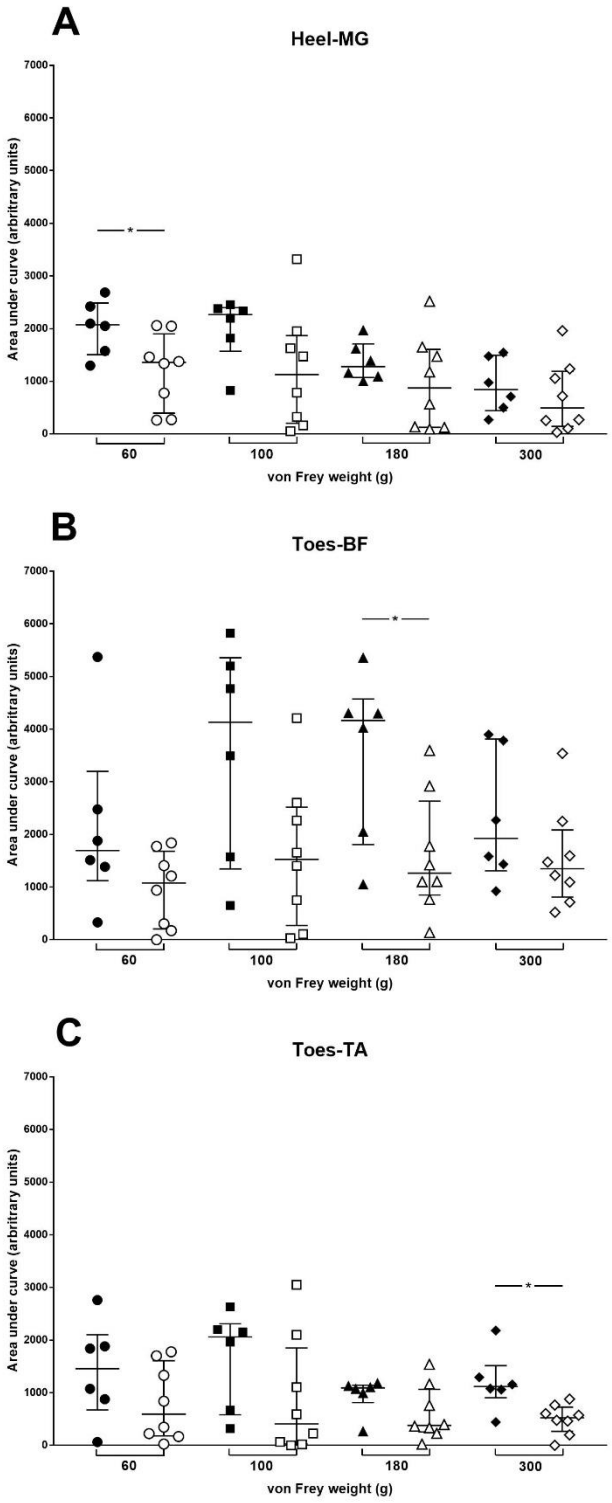

Figure 5.8. Effect of intramuscular injection of 50 µg capsaicin into the contralateral hindlimb on mechanically evoked (A) heel-medial gastrocnemius (MG), (B) toes-biceps femoris (BF) and (C) toes-tibialis anterior (TA) reflexes using 60 – 300 g von Frey (vF) monofilaments in 3-4 day saline (n = 6, closed symbols) and MIA-injected (n = 8, open symbols) animals. Values plotted are area under curve (AUC) determinations for each animal with horizontal bars indicating medians and interquartile ranges. *p < 0.05 denotes significant difference between saline and MIA-injected animals (unpaired t-test).

5.3.4.2. Injection into the contralateral forelimb

Following 50 μg capsaicin to the contralateral forelimb, heel-MG responses were significantly inhibited ($p = 0.0001$, $p < 0.0001$, $p = 0.0070$ and $p < 0.0001$ respectively, Friedman's ANOVA) by 60 g, 100 g, 180 g and 300 g vF filaments to medians of 23% (IQR 7 – 56%), 49% (IQR 33 – 62%), 70% (IQR 69 – 84%) and 72% (IQR 71 – 99%) of controls in saline-injected animals (n = 7; Figures 5.9A, 5.10A, 5.11A and 5.12A). Similarly, in MIA-injected animals (n = 9), heel-MG responses evoked by the corresponding vF weights were inhibited to medians of 28% (IQR 9 – 46%), 67% (IQR 55 – 82%), 83% (IQR 65 – 90%) and 87% (IQR 75 – 93%) of controls, however responses evoked by 300 g were not found to be significant ($p < 0.0001$, $p < 0.0001$, $p = 0.0050$ and $p = 0.2171$ respectively, Friedman's ANOVA). Median duration of inhibition in saline-injected animals was 25 min (IQR 9 – 25 min), 25 min (IQR 21 – 25 min), 13 min (IQR 13 – 37 min) and 21 min (IQR 13 – 29 min) for 60 g, 100 g, 180 g and 300 g vF weights respectively and 21 min (IQR 7 – 35 min), 17 min (IQR 0 – 31 min) and 21 min (IQR 5 – 29 min) for MIA-injected animals; these durations were not significantly different between groups ($p = 0.7374$, $p = 0.1122$, $p = 0.9430$ and $p = 0.7749$, Mann-Whitney test). Furthermore, analysis of negative AUC values revealed no significant difference in overall inhibition of responses to 60 – 300 g vF filaments between treatment groups ($p = 0.7082$, $p = 0.4612$, $p= 0.5373$ and $p = 0.2923$ respectively, unpaired t-test; Figure 5.13A).

In saline-injected animals (n = 7), significant inhibition of toes-BF responses evoked by 60 g, 100 g, 180 g and 300 g monofilaments was induced ($p < 0.0001$, Friedman's ANOVA; Figures 5.9B, 5.10B, 5.11B and 5.12B) to medians of 56% (IQR 44 – 85%), 61% (IQR 38 – 82%), 60% (IQR 26 – 93%) and 55% (IQR 29 – 73%) of controls respectively. The corresponding level of inhibition in MIA-injected animals (n = 9) was to medians of 53% (IQR 41 – 72%), 83% (IQR 75 – 95%), 66% (IQR 42 – 83%) and 85% (IQR 39 – 87%) of controls respectively ($p = 0.0001$, $p < 0.0001$, $p < 0.0001$ and $p < 0.0001$ respectively, Friedman's ANOVA). Median duration of inhibition was 19 min (IQR 0 – 23 min), 19 min (IQR 0 – 19 min), 23 min (IQR 0 – 47 min) and 35 min (IQR 19 – 63 min) for 60 g, 100 g, 180 g and 300 g vF weights respectively in saline-injected animals and 15 min (IQR 0 – 23 min), 15 min (IQR 13 – 29 min), 23 min (IQR 2 – 49 min) and 39 min (IQR 14 –61 min) for the corresponding vF weights in MIA-injected animals; these durations were not significantly different between groups ($p = 0.6148$, $p = 0.6153$, $p = 0.9855$ and $p = 0.8959$, Mann-Whitney test). Analysis of negative AUC values indicated no significant differences in overall inhibition between saline and MIA-injected animals for toes-BF responses evoked by 60 – 300 g vF filaments ($p = 0.3099$, $p = 0.8179$, $p = 0.7947$ and $p = 0.8411$ respectively, unpaired t-test; Figure 5.13B).

Following capsaicin administration, toes-TA reflex responses evoked by 60 g, 100 g, 180 g and 300 g vF filaments were significantly inhibited in saline-injected animals (n = 7; $p < 0.0001$, $p < 0.0001$, $p = 0.0007$ and $p = 0.0005$ respectively,

Friedman's ANOVA) to medians of 66% (IQR 50 – 95%), 78% (IQR 55 – 101%), 96% (IQR 79 – 99%) and 74% (IQR 65 – 85%) of controls respectively (Figures 5.9C, 5.10C, 5.11C and 5.12C); for MIA-injected animals (n = 9), significant inhibition ($p = 0.0002$, $p < 0.0001$, $p = 0.0049$ and $p = 0.0036$ respectively, Friedman's ANOVA) to medians of 55% (IQR 52 – 84%), 79% (IQR 68 – 104%), 95% (IQR 86 – 107%) and 99% (IQR 69 – 108%) of controls was produced in toes-TA reflexes by these same respective vF filaments. Median duration of inhibition was 15 min (IQR 11 – 35 min), 19 min (IQR 15 – 23 min), 15 min (IQR 0 – 35 min) and 27 min (IQR 7 – 35 min) for 60 g, 100 g, 180 g and 300 g vF weights respectively in saline-injected animals and correspondingly 19 min (IQR 6 – 43 min), 19 min (IQR 9 – 33 min), 11 min (IQR 0 – 29 min) and 11 min (IQR 4 – 31 min) in MIA-injected animals; these durations were not significantly different between groups ($p = 0.9366$, $p = 0.8552$, $p = 0.7053$ and $p = 0.4492$ respectively, Mann-Whitney test). Comparison of negative AUC values found that overall inhibition of toes-TA responses was not significantly different between saline and MIA-injected animals for any (60 – 300 g) vF weight ($p = 0.9899$, $p = 0.5953$, $p = 0.5935$ and $p = 0.8123$ respectively, unpaired t-test; Figure 5.13C).

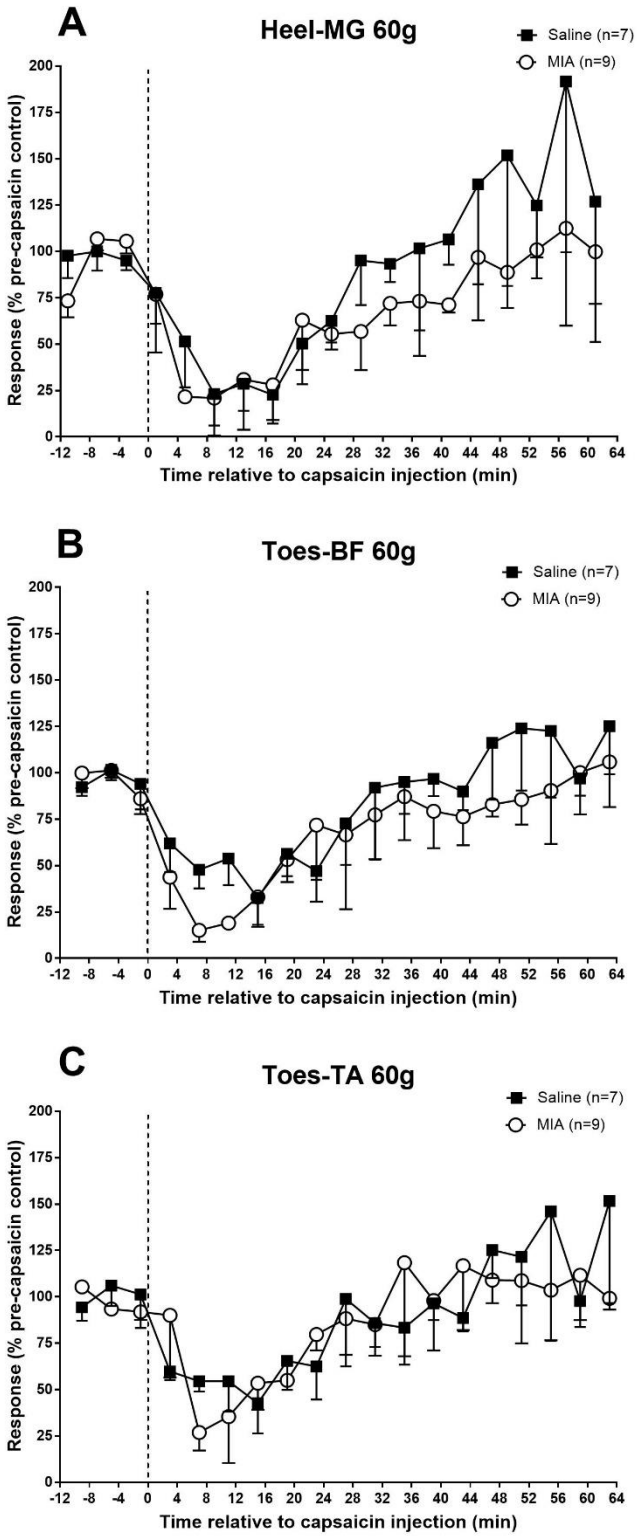

Figure 5.9. Effect of intramuscular injection of 50 µg capsaicin into the contralateral forelimb on mechanically evoked (A) heel-medial gastrocnemius (MG), (B) toes-biceps femoris (BF) and (C) toes-tibialis anterior (TA) reflexes using a 60 g von Frey (vF) monofilament in 3-4 day saline and MIA-injected animals. Values plotted are medians and errors are interquartile ranges.

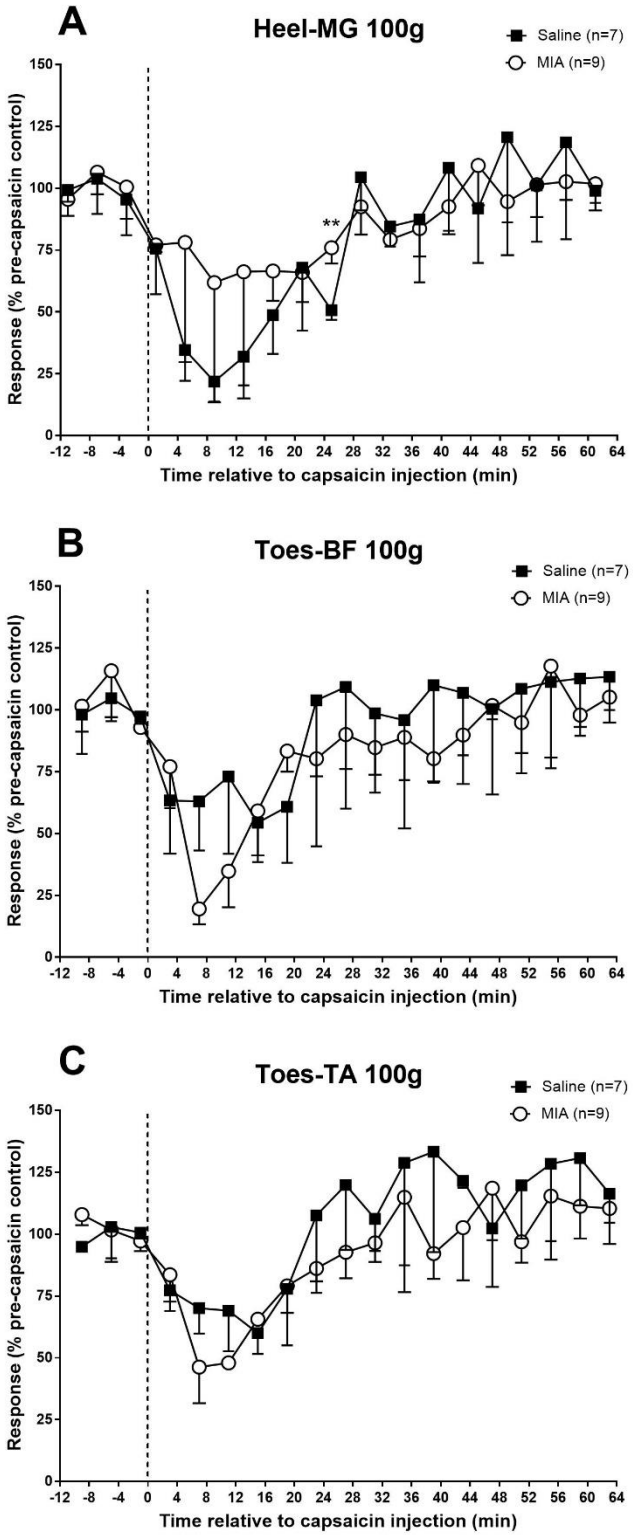

Figure 5.10. Effect of intramuscular injection of 50 µg capsaicin into the contralateral forelimb on mechanically evoked (A) heel-medial gastrocnemius (MG), (B) toes-biceps femoris (BF) and (C) toes-tibialis anterior (TA) reflexes using a 100 g von Frey (vF) monofilament in 3-4 day saline and MIA-injected animals. Values plotted are medians and errors are interquartile ranges. **p < 0.01 denotes significant difference between saline and MIA-injected animals at the same post-capsaicin time points (Mann-Whitney test).

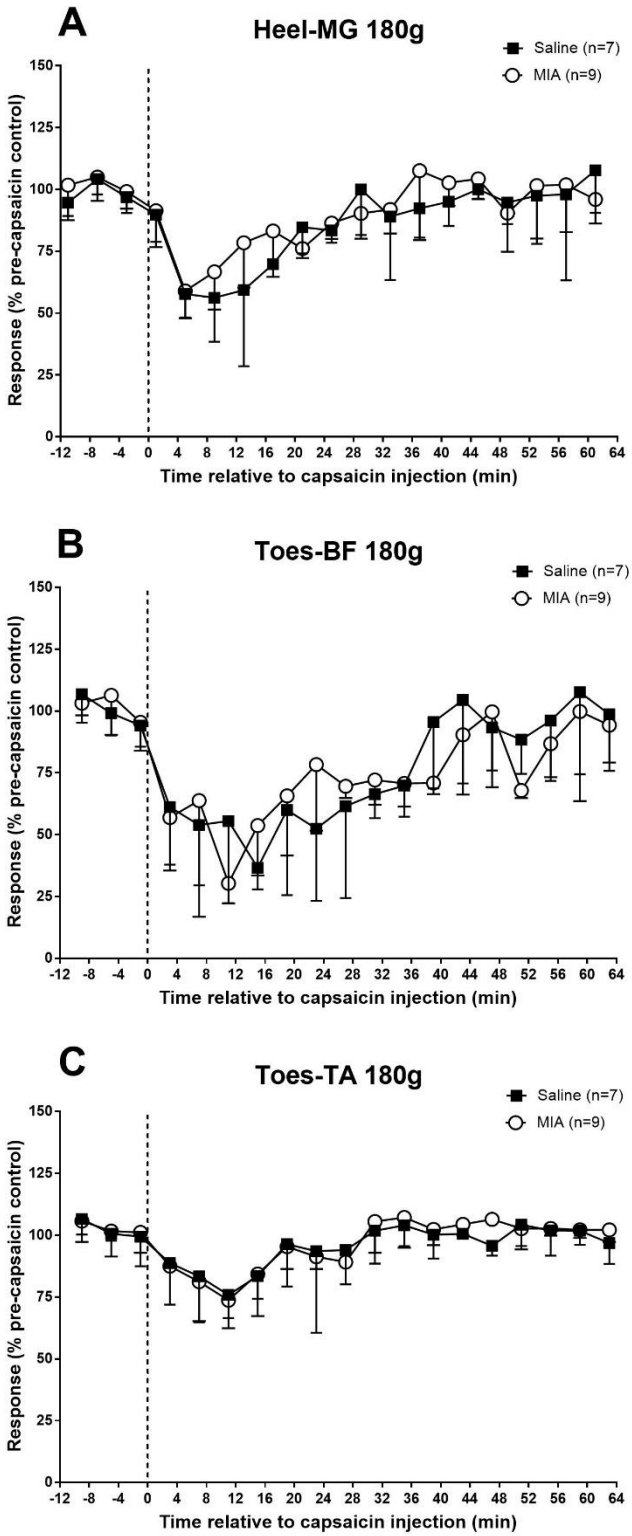

Figure 5.11. Effect of intramuscular injection of 50 µg capsaicin into the contralateral forelimb on mechanically evoked (A) heel-medial gastrocnemius (MG), (B) toes-biceps femoris (BF) and (C) toes-tibialis anterior (TA) reflexes using a 180 g von Frey (vF) monofilament in 3-4 day saline and MIA-injected animals. Values plotted are medians and errors are interquartile ranges.

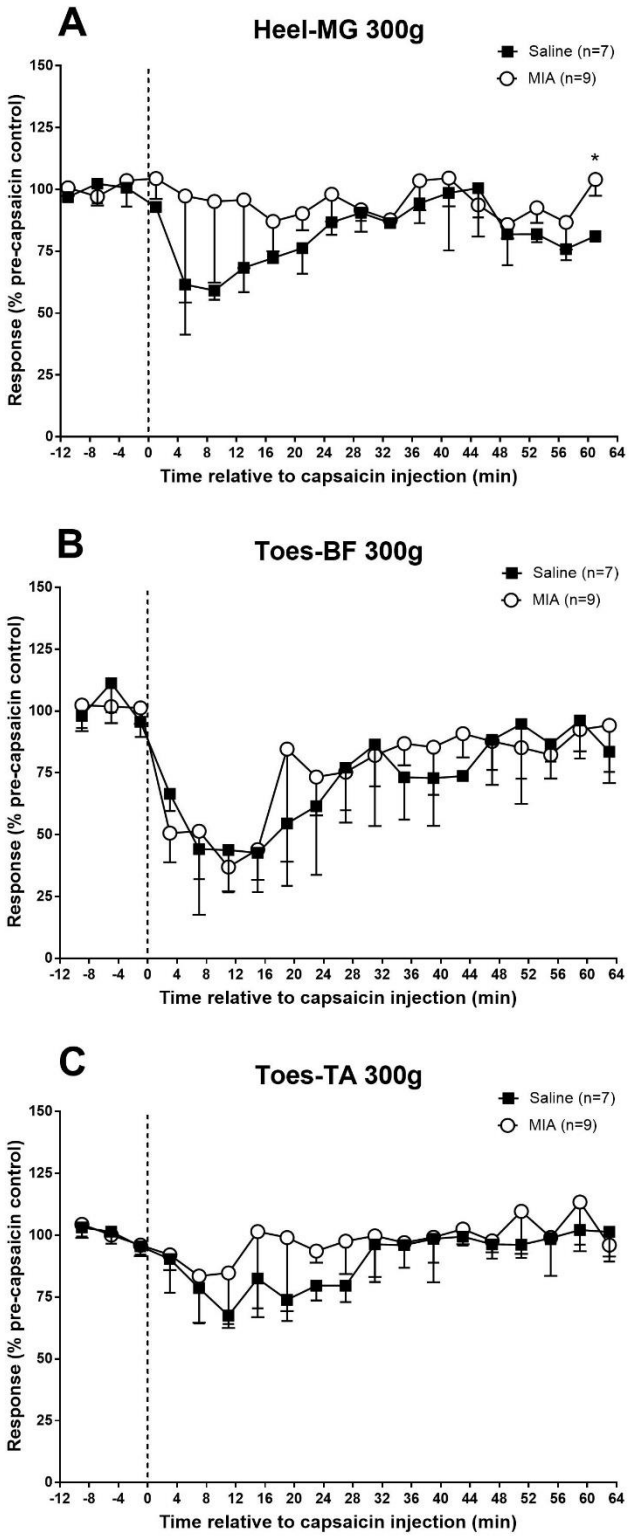

Figure 5.12. Effect of intramuscular injection of 50 µg capsaicin into the contralateral forelimb on mechanically evoked (A) heel-medial gastrocnemius (MG), (B) toes-biceps femoris (BF) and (C) toes-tibialis anterior (TA) reflexes using a 300 g von Frey (vF) monofilament in 3-4 day saline and MIA-injected animals. Values plotted are medians and errors are interquartile ranges. *$p < 0.05$ denotes significant difference between saline and MIA-injected animals at the same post-capsaicin time points (Mann-Whitney test).

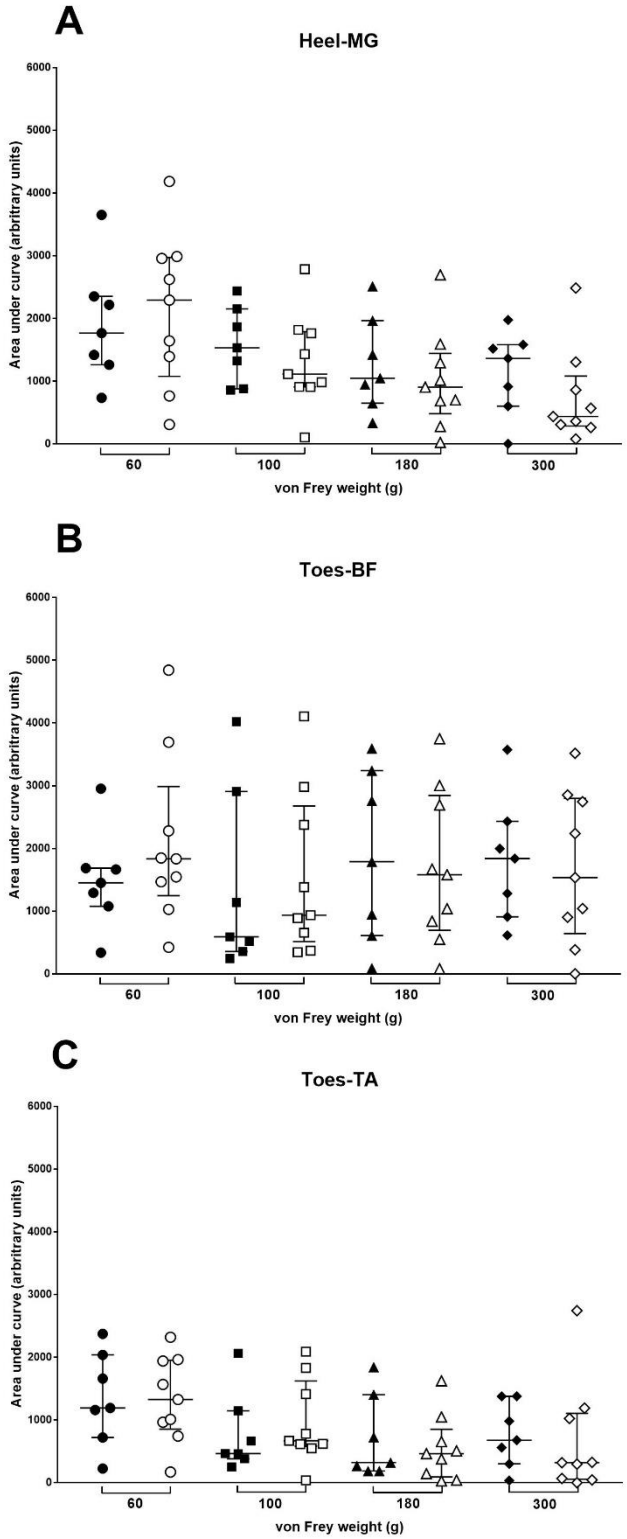

Figure 5.13. Effect of intramuscular injection of 50 µg capsaicin into the contralateral forelimb on mechanically evoked (A) heel-medial gastrocnemius (MG), (B) toes-biceps femoris (BF) and (C) toes-tibialis anterior (TA) reflexes using 60 – 300 g von Frey (vF) monofilaments in 3-4 day saline (n = 7, closed symbols) and MIA-injected (n = 9, open symbols) animals. Values plotted are area under curve (AUC) determinations for each animal with horizontal bars indicating medians and interquartile ranges.

5.3.4.3. Effect of capsaicin injection site

In nearly all cases, comparison of heel-MG, toes-BF and toes-TA responses between hindlimb and forelimb capsaicin injection sites indicated no significant difference in the degree, duration or overall inhibition between saline or MIA-injected animals ($p > 0.05$, Mann-Whitney or unpaired t-test). The exceptions being that degree of inhibition was significantly smaller after hindlimb compared to forelimb injection for heel-MG reflexes evoked by the 60 g vF weight in MIA-injected animals with medians of 71% (IQR 51 – 89%) and 28% (IQR 9 – 46%) respectively ($p = 0.0464$, Mann-Whitney test). In saline-injected animals, duration of inhibition was significantly shorter after forelimb compared to hindlimb injection for toes-BF reflexes evoked by the 180 g monofilament with medians of 23 min (IQR 0 – 47 min) and 63 min (IQR 44 – 63 min) respectively ($p = 0.0379$, Mann-Whitney test) and overall inhibition of toes-BF responses evoked by the 100 g vF weight was significantly smaller after forelimb compared to hindlimb injection with values of 590 (IQR 355 – 2909) and 4132 (IQR 1344 – 5356) respectively ($p = 0.0489$, unpaired t-test).

5.4. Discussion

Joint pathology of 3-4 day MIA-injected (2 mg dose) animals indicate little to no cartilage degradation and often do not have significant joint scoring compared to controls, indicating gross pathology is virtually unchanged from controls (Lockwood et al., 2019b). However, staining of the joints with safranin-O reveals that weak cartilage staining can be detected at 3 days post-MIA (1 mg dose) injection in both the patellofemoral and tibiofemoral joints, indicating that histologically cartilage degradation has started to occur and no staining was present by 1 week post injection (Takahashi et al., 2018). Histologically on day 1 after 1 mg dose of MIA, synovial membrane and subjacent connective tissue necrosis were present with acute inflammatory cell infiltration and oedema into the fat pad and nearby connective tissues (Clements et al., 2009). In keeping with the biphasic response, there is an initial period of knee swelling, implying transient synovial inflammation, which correlates with human OA, however it is not currently known why this resolves in the MIA model whereas in human disease recurrent inflammatory phases are noted (Saxne, 2003; Fernihough et al., 2004). The knee swelling is not always observed in knee diameter measurements in 1 mg MIA models which are often not significantly different from controls (Nwosu et al., 2016a), but is observed after a 2 mg dose MIA where knee diameter measurements were found to increase by approximately 2 mm at day 3 post injection, indicating a robust inflammatory response which returned to normal levels by day 5 (Fernihough et al., 2004). The inflammatory response is strongly observed histologically in the infiltration

of inflammatory cells including monocytes, neutrophils and basophils, all of which are present from day 1 and increase exponentially to day 3, after which they begin to subside (Clements et al., 2009). Gross examination of the joints in the present study and subsequent severity scoring indicated there were no gross lesions with very little to no cartilage damage in the ipsilateral MIA-injected joint which is in-keeping with previous studies. However, the surface of the joints had brown homogenous discolouration and, in some animals, superficial fibrillation and a lightly broken surface was observed more commonly in the tibial plateau compared to saline-injected animals, which had a smooth and unbroken surface and was a white to off-white colour. MIA-injected animals in the present study had joint scores that indicated more damage in the ipsilateral limb compared to the contralateral side and the hindlimbs of saline controls.

Pain behaviour in the form of weight bearing asymmetry and mechanical allodynia are observed in the MIA model from an early stage (Bove et al., 2003; Ferland et al., 2011; Nwosu et al., 2016a; Lockwood et al., 2019b). As early as day 1 post 1 mg MIA injection weight bearing asymmetry was apparent in previous studies, which often recovers slightly by day 7 and maintains a deficit in weight bearing for the duration of the study, which is consistent with the biphasic response observed in this model (Clements et al., 2009; Nwosu et al., 2016a). Contrastingly, mechanical allodynia measured in the form of PWTs often reduce on day 1 post MIA injection (1 mg and 2 mg doses) and remain at

this low level for the duration of the study (Nwosu et al., 2016a; Lockwood et al., 2019b). In the current study, pain behaviour testing indicated MIA animals favoured the contralateral uninjured hindlimb and exhibited significant mechanical allodynia in the ipsilateral hindlimb as early as day 1 post-injection, and this was maintained over the 3-4 day testing period which is consistent with previous studies (Bove et al., 2003; Ferland et al., 2011; Nwosu et al., 2016a; Lockwood et al., 2019b). When compared to animals tested at a later stage of model development (day 28-35), no greater difference in weight-bearing appeared to be present, however PWTs were significantly lower at the later stage suggesting an increase in pain sensitivity at this point (data not shown). This contradicts previous studies which indicate that weight bearing asymmetry is more sensitive to the biphasic nature of the MIA model, with an initial indication of pain behaviour during the inflammatory phase which recovers when this has dissipated and worsens again due to progressive damage within the joint (Fernihough et al., 2004; Nwosu et al., 2016a; Lockwood et al., 2019b). This direct comparison was not made in the present studies as 28-35 day animals did not have behavioural testing on day 3-4. However this does differ in mechanical allodynia which has previously decreased in the injured paw and stayed consistently low for the duration of the study using both a 1 mg and 2 mg dose (Fernihough et al., 2004; Nwosu et al., 2016a; Abaei et al., 2016; Lockwood et al., 2019b).

DNIC investigations during the early phase of the model have indicated that there does appear to be a difference in the level of inhibition evoked between early and late phase in the MIA model (Danziger et al., 1999; Lockwood et al., 2019b). In the current study, injection of capsaicin into the contralateral hind and forelimb induced significant inhibition of reflex responses evoked by a range of vF monofilaments (60 – 300 g) in the early MIA model as well as saline controls. However, interestingly, when capsaicin was injected into the contralateral hindlimb there were significant indications that the efficacy of observed inhibition in reflex responses was reduced in MIA-injected animals compared to saline controls, although this deficit in DNIC appeared to be sensitive to the strength of the test stimulus and the reflex response measured. Contrastingly, previous studies in early phase animal OA models have indicated that there is no difference in the efficacy of DNIC compared to controls (Danziger et al., 1999; Lockwood et al., 2019b). In early phase (2-6 day) MIA-injected animals, DNIC induced inhibition of mechanically evoked neuronal firing in spinal single unit recordings evoked by noxious pinch to the ear and knee was comparable to early phase sham-injected animals, indicating DNIC induced inhibition is not altered in the early inflammatory stages (Lockwood et al., 2019b, 2019a). Similarly, other animal models of early OA have shown DNIC induced inhibitions triggered by thermal or mechanical conditioning stimulation are not altered compared to controls (Danziger et al., 1999). Acute (24 – 48 hour) and chronic (3-4 week) monoarthritis induced by injection of CFA into the ankle joint was found to mimic each other during behavioural testing, whereby both groups had increased sensitivity to mechanical stimuli applied to

the arthritic joint, however they showed different electrophysiological profiles (Danziger et al., 1999). Acute monoarthritic animals displayed increased DNIC-induced inhibition of trigeminal neurons in response to mechanical and thermal stimulation of the arthritic joint compared to the same stimulations of the normal joint, however chronic monoarthritic animals exhibited similar DNIC-induced inhibitions after mechanical and thermal stimulation to the arthritic and normal joint (Danziger et al., 1999). This would suggest that inputs activated during chronic monoarthritis fail to recruit DNIC and therefore may be functionally different to those activated during the acute inflammatory stage (Danziger et al., 1999). Chronic pain is known to lead to peripheral and central sensitization (see section 1.2.5) which would be the case with the MIA model. However, most previous studies have evaluated the histological changes and pain related behaviours; not much is known about the changes in transmission of nociceptive information from the damaged joint to the CNS (Schuelert and McDougall, 2009). Some recent studies have shown that MIA-induced OA leads to an increased firing rate and reduced activation threshold of afferent nerve fibres (Schuelert and McDougall, 2006) which subsequently leads to sensitization of spinal neurons in the dorsal horn (Harvey and Dickenson, 2009). Another study revealed that there was a direct relationship between the concentration of MIA injected and afferent nerve fibre activity where an increase in concentration of MIA produced graded sensitization of joint nociceptors (Schuelert and McDougall, 2009). The MIA model can therefore alter the excitability of spinal neurons resulting in sensitization which is evident at day 14 post MIA injection in animals given a 40 times lower dose

of MIA intra-articularly (Harvey and Dickenson, 2009). This therefore shows that changes to the CNS in the MIA model in the later chronic phase (day 28-35) of the model may be different than the changes in the initial phase (day 3-4). The study of this thesis therefore offers a new insight into DNIC in acute OA pain whereby recordings from the periphery are not the same as recordings from the spinal cord, this is an important finding that highlights the complex nature of DNIC and that the methodology of the study should be carefully considered as reflex responses offer an additional layer of knowledge to this subject.

These studies have also indicated that the site of the conditioning stimulus may be important in trying to detect a difference in DNIC in pre-clinical models. This reduction in efficacy of DNIC does not appear to be mirrored in the reflex responses after capsaicin injection to the forelimb which may suggest injection sites are utilising different mechanisms of action in early MIA-injected animals. Previous investigations of the effect of high intensity stimulation on spinal reflex responses indicated that significant depressions of the MG muscle could be induced in spinalized animals for periods greater than 20 mins which could be supressed with very low doses of naloxone, suggesting this inhibition was mediated by opioid μ receptors (Clarke et al., 1989). Another study indicated site specific differences in inducing long-lasting depression of reflex responses in response to high-intensity stimulation of the ipsilateral and contralateral hindlimbs and forelimbs which indicated contralateral hindlimb induced

inhibitions were significantly reduced by idazoxan but were unaffected by naloxone, however forelimb induced inhibitions could be reduced by idazoxan and naloxone given independently and complete abolishment of the inhibition could be achieved giving both together (Taylor et al., 1991). These studies indicate that both noradrenergic and opioidergic mechanisms mediate heterotrophic inhibition indicating that in the present studies, early inflammatory MIA-injected animals may be activating different descending mechanisms depending on the site of conditioning stimulation (Harris, 2016).

Chapter Six

General Discussion

6.1. Discussion of findings

Overall, the findings in this thesis highlight the complexity of investigating underlying mechanisms of OA knee pain in experimental models and the influence of 'test' versus 'conditioning' stimuli, the stage of the model, the location of the conditioning stimulus and the reflex response chosen, when studying DNIC. DNIC has been extensively studied in humans, where it is termed CPM, in order to represent the human behavioural aspect of the phenomena (Kennedy et al., 2016). Despite DNIC having many variables by which it is affected (see section 1.3.3) it is considered to be a consistent measure with its reliability dependent on stimulation parameters and the methodology of the study (Kennedy et al., 2016). Different test stimulus modalities in the current study used electrical stimulation as an excellent way to deliver consistent quantifiable stimuli, whilst mechanical stimulation, although more variable in its application, was more physiologically relevant and could be graded with the use of multiple vF filaments. In human studies, various stimulus modalities have been used to evoke test responses, such as thermal contact-heat via a thermode, mechanical pressure applied using vF filaments and electrical stimulation, whilst typical conditioning stimuli consist of thermal contact-heat, cold pressor test and hot water baths (Nir and Yarnitsky, 2015). Using thermal and mechanical modalities, pain thresholds, suprathreshold pain and temporal summation as the test stimulus indicated that varying its modality in human studies results in varying DNIC responses to each DNIC paradigm (Nahman-Averbucha et al., 2013). The most effective test stimulation in humans were

pressure pain threshold (PPT) and thermal temporal summation which were both inhibited during the conditioning stimulus, however the other test stimuli did not (Nahman-Averbucha et al., 2013). These electrophysiological studies demonstrated that a capsaicin conditioning stimulus inhibited test reflex responses in a dose-related manner whereby inhibition was increased by increasing the dosage in the smaller two doses but was not increased any more by the largest dose. Previous investigations in humans have found that DNIC inhibition is dependent on intensity of the conditioning stimulus, with two temperatures of a water bath used as the conditioning stimulus (41 °C and 45 °C), whereby the higher temperature elicited significant inhibition but the lower temperature did not (Kakigi, 1994). Another study investigating more conditioning stimuli intensities found that temperatures above 45 °C reduced evoked responses in a dose-dependent manner when applied to the contralateral hand, where 45 °C, 46 °C and 47 °C produced increasingly larger inhibitory effects on a nociceptive flexion reflex (Willer et al., 1989). Location of the conditioning stimulus is also an important factor in DNIC with previous human studies indicating that applying the conditioning stimulus to the shoulder and the hand resulted in greater inhibition from stimulation at the shoulder (Haefeli et al., 2014). However, another study investigating the back and forearms as conditioning stimulation sites found no differences in the evoked inhibition between the two locations (Klyne et al., 2015). This agrees with the results in the present study which found site specific differences between forelimb and hindlimb injection sites; generally, forelimb injection

appeared to have larger and longer lasting inhibitory effects compared to hindlimb.

The capsaicin induced inhibition in the present study could be completely abolished in spinalized animals, agreeing with previous studies that the mechanisms underlying DNIC arise entirely from supraspinal sources (Le Bars et al., 1979a, 1979b; Hall et al., 1982; Cadden et al., 1983; Dickhaus et al., 1985; Morton et al., 1987; Gjerstad et al., 1999). In humans with spinal cord injury (SCI), individuals with SCI and neuropathic pain associated with their condition were found to have reduced DNIC, however individuals that had SCI but no neuropathic pain were found to have DNIC reductions that were to a similar degree as healthy controls (Albu et al., 2015; Gruener et al., 2016). Contrastingly, individuals with tetraplegia due to a traumatic section of the C5, C6 or C7 spinal cord had an inability to trigger inhibitory effects on a nociceptive flexion reflex in the leg in response to a clearly nociceptive stimulus applied to the contralateral fingers (Roby-Brami et al., 1987). This indicates that in humans with complete transection of the spinal cord the inhibitory effects triggered by heteroptopic nociceptive stimuli are therefore sustained by a loop which includes supraspinal structures (Roby-Brami et al., 1987; Le Bars et al., 1991; Albu et al., 2015; Gruener et al., 2016). DNIC inhibition in the present studies was reduced by pre-collicular decerebration, indicating inhibition of reflexes in these studies may be partially controlled by structures rostral to the colliculi exerting influence on structures caudal to the colliculi (i.e. midbrain and

brainstem regions). Previous animal studies have indicated regions responsible for the source of DNIC pathways, however lesioning these regions has never fully abolished DNIC (see section 1.3.1). The results in this study contradict previous results in humans which suggest that only brainstem structures are involved in mediating DNIC and specifically that spinothalamic pathways are not involved in DNIC. Profound inhibition could be induced in the flexion reflex in patients with unilateral thalamic vascular lesions when conditioning stimuli was applied to the analgesic hand, whereas it could not be induced in patients with unilateral lesions of the retro-olivary portion of the medulla (Wallenberg's syndrome, WS)(De Broucker et al., 1990). The same conditioning procedure applied to the non-analgesic hand of WS patients resulted in inhibition that was not different from healthy controls (De Broucker et al., 1990). This research therefore suggests that spinoreticular tracts are key neuronal links in endogenous analgesia (Pud et al., 2005). Similarly in humans, involvement of an opioidergic link was found by investigating DNIC in healthy subjects where i.v. naloxone resulted in complete abolition of flexion reflex inhibitions, indicating inhibitions triggered by DNIC involve endogenous opioids (Willer et al., 1990). This thesis also investigated the effect of alfaxalone anaesthesia on DNIC for the first time and, concurring with previous work on anaesthetics, found under low alfaxalone levels animals had greater DNIC than under normal alfaxalone conditions (Tomlinson et al., 1983; Jinks et al., 2003a). In human experiments, DNIC is investigated in conscious subjects and therefore it is difficult to determine the effect of anaesthesia on DNIC in humans.

There are very few studies investigating DNIC in reflex responses in humans, however DNIC has been shown to have strong inhibitory effects on electrically stimulated nociceptive reflexes with thermal, mechanical or chemical conditioning stimuli (Willer et al., 1984, 1989). Reflex responses measured in the BF muscles in humans were significantly inhibited by ice water applied to the contralateral hand and foot with no significant interaction measured between the size of the reflex and the intensity of the pain (Terkelsen et al., 2001). In all of these studies the test stimulus for evoking the reflex response was electrical stimulation of the sural nerve in the form of surface electrodes which is a very similar method to the electrically stimulated responses used in this thesis (Willer et al., 1984; Terkelsen et al., 2001). There are no human studies comparable to the mechanical stimulation used in the present studies to evoke reflex responses however mechanical stimulation is often used in pain studies in humans in the form of PPT measurement which is very reliable for analysing pain. None of these studies have compared multiple reflex responses like the experiments undertaken in this thesis. The current study indicated that the flexor reflexes are more susceptible to DNIC than extensor reflexes which would suggest that muscles are differentially controlled (section 1.4.2) and therefore differentially modulated via descending controls (Schouenborg and Kalliomäki, 1990).

DNIC has been extensively investigated in humans with OA (Kosek and Ordeberg, 2000; Quante et al., 2008; Graven-Nielsen et al., 2012; Arendt-Nielsen et al., 2015) but also in other chronic pain conditions such as myofascial TMD (Maixner et al., 1995; Bragdon et al., 2002), fibromyalgia (Kosek and Hansson, 1997; Lautenbacher and Rollman, 1997; Staud et al., 2003; Julien et al., 2005), chronic lower back pain (Peters et al., 1992), irritable bowel syndrome (IBS)(Wilder-Smith et al., 2004; Song et al., 2006) and chronic tension headaches (Pielsticker et al., 2005; Sandrini et al., 2006), where it has been found to be less efficacious. In contrast, DNIC was found to be preserved in patients with long-term trapezius myalgia (Leffler et al., 2002a), acute and chronic rheumatoid arthritis (Leffler et al., 2002b), vestibulodynia (Johannesson et al., 2007) and Parkinson's disease (Mylius et al., 2009), which was the case in the chronic pain animals in the present study. A potential cause for these differences between chronic pain conditions may be due to different physiological mechanisms underlying pain, different noxious conditioning procedures, different testing techniques as well as differences in pain duration/intensity (Leffler et al., 2002b). Electrophysiologically, the present study investigated the efficacy of DNIC in both acute and chronic phases of the MIA model, finding DNIC less efficacious in the acute phase but restored in the chronic phase. This was surprising as previous animal studies had shown the opposite results with DNIC reduced as the disease progresses (Lockwood et al., 2019b). However, one study has shown a complete lack of DNIC in human OA separated into high and low pain groups suggesting the acute pain (low pain) was completely abolished in this study (King et al., 2013). The difference in the

current study may possibly be attributed to the measured response whereby the present study recorded functionally relevant multi-synaptic reflex responses in peripheral muscles, whereas previous work investigated single spinal dorsal horn neurons (Lockwood et al., 2019b). It is currently unknown whether less efficacious DNIC is a result of the ongoing chronic pain or whether it predisposes them to acute or chronic pain (Granovsky, 2013). Results of one previous animal study suggested that efficient descending inhibition can provide protection against the development of experimental chronic neuropathic pain and particularly the transition of acute to chronic neuropathic pain (De Felice et al., 2011). This hypothesis compliments a study in humans which indicated impaired DNIC may predict the development of chronic pain, where patients with less efficacious DNIC in a pain-free state before thoracotomy surgery had a higher chance for development of chronic but not acute pain post-surgery (Yarnitsky et al., 2008). Similarly, effective DNIC was linked to a lower risk of developing chronic post-surgery pain with an odds ratio of 0.52 (Yarnitsky et al., 2008). Another study investigating DNIC in acute post-caesarean pain found the opposite, suggesting more research is needed in this area (Landau et al., 2010). Other studies have reported that impairment of DNIC was present in patients with painful hip and knee OA but that DNIC function was restored after successful joint replacement surgery which suggests that reduced efficacy of DNIC was maintained by the chronic pain and that ongoing pain from one site may interact with DNIC evoked by pain in another area (Kosek and Ordeberg, 2000; Arendt-Nielsen et al., 2010; Graven-Nielsen et al., 2012). The mechanism of this change in DNIC efficacy is not fully known,

although what is clear is that the loss of DNIC provides evidence of altered central pain processing (Graven-Nielsen et al., 2012). It has been postulated that descending inhibition is reorganised in that neurons in the dorsal horn and at supraspinal sites change their response characteristics following peripheral nerve damage and that these changes in plasticity are time dependent (Pertovaara et al., 1997; Chapman et al., 1998; Sotgiu and Biella, 1998; Woolf and Mannion, 1999). In studies investigating the loss of DNIC in animal chronic pain models it has been found that a reduction in descending noradrenergic inhibition and enhanced descending serotonergic facilitation acting at 5-HT_3 receptors has been shown in the chronic pain phase of the MIA and SNL models (Bannister et al., 2015; Lockwood et al., 2019a).

In the current study the difference between acute and chronic stages of OA was ascertained by the degree of gross macroscopic joint damage and this was compared to pain behaviour and the effectiveness of DNIC. MIA-injected animals exhibited significant pain behaviour by day 1 post-injection with gross joint pathology expressing key indicators of the progression of OA over short (day 3-4) and later (day 28-35) stages of the model, which has been well documented in previous work (Schaible, 2013; Mapp et al., 2013; Nwosu et al., 2016b). However, in human OA there is often a large discrepancy between joint damage and pain symptoms (Arendt-Nielsen et al., 2010); this was reflected in the current study with pain behaviours in acute and chronic states of the MIA model being similar between groups despite the large variations in joint

pathology. A recent study has been able to subgroup patients based on the degree of knee OA and pain using quantitative sensory testing (QST) and Kellgren and Lawrence (KL) grading scores whereby 217 individuals were categorised into four groups; low pain/low KL, low pain/high KL, high pain/low KL and high pain/high KL (Arendt-Nielsen et al., 2015). DNIC was assessed between groups and found that higher pain groups had significantly less effective DNIC (Arendt-Nielsen et al., 2015). This postulates the question that if joint damage is not a reliable measure for predicting pain in human OA, could DNIC be a better predictor? However, other investigations looking at the same four groups in human OA found there was no significant difference with respect to DNIC (Finan et al., 2013). Despite these variations there is a strong belief that DNIC and its underlying mechanisms can be useful in predicting and treating chronic pain (Granovsky, 2013). This can only be utilised for making better individual patient decisions if there is a greater understanding of the physiology of DNIC (Granovsky, 2013).

6.1.1. Future directions

An initial future direction to the current studies would be to analyse the C-fibre responses from electrically stimulated recordings. Whilst DNIC is observed in A-fibre responses, its inhibitory effects are to a much stronger degree in C-fibre responses and so adding this element to the analysis would give a greater idea of the effect of capsaicin on reflex responses but also would fully analyse the levels of evoked inhibition.

The work presented in this thesis suggests a difference in capsaicin-induced DNIC of electrophysiologically recorded reflexes in the MIA model of OA pain depending on the post-injection time period i.e. on days 3-4 or days 28-35, which in this model of OA pain can be regarded as acute and chronic pain states, as well as inflammatory and neuropathic pain. A future study investigating change in DNIC efficacy at post-injection time points between these acute and chronic states e.g. on day 7, 14 and 21 post MIA injection, would allow better understanding of when DNIC in this preparation switches and give greater insight into the gross joint pathology that is present when DNIC efficacy is no longer altered.

The MIA model combined with the measurement of spinally organised reflexes is ideal for investigating mechanistic changes occurring within the CNS and as such could be used to determine which pathways are affected when DNIC is altered. Thus, spinal administration of 5-HT and NA antagonists via an intrathecal cannula would help to determine which of these transmitters and their receptors may alter as OA develops. Alongside this it would be possible to investigate the immunohistochemistry of the changes in receptor populations (e.g. α_2 adrenoceptors) within the spinal cord at various stages of the MIA model, again linking these changes to alterations in DNIC efficacy between acute and chronic disease states.

As decerebration affected the efficacy of DNIC in 'normal' healthy animals, in addition to midbrain/brainstem areas, a role for higher brain regions is suggested. This opens the possibility of lesioning specific areas of the brain to try to determine the location of regions contributing to the inhibition.

6.2. Concluding remarks

Overall, the studies presented in this thesis provide new information on the effects of variables on DNIC such as anaesthesia, which is often disregarded in such studies, as well as the importance of the balance between test versus conditioning stimuli. This thesis has demonstrated that animals with chronic OA pain do not have compromised DNIC of reflex responses and that the acute inflammatory phase of the disease can have less effective DNIC. These findings demonstrate that DNIC is highly variable, depending on the investigation parameters, and show that reflex responses should be considered as a test response when investigating DNIC. This thesis ultimately adds to the wealth of information regarding chronic pain in OA and understanding these underlying mechanisms behind OA pain is key to developing novel therapies.

References

Aagaard, H. and Verdonk, R. (1999) Function of the normal meniscus and consequences of meniscal resection. Scandinavian Journal of Medicine & Science in Sports, **9**: 134–140

Abaei, M., Sagar, D.R., Stockley, E.G., et al. (2016) Neural correlates of hyperalgesia in the monosodium iodoacetate model of osteoarthritis pain. Molecular Pain, **12**: 1–12

Adams, J.G., McAdlindon, T., Dimasi, M., et al. (1999) Contribution of meniscal extrusion and cartilage loss to joint space narrowing in osteoarthritis. Clinical Radiology, **54**: 502–506

Adams, M.E., Billingham, M.E.J. and Muir, H. (1983) The glycosaminoglycans in menisci in experimental and natural osteoarthritis. Arthritis & Rheumatism, **26** (1): 69–76

Akgun, U., Kocaoglu, B., Orhan, E.K., et al. (2008) Possible reflex pathway between medial meniscus and semimembranosus muscle: An experimental study in rabbits. Knee Surgery, Sports Traumatology, Arthroscopy, **16** (9): 809–814

Alarcón, G. and Cervero, F. (1989) Effects of two anaesthetic regimes on the heterotopic inhibition of rat dorsal horn neurones. The Journal of Physiology, **416** (19P)

Albu, S., Gómez-Soriano, J., Avila-Martin, G., et al. (2015) Deficient conditioned pain modulation after spinal cord injury correlates with clinical spontaneous pain measures. PAIN, **156** (2): 260–272

Ameye, L.G. and Young, M.F. (2006) Animal models of osteoarthritis: lessons learned while seeking the 'Holy Grail'. Current Opinion in Rheumatology, **18** (5): 537–547

Amiel, D., Frank, C., Harwood, F., et al. (1983) Tendons and ligaments: A morphological and biochemical comparison. Journal of Orthopaedic Research, **1** (3): 257–265

Andersen, O.K. (2007) Studies of the organization of the human nociceptive withdrawal reflex. Acta Physiologica, **189**: 1–35

Andriacchi, T.P., Mündermann, A., Smith, R.L., et al. (2004) A framework for the in vivo pathomechanics of osteoarthritis at the knee. Annals of Biomedical Engineering, **32** (3): 447–457

Arendt-Nielsen, L., Egsgaard, L.L., Petersen, K.K., et al. (2015) A mechanism-based pain sensitivity index to characterize knee osteoarthritis patients with different disease stages and pain levels. European Journal of Pain, **19** (10): 1406–1417

Arendt-Nielsen, L., Nie, H.L., Laursen, M.B., et al. (2010) Sensitization in patients with painful knee osteoarthritis. Pain, **149** (3): 573–581

Arendt-Nielsen, L., Sluka, K.A. and Nie, H.L. (2008) Experimental muscle pain impairs descending inhibition. Pain, **140** (3): 465–471

Arthritis Research UK (2012) Osteoarthritis. Chesterfield: Arthritis Research UK

Arthritis Research UK (2013) Osteoarthritis in general practice. Chesterfield: Arthritis Research UK

Ashraf, S., Mapp, P.I. and Walsh, D.A. (2011) Contributions of angiogenesis to inflammation, joint damage, and pain in a rat model of osteoarthritis. Arthritis and Rheumatism, **63** (9): 2700–2710

Ashraf, S., Wibberley, H., Mapp, P.I., et al. (2010) Increased vascular penetration and nerve growth in the meniscus: A potential source of pain in osteoarthritis. Osteoarthritis and Cartilage, **18** (2): S20–S21

Ateshian, G.A. and Hung, C.T. (2013) Patellofemoral joint biomechanics and tissue engineering. Clinical Orthopaedics and Related Research, **436**: 81–90

Ayral, X., Gueguen, A., Listrat, V., et al. (1994) Simplified arthroscopy scoring system for chondropathy of the knee (revised SFA score). Revue du Rhumatisme [Eng Ed], **61** (2): 88–90

Ayral, X., Pickering, E.H., Woodworth, T.G., et al. (2005) Synovitis: a potential predictive factor of structural progression of medial tibiofemoral knee osteoarthritis - results of a 1 year longitudinal arthroscopic study in 422 patients. Osteoarthritis and Cartilage, **13**: 361–367

Baad-Hansen, L., Poulsen, H.F., Jensen, H.M., et al. (2005) Lack of sex differences in modulation of experimental intraoral pain by diffuse noxious inhibitory controls (DNIC). Pain, **116** (3): 359–365

van Baar, M.E., Dekker, J., Lemmens, J.A., et al. (1998) Pain and disability in patients with osteoarthritis of hip or knee: the relationship with articular, kinesiological, and psychological characteristics. Journal of Rheumatology, **25** (1): 125–133

Ball, J., Chapman, J.A. and Muirden, K.D. (1964) The uptake of iron in rabbit synovial tissue following intra-articular injection of iron dextran: a light and electron microscope study. The Journal of Cell Biology, **22**: 351–364

Bannister, K., Bee, L.A. and Dickenson, A.H. (2009) Preclinical and early clinical investigations related to monoaminergic pain modulation. Neurotherapeutics, **6** (4): 703–712

Bannister, K., Lockwood, S., Goncalves, L., et al. (2017) An investigation into the inhibitory function of serotonin in diffuse noxious inhibitory controls in the neuropathic rat. European Journal of Pain, **21** (4): 750–760

Bannister, K., Patel, R., Goncalves, L., et al. (2015) Diffuse noxious inhibitory controls and nerve injury: Restoring an imbalance between descending monoamine inhibitions and facilitations. Pain, **156** (9): 1803–1811

Le Bars, D. (2002) The whole body receptive field of dorsal horn multireceptive neurones. Brain Research Reviews, **40** (1–3): 29–44

Le Bars, D., Dickenson, A.H. and Besson, J.-M. (1979a) Diffuse noxious inhibitory controls (DNIC). I. Effects on dorsal horn convergent neurones in the rat. Pain, **6**: 283–304

Le Bars, D., Dickenson, A.H. and Besson, J.-M. (1979b) Diffuse noxious inhibitory controls (DNIC). II. Lack of effect on non-convergent neurones, supraspinal involvement and theoretical implications. Pain, **6**: 305–327

Le Bars, D., Villanueva, L., Willer, J.C., et al. (1991) Diffuse noxious inhibitory controls (DNIC) in animals and in man. Acupuncture in Medicine, **9** (2): 47–56

Le Bars, D. and Willer, J.C. (2010) Diffuse Noxious Inhibitory Controls (DNIC). The Senses: A Comprehensive Reference, **5** (January 2010): 763–773

Basbaum, A.I., Bautista, D.M., Scherrer, G., et al. (2009) Cellular and Molecular Mechanisms of Pain. Cell, **139** (2): 267–284

Basbaum, A.I. and Fields, H.L. (1978) Endogenous pain control mechanisms: review and hypothesis. Annals of Neurology, **4** (5): 451–462

Basbaum, A.I. and Fields, H.L. (1979) The origin of descending pathways in the dorsolateral funiculus of the spinal cord of the cat and rat: Further studies on the anatomy of pain modulation. Journal of Comparative Neurology, **187** (3): 513–531

Bellamy, N., Campbell, J., Robinson, V., et al. (2006) Intraarticular corticosteroid for treatment of osteoarthritis of the knee. Cochrane Database of Systematic Reviews, **19** (2): 1–221

Bellemans, J. (2003) Biomechanics of anterior knee pain. The Knee, **10**: 123–126

Bendele, A.M. (2001) Animal models of osteoarthritis. Journal of Musculoskeletal and Neuronal Interactions, **1** (4): 363–376

Bendele, A.M. and Hulman, J.F. (1988) Spontaneous cartilage degeneration in guinea pigs. Arthritis & Rheumatism, **31** (4): 561–565

Bendele, A.M. and Hulman, J.F. (1991) Effects of body weight restriction on the development and progression of spontaneous osteoarthritis in guinea pigs. Arthritis & Rheumatism, **34** (9): 1180–1184

Berge, O.-G. (2013) “Animal Models of Pain.” In McMahon, S.B., Koltzenburg, M., Tracey, I., et al. (eds.) Wall and Melzack’s Textbook of Pain. 6th ed. Philadelphia: Elsevier Saunders

Berkley, K.J. (1997) Sex differences in pain. Behavioural and Brain Sciences, **20**: 371–380

Bernard, J.F., Villanueva, L., Carroué, J., et al. (1990) Efferent projections from the subnucleus reticularis dorsalis (SRD): A Phaseolus vulgaris leucoagglutinin study in the rat. Neuroscience Letters, **116**: 257–262

Bessou, P. and Perl, E.R. (1969) Response of cutaneous sensory units with unmyelinated fibers to noxious stimuli. Journal of neurophysiology, **32** (6): 1025–1043

Bevan, S. and Szolcsányi, J. (1990) Sensory neuron-specific actions of capsaicin: mechanisms and applications. Trends in Pharmacological Sciences, **11** (8): 331–333

Bhattachayya, T., Gale, D., Dewire, P., et al. (2003) The clinical importance of meniscal tears demonstrated by Magnetic Resonance Imaging in osteoarthritis of the knee. The Journal of Bone and Joint Surgery, **85A** (1): 4–9

Bhosale, A.M. and Richardson, J.B. (2008) Articular cartilage: Structure, injuries and review of management. British Medical Bulletin, **87** (1): 77–95

Bird, H.A., Tribe, C.R. and Bacon, P.A. (1978) Joint hypermobility leading to osteoarthrosis nd chondrocalcinosis. Annals of the Rheumatic Diseases, **37**: 203–211

Bird, M.D.T. and Sweet, M.B.E. (1987) A system of canals in semilunar menisci. Annals of the Rheumatic Diseases, **46** (9): 670–673

Bird, M.D.T. and Sweet, M.B.E. (1988) Canals in the semilunar meniscus: Brief report. Journal of Bone and Joint Surgery: Brief Reports, **70**-**B** (5): 839

Bishop, G.H. (1946) Neural mechanisms of cutaneous sense. Physiological Reviews, **26** (1): 77–102

Bitton, R. (2009) The economic burden of osteoarthritis. The American journal of managed care, **15** (8 Suppl): S230–S235

Biurrun Manresa, J.A., Fritsche, R., Vuilleumier, P.H., et al. (2014) Is the conditioned pain modulation paradigm reliable? A test-retest assessment using the nociceptive withdrawal reflex. PLoS ONE, **9** (6)

Biurrun Manresa, J.A., Neziri, A.Y., Curatolo, M., et al. (2013) Reflex receptive fields are enlarged in patients with musculoskeletal low back and neck pain. Pain, **154**: 1318–1324

Boegård, T. and Jonsson, K. (1999) Radiography in osteoarthritis of the knee. Skeletal Radiology, **28** (11): 605–615

Bolbos, R.I., Zuo, J., Banerjee, S., et al. (2008) Relationship between trabecular bone structure and articular cartilage morphology and relaxation times in early OA of the knee joint using parallel MRI at 3T. Osteoarthritis and Cartilage, **16** (10): 1150–1159

Bonnet, C.S. and Walsh, D.A. (2005) Osteoarthritis, angiogenesis and inflammation. Rheumatology, **44** (1): 7–16

Bouhassira, D., Bing, Z. and Le Bars, D. (1990) Studies of the brain structures involved in diffuse noxious inhibitory controls: the mesencephalon. Journal of Neurophysiology, **64** (6): 1712–1723

Bouhassira, D., Bing, Z. and Le Bars, D. (1992a) Effects of lesions of locus coeruleus/subcoeruleus on diffuse noxious inhibitory controls in the rat. Brain Research, **571**: 140–144

Bouhassira, D., Chitour, D., Villanueva, L., et al. (1993) Studies of brain structures involved in diffuse noxious inhibitory controls in the rat: The rostral ventromedial medulla. Journal of Pharmacology, **463**: 667–687

Bouhassira, D., Villanueva, L., Bing, Z., et al. (1992b) Involvement of the subnucleus reticularis dorsalis in diffuse noxious inhibitory controls in the rat. Brain Research, **595**: 353–357

Bove, S.E., Calcaterra, S.L., Brooker, R.M., et al. (2003) Weight bearing as a measure of disease progression and efficacy of anti-inflammatory compounds in a model of monosodium iodoacetate-induced osteoarthritis. Osteoarthritis and Cartilage, **11** (11): 821–830

Bove, S.E., Laemont, K.D., Brooker, R.M., et al. (2006) Surgically induced osteoarthritis in the rat results in the development of both osteoarthritis-like joint pain and secondary hyperalgesia. Osteoarthritis and Cartilage, **14** (10): 1041–1048

Boyd, S.K., Müller, R., Leonard, T., et al. (2005) Long-term periarticular bone adaptation in a feline knee injury model for post-traumatic experimental

osteoarthritis. Osteoarthritis and Cartilage, **13**: 235–242

Bragdon, E.E., Light, K.C., Costello, N.L., et al. (2002) Group differences in pain modulation: Pain-free women compared to pain-free men and to women with TMD. Pain, **96** (3): 227–237

Brandt, K.D. (2002) Animal models of osteoarthritis. Biorheology, **39**: 221–235

Bray, R.C., Salo, P.T., Lo, I.K., et al. (2005) Normal ligament structure, physiology and function. Sports Medicine and Arthroscopy Review, **13** (3): 127–135

Breitenseher, M.J., Trattni, S., Dobrocky, I., et al. (1997) MR imaging of meniscal subluxation in the knee. Acta Radiologica, **38**: 876–879

Breivik, H., Collett, B., Ventafridda, V., et al. (2006) Survey of chronic pain in Europe: Prevalence, impact on daily life, and treatment. European Journal of Pain, **10** (4): 287–333

Brennan, H.C., Nijjar, S. and Jones, E.A. (1998) The specification of the pronephric tubules and duct in Xenopuslaevis. Mechanisms of Development, **75**: 127–137

Brody, L.T. (2015) Knee osteoarthritis: Clinical connections to articular cartilage structure and function. Physical Therapy in Sport, **16** (4): 301–316

De Broucker, T.H., Cesaro, P., Willer, J.C., et al. (1990) Diffuse noxious inhibitory controls in man: Involvement of the spinorecticular tract. Brain, **113**: 1223–1234

Bryceland, J.K., Powell, A.J. and Nunn, T. (2017) Knee Menisci: Structure, Function, and Management of Pathology. Cartilage, **8** (2): 99–104

Buckland-Wright, C. (2004) Subchondral bone changes in hand and knee osteoarthritis detected by radiography. Osteoarthritis and Cartilage, **12**: 10–19

Buckwalter, J.A. and Mankin, H.J. (1997) Articular Cartilage. Part I: Tissue Design and Chondrocyte-Matrix Interactions. Amercian Academy of Orthopaedic Surgeons: Instructional Course Lectures, **47**: 600–611

Buckwalter, J.A. and Mankin, H.J. (1998) Articular cartilage. Part II: Degeneration and osteoarthrosis, repair, regeneration, and transplantation. Amercian Academy of Orthopaedic Surgeons: Instructional Course Lectures, **47**: 612–632

Buckwalter, J.A. and Martin, J.A. (2006) Osteoarthritis. Advanced Drug Delivery Reviews, **58** (2): 150–167

Budai, D. (2000) Neurotransmitters and receptors in the dorsal horn of the spinal cord. Acta Biologica Szegediensis, **44** (1–4): 21–38

Burgess, P.R. and Perl, E.R. (1967) Myelinated afferent fibres responding specifically to noxious stimulation of the skin. The Journal of Physiology, **190** (3): 541–62

Burke, R.E. (1999) The use of state-dependent modulation of spinal reflexes as a tool to investigate the organization of spinal interneurons. Experimental Brain Research, **128** (3): 263–277

Burr, D.B. and Gallant, M.A. (2012) Bone remodelling in osteoarthritis. Nature Reviews Rheumatology, **8**: 665–673

Burr, D.B., Schaffler, M.B. and Frederickson, R.G. (1988) Composition of the

cement line and its possible mechanical role as a local interface in human compact bone. Journal of Biomechanics, **21** (11)

Cadden, S.W., Villanueva, L., Chitour, D., et al. (1983) Depression of activities of dorsal horn convergent neurones by propriospinal mechanisms triggered by noxious inputs; comparison with diffuse noxious inhibitory controls (DNIC). Brain Research, **275** (1): 1–11

Calvo, E., Palacios, I., Delgado, E., et al. (2004) Histopathological correlation of cartilage swelling detected by magnetic resonance imaging in early experimental osteoarthritis. Osteoarthritis and Cartilage, **12**: 878–886

Campbell, C.M., France, C.R., Robinson, M.E., et al. (2008) Ethnic differences in diffuse noxious inhibitory controls (DNIC). Journal of Pain, **9** (8): 759–766

Carlson, C.S., Loeser, R.F., Jayo, M.J., et al. (1994) Osteoarthritis in cynomolgus macaques: A primate model of naturally occurring disease. Journal of Orthopaedic Research, **12** (3): 331–339

Carlson, C.S., Loeser, R.F., Purser, C.B., et al. (1996) Osteoarthritis in cynomolgus macaques III: Effects of age, gender, and subchondral bone thickness on the severity of disease. Journal of Bone and Mineral Research, **11** (9): 1209–1217

Carrino, J.A., Blum, J., Parellada, J.A., et al. (2006) MRI of bone marrow edema-like signal in the pathogenesis of subchondral cysts. Osteoarthritis and Cartilage, **14**: 1081–1085

Caterina, M.J., Leffler, A., Malmberg, A.B., et al. (2000) Impaired nociception

and pain sensation in mice lacking the capsaicin receptor. Science, **288** (5464): 306–313

Cervero, F., Schaible, H.-G. and Schmidt, R.F. (1991) Tonic descending inhibition of spinal cord neurones driven by joint afferents in normal cats and in cats with an inflamed knee joint. Experimental Brain Research, **83** (3): 675–678

Chan, W.P., Lang, P., Stevens, M.P., et al. (1991) Osteoarthritis of the knee: comparison of radiography, CT, and MR Imaging to assess extent and severity. American Journal of Roentgenology, **157** (4): 799–806

Chang, H.-T. and Ruch, T.C. (1949) Spinal origin of the ventral supraoptic decussation (Gudden's commissure) in the spider monkey. Journal of Anatomy, **83** (1): 1–9

Chaplan, S.R., Bach, F.W., Pogrel, J.W., et al. (1994) Quantitative assessment of tactile allodynia in the rat paw. Journal of Neuroscience Methods, **53** (1): 55–63

Chapman, V., Suzuki, R. and Dickenson, A.H. (1998) Electrophysiological characterization of spinal neuronal response properties in anaesthetized rats after ligation of spinal nerves L5-L6. The Journal of physiology, **507 (Pt 3** (Pt 3): 881–94

Child, K.J., Davis, B., Dodds, M.G., et al. (1972) Anaesthetic, cardiovascular and respiratory effects of a new steroidal agent CT 1341: a comparison with other intravenous anaesthetic drugs in the unrestrained cat. British Journal of Pharmacology, **46**: 189–200

Chitour, D., Dickenson, A.H. and Le Bars, D. (1982) Pharmacological evidence for the involvement of serotonergic mechanisms in diffuse noxious inhibitory controls (DNIC). Brain Research, **236** (2): 329–337

Chopra, A. (2013) The COPCORD world of musculoskeletal pain and arthritis. Rheumatology, **52** (11): 1925–1928

Christina, A.J.M., Merlin, N.J., Vijaya, C., et al. (2004) Daily rhythm of nociception in rats. Journal of Circadian Rhythms, **2** (1): 1–3

Cimmino, M.A. and Parodi, M. (2004) Risk factors for osteoarthritis. Seminars in Arthritis and Rheumatism, **34** (2 SUPPL.): 29–34

Claes, S., Vereecke, E., Maes, M., et al. (2013) Anatomy of the anterolateral ligament of the knee. Journal of Anatomy, **223** (4): 321–328

Clarke, R.W., Ford, T.W. and Taylor, J.S. (1989) Activation by high intensity peripheral nerve stimulation of adrenergic and opioidergic inhibition of a spinal reflex in the decerebrated rabbit. Brain Research, **505** (1): 1–6

Clarke, R.W. and Harris, J. (2004) The organization of motor responses to noxious stimuli. Brain Research Reviews, **46** (2): 163–172

Clarke, R.W., Harris, J. and Houghton, A.K. (1996) Spinal 5-HT-receptors and tonic modulation of transmission through a withdrawal reflex pathway in the decerebrated rabbit. British Journal of Pharmacology, **119** (6): 1167–1176

Clarke, R.W. and Matthews, B. (1985) The effects of anaesthetics and remote noxious stimuli on the jaw-opening reflex evoked by tooth-pulp stimulation in the cat. Brain Research, **327** (1–2): 105–111

Clements, K.M., Ball, A.D., Jones, H.B., et al. (2009) Cellular and histopathological changes in the infrapatellar fat pad in the monoiodoacetate model of osteoarthritis pain. Osteoarthritis and Cartilage, **17**: 805–812

Coimbra, I.B., Jimenez, S.A., Hawkins, D.F., et al. (2004) Hypoxia inducible factor-1 alpha expression in human normal and osteoarthritic chondrocytes. Osteoarthritis and Cartilage, **12**: 336–345

Collins, D.H. (1949) The Pathology of Articular and Spinal Diseases. London: Edward Arnold & Co

Combe, R., Bramwell, S. and Field, M.J. (2004) The monosodium iodoacetate model of osteoarthritis: a model of chronic nociceptive pain in rats? Neuroscience Letters, **370** (2–3): 236–240

Cooper, C., Javaid, M.K. and Arden, N. (2015) "Epidemiology of osteoarthritis." In Arden, N., Blanco, F.J., Cooper, C., et al. (eds.) Atlas of osteoarthritis. 1st ed. London: Springer Healthcare

Craig, A.D. (2003) PAIN MECHANISMS: Labeled lines versus convergence in central processing. Annu. Rev. Neurosci, **26**: 1–30

Craig, A.D., Heppelmann, B. and Schaible, H.-G. (1988) The projection of the medial and posterior articular nerves of the cat's knee to the spinal cord. Journal of Comparative Neurology, **276** (2): 279–288

Craig, A.D., Zhang, E.T. and Blomqvist, A. (2002) Association of spinothalamic lamina I neurons and their ascending axons with calbindin-immunoreactivity in monkey and human. Pain, **97** (1–2): 105–115

Crema, M.D., Roemer, F.W., Zhu, Y., et al. (2010) Subchondral cystlike lesions develop longitudinally in areas of bone marrow edema-like lesions in patients with or at risk for knee osteoarthritis: detection with MR imaging--the MOST study. Radiology, **256** (3): 855–862

Crosby, E.B. and Insall, J. (1976) Recurrent dislocation of the patella. The Journal of Bone and Joint Surgery, **58A** (1): 9–13

Cross, M., Smith, E., Hoy, D., et al. (2014) The global burden of hip and knee osteoarthritis: estimates from the global burden of disease 2010 study. Ann Rheum Dis, **73** (7): 1323–1330

Cushner, F.D., La Rosa, D.F., Vigorita, V.J., et al. (2003) A quantitative histologic comparison : ACL degeneration in the osteoarthritic knee. The Journal of Arthroplasty, **18** (6): 687–692

Dado, R.J., Katter, J.T. and Giesler Jr., G.J. (1994a) Spinothalamic and spinohypothalamic tract neurons in the cervical enlargement of rats. I. Locations of the antidromically identified axons in the thalamus and hypothalamus. Journal of Neurophysiology, **71** (3): 959–980

Dado, R.J., Katter, J.T. and Giesler Jr., G.J. (1994b) Spinothalamic and spinohypothalamic tract neurons in the cervical enlargement of rats. II. Responses to innocuous and noxious mechanical and thermal stimuli. Journal of Neurophysiology, **71** (3): 981–1002

Dallas, S.L., Prideaux, M. and Bonewald, L.F. (2013) The osteocyte: An endocrine cell . . . and more. Endocrine Reviews, **34** (5): 658–690

Dallel, R., Duale, C., Luccarini, P., et al. (1999) Stimulus-function, wind-up and modulation by diffuse noxious inhibitory controls of responses of convergent neurons of the spinal trigeminal nucleus oralis. European Journal of Neuroscience, **11** (1): 31–40

Danziger, N., Gautron, M., Le Bars, D., et al. (2001) Activation of diffuse noxious inhibitory controls (DNIC) in rats with an experimental peripheral mononeuropathy. Pain, **91** (3): 287–296

Danziger, N., Weil-Fugazza, J., Le Bars, D., et al. (1999) Alteration of descending modulation of nociception during the course of monoarthritis in the rat. The Journal of Neuroscience, **19** (6): 2394–2400

Davis, M.A., Ettinger, W.H., Neuhaus, J.M., et al. (1989) The association of knee injury and obesity with unilateral and bilateral osteoarthritis of the knee. American Journal of Epidemiology, **130** (2): 278–288

DeGroot, J., Verzijl, N., Bank, R.A., et al. (1999) Age-related decrease in proteoglycan synthesis of human articular chondrocytes: the role of nonenzymatic glycation. Arthritis and Rheumatism, **42** (5): 1003–9

Department of Health (2016) Reference Costs 2015-16. London: Department of Health

Dickenson, A.H., Le Bars, D. and Besson, J.-M. (1980) Diffuse noxious inhibitory controls (DNIC). Effects on trigeminal nucleus caudalis neurones in the rat. Brain Research, **200** (2): 293–305

Dickenson, A.H., Rivot, J.-P.P., Chaouch, A., et al. (1981) Diffuse noxious

inhibitory controls (DNIC) in the rat with or without pCPA pretreatment. Brain Research, **216** (2): 313–321

Dickhaus, H., Pauser, G. and Zimmermann, M. (1985) Tonic descending inhibition affects intensity coding of nociceptive responses of spinal dorsal horn neurones in the cat. Pain, **23** (2): 145–158

Dieppe, P.A. (2005) Relationship between symptoms and structural change in osteoarthritis: what are the important targets for therapy? The Journal of Rheumatology, **32** (6): 1147–1149

Dieppe, P.A. and Lohmander, L.S. (2005) Pathogenesis and management of pain in osteoarthritis. The Lancet, **365** (9463): 965–973

Ding, M. (2010) Microarchitectural adaptations in aging and osteoarthrotic subchondral bone issues. Acta Orthopaedica, **81** (SUPPL. 340): 1–53

Djouhri, L. and Lawson, S.N. (2004) Aβ-fiber nociceptive primary afferent neurons: A review of incidence and properties in relation to other afferent A-fiber neurons in mammals. Brain Research Reviews, **46** (2): 131–145

Dobson, K.L. and Harris, J. (2012) A detailed surgical method for mechanical decerebration of the rat. Experimental Physiology, **97** (6): 693–698

Dostrovsky, J.O. and Craig, A.D. (2013) "Ascending Projection Systems." In McMahon, S.B., Koltzenburg, M., Tracey, I., et al. (eds.) Wall and Melzack's Textbook of Pain. 6th ed. Philadelphia: Elsevier Saunders

Dougados, M., Ayral, X., Listrat, V., et al. (1994) The SFA system for assessing articular cartilage lesions at arthroscopy of the knee. Arthroscopy: The Journal

of Arthroscopic & Related Surgery, **10** (1): 69–77

Dunham, J., Hoedt-Schmidt, S. and Kalbhen, D.A. (1992) Structural and metabolic changes in articular cartilage induced by iodoacetate. International Journal of Experimental Pathology, **73** (4): 455–464

Dürr, H.R., Martin, H., Pellengahr, C., et al. (2004) The cause of subchondral bone cysts in osteoarthrosis: A finite element analysis. Acta Orthopaedica Scandinavica, **75** (5): 554–558

Edwards, C.L., Fillingim, R.B. and Keefe, F. (2001) Race, ethnicity and pain. Pain, **94** (2): 133–137

Edwards, R.R., Fillingim, R.B. and Ness, T.J. (2003) Age-related differences in endogenous pain modulation: A comparisom of diffuse noxious inhibitory controls in healthy older and younger adults. Pain, **101**: 155–165

Edwards, R.R., Grace, E., Peterson, S., et al. (2009) Sleep continuity and architecture: Assocations with pain-inhibitory processes in patients with temporomandibular joint disorder. European Journal of Pain, **13** (10): 1043–1047

Eleswarapu, S. V., Responte, D.J. and Athanasiou, K.A. (2011) Tensile properties, collagen content, and crosslinks in connective tissues of the immature knee joint. PLoS ONE, **6** (10): 1–7

Englund, M. (2009) The role of the meniscus in osteoarthritis genesis. Medical Clinics of North America, **93** (1): 37–43

Englund, M., Guermazi, A., Gale, D., et al. (2008) Incidental meniscal findings on

knee MRI in middle-aged and elderly persons. New England Journal of Medicine, **359** (11): 1108–1115

Englund, M., Guermazi, A. and Lohmander, S.L. (2009) The role of the meniscus in knee osteoarthritis: a cause or consequence ? Radiologic Clinics of North America, **47** (4): 703–712

Eriksen, E.F. (2010) Cellular mechanisms of bone remodeling. Reviews in Endocrine and Metabolic Disorders, **11**: 219–227

Eriksen, E.F. (2015) Treatment of bone marrow lesions (bone marrow edema). BoneKEy Reports, **4**: 1–6

Fairbank, T.J. (1948) Knee joint changes after meniscetomy. The Journal of Bone and Joint Surgery, **30** (4): 664–670

Fein, A. (2012) Nociceptors and the perception of pain. PhD Thesis: University of Connecticut Health Center, Connnecticut

De Felice, M., Sanoja, R., Wang, R., et al. (2011) Engagement of descending inhibition from the rostral ventromedial medulla protects against chronic neuropathic pain. Pain, **152** (12): 2701–9

Felson, D.T. (2005) The sources of pain in knee osteoarthritis. Current Opinion in Rheumatology, **17** (5): 624–628

Felson, D.T. (2006) Osteoarthritis of the Knee. New England Journal of Medicine, **354** (8): 841–848

Felson, D.T., Chaisson, C.E., Hill, C.L., et al. (2001) The association of bone marrow lesions with pain in knee osteoarthritis. Annals of Internal Medicine,

134 (7): 541–549

Ferland, C.E., Laverty, S., Beaudry, F., et al. (2011) Gait analysis and pain response of two rodent models of osteoarthritis. Pharmacology Biochemistry and Behavior, **97** (3): 603–610

Fernihough, J., Gentry, C., Malcangio, M., et al. (2004) Pain related behaviour in two models of osteoarthritis in the rat knee. Pain, **112** (1–2): 83–93

Ferreira-Gomes, J., Adães, S. and Castro-Lopes, J.M. (2008) Assessment of movement-evoked pain in osteoarthritis by the knee-bend and CatWalk tests: A clinically relevant study. Journal of Pain, **9** (10): 945–954

Fields, H.L. and Basbaum, A.I. (1978) Brainstem control of spinal pain-transmission neurons. Ann. Rev. Physiol, **40**: 217–48

Fife, R.S., Brandt, K.D., Braunstein, E.M., et al. (1991) Relationship between arthroscopic radiographic evidence of joint space of the knee. Arthritis & Rheumatism, **34** (4): 377–382

Finan, P.H., Buenaver, L.F., Bounds, S.C., et al. (2013) Discordance between pain and radiographic severity in knee osteoarthritis: findings from quantitative sensory testing of central sensitization. Arthritis and rheumatism, **65** (2): 1–16

Finnilä, M.A.J., Thevenot, J., Aho, O.M., et al. (2017) Association between subchondral bone structure and osteoarthritis histopathological grade. Journal of Orthopaedic Research, **35** (4): 785–792

Fitzgerald, M. (1982) The contralateral input to the dorsal horn of the spinal cord in the decerebrate spinal rat. Brain Research, **236** (2): 275–287

Fleischmann, A. and Urca, G. (1989) Clip-induced analgesia: Noxious neck pinch suppresses spinal and mesencephalic neural responses to noxious peripheral stimulation. Physiology & Behavior, **46** (2): 151–157

Fox, A.J.S., Bedi, A. and Rodeo, S.A. (2009) The basic science of articular cartilage: Structure, composition, and function. Sports Health, **1** (6): 461–468

Fox, A.J.S., Bedi, A. and Rodeo, S.A. (2012a) The basic science of human knee menisci: Structure, composition and function. Sports Health, **4** (4): 340–351

Fox, A.J.S., Wanivenhaus, F. and Rodeo, S.A. (2012b) The basic science of the patella: Structure, composition and function. The Journal of Knee Surgery, **25** (2): 127–141

Frank, C.B. (2004) Ligament structure, physiology and function. Journal of Musculoskeletal Neuronal Interactions, **4** (2): 199–201

Freehafer, A.A. (1962) A study of the function of the patella. Clinical Orthopaedics and Related Research, **25**: 162–170

Froimson, M.I., Ratcliffe, A., Gardner, T.R., et al. (1997) Differences in patellofemoral joint cartilage material properties and their significance to the etiology of cartilage surface fibrillation. Osteoarthritis and Cartilage, **5** (6): 377–386

Fruhstorfer, H., Gross, W. and Selbmann, O. (2001) von Frey hairs: new materials for a new design. European Journal of Pain, **5**: 341–342

Fukubayashi, T. and Kurosawa, H. (1980) The contact area and pressure distribution pattern of the knee: A study of normal and osteoarthrotic knee

joints. Acta Orthopaedica Scandinavica, **51** (1–6): 871–879

Gabriel, S.E., Jaakkimainen, L. and Bombardier, C. (1991) Risk for serious gastrointestinal complications related to use of nonsteroidal anti-inflammatory drugs. A meta-analysis. Annals of internal medicine, **115** (10): 787–796

Gaffen, J.D., Gleave, S.J., Crossman, M. V, et al. (1995) Articular cartilage proteoglycans in osteoarthritic STR/Ort mice. Osteoarthritis and Cartilage, **3** (2): 95–104

Gale, D.R., Chaisson, C.E., Totterman, S.M.S., et al. (1999) Meniscal subluxation: association with osteoarthritis and joint space narrowing. Osteoarthritis and Cartilage, **7**: 526–532

Gauriau, C. and Bernard, J.-F. (2002) Pain pathways and parabrachial circuits in the rat. Experimental Physiology, **87** (2): 251–258

Ge, H.Y., Madeleine, P. and Arendt-Nielsen, L. (2004) Sex differences in temporal characteristics of descending inhibitory control: an evaluation using repeated bilateral experimental induction of muscle pain. Pain, **110** (1–2): 72–78

Ge, H.Y., Madeleine, P. and Arendt-Nielsen, L. (2005) Gender differences in pain modulation evoked by repeated injections of glutamate into the human trapezius muscle. Pain, **113** (1–2): 134–140

Gehling, J., Mainka, T., Vollert, J., et al. (2016) Short-term test-retest-reliability of conditioned pain modulation using the cold-heat-pain method in healthy subjects and its correlation to parameters of standardized quantitative sensory

testing. BMC Neurology, **16** (1)

Gelber, A.C., Hochberg, M.C., Mead, L.A., et al. (2000) Joint injury in young adults and risk for subsequent knee and hip osteoarthritis. Annals of Internal Medicine, **133** (5): 321-328+I16

Gerhart, K.D., Yezierski, R.P., Giesler, G.J., et al. (1981) Inhibitory receptive fields of primate spinothalamic tract cells. Journal of neurophysiology, **46** (6): 1309–25

Gjerstad, J., Tjølsen, A., Svendsen, F., et al. (1999) Inhibition of evoked C-fibre responses in the dorsal horn after contralateral intramuscular injection of capsaicin involves activation of descending pathways. Pain, **80** (1): 413–418

Gjerstad, J., Tjølsen, A., Svendsen, F., et al. (2000) Inhibition of spinal nociceptive responses after intramuscular injection of capsaicin involves activation of noradrenergic and opioid systems. Brain Research, **859** (1): 132–136

Glasson, S.S., Askew, R., Sheppard, B., et al. (2005) Deletion of active ADAMTS5 prevents cartilage degradation in a murine model of osteoarthritis. Nature, **434**: 644–648

Glasson, S.S., Chambers, M.G., Van Den Berg, W.B., et al. (2010) The OARSI histopathology initiative – recommendations for histological assessments of osteoarthritis in the mouse. Osteoarthritis and Cartilage, **18**: S17–S23

Goldring, M.B. and Goldring, S.R. (2010) Articular cartilage and subchondral bone in the pathogenesis of osteoarthritis. Annals of the New York Academy of

Sciences, **1192**: 230–237

Goldring, M.B. and Marcu, K.B. (2009) Cartilage homeostasis in health and rheumatic diseases. Arthritis Research and Therapy, **11** (3): 224–240

Goldring, S.R. and Goldring, M.B. (2016) Changes in the osteochondral unit during osteoarthritis: structure, function and cartilage-bone crosstalk. Nature Reviews. Rheumatology, **12** (11): 632–644

Goldstein, D.S. (2010) Catecholamines 101. Clinical Autonomic Research, **20** (6): 331–352

Goodin, B.R., Kronfli, T., King, C.D., et al. (2013) Testing the relation between dispositional optimism and conditioned pain modulation: Does ethnicity matter? Journal of Behavioural Medicine, **36** (2): 165–174

Goodin, B.R., McGuire, L., Allshouse, M., et al. (2009) Associations between catastrophizing and endogenous pain-inhibitory processes: Sex Differences. Journal of Pain, **10** (2): 180–190

Granot, M., Weissman-Fogel, I., Crispel, Y., et al. (2008) Determinants of endogenous analgesia magnitude in a diffuse noxious inhibitory control (DNIC) paradigm: Do conditioning stimulus painfulness, gender and personality variables matter? Pain, **136** (1–2): 142–149

Granovsky, Y. (2013) Conditioned pain modulation: a predictor for development and treatment of neuropathic pain. Current Pain and Headache Reports, **17** (9): 361

Granovsky, Y., Miller-Barmak, A., Goldstein, O., et al. (2016) CPM test-retest

reliability: “standard” vs “single test-stimulus” protocols. Pain Medicine, **17** (3): 521–529

Grashorn, W., Sprenger, C., Forkmann, K., et al. (2013) Age-dependent decline of endogenous pain control: Exploring the effect of expectation and depression. PLoS ONE, **8** (9): 1–7

Graven-Nielsen, T., Wodehouse, T., Langford, R.M., et al. (2012) Normalization of widespread hyperesthesia and facilitated spatial summation of deep-tissue pain in knee osteoarthritis patients after knee replacement. Arthritis & Rheumatism, **64** (9): 2907–2916

Gregory, M.H., Capito, N., Kuroki, K., et al. (2012) A review of translational animal models for knee osteoarthritis. Arthritis, **2012**: 14

Greis, P.E., Bardana, D.D., Holmstrom, M.C., et al. (2002) Meniscal injury: I. Basic science and evaluation. The Journal of the American Academy of Orthopaedic Surgeons, **10** (3): 168–176

Grelsamer, R.P. and Weinstein, C.H. (2001) Applied biomechanics of the patella. Clinical Orthopaedics and Related Research, **389**: 9–14

Grönblad, M., Korkala, O., Liesi, P., et al. (1985) Innervation of synovial membrane and meniscus. Acta Orthopaedica Scandinavica, **56** (6): 484–6

Gruener, H., Zeilig, G., Laufer, Y., et al. (2016) Differential pain modulation properties in central neuropathic pain after spinal cord injury. PAIN, **157** (7): 1415–1424

Guerne, P.A., Blanco, F., Kaelin, A., et al. (1995) Growth factor responsiveness

of human articular chondrocytes in aging and development. Arthritis and Rheumatism, **38** (7): 960–968

Guilak, F., Ratcliffe, A., Lane, N., et al. (1994) Mechanical and biochemical changes in the superficial zone of articular cartilage in canine experimental osteoarthritis. Journal of Orthopaedic Research, **12** (4): 474–484

Guingamp, C., Gegout-Pottie, P., Philippe, L., et al. (1997) Mono-iodoacetate-induced experimental osteoarthritis. A dose-response study of loss of mobility, morphology, and biochemistry. Arthritis & Rheumatism, **40** (9): 1670–1679

Guzman, R.E., Evans, M.G., Bove, S.E., et al. (2003) Mono-iodoacetate-induced histologic changes in subchondral bone and articular cartilage of rat femorotibial joints: An animal model of osteoarthritis. Toxicologic Pathology, **31** (6): 619–624

Hadler, N.M., Gillings, D.B., Imbus, H.R., et al. (1978) Hand structure and function in an industrial setting. Arthritis & Rheumatism, **21** (2): 210–220

Haefeli, J., Kramer, J.L.K., Blum, J., et al. (2014) Heterotopic and homotopic nociceptive conditioning stimulation: Distinct effects of pain modulation. European Journal of Pain, **18** (8): 1112–1119

Hagbarth, K.E. (1960) Spinal withdrawal reflexes in the human lower limbs. Journal of neurology, neurosurgery, and psychiatry, **23** (3): 222

Hall, J.G., Duggan, A.W., Morton, C.R., et al. (1982) The location of brainstem neurones tonically inhibiting dorsal horn neurones of the cat. Brain Research, **244** (2): 215–222

Hame, S.L. and Alexander, R.A. (2013) Knee osteoarthritis in women. Current Reviews in Musculoskeletal Medicine, **6** (2): 182–187

Hanna, F.S., Teichtahl, A.J., Wluka, A.E., et al. (2009) Women have increased rates of cartilage loss and progression of cartilage defects at the knee than men: a gender study of adults without clinical knee osteoarthritis. Menopause (New York, N.Y.), **16** (4): 666–670

Hannan, M.T., Anderson, J.J., Zhang, Y., et al. (1993) Bone mineral density and knee osteoarthritis in elderly men and women. The Framingham Study. Arthritis & Rheumatism, **36** (12): 1671–80

Harper, A.A. and Lawson, S.N. (1985a) Conduction velocity is related to morphological cell type in rat dorsal root ganglion neurones. The Journal of Physiology, **359**: 31–46

Harper, A.A. and Lawson, S.N. (1985b) Electrical properties of rat dorsal root ganglion neurones with different peripheral nerve conduction velocities. The Journal of Physiology, **359**: 47–63

Harris, J. (2016) Involvement of spinal α2-adrenoceptors in prolonged modulation of hind limb withdrawal reflexes following acute noxious stimulation in the anaesthetized rabbit. European Journal of Neuroscience, **43** (6): 834–845

Harris, J. and Clarke, R.W. (2003) Organisation of sensitisation of hind limb withdrawal reflexes from acute noxious stimuli in the rabbit. Journal of Physiology, **546** (1): 251–265

Harrison, N.L. and Simmonds, M.A. (1984) Modulation of the GABA receptor complex by a steroid anaesthetic. Brain Research, **323** (2): 287–292

Harvey, V.L. and Dickenson, A.H. (2009) Behavioural and electrophysiological characterisation of experimentally induced osteoarthritis and neuropathy in C57Bl/6 mice. Molecular Pain, **5** (18): 1–11

Hasegawa, A., Otsuki, S., Pauli, C., et al. (2012) Anterior cruciate ligament changes in the human knee joint in aging and osteoarthritis. Arthritis & Rheumatism, **64** (3): 696–704

Hawker, G.A., Mian, S., Kendzerska, T., et al. (2011) Measures of adult pain: Visual Analog Scale for Pain (VAS Pain), Numeric Rating Scale for Pain (NRS Pain), McGill Pain Questionnaire (MPQ), Short-Form McGill Pain Questionnaire (SF-MPQ), Chronic Pain Grade Scale (CPGS), Short Form-36 Bodily Pain Scale (SF. Arthritis Care and Research, **63** (SUPPL. 11): 240–252

Hayami, T., Pickarski, M., Zhuo, Y., et al. (2006) Characterization of articular cartilage and subchondral bone changes in the rat anterior cruciate ligament transection and meniscectomized models of osteoarthritis. Bone, **38** (2): 234–243

Haywood, L., McWilliams, D.F., Pearson, C.I., et al. (2003) Inflammation and angiogenesis in osteoarthritis. Arthritis & Rheumatism, **48** (8): 2173–2177

Hehne, H.J. (1990) Biomechanics of the patellofemoral joint and its clinical relevance. Clinical Orthopaedics and Related Research, **258**: 73–85

Hensel, H. (1973) “Cutaneous thermoreceptors.” In Iggo, A. (ed.)

Somatosensory System. Springer Berlin Heidelberg. pp. 79–110

Hensel, H. and Boman, K.K.A. (1960) Afferent impulses in cutaneous sensory nerves in human subjects. Journal of Neurophysiology, **23** (5): 564–578

Herwig, J., Egner, E. and Buddecke, E. (1984) Chemical changes of human knee joint menisci in various stages of degeneration. Annals of the Rheumatic Diseases, **43**: 635–640

Hill, C.L., Hunter, D.J., Niu, J., et al. (2007) Synovitis detected on magnetic resonance imaging and its relation to pain and cartilage loss in knee osteoarthritis. Annals of the Rheumatic Diseases, **66** (12): 1599–1603

Hinman, R.S. and Crossley, K.M. (2007) Patellofemoral joint osteoarthritis: an important subgroup of knee osteoarthritis. Rheumatology, **46** (7): 1057–1062

Hopman, W.M., Harrison, M.B., Coo, H., et al. (2009) Associations between chronic disease, age and physical and mental health status. Chronic Diseases in Canada, **29** (3): 108–117

Huberti, H.H. and Hayes, W.C. (1984) Patellofemoral contact pressures. The influence of q-angle and tendofemoral contact. Journal of Bone and Joint Surgery American, **66** (5): 715–724

Hunt, J., Murrell, J., Knazovicky, D., et al. (2016) Alfaxalone anaesthesia facilitates electrophysiological recordings of nociceptive withdrawal reflexes in dogs (Canis familiaris) Sakakibara, M. (ed.). PLoS ONE, **11** (7): 1–18

Hunt, J.R., Goff, M., Jenkins, H., et al. (2018) Electrophysiological characterisation of central sensitisation in canine spontaneous osteoarthritis.

Pain, **159** (11): 2318–2330

Hunter, D.J., Guermazi, A., Roemer, F., et al. (2013) Structural correlates of pain in joints with osteoarthritis. Osteoarthritis and Cartilage, **21** (9): 1170–1178

Hunter, D.J., March, L. and Sambrook, P.N. (2003) The association of cartilage volume with knee pain. Osteoarthritis and Cartilage, **11**: 725–729

Hunter, D.J. and Spector, T.D. (2003) The role of bone metabolism in osteoarthritis. Current rheumatology reports, **5** (1): 15–9

Hunter, D.J., Zhang, Y.Q., Niu, J.B., et al. (2007) Patella malalignment, pain and patellofemoral progression: the Health ABC Study. Osteoarthritis and cartilage, **15** (10): 1120–1127

Hwang, H.S. and Kim, H.A. (2015) Chondrocyte apoptosis in the pathogenesis of osteoarthritis. International Journal of Molecular Sciences, **16**: 26035–26054

Ikeuchi, M., Izumi, M., Aso, K., et al. (2013) Clinical characteristics of pain originating from intra-articular structures of the knee joint in patients with medial knee osteoarthritis. SpringerPlus, **2** (628): 1–6

Imhof, H., Breitenseher, M., Kainberger, F., et al. (1999) Importance of subchondral bone to articular cartilage in health and disease. Topics in Magnetic Resonance Imaging, **10** (3): 180–192

Imhof, H., Sulzbacher, I., Grampp, S., et al. (2000) Subchondral bone and cartilage disease: A rediscovered functional unit. Investigative Radiology, **35** (10): 581–588

Intema, F., Hazewinkel, H.A.W., Gouwens, D., et al. (2010a) In early OA, thinning

of the subchondral plate is directly related to cartilage damage: Results from a canine ACLT-meniscectomy model. Osteoarthritis and Cartilage, **18**: 691–698

Intema, F., Sniekers, Y.H., Weinans, H., et al. (2010b) Similarities and discrepancies in subchondral bone structure in two differently induced canine models of osteoarthritis. Journal of Bone and Mineral Research, **25** (7): 1650–1657

Iwanaga, T., Shikichi, M., Kitamura, H., et al. (2000) Morphology and functional roles of synoviocytes in the joint. Archives of Histology and Cytology, **63** (1): 17–31

Jankowska, E. and Lundberg, A. (1981) Interneurones in the spinal cord. Trends in Neurosciences, **4**: 230–233

Janusz, M.J., Hookfin, E.B., Heitmeyer, S.A., et al. (2001) Moderation of iodoacetate-induced experimental osteoarthritis in rats by matrix metalloproteinase inhibitors. Osteoarthritis and Cartilage, **9** (8): 751–760

Jerosch, J., Prymka, M. and Castro, W.H.M. (1996) Proprioception of the knee joints with a lesion of the medial meniscus. Acta Orthopaedica Belgica, **62** (1): 41–45

Jimenez, P.A., Glasson, S.S., Trubetskoy, O. V, et al. (1997) Spontaneous osteoarthritis in Dunkin Hartley guinea pigs: histologic, radiologic, and biochemical changes. Laboratory Animal Science, **47** (6): 598–601

Jinks, S.L., Antognini, J.F. and Carstens, E. (2003a) Isoflurane depresses diffuse noxious inhibitory controls in rats between 0.8 and 1.2 minimum alveolar

anesthetic concentration. Anesthesia & Analgesia, **97**: 111–116

Jinks, S.L., Martin, J.T., Carstens, E., et al. (2003b) Peri-MAC depression of a nociceptive withdrawal reflex is accompanied by reduced dorsal horn activity with halothane but not isoflurane. Anesthesiology, **98** (5): 1128–1138

Johannesson, U., de Boussard, C.N., Brodda-Jansen, G., et al. (2007) Evidence of diffuse noxious inhibitory controls (DNIC) elicited by cold noxious stimulation in patients with provoked vestibulodynia. Pain, **130** (1): 31–39

Johnston, S.A. (1997) Osteoarthritis: Joint anatomy, physiology, and pathobiology. The Veterinary Clinics of North America. Small Animal Practice, **27** (4): 699–723

Jones, I. and Johnson, M.I. (2009) Transcutaneous electrical nerve stimulation. Continuing Education in Anaesthesia, Critical Care & Pain, **9** (4): 130–135

Jones, S.L. (1991) Descending noradrenergic influences on pain. Progress in Brain Research, **88**: 381–94

Jordan, K.M., Arden, N.K., Doherty, M., et al. (2003) EULAR Recommendations 2003: an evidence based approach to the management of knee osteoarthritis: Report of a Task Force of the Standing Committee for International Clinical Studies Including Therapeutic Trials (ESCISIT). Annals of the Rheumatic Diseases, **62** (12): 1145–1155

Julien, N., Goffaux, P., Arsenault, P., et al. (2005) Widespread pain in fibromyalgia is related to a deficit of endogenous pain inhibition. Pain, **114**: 295–302

Julius, D. and Basbaum, A.I. (2001) Molecular mechanisms of nociception. Nature, **413** (6852): 203–210

Kakigi, R. (1994) Diffuse noxious inhibitory control. Reappraisal by pain-related somatosensory evoked potentials following CO2 laser stimulation. Journal of the Neurological Sciences, **125** (2): 198–205

Kalliomäki, J., Schouenborg, J. and Dickenson, A.H. (1992) Differential effects of a distant noxious stimulus on hindlimb nociceptive withdrawal reflexes in the rat. European Journal of Neuroscience, **4** (7): 648–652

Kandel, E.R., Schwartz, J.H., Jessell, T.M., et al. (2013) Principles of Neural Science. 5th ed. New York: McGraw Hill Medical

Karahan, M., Kocaoglu, B., Cabukoglu, C., et al. (2010) Effect of partial medial meniscectomy on the proprioceptive function of the knee. Archives of Orthopaedic and Trauma Surgery, **130** (3): 427–431

Katsuragawa, Y., Saitoh, K., Tanaka, N., et al. (2010) Changes of human menisci in osteoarthritic knee joints. Osteoarthritis and Cartilage, **18** (9): 1133–1143

Kearns, K., Dee, A., Fitzgerald, A.P., et al. (2014) Chronic disease burden associated with overweight and obesity in Ireland: the effects of a small BMI reduction at population level. BMC Public Health, **14** (1): 143

Kelly, S., Chapman, R.J., Woodhams, S., et al. (2013a) Increased function of pronociceptive TRPV1 at the level of the joint in a rat model of osteoarthritis pain. Annals of the Rheumatic Diseases, **71** (1): 252–259

Kelly, S., Dobson, K.L. and Harris, J. (2013b) Spinal nociceptive reflexes are

sensitized in the monosodium iodoacetate model of osteoarthritis pain in the rat. Osteoarthritis and Cartilage, **21** (9): 1327–1335

Kelly, S., Dunham, J.P., Murray, F., et al. (2012) Spontaneous firing in C-fibers and increased mechanical sensitivity in A-fibers of knee joint-associated mechanoreceptive primary afferent neurones during MIA-induced osteoarthritis in the rat. Osteoarthritis and Cartilage, **20** (4): 305–313

Kempson, G.E. (1982) Relationship between the Tensile Properties of Articular-Cartilage from the Human Knee and Age. Annals of the Rheumatic Diseases, **41**: 508–511

Kennedy, D.L., Kemp, H.I., Ridout, D., et al. (2016) Reliability of conditioned pain modulation. Pain, **157** (11): 2410–2419

Key, J.A. (1928) Cytology of the synovial fluid of normal joints. The Anatomical Record, **40** (2): 193–211

King, C.D.T., Sibille, K., Goodin, B.R., et al. (2013) Experimental pain sensitivity differs as a function of clinical pain severity in symptomatic knee osteoarthritis. Osteoarthritis and Cartilage, **21** (9): 1243–52

Klyne, D.M., Schmid, A.B., Moseley, G.L., et al. (2015) Effect of types and anatomic arrangement of painful stimuli on conditioned pain modulation. Journal of Pain, **16** (2): 176–185

Knotek, Z., Hrdá, A., Knotková, Z., et al. (2013) Alfaxalone anaesthesia in the green iguana (Iguana iguana). Acta Veterinaria Brno, **82** (1): 109–114

Kolstad, K., Sahlstedt, B. and Wigren, A. (1980) Extension deficit and lateral

instability in degenerative disease of the knee. Acta Orthopaedica Scandinavica, **51** (1–6): 667–672

Konecka, A.M. and Sroczynska, I. (1998) Circadian rhythm of pain in male mice. General Pharmacology, **31** (5): 809–810

Kornaat, P.R., Bloem, J.L., Ceulemans, R.Y.T., et al. (2006) Osteoarthritis of the knee: association between clinical features and MR Imaging findings. Radiology, **239** (3): 811–817

Kosek, E. and Hansson, P. (1997) Modulatory influence on somatosensory perception from vibration and heterotopic noxious conditioning stimulation (HNCS) in fibromyalgia patients and healthy subjects. Pain, **70**: 41–51

Kosek, E. and Ordeberg, G. (2000) Lack of pressure pain modulation by heterotopic noxious conditioning stimulation in patients with painful osteoarthritis before, but not following, surgical pain relief. Pain, **88**: 69–78

Kothari, A., Guermazi, A., Chmiel, J.S., et al. (2010) The within-subregion relationship between bone marrow lesions and subsequent cartilage loss in knee osteoarthritis. Arthritis Care & Research, **62** (2): 198–203

van der Kraan, P.M. and van den Berg, W.B. (2007) Osteophytes: relevance and biology. Osteoarthritis and Cartilage, **15**: 237–244

van der Kraan, P.M., Vitters, E.L., van de Putte, L.B., et al. (1989) Development of osteoarthritic lesions in mice by “metabolic” and “mechanical” alterations in the knee joints. The American Journal of Pathology, **135** (6): 1001–14

Kuhtz-Buschbeck, J.P., Andresen, W., Göbel, S., et al. (2010) Thermoreception

and nociception of the skin: a classic paper of Bessou and Perl and analyses of thermal sensitivity during a student laboratory exercise. Advances in physiology education, **34**: 25–34

Kwak, S.D., Colman, W.W., Ateshian, G.A., et al. (1997) Anatomy of the human patellofemoral joint articular cartilage: surface curvature analysis. Journal of Orthopaedic Research, **15** (3): 468–472

Labek, G., Thaler, M., Janda, W., et al. (2011) Revision rates after total joint replacement. J Bone Joint Surg [Br], **93** (3): 293–7

Lajeunesse, D. (2004) The role of bone in the treatment of osteoarthritis. Osteoarthritis and Cartilage, **12**: 34–38

Lambert, J.J., Belelli, D., Peden, D.R., et al. (2003) Neurosteroid modulation of GABA A receptors. Progress in Neurobiology, **71** (1): 67–80

Landau, R., Kraft, J.C., Flint, L.Y., et al. (2010) An experimental paradigm for the prediction of Post-Operative Pain (PPOP). J. Vis. Exp, (35): 1671

Landells, J. (1953) The bone cyst of osteoarthritis. The Journal of Bone and Joint Surgery, **35 B** (4): 643–649

Lapirot, O., Chebbi, R., Monconduit, L., et al. (2009) NK1 receptor-expressing spinoparabrachial neurons trigger diffuse noxious inhibitory controls through lateral parabrachial activation in the male rat. Pain, **142** (3): 245–254

Larivière, M., Goffaux, P., Marchand, S., et al. (2007) Changes in pain perception and descending inhibitory controls start at middle age in healthy adults. The Clinical Journal of Pain, **23** (6): 506–510

Lascelles, B.D.X. and Main, D.C. (2002) Surgical trauma and chronically painful conditions--within our comfort level but beyond theirs? Journal of the Amercian Veterinary Association, **221** (2): 1–5

Latremoliere, A. and Woolf, C.J. (2009) Central Sensitization: A Generator of Pain Hypersensitivity by Central Neural Plasticity. The Journal of Pain, **10** (9): 895–926

Lautenbacher, S., Kundermann, B. and Krieg, J.-C. (2006) Sleep deprivation and pain perception. Sleep Medicine Reviews, **10** (5): 357–369

Lautenbacher, S. and Rollman, G.B. (1997) Possible deficiencies of pain modulation in fibromyalgia. The Clinical Journal of Pain, **13** (3): 189–196

Lawrence, R.C., Felson, D.T., Helmick, C.G., et al. (2008) Estimates of the prevalence of arthritis and other rheumatic conditions in the United States. Part II. Arthritis and rheumatism, **58** (1): 26–35

Lawson, S.N. (2002) Phenotype and function of somatic primary afferent nociceptive neurones with C-, Aδ- or Aα/β-fibres. Experimental physiology, **87** (2): 239–244

Lawson, S.N. (2005) "The Peripheral Sensory Nervous System: Dorsal Root Ganglion Neurons." In Dyck, P.J. and Thomas, P.K. (eds.) Peripheral Neuropathy. 4th ed. Philadelphia: W.B. Saunders. pp. 163–202

Leach, D.H., Caldwell, S.J. and Ferguson, J.G. (1988) Ultrastructural study of synovial membrane from the antebrachiocarpal joint of calves. Acta Anatomica, **133**: 234–246

Leffler, A.-S., Kosek, E., Lerndal, T., et al. (2002a) Somatosensory perception and function of diffuse noxious inhibitory controls (DNIC) in patients suffering from long-term trapezius myalgia. European Journal of Pain, **6** (2): 149–159

Leffler, A.-S., Kosek, E., Lerndal, T., et al. (2002b) Somatosensory perception and function of diffuse noxious inhibitory controls (DNIC) in patients suffering from rheumatoid arthritis. European Journal of Pain, **6** (2): 161–176

Lerner, D., Reed, J.I., Massarotti, E., et al. (2002) The Work Limitations Questionnaire's validity and reliability among patients with osteoarthritis. Journal of Clinical Epidemiology, **55** (2): 197–208

Levine, J.D., Fields, H.L. and Basbaum, A.I. (1993) Peptides and the primary afferent nociceptor. The Journal of Neuroscience, **13** (6): 2273–2286

Levy, I.M., Torzilli, P.A. and Warren, R.F. (1982) The effect of medial meniscectomy on anterior-posterior motion of the knee. The Journal of Bone and Joint Surgery. American Volume, **64** (6): 883–888

Li, B. and Aspden, R.M. (1997) Composition and mechanical properties of cancellous bone from the femoral head of patients with osteoporosis or osteoarthritis. Journal of Bone and Mineral Research, **12** (4): 641–51

Li, G., Yin, J., Gao, J., et al. (2013) Subchondral bone in osteoarthritis: insight into risk factors and microstructural changes. Arthritis Research & Therapy, **15** (223): 1–12

Lin, E.H.B., Katon, W., Williams, J.W., et al. (2003) Effect of improving depression care on pain and functional outcomes. JAMA : the Journal of the

American Medical Association, **290** (18): 2428–2434

Litwic, A., Edwards, M.H., Dennison, E.M., et al. (2013) Epidemiology and burden of osteoarthritis. British medical bulletin, **105**: 185–99

Lockwood, S.M., Bannister, K. and Dickenson, A.H. (2019a) An investigation into the noradrenergic and serotonergic contributions of diffuse noxious inhibitory controls in a monoiodoacetate model of osteoarthritis. Journal of Neurophysiology, **121** (1): 96–104

Lockwood, S.M., Lopes, D.M., McMahon, S.B., et al. (2019b) Characterisation of peripheral and central components of the rat monoiodoacetate model of Osteoarthritis. Osteoarthritis and Cartilage, **27** (4): 712–722

Loeser, J.D. and Treede, R.-D. (2008) The Kyoto protocol of IASP basic pain terminology. Pain, **137** (3): 473–477

Loeser, R.F., Goldring, S.R., Scanzello, C.R., et al. (2012) Osteoarthritis: A disease of the joint as an organ. Arthritis & Rheumatism, **64** (6): 1697–1707

Longstaff, A. (2000) Neuroscience. 3rd ed. New York: BIOS Scientific

Lyons, T.J., McClure, S.F., Stoddart, R.W., et al. (2006) The normal human chondro-osseous junctional region: Evidence for contact of uncalcified cartilage with subchondral bone and marrow spaces. BMC Musculoskeletal Disorders, **7** (52): 1–8

MacConaill, M.A. (1932) The function of intra-articular fibrocartilages, with special reference to the knee and inferior radio-ulnar joints. Journal of Anatomy, **6**: 210–227

Maixner, W., Fillingim, R., Booker, D., et al. (1995) Sensitivity of patients with painful temporomandibular disorders to experimentally evoked pain. Pain, **63**: 341–351

Makris, E.A., Hadidi, P. and Athanasiou, K.A. (2011) The knee meniscus: Structure-function, pathophysiology, current repair techniques, and prospects for regeneration. Biomaterials, **32** (30): 7411–7431

Malfait, A.-M. and Schnitzer, T.J. (2013) Towards a mechanism-based approach to pain management in osteoarthritis. Nature Reviews. Rheumatology, **9** (11): 654–664

Malmberg, A.B. and Yaksh, T.L. (1994) Voltage-sensitive calcium channels in spinal nociceptive processing: blockade of N- and P-type channels inhibits formalin-induced nociception. The Journal of Neuroscience, **14** (8): 4882–90

Mapp, P.I. (1995) Innervation of the synovium. Annals of the Rheumatic Diseases, **54** (5): 398–403

Mapp, P.I., Avery, P.S., McWilliams, D.F., et al. (2008) Angiogenesis in two animal models of osteoarthritis. Osteoarthritis and Cartilage, **16** (1): 61–69

Mapp, P.I. and Revell, P.A. (1985) Fibronectin production by synovial intimal cells. Rheumatology International, **5** (5): 229–237

Mapp, P.I., Sagar, D.R., Ashraf, S., et al. (2013) Differences in structural and pain phenotypes in the sodium monoiodoacetate and meniscal transection models of osteoarthritis. Osteoarthritis and Cartilage, **21** (9): 1336–1345

March, L.M. and Bachmeier, C.J.M. (1997) Economics of osteoarthritis: A global

perspective. Bailliere's Clinical Rheumatology, **11** (4): 817–834

Markolf, K.L., Mensch, J.S. and Amstutz, H.C. (1976) Stiffness and laxity of the knee: The contributions of supporting structures. The Journal of Bone and Joint Surgery, **58A** (5): 583–594

Martin, J.A. and Buckwalter, J.A. (2002) Aging, articular cartilage chondrocyte senscence and osteoarthritis. Biogerontology, **3**: 257–264

Mason, R.M., Chambers, M.G., Flannelly, J., et al. (2001) The STR/ort mouse and its use as a model of osteoarthritis. Osteoarthritis and Cartilage, **9**: 85–91

Matos, F.F., Rollema, H., Brown, J.L., et al. (1992) Do opioids evoke the release of serotonin in the spinal cord? An in vivo microdialysis study of the regulation of extracellular serotonin in the rat. Pain, **48** (3): 439–447

Matsubara, T., Spycher, M.A., Rüttner, J.R., et al. (1983) The ultrastructural localization of fibronectin in the lining layer of rheumatoid arthritis synovium: the synthesis of fibronectin by type B lining cells. Rheumatology International, **3** (2): 75–79

Mazzuca, S.A., Brandt, K.D., Katz, B.P., et al. (2006) Risk factors for progression of tibiofemoral osteoarthritis: an analysis based on fluoroscopically standardised knee radiography. Annals of the Rheumatic Diseases, **65** (4): 515–519

Mcdougall, J.J., Andruski, B., Schuelert, N., et al. (2009) Unravelling the relationship between age, nociception and joint destruction in naturally occurring osteoarthritis of Dunkin Hartley guinea pigs. Pain, **141**: 222–232

McDougall, J.J., Bray, R.C. and Sharkey, K.A. (1997) Morphological and immunohistochemical examination of nerves in normal and injured collateral ligaments of rat, rabbit, and human knee joints. Anatomical Record, **248** (1): 29–39

McDougall, J.J. and Linton, P. (2012) Neurophysiology of arthritis pain. Current Pain and Headache Reports, **16** (6): 485–491

McGaraughty, S. and Henry, J.L. (1997) Effects of noxious hindpaw immersion on evoked and spontaneous firing of contralateral convergent dorsal horn neurons in both intact and spinalized rats. Brain Research Bulletin, **43** (3): 263–267

McGlashan, S.R., Cluett, E.C., Jensen, C.G., et al. (2008) Primary cilia in osteoarthritic chondrocytes: From chondrons to clusters. Developmental Dynamics, **237**: 2013–2020

McGlone, F. and Reilly, D. (2010) The cutaneous sensory system. Neuroscience & Biobehavioral Reviews, **34** (2): 148–159

Meachim, G., Bentley, G. and Baker, R. (1977) Effect of age on thickness of adult patellar articular cartilage. Annals of the Rheumatic Diseases, **36**: 563–568

Meerding, W.J., IJzelenberg, W., Koopmanschap, M.A., et al. (2005) Health problems lead to considerable productivity loss at work among workers with high physical load jobs. Journal of Clinical Epidemiology, **58** (5): 517–523

Megirian, D. (1962) Bilateral facilitatory and inhibitory skin areas of spinal motorneurones of cat. Journal of Neurophysiology, **25** (1): 127–137

Melzack, R. (1975) The McGill Pain Questionnaire: Major properties and scoring methods. Pain, **1** (3): 277–299

Mendez, K.T. (2017) Knee & Shoulder Center [online]. Available from: http://mendezortho.com/specialties-and-procedures/hip-knee-arthritis.php [Accessed 10 August 2017]

Merchant, A.C., Arendt, E.A., Dye, S.F., et al. (2008) The female knee: Anatomic variations and the female-specific total knee design. Clinical Orthopaedics and Related Research, **466** (12): 3059–3065

Messner, K. and Gao, J. (1998) The menisci of the knee joint. Anatomical and functional characteristics, and a rationale for clinical treatment. Journal of Anatomy, **193**: 161–178

Michou, J.N., Leece, E.A. and Brearley, J.C. (2012) Comparison of pain on injection during induction of anaesthesia with alfaxalone and two formulations of propofol in dogs. Veterinary Anaesthesia and Analgesia, **39** (3): 275–281

Milgram, J.W. (1983) Morphologic alterations of the subchondral bone in advanced degenerative arthritis. Clinical Orthopaedics and Related Research, **173**: 293–312

Millan, M.J. (1999) The induction of pain: an integrative review. Progress in Neurobiology, **57** (1): 1–164

Millan, M.J. (2002) Descending control of pain. Progress in Neurobiology, **66** (6): 355–474

Mine, T., Kimura, M., Sakka, A., et al. (2000) Innervation of nociceptors in the

menisci of the knee joint: an immunohistochemical study. Archives of Orthopaedic and Trauma Surgery, **120** (3–4): 201–204

Moilanen, L.J., Hämäläinen, M., Nummenmaa, E., et al. (2015) Monosodium iodoacetate-induced inflammation and joint pain are reduced in TRPA1 deficient mice - potential role of TRPA1 in osteoarthritis. Osteoarthritis and Cartilage, **23** (11): 2017–2026

Molander, C. and Grant, G. (1986) Laminar distribution and somatotopic organization of primary afferent fibers from hindlimb nerves in the dorsal horn. A study by transganglionic transport of horseradish peroxidase in the rat. Neuroscience, **19** (1): 297–312

Molander, C., Xu, Q. and Grant, G. (1984) Cytoarchitectonic organization of the spinal cord in the rat: I. The lower thoracic and lumbosacral cord. Journal of Comparative Neurology, **230** (1): 133–141

Molander, C., Xu, Q., Rivero-Melian, C., et al. (1989) Cytoarchitectonic organization of the spinal cord in the rat: II. The cervical and upper thoracic cord. Journal of Comparative Neurology, **289** (3): 375–385

Morgan, M.M., Heinricher, M.M. and Fields, H.L. (1994) Inhibition and facilitation of different nocifensor reflexes by spatially remote noxious stimuli. Journal of Neurophysiology, **72** (3): 1152–1160

Morin, F., Schwartz, H.G. and O'Leary, J.L. (1951) Experimental study of the spinothalamic and related tracts. Acta Psychiatr Neurol Scand, **26** (3–4): 371–96

Morton, C.R., Du, H.J., Xiao, H.M., et al. (1988) Inhibition of nociceptive responses of lumbar dorsal horn neurones by remote noxious afferent stimulation in the cat. Pain, **34** (1): 75–83

Morton, C.R., Maisch, B. and Zimmermann, M. (1987) Diffuse noxious inhibitory controls of lumbar spinal neurons involve a supraspinal loop in the cat. Brain Research, **410** (2): 347–352

Mullaji, A.B., Marawar, S. V, Simha, M., et al. (2008) Cruciate ligaments in arthritic knees: a histologic study with radiologic correlation. The Journal of Arthroplasty, **23** (4): 567–572

Muraki, S., Akune, T., Oka, H., et al. (2009) Association of occupational activity with radiographic knee osteoarthritis and lumbar spondylosis in elderly patients of population-based cohorts: A large-scale population-based study. Arthritis Care and Research, **61** (6): 779–786

Murray, C.J.L., Richards, M.A., Newton, J.N., et al. (2013) UK health performance: Findings of the Global Burden of Disease Study 2010. The Lancet, **381** (9871): 997–1020

Mylius, V., Engau, I., Teepker, M., et al. (2009) Pain sensitivity and descending inhibition of pain in Parkinson's disease. Journal of Neurology, Neurosurgery & Psychiatry, **80** (1): 24–28

Nahman-Averbucha, H., Yarnitsky, D., Granovsky, Y., et al. (2013) The role of stimulation parameters on the conditioned pain modulation response. Scandinavian Journal of Pain, **4** (1): 10–14

National Center for Biotechnology Information (2019) PubChem Compound Database. Capsaicin, CID=1548943 [online]. Available from: https://pubchem.ncbi.nlm.nih.gov/compound/Capsaicin [Accessed 10 January 2019]

National Joint Registry (2016) National Joint Registry 13th Annual report. Hertfordshire: National Joint Registry

Naugle, K.M. and Riley, J.L. (2014) Self-reported physical activity predicts pain inhibitory and facilitatory function. Medicine and Science in Sports and Exercise, **46** (3): 622–629

Neogi, T., Felson, D., Niu, J., et al. (2009) Cartilage loss occurs in the same subregions as subchondral bone attrition: A within-knee subregions-matched approch from the Multicenter Osteoarthritis Study. Arthritis & Rheumatism, **61** (11): 1539–1544

Neogi, T. and Felson, D.T. (2013) "Osteoarthritis and Rheumatoid Arthritis." In McMahon, S.B., Koltzenburg, M., Tracey, I., et al. (eds.) Wall and Melzack's Textbook of Pain. 6th ed. Philadelphia: Elsevier Saunders. pp. 645–657

Neogi, T., Nevitt, M., Niu, J., et al. (2010) Subchondral bone attrition may be a reflection of compartment-specific mechanical load: The MOST Study. Annals of the Rheumatic Diseases, **69**: 841–844

Neugebauer, V., Rümenapp, P. and Schaible, H.-G. (1996) Calcitonin gene-related peptide is involved in the spinal processing of mechanosensory input from the rat's knee joint and in the generation and maintenance of

hyperexcitability of dorsal horn neurons during development of acute inflammation. Neuroscience, **71** (4): 1095–1109

Nevitt, M.C., Cummings, S.R., Lane, N.E., et al. (1996) Association of estrogen replacement therapy with the risk of osteoarthritis of the hip in elderly white women. Archives of Internal Medicine, **156** (18): 2073–2080

NHS Digital (2017) Prescription Cost Analysis Data 2016

Niissalo, S., Hukkanen, M., Imai, S., et al. (2002) Neuropeptides in experimental and degenerative arthritis. Annals of the New York Academy of Sciences, **966**: 384–99

Nir, R.R. and Yarnitsky, D. (2015) Conditioned pain modulation. Current Opinion in Supportive and Palliative Care, **9** (2): 131–137

Noble, J. and Hamblen, D.L. (1975) The pathology of the degenerate meniscus lesion. The Journal of Bone and Joint Surgery. British Volume, **57B**: 180–186

North, R.A. (2004) P2X3 receptors and peripheral pain mechanisms. Journal of Physiology, **554** (2): 301–308

Nwosu, L.N., Mapp, P.I., Chapman, V., et al. (2016a) Blocking the tropomyosin receptor kinase A (TrkA) receptor inhibits pain behaviour in two rat models of osteoarthritis. Annals of the rheumatic diseases, **75** (6): 1246–54

Nwosu, L.N., Mapp, P.I., Chapman, V., et al. (2016b) Relationship between structural pathology and pain behaviour in a model of osteoarthritis (OA). Osteoarthritis and Cartilage, **24** (11): 1910–1917

O'Connell, J.X. (2000) Pathology of the synovium. American Journal of Clinical

Pathology, **114**: 773–784

Ogbonna, A.C., Clark, A.K., Gentry, C., et al. (2013) Pain-like behaviour and spinal changes in the monosodium iodoacetate model of osteoarthritis in C57Bl/6 mice. European Journal of Pain, **17**: 514–526

Øiestad, B.E., Engebretsen, L., Storheim, K., et al. (2009) Knee osteoarthritis after anterior cruciate ligament injury: a systematic review. The American journal of sports medicine, **37** (7): 1434–43

Okada-Ogawa, A., Porreca, F. and Meng, I.D. (2009) Sustained morphine-induced sensitization and loss of diffuse noxious inhibitory controls in dura-sensitive medullary dorsal horn neurons. The Journal of neuroscience : the official journal of the Society for Neuroscience, **29** (50): 15828–35

Oliveria, S.A., Felson, D.T., Reed, J.I., et al. (1995) Incidence of symptomatic hand, hip, and knee osteoarthritis among patients in a health maintenance organization. Arthritis and rheumatism, **38** (8): 1134–1141

Osiri, M., Welch, V., Brosseau, L., et al. (2009) Transcutaneous electrical nerve stimulation for knee osteoarthritis. Cochrane Database of Systematic Reviews, **4**

Ossipov, M.H., Morimura, K. and Porreca, F. (2014) Descending pain modulation and chronification of pain. Current Opinion in Supportive and Palliative Care, **8** (2): 143–51

Palazzo, C., Nguyen, C., Lefevre-Colau, M.M., et al. (2016) Risk factors and burden of osteoarthritis. Annals of Physical and Rehabilitation Medicine, **59** (3):

134–138

Parsons, S., Ingram, M., Clarke-Cornwell, A.M., et al. (2011) A Heavy Burden: the occurrence and impact of musculoskeletal conditions in the United Kingdom today. Manchester

Patel, R. and Dickenson, A.H. (2019) A study of cortical and brainstem mechanisms of diffuse noxious inhibitory controls in anaesthetised normal and neuropathic rats. European Journal of Neuroscience, (October)

Pauli, C., Grogan, S.P., Patil, S., et al. (2011) Macroscopic and histopathologic analysis of human knee menisci in aging and osteoarthritis. Osteoarthritis and Cartilage, **19** (9): 1132–1141

Pearle, A.D., Scanzello, C.R., George, S., et al. (2007) Elevated high-sensitivity C-reactive protein levels are associated with local inflammatory findings in patients with osteoarthritis. Osteoarthritis and Cartilage, **15**: 516–523

Penninx, B.W.J.H., Beekman, A.T.F., Ormel, J., et al. (1996) Psychological status among elderly people with chronic diseases: Does type of disease play a part? Journal of Psychosomatic Research, **40** (5): 521–534

Pertovaara, A. (2006) Noradrenergic pain modulation. Progress in Neurobiology, **80** (2): 53–83

Pertovaara, A. (2013) The noradrenergic pain regulation system: A potential target for pain therapy. European Journal of Pharmacology, **716** (1–3): 2–7

Pertovaara, A., Kontinen, V.K. and Kalso, E.A. (1997) Chronic spinal nerve ligation induces changes in response characteristics of nociceptive spinal dorsal

horn neurons and in their descending regulation originating in the periaqueductal gray in the rat. Experimental Neurology, **147** (2): 428–436

Peters, M.L., Schmidt, A.J.M., Van den Hout, M.A., et al. (1992) Chronic back pain, acute postoperative pain and the activation of diffuse noxious inhibitory controls (DNIC). Pain, **50** (2): 177–187

Pielsticker, A., Haag, G., Zaudig, M., et al. (2005) Impairment of pain inhibition in chronic tension-type headache. Pain, **118** (1–2): 215–223

Pomonis, J.D., Boulet, J.M., Gottshall, S.L., et al. (2005) Development and pharmacological characterization of a rat model of osteoarthritis pain. Pain, **114** (3): 339–346

Poole, R., Blake, S., Buschmann, M., et al. (2010) Recommendations for the use of preclinical models in the study and treatment of osteoarthritis. Osteoarthritis and Cartilage, **18**: S10–S16

Pottenger, L.A., Phillips, F.M. and Draganich, L.F. (1990) The effect of marginal osteophytes on reduction of varus-valgus instability in osteoarthritic knees. Arthritis & Rheumatism, **33** (6): 853–858

Pritzker, K.P.H., Gay, S., Jimenez, S.A., et al. (2006) Osteoarthritis cartilage histopathology: Grading and staging. Osteoarthritis and Cartilage, **14**: 13–29

Pud, D., Granovsky, Y. and Yarnitsky, D. (2009) The methodology of experimentally induced diffuse noxious inhibitory control (DNIC)-like effect in humans. Pain, **144** (1–2): 16–19

Pud, D., Sprecher, E. and Yarnitsky, D. (2005) Homotopic and heterotopic

effects of endogenous analgesia in healthy volunteers. Neuroscience Letters, **380** (3): 209–213

Quante, M., Hille, S., Schofer, M.D., et al. (2008) Noxious counterirritation in patients with advanced osteoarthritis of the knee reduces MCC but not SII pain generators: A combined use of MEG and EEG

Ralphs, J.R. and Benjamin, M. (1994) The joint capsule: structure, composition, ageing and disease. Journal of Anatomy, **184** (3): 503–509

Reichenbach, S., Guermazi, A., Niu, J., et al. (2008) Prevalence of bone attrition on knee radiographs and MRI in a community-based cohort. Osteoarthritis and Cartilage, **16** (9): 1005–1010

Reider, B., Arcand, M.A., Diehl, L.H., et al. (2003) Proprioception of the knee before and after anterior cruciate ligament reconstruction. Arthroscopy - Journal of Arthroscopic and Related Surgery, **19** (1): 2–12

Rexed, B. (1952) The cytoarchitectonic organization of the spinal cord in the cat. Journal of Comparative Neurology, **96** (3): 415–495

Richmond, R.S., Carlson, C.S., Register, T.C., et al. (2000) Functional estrogen receptors in adult articular cartilage: estrogen replacement therapy increases chondrocyte synthesis of proteoglycans and insulin-like growth factor binding protein 2. Arthritis and rheumatism, **43** (9): 2081–2090

Riley, J.L., Cruz-Almeida, Y., Glover, T.L., et al. (2014) Age and race effects on pain sensitivity and modulation among middle-aged and older adults. Journal of Pain, **15** (3): 272–282

Riley, J.L., King, C.D., Wong, F., et al. (2010) Lack of endogenous modulation but enhanced decay of prolonged heat pain in older adults. Pain, **150** (1): 153–160

Ringkamp, M., Raja, S.N., Campbell, J.N., et al. (2013) "Peripheral Mechanisms of Cutaneous Nociception." In McMahon, S.B., Koltzenburg, M., Tracey, I., et al. (eds.) Wall and Melzack's Textbook of Pain. 6th ed. Philadelphia: Elsevier Saunders. pp. 1–30

Rivot, J.P., Chaouch, A. and Besson, J.-M. (1979) The influence of naloxone on the C fiber response of dorsal horn neurons and their inhibitory control by raphe magus stimulation. Brain Research, **176**: 355–364

Rivot, J.P., Chaouch, A. and Besson, J.-M. (1980) Nucleus raphe magnus modulation of response of rat dorsal horn neurons to unmyelinated fiber inputs: Partial involvement of serotonergic pathways. Journal of Neurophysiology, **44** (6): 1039–1057

Roberts, S., Weightman, B., Urban, J., et al. (1986) Mechanical and biochemical properties of human articular cartilage in osteoarthritic femoral heads and in autopsy specimens. Journal of Bone & Joint Surgery, **68**-**B** (2): 278–288

Roby-Brami, A., Bussel, B., Willer, J.C., et al. (1987) An electrophysiological investigation into the pain-relieving effects of heterotopic nociceptive stimuli: Probable involvement of a supraspinal loop. Brain, **110** (6): 1497–1508

Roemer, F.W., Guermazi, A., Felson, D.T., et al. (2011) Presence of MRI-detected joint effusion and synovitis increases the risk of cartilage loss in knees without osteoarthritis at 30-month follow-up: the MOST study: a longitudinal

Multicenter Study of Knee Osteoarthritis. Annals of the Rheumatic Diseases2, **70** (10): 1804–1809

Roemer, F.W., Javaid, M.K., Guermazi, A., et al. (2010) Anatomical distribution of synovitis in knee osteoarthritis and its association with joint effusion assessed on non-enhanced and contrast-enhanced MRI. Osteoarthritis and Cartilage, **18** (10): 1269–1274

Roemer, F.W., Lynch, J.A., Crema, M.D., et al. (2009) Tibiofemoral joint osteoarthritis: risk factors for MR-depicted fast cartilage loss over a 30-month period in the Multicenter Osteoarthritis Study 1 Purpose : Methods : Results : Conclusion : Radiology, **252** (3): 772–789

Roos, H., Adalberth, T., Dahlberg, L., et al. (1995) Osteoarthritis of the knee after injury to the anterior cruciate ligament or meniscus: the influence of time and age. Osteoarthritis and Cartilage, **3** (4): 261–267

Roughley, P.J. and Mort, J.S. (2014) The role of aggrecan in normal and osteoarthritic cartilage. Journal of Experimental Orthopaedics, **1** (8): 11

Sagar, D.R., Burston, J.J., Hathway, G.J., et al. (2011) The contribution of spinal glial cells to chronic pain behaviour in the monosodium iodoacetate model of osteoarthritic pain. Molecular Pain, **7** (88): 1–12

Sagar, D.R., Staniaszek, L.E., Okine, B.N., et al. (2010) Tonic modulation of spinal hyperexcitability by the endocannabinoid receptor system in a rat model of osteoarthritis pain. Arthritis & Rheumatism, **62** (12): 3666–3676

Sagar, D.R., Suokas, A.K., Kelly, S., et al. (2014) “Mechanisms of Nociception in

Models of Osteoarthritic Pain." In Graven-Nielsen, T. and Arendt-Nielsen, L. (eds.) Musculoskeletal Pain: Basic Mechanisms and Implications. Washington, D.C.: IASP Press. pp. 275–297

Saleh, K.J., Arendt, E.A., Eldridge, J., et al. (2005) Symposium: Operative treatment of patellofemoral arthritis. The Journal of Bone and Joint Surgery (American), **87A** (3): 659–671

Sandkühler, J., Stelzer, B. and Fu, Q.-G. (1993) Characteristics of propriospinal modulation of nociceptive lumbar spinal dorsal horn neurons in the cat. Neuroscience, **54** (4): 957–967

Sandrini, G., Rossi, P., Milanov, I., et al. (2006) Abnormal modulatory influence of diffuse noxious inhibitory controls in migraine and chronic tension-type headache patients. Cephalalgia, **26** (7): 782–789

Santos González, M., Bertrán de Lis, B.T. and Tendillo Cortijo, F.J. (2013) Effects of intramuscular alfaxalone alone or in combination with diazepam in swine. Veterinary Anaesthesia and Analgesia, **40** (4): 399–402

Sapru, H.N. and Krieger, A.J. (1978) Procedure for the decerebration of the rat. Brain Research Bulletin, **3** (6): 675–679

Saxne, T. (2003) Inflammation is a feature of the disease process in early knee joint osteoarthritis. Rheumatology, **42** (7): 903-a-905

Saygi, B., Yildirim, Y., Berker, N., et al. (2005) Evaluation of the neurosensory function of the medial meniscus in humans. Arthroscopy - Journal of Arthroscopic and Related Surgery, **21** (12): 1468–1472

Scanzello, C.R. and Goldring, S.R. (2012) The role of synovitis in osteoarthritis pathogenesis. Bone, **51** (2): 249–257

Schaible, H.-G. (2013) "Joint Pain: Basic Mechanisms." In McMahon, S.B., Koltzenburg, M., Tracey, I., et al. (eds.) Wall and Melzack's Textbook of Pain. 6th ed. Philadelphia: Elsevier Saunders. p. 609

Schaible, H.-G., Ebersberger, A. and Von Banchet, G.S. (2002) Mechanisms of Pain in Arthritis. Annals of the New York Academy of Sciences, **966** (1): 343–354

Schaible, H.-G. and Grubb, B.D. (1993) Afferent and spinal mechanisms of joint pain. Pain, **55** (1): 5–54

Schaible, H.-G., Richter, F., Ebersberger, A., et al. (2009) Joint pain. Experimental Brain Research, **196**: 153–162

Schaible, H.-G., Schmidt, R.F. and Willis, W.D. (1987) Convergent inputs from articular, cutaneous and muscle receptors onto ascending tract cells in the cat spinal cord. Experimental Brain Research, **66** (3): 479–488

Schmidt, D. and Mackay, B. (1982) Ultrastructure of human tendon sheath and synovium: implications for tumor histogenesis. Ultrastructural Pathology, **3**: 269–283

Schmidt, R., Schmelz, M., Forster, C., et al. (1995) Novel classes of responsive and unresponsive C nociceptors in human skin. The Journal of Neuroscience, **15** (1): 333–341

Schouenborg, J. (2002) Modular organisation and spinal somatosensory imprinting. Brain Research Reviews, **40**: 80–91

Schouenborg, J. and Dickenson, A.H. (1985) The effects of a distant noxious stimulation on A and C fibre-evoked flexion reflexes and neuronal activity in the dorsal horn of the rat. Brain Research, **328** (1): 23–32

Schouenborg, J., Holmberg, H. and Weng, H.-R. (1992) Functional organization of the nociceptive withdrawal reflexes. 2 Changes of excitability and receptive fields after spinalization in the rat. Experimental Brain Research, **90**: 469–478

Schouenborg, J. and Kalliomäki, J. (1990) Functional organization of the nociceptive withdrawal reflexes. Experimental Brain Research, **83**: 67–78

Schouenborg, J., Weng, H.-R. and Holmberg, H. (1994) Modular organization of spinal nociceptive reflexes: A new hypothesis. Physiology, **9** (6): 261–265

Schuelert, N. and McDougall, J.J. (2006) Electrophysiological evidence that the vasoactive intestinal peptide receptor antagonist VIP6–28 reduces nociception in an animal model of osteoarthritis. Osteoarthritis and Cartilage, **14** (11): 1155–1162

Schuelert, N. and McDougall, J.J. (2009) Grading of monosodium iodoacetate-induced osteoarthritis reveals a concentration-dependent sensitization of nociceptors in the knee joint of the rat. Neuroscience Letters, **465** (2): 184–188

Shahani, B.T. and Young, R.R. (1971) Human flexor reflexes. J Neurol Neurosurg Psychiatry, **34** (5): 616–627

Sherrington, C.S. (1898) Decerebrate rigidity, and reflex coordination of movements. The Journal of Physiology, **22** (4): 319–332

Sherrington, C.S. (1906) Observations on the scratch-reflex in the spinal dog.

The Journal of Physiology, **34** (1–2): 1–50

Sherrington, C.S. (1910) Flexion-reflex of the limb, crossed extension-reflex, and reflex stepping and standing. The Journal of Physiology, **40** (1–2): 28–121

Da Silva, J.T., Zhang, Y., Asgar, J., et al. (2018) Diffuse noxious inhibitory controls and brain networks are modulated in a testosterone-dependent manner in Sprague Dawley rats. Behavioural Brain Research, **349**: 91–97

Silverman, J., Garnett, N.L., Giszter, S.F., et al. (2005) Decerebrate mammalian preparations: unalleviated or fully alleviated pain? A review and opinion. Contemporary Topics in Laboratory Animal Science, **44** (4): 34–36

Silverwood, V., Blagojevic-Bucknall, M., Jinks, C., et al. (2015) Current evidence on risk factors for knee osteoarthritis in older adults: A systematic review and meta-analysis. Osteoarthritis and Cartilage, **23** (4): 507–515

Simon, W.H. (1970) Scale effects in animal joints. I. articular cartilage thickness and compressive stress. Arthritis & Rheumatism, **13** (3): 244–255

Singh, I. (1978) The architecture of cancellous bone. Journal of Anatomy, **127** (2): 305–310

Smith, M.D. (2011) The normal synovium. The Open Rheumatology Journal, **5** (1): 100–106

Smith, M.T., Edwards, R.R., McCann, U.D., et al. (2007) The effects of sleep deprivation on pain inhibition and spontaneous pain in women. Sleep, **30** (4): 494–505

Smith, M.T. and Haythornthwaite, J.A. (2004) How do sleep disturbance and

chronic pain inter-relate? Insights from the longitudinal and cognitive-behavioral clinical trials literature. Sleep Medicine Reviews, **8** (2): 119–132

Sommer, C. (2004) Serotonin in Pain and Analgesia: Actions in the Periphery. Molecular Neurobiology, **30** (2): 117–126

Sommer, C. (2006) Is serotonin hyperalgesic or analgesic? Current Pain and Headache Reports, **10** (2): 101–106

Song, G.H., Venkatraman, V., Ho, K.Y., et al. (2006) Cortical effects of anticipation and endogenous modulation of visceral pain assessed by functional brain MRI in irritable bowel syndrome patients and healthy controls. Pain, **126**: 79–90

Sorkin, L.S. and Yaksh, T.L. (2013) "Spinal Pharmacology of Nociceptive Transmission." In McMahon, S.B., Koltzenburg, M., Tracey, I., et al. (eds.) Wall and Melzack's Textbook of Pain. 6th ed. Philadelphia: Elsevier Saunders. pp. 375–401

Sotgiu, M.L. and Biella, G. (1998) Spinal neuron sensitization facilitates contralateral input in rats with peripheral mononeuropathy. Neuroscience Letters, **241** (2–3): 127–130

Southwick, W.O. and Bensch, K.G. (1971) Phagocytosis of colloidal gold by cells of synovial membrane. The Journal of Bone and Joint Surgery, **53A** (4): 729–741

Spector, T.D. and MacGregor, A.J. (2004) Risk factors for osteoarthritis: Genetics. Osteoarthritis and Cartilage, **12** (SUPLL.)

Stamford, J.A. (1995) Descending control of pain. British Journal of Anaesthesia,

75 (2): 217–227

Staud, R., Robinson, M.E., Vierck, C.J., et al. (2003) Diffuse noxious inhibitory controls (DNIC) attenuate temporal summation of second pain in normal males but not in normal females or fibromyalgia patients. Pain, **101** (1–2): 167–174

Stoop, R., Buma, P., van der Kraan, P.M., et al. (2000) Differences in type II collagen degradation between peripheral and central cartilage of rat stifle joints after cranial cruciate ligament transection. Arthritis & Rheumatism, **43** (9): 2121–2131

Strickland, I.T., Martindale, J.C., Woodhams, P.L., et al. (2008) Changes in the expression of NaV1.7, NaV1.8 and NaV1.9 in a distinct population of dorsal root ganglia innervating the rat knee joint in a model of chronic inflammatory joint pain. European Journal of Pain, **12** (5): 564–572

Stürmer, T., Günther, K.-P. and Brenner, H. (2000) Obesity, overweight and patterns of osteoarthritis. Journal of Clinical Epidemiology, **53** (3): 307–313

Sun, Y., Mauerhan, D.R., Kneisl, J.S., et al. (2012) Histological examination of collagen and proteoglycan changes in osteoarthritic menisci. The Open Rheumatology Journal, **6**: 24–32

Suokas, A.K., Walsh, D.A., McWilliams, D.F., et al. (2012) Quantitative sensory testing in painful osteoarthritis: a systematic review and meta-analysis. Osteoarthritis and Cartilage, **20** (10): 1075–1085

Suri, S., Gill, S.E., Massena de Camin, S., et al. (2007) Neurovascular invasion at the osteochondral junction and in osteophytes in osteoarthritis. Annals of the

Rheumatic Diseases, **66** (11): 1423–8

Suri, S. and Walsh, D.A. (2012) Osteochondral alterations in osteoarthritis. Bone, **51**: 204–211

Suzuki, R., Rygh, L.J. and Dickenson, A.H. (2004) Bad news from the brain: Descending 5-HT pathways that control spinal pain processing. Trends in Pharmacological Sciences, **25** (12): 613–617

Swagerty, D. and Hellinger, D. (2001) Radiographic assessment of osteoarthritis. American Family Physician, **64** (2): 279–287

Szebenyi, B., Hollander, A.P., Dieppe, P., et al. (2006) Associations between pain, function, and radiographic features in osteoarthritis of the knee. Arthritis and Rheumatism, **54** (1): 230–235

Takahashi, I., Matsuzaki, T., Kuroki, H., et al. (2018) Induction of osteoarthritis by injecting monosodium iodoacetate into the patellofemoral joint of an experimental rat model. PLoS ONE, **13** (4): 1–15

Tambeli, C.H., Quang, P., Levine, J.D., et al. (2003) Contribution of spinal inhibitory receptors in heterosegmental antinociception induced by noxious stimulation. European Journal of Neuroscience, **18** (11): 2999–3006

Tan, A.L., Toumi, H., Benjamin, M., et al. (2006) Combined high-resolution magnetic resonance imaging and histological examination to explore the role of ligaments and tendons in the phenotypic expression of early hand osteoarthritis. Annals of the Rheumatic Diseases, **65** (10): 1267–1272

Tanamas, S.K., Wluka, A.E., Pelletier, J.-P., et al. (2010) The association between

subchondral bone cysts and tibial cartilage volume and risk of joint replacement in people with knee osteoarthritis: A longitudinal study. Arthritis Research and Therapy, **12**: 1–7

Taylor, J.S., Neal, R.I., Harris, J., et al. (1991) Prolonged inhibition of a spinal reflex after intense stimulation of distant peripheral nerves in the decerebrated rabbit. Journal of Physiology, **437**: 71–83

Terkelsen, A.J., Andersen, O.K., Hansen, P.O., et al. (2001) Effects of heterotopic- and segmental counter-stimulation on the nociceptive withdrawal reflex in humans. Acta Physiologica Scandinavica, **172** (3): 211–7

Thakur, M., Rahman, W., Hobbs, C., et al. (2012) Characterisation of a peripheral neuropathic component of the rat monoiodoacetate model of osteoarthritis. PloS one, **7** (3): e33730

The McGraw-Hill Companies (2018) Withdrawal reflex [image] [online]. Available from: http://highered.mheducation.com/sites/0072507470/student_view0/chapter12/multiple_choice_quiz_1.html [Accessed 25 May 2018]

Thonar, E.J.-M.A., Buckwalter, J.A. and Kuettner, K.E. (1986) Maturation-related differences in the structure and composition of proteoglycans synthesized by chondrocytes from bovine articular cartilage. Journal of Biological Chemistry, **261** (5): 2467–2474

Todd, A.J. (2010) Neuronal circuitry for pain processing in the dorsal horn. Nature reviews. Neuroscience, **11** (12): 823–36

Todd, A.J. and Koerber, H.R. (2013) “Neuroanatomical Substrates of Spinal Nociception.” In McMahon, S.B., Koltzenburg, M., Tracey, I., et al. (eds.) Wall and Melzack’s Textbook of Pain. 6th ed. Philadelphia: Elsevier Saunders

Tomlinson, R.W., Gray, B.G. and Dostrovsky, J.O. (1983) Inhibition of rat spinal cord dorsal horn neurons by non-segmental, noxious cutaneous stimuli. Brain Research, **279** (1–2): 291–294

Treister, R., Eisenberg, E., Gershon, E., et al. (2010) Factors affecting - And relationships between - Different modes of endogenous pain modulation in healthy volunteers. European Journal of Pain, **14** (6): 608–614

Tyce, G.M. and Yaksh, T.L. (1981) Monoamine release from cat spinal cord by somatic stimuli: an intrinsic modulatory system. The Journal of Physiology, **314** (1): 513–529

Vainio, O. (2012) Translational animal models using veterinary patients – An example of canine osteoarthritis (OA). Scandinavian Journal of Pain, **3** (2): 84–89

Vanegas, H. and Schaible, H.-G. (2004) Descending control of persistent pain: inhibitory or facilitatory? Brain Research Reviews, **46** (3): 295–309

Vanegas, H., Vazquez, E. and Tortorici, V. (2010) NSAIDS, opioids, cannabinoids and the control of pain by the central nervous system. Pharmaceuticals, **3** (5): 1335–1347

Velo, P., Leiras, R. and Canedo, A. (2013) Electrophysiological study of supraspinal input and spinal output of cat’s subnucleus reticularis dorsalis (SRD)

neurons. PLoS ONE, **8** (3): 1–14

Venn, M. and Maroudas, A. (1977) Chemical composition and swelling of normal and osteoarthrotic femoral head cartilage. I. Chemical composition. Annals of the Rheumatic Diseases, **36**: 121–129

Verzijl, N., DeGroot, J., Oldehinkel, E., et al. (2000) Age-related accumulation of Maillard reaction products in human articular cartilage collagen. The Biochemical Journal, **350**: 381–387

Villanueva, L., Bouhassira, D. and Le Bars, D. (1996) The medullary subnucleus reticularis dorsalis (SRD) as a key link in both the transmission and modulation of pain signals. Pain, **67** (2–3): 231–240

Villanueva, L., Bouhassira, D., Bing, Z., et al. (1988) Convergence of heterotopic nociceptive information onto subnucleus reticularis dorsalis neurons in the rat medulla. Journal of Neurophysiology, **60** (3): 980–1009

Villanueva, L., Cadden, S.W. and Le Bars, D. (1984) Diffuse noxious inhibitory controls (DNIC): evidence for post-synaptic inhibition of trigeminal nucleus caudalis convergent neurones. Brain Research, **321** (1): 165–168

Villanueva, L., Chitour, D. and Le Bars, D. (1986a) Involvement of the dorsolateral funiculus in the descending spinal projections responsible for diffuse noxious inhibitory controls in the rat. Journal of Neurophysiology, **56** (4): 1185–1195

Villanueva, L., Peschanski, M., Calvino, B., et al. (1986b) Ascending pathways in the spinal cord involved in triggering of diffuse noxious inhibitory controls in

the rat. Journal of Neurophysiology, **55** (1): 34–55

Voloshin, A.S. and Wosk, J. (1983) Shock absorption of meniscectomized and painful knees: A comparative in vivo study. Journal of Biomedical Engineering, **5** (2): 157–161

Vuori, I.M. (2001) Dose-response of physical activity and low back pain, osteoarthritis and osteoporosis. Medicine and Science in Sports and Exercise, **33** (6): 551–586

Wada, M., Imura, S., Baba, H., et al. (1996) Knee laxity in patients with osteoarthritis and rheumatoid arthritis. British Journal of Rheumatology, **35** (6): 560–563

Wada, M., Tatsuo, H., Baba, H., et al. (1999) Femoral intercondylar notch measurements in osteoarthritic knees. Rheumatology, **38** (6): 554–558

Walker, P.S. and Erkman, M.J. (1975) The role of the menisci in force transmission across the knee. Clinical Orthopaedics and Related Research, (109): 184–192

Walsh, D.A., Bonnet, C.S., Turner, E.L., et al. (2007) Angiogenesis in the synovium and at the osteochondral junction in osteoarthritis. Osteoarthritis and Cartilage, **15** (7): 743–751

Walsh, D.A., Mcwilliams, D.F., Turley, M.J., et al. (2010) Angiogenesis and nerve growth factor at the osteochondral junction in rheumatoid arthritis and osteoarthritis. Rheumatology, **49** (10): 1852–1861

Walsh, D.A., Yousef, A., McWilliams, D.F., et al. (2009) Evaluation of a

Photographic Chondropathy Score (PCS) for pathological samples in a study of inflammation in tibiofemoral osteoarthritis. Osteoarthritis and Cartilage, **17** (3): 304–312

Warne, L.N., Beths, T., Whittem, T., et al. (2015) A review of the pharmacology and clinical application of alfaxalone in cats. The Veterinary Journal, **203** (2): 141–148

Washington, L.L., Gibson, S.J. and Helme, R.D. (2000) Age-related differences in the endogenous analgesic response to repeated cold water immersion in human volunteers. Pain, **89** (1): 89–96

Watanabe, A., Kanamori, A., Ikeda, K., et al. (2011) Histological evaluation and comparison of the anteromedial and posterolateral bundle of the human anterior cruciate ligament of the osteoarthritic knee joint. The Knee, **18**: 47–50

Weissman-Fogel, I., Sprecher, E. and Pud, D. (2008) Effects of catastrophizing on pain perception and pain modulation. Experimental Brain Research, **186** (1): 79–85

Wen, Y.-R., Wang, C.-C., Yeh, G.-C., et al. (2010) DNIC-mediated analgesia produced by a supramaximal electrical or a high-dose formalin conditioning stimulus: roles of opioid and alpha2-adrenergic receptors. Journal of Biomedical Science, **17** (19): 1–13

Weng, H.-R. and Schouenborg, J. (1996) Nociceptive inhibition of withdrawal reflex responses increases over time in spinalized rats. NeuroReport, **7** (7): 1310–1314

White, K.L., Paine, S. and Harris, J. (2017) A clinical evaluation of the pharmacokinetics and pharmacodynamics of intravenous alfaxalone in cyclodextrin in male and female rats following a loading dose and constant rate infusion. Veterinary Anaesthesia and Analgesia, **44** (4): 865–875

Wiberg, M., Westman, J. and Blomqvist, A. (1987) Somatosensory projection to the mesencephalon: An anatomical study in the monkey. Journal of Comparative Neurology, **264** (1): 92–117

van Wijk, G. and Veldhuijzen, D.S. (2010) Perspective on diffuse noxious inhibitory controls as a model of endogenous pain modulation in clinical pain syndromes. The Journal of Pain, **11** (5): 408–419

Wilder-Smith, C.H., Schindler, D., Lovblad, K., et al. (2004) Brain functional magnetic resonance imaging of rectal pain and activation of endogenous inhibitory mechanisms in irritable bowel syndrome patient subgroups and healthy controls. Gut, **53** (11): 1595–601

Willer, J.C., Le Bars, D. and De Broucker, T. (1990) Diffuse noxious inhibitory controls in man: Involvement of an opioidergic link. European Journal of Pharmacology, **182** (2): 347–355

Willer, J.C., De Broucker, T. and Le Bars, D. (1989) Encoding of nociceptive thermal stimuli by diffuse noxious inhibitory controls in humans. Journal of Neurophysiology, **62** (5): 1028–1038

Willer, J.C., Roby, A. and Le Bars, D. (1984) Psychophysical and electrophysiological approaches to the pain-relieving effects of heterotopic

nociceptive stimuli. Brain, **107** (4): 1095–1112

Wise, B.L., Niu, J., Zhang, Y., et al. (2010) Psychological factors and their relation to osteoarthritis pain. Osteoarthritis and Cartilage, **18** (7): 883–887

Wluka, A.E., Lombard, C.B. and Cicuttini, F.M. (2013) Tackling obesity in knee osteoarthritis. Nature reviews. Rheumatology, **9**: 225–235

Wojtys, E.M., Beaman, D.N., Glover, R.A., et al. (1990) Innervation of the human knee joint by substance-P fibers. Arthroscopy: The Journal of Arthroscopic and Related Surgery, **6** (4): 254–63

Woo, S.L.-Y., Abramowitch, S.D., Kilger, R., et al. (2006) Biomechanics of knee ligaments: injury, healing, and repair. Journal of Biomechanics, **39** (1): 1–20

Woolf, C.J. and Costigan, M. (1999) Transcriptional and posttranslational plasticity and the generation of inflammatory pain. Proceedings of the National Academy of Sciences of the United States of America, **96** (14): 7723–7730

Woolf, C.J. and Ma, Q. (2007) Nociceptors noxious stimulus detectors. Neuron, **55** (3): 353–364

Woolf, C.J. and Mannion, R.J. (1999) Neuropathic pain: aetiology, symptoms, mechanisms, and management. The Lancet, **353** (9168): 1959–1964

Wu, Q. and Henry, J.L. (2010) Changes in Abeta non-nociceptive primary sensory neurons in a rat model of osteoarthritis pain. Molecular pain, **6** (37): 13

Xu, H., Edwards, J., Banerji, S., et al. (2003) Distribution of lymphatic vessels in normal and arthritic human synovial tissues. Annals of the Rheumatic Diseases, **62**: 1227–1229

Yaksh, T.L. and Tyce, G.M. (1979) Microinjection of morphine into the periaqueductal gray evokes the release of serotonin from spinal cord. Brain Research, **171** (1): 176–181

Yam, M.F., Loh, Y.C., Tan, C.S., et al. (2018) General pathways of pain sensation and the major neurotransmitters involved in pain regulation. International Journal of Molecular Sciences, **19** (8): 1–23

Yamada, K., Healey, R., Amiel, D., et al. (2002) Subchondral bone of the human knee joint in aging and osteoarthritis. Osteoarthritis and Cartilage, **10**: 360–369

Yarnitsky, D. (2010) Conditioned pain modulation (the diffuse noxious inhibitory control-like effect): Its relevance for acute and chronic pain states. Current Opinion in Anaesthesiology, **23** (5): 611–615

Yarnitsky, D., Arendt-Nielsen, L., Bouhassira, D., et al. (2010) Recommendations on terminology and practice of psychophysical DNIC testing. European Journal of Pain, **14** (4): 339

Yarnitsky, D., Crispel, Y., Eisenberg, E., et al. (2008) Prediction of chronic post-operative pain: Pre-operative DNIC testing identifies patients at risk. Pain, **138** (1): 22–28

Young, M.R., Fleetwood-Walker, S.M., Mitchell, R., et al. (1995) The involvement of metabotropic glutamate receptors and their intracellular signalling pathways in sustained nociceptive transmission in rat dorsal horn neurons. Neuropharmacology, **34** (8): 1033–1041

Yusuf, E., Kortekaas, M.C., Watt, I., et al. (2011) Do knee abnormalities

visualised on MRI explain knee pain in knee osteoarthritis? A systematic review. Annals of the Rheumatic Diseases, **70** (1): 60–7

Zhang, E.T. and Craig, A.D. (1997) Morphology and distribution of spinothalamic lamina I neurons in the monkey. The Journal of Neuroscience, **17** (9): 3274–3284

Zhang, Y., McAlindon, T.E., Hannan, M.T., et al. (1998) Worsening of radiographic knee osteoarthritis: The Framingham study. Arthritis and Rheumatism, **41** (10): 1867–1873